Development of Novel Therapies, Models, and Biomarkers for Osteoclast-Related Diseases

Löfvall, Henrik

2018

Document Version:
Publisher's PDF, also known as Version of record

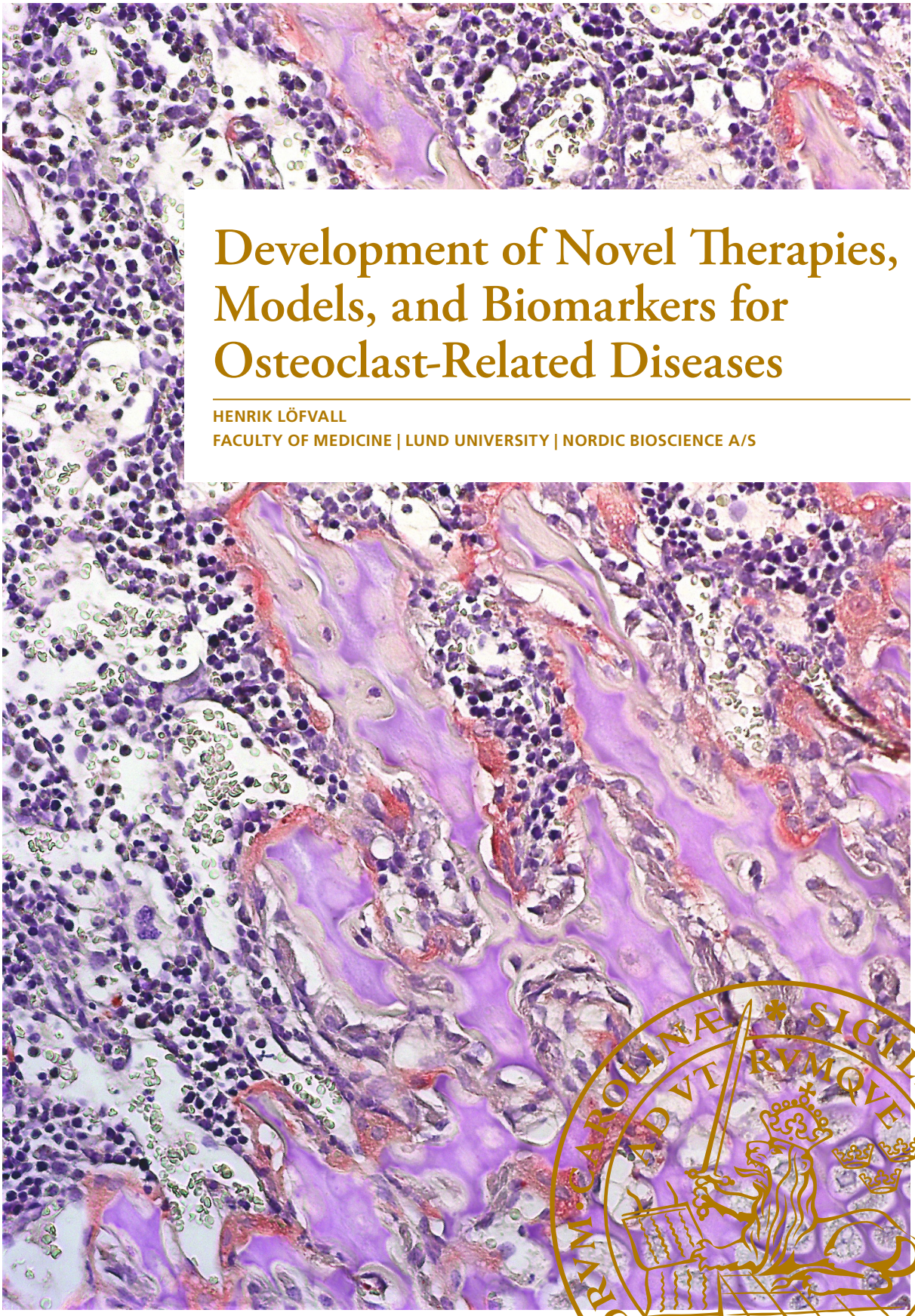

Development of Novel Therapies, Models, and Biomarkers for Osteoclast-Related Diseases

HENRIK LÖFVALL
FACULTY OF MEDICINE | LUND UNIVERSITY | NORDIC BIOSCIENCE A/S

Development of Novel Therapies, Models, and Biomarkers for Osteoclast-Related Diseases

Development of Novel Therapies, Models, and Biomarkers for Osteoclast-Related Diseases

Henrik Löfvall

LUND
UNIVERSITY

DOCTORAL DISSERTATION
by due permission of the Faculty of Medicine, Lund University, Sweden.
To be defended at Segerfalksalen, BMC A10, Sölvegatan 19, Lund, Sweden
on October 26th, 2018, at 13:00.

Faculty opponent
Emeritus Professor Miep Helfrich
The Institute of Medical Sciences, University of Aberdeen
Aberdeen, United Kingdom

Organization LUND UNIVERSITY	Document name Doctoral Dissertation
Department of Laboratory Medicine Division of Molecular Medicine and Gene Therapy	Date of issue 2018-10-26
Author(s) Henrik Löfvall	Sponsoring organization

Title and subtitle

Development of Novel Therapies, Models, and Biomarkers for Osteoclast-Related Diseases

Abstract

Osteoclasts are derived from hematopoietic stem cells (HSCs) and form upon stimulation of osteoclast precursors by macrophage colony-stimulating factor (M-CSF) and receptor activator of nuclear factor κB ligand (RANKL). Osteoclasts resorb bone by secreting hydrochloric acid, matrix metalloproteinases (MMPs) and cathepsin K. Failure of bone resorption or bone formation results in metabolic bone diseases. Osteopetrosis (excess bone) is caused by mutations impairing osteoclastogenesis or osteoclast function, and can only be treated with a hematopoietic stem cell (HSC) transplant (HSCT). Infantile malignant osteopetrosis (IMO) is typically lethal without HSCT. 50% of IMO patients have mutations in TCIRG1, a component of the osteoclast V-ATPase that is crucial for acidification. The first aim of this dissertation was to develop a clinically applicable TCIRG1-targeting gene therapy, to circumvent the need for HSC donors, and assess its efficacy and safety.

Osteoclasts have also been implicated as mediators of bone and cartilage degradation in rheumatic diseases. The increased bone degradation in rheumatoid arthritis and osteoarthritis has been strongly linked to increased osteoclast presence and activity, but the role of osteoclasts in the pathological degradation of cartilage—and type II collagen, its main component—remains unclear. Therefore, the second aim of this dissertation was to develop novel models and biomarkers for the investigation of osteoclast-mediated cartilage degradation.

In **Paper I**, we demonstrated that a proof-of-concept lentiviral vector, with a viral promoter, used to transduce IMO HSCs only induces TCIRG1 expression in osteoclasts, not in precursors or macrophages, and that a small percentage of treated cells is sufficient to restore resorption. In **Paper II**, we developed a clinically applicable vector, with a human promoter, and demonstrated that transduced human IMO HSCs transplanted into mice maintained the ability to generate functional osteoclasts *ex vivo* long-term. These studies are promising progress for the development of IMO gene therapy. In **Paper III**, we developed a mouse model with human HSCs expressing human M-CSF—to bypass the incompatibility of the human M-CSF receptor and mouse M-CSF—by transducing the HSCs with a human M-CSF vector and transplanting them into immunodeficient mice. These mice had improved human monocyte and myeloid reconstitution, but human osteoclasts could not be detected.

In **Paper IV**, we developed a cell culture model of human osteoclasts resorbing cartilage; using protease inhibitors and the C2M biomarker of type II collagen degradation, we demonstrated that cartilage resorption was mediated by MMPs and, to some extent, cathepsin K. In **Paper V**, we developed the type II collagen degradation biomarker assay GPDPLQ$_{1237}$, targeting an elongated version of the CTX-II neo-epitope that has been speculated to be osteoclast- and cathepsin K-specific. Both MMPs and cathepsin K contributed to GPDPLQ$_{1237}$ release from cartilage resorption, but only MMPs contributed to CTX-II release. Pro-inflammatory stimulation of cartilage without osteoclasts also resulted in MMP-mediated GPDPLQ$_{1237}$ and CTX-II release. Hence, GPDPLQ$_{1237}$ is a multi-protease biomarker of osteoclast- and inflammation-mediated cartilage degradation. However, GPDPLQ$_{1237}$ could not be detected at sufficient levels in blood or urine from humans or rats to validate the assay *in vivo*. These studies highlight the potential contribution of osteoclastic cartilage degradation to rheumatic diseases, and that novel biomarkers of cartilage degradation covering a wider range of cartilage degradation processes are needed to better understand relevant disease mechanisms.

Key words

Osteoclast, Extracellular matrix, Gene therapy, Osteopetrosis, Cell culture, Biomarker

Classification system and/or index terms (if any)

Supplementary bibliographical information		Language English
ISSN and key title 1652-8220		ISBN 978-91-7619-676-2
Recipient's notes	Number of pages 198	Price
	Security classification	

Signature  Date 2018-09-14

Development of Novel Therapies, Models, and Biomarkers for Osteoclast-Related Diseases

Henrik Löfvall

LUND
UNIVERSITY

Division of Molecular Medicine and Gene Therapy
Department of Laboratory Medicine
Faculty of Medicine, Lund University
Lund, Sweden
and
Nordic Bioscience A/S
Herlev, Denmark

Cover photo by Henrik Löfvall

The work described in this dissertation was performed in collaboration between Lund University and Nordic Bioscience A/S, and received funding from the Marie Skłodowska-Curie Actions ITN Euroclast.

Lund University, Faculty of Medicine
Department of Laboratory Medicine
Division of Molecular Medicine and Gene Therapy

Lund University, Faculty of Medicine Doctoral Dissertation Series 2018:108
ISBN 978-91-7619-676-2
ISSN 1652-8220

Printed in Sweden by Media-Tryck, Lund University
Lund 2018

MADE IN SWEDEN

To Eva and Anders, my supportive parents

Table of Contents

List of Publications

Papers included in this dissertation

I. Regulation and Function of Lentiviral Vector-Mediated TCIRG1 Expression in Osteoclasts from Patients with Infantile Malignant Osteopetrosis: Implications for Gene Therapy.
Thudium CS, Moscatelli I, **Löfvall H**, Kertész Z, Montano C, Bjurström CF, Karsdal MA, Schulz A, Richter J, Henriksen K.
Calcif. Tissue Int. 99, 638–648 (2016). doi: 10.1007/s00223-016-0187-6

II. Targeting NSG Mice Engrafting Cells with a Clinically Applicable Lentiviral Vector Corrects Osteoclasts in Infantile Malignant Osteopetrosis.
Moscatelli I, **Löfvall H**, Schneider Thudium C, Rothe M, Montano C, Kertész Z, Sirin M, Schulz A, Schambach A, Henriksen K, Richter J.
Hum. Gene Ther. 29, 938–949 (2018). doi: 10.1089/hum.2017.053

III. Forced Expression of Human Macrophage Colony-Stimulating Factor in $CD34^+$ Cells Promotes Monocyte Differentiation In Vitro and In Vivo but Blunts Osteoclastogenesis In Vitro.
Montano Almendras CP, Thudium CS, **Löfvall H**, Moscatelli I, Schambach A, Henriksen K, Richter J.
Eur. J. Haematol. 98, 517–526 (2017). doi: 10.1111/ejh.12867

IV. Osteoclasts Degrade Bone and Cartilage Knee Joint Compartments Through Different Resorption Processes.
Löfvall H, Newbould H, Karsdal MA, Dziegiel MH, Richter J, Henriksen K, Thudium CS.
Arthritis Res. Ther. 20, 67 (2018). doi: 10.1186/s13075-018-1564-5

V. $GPDPLQ_{1237}$—A Type II Collagen Neo-Epitope Biomarker of Osteoclast- and Inflammation-Derived Multi-Protease Cartilage Degradation In Vitro.
Löfvall H, Katri A, Dąbrowska A, Karsdal MA, Luo Y, He Y, Manon-Jensen T, Dziegiel MH, Bay-Jensen AC, Thudium CS, Henriksen K.
Manuscript.

Papers not included in this dissertation

1. Protein Biomarkers Associated with Pain Mechanisms in Osteoarthritis.
   Thudium CS, **Löfvall H**, Karsdal MA, Bay-Jensen AC, Bihlet AR.
   J. Proteomics (2018). doi:10.1016/j.jprot.2018.04.030
2. Combining Naproxen and a Dual Amylin and Calcitonin Receptor Agonist Improves Pain and Structural Outcomes in the Collagen-Induced Arthritis Rat Model.
   Katri A, Dąbrowska A, Ding M, **Löfvall H**, Karsdal MA, Andreassen KV, Thudium CS, Henriksen K.
   Manuscript.

Popular Scientific Summary

Restoring Osteoclast Functionality with Gene Therapy

Osteoclasts are the only human cells capable of degrading bone. Osteoclasts degrade the calcium-containing component of bone by secreting hydrochloric acid that dissolves the mineral. To degrade the protein component of bone, mainly type I collagen, the osteoclasts secrete enzymes including matrix metalloproteinases (MMPs) and cathepsin K.

Bone is an important extracellular matrix (ECM) as it, together with cartilage, makes up the human skeleton that protects our internal organs and provides structural support. Osteoclasts degrade bone and osteoblasts reform it in a continuous balancing act that is crucial for healthy skeletal growth and repair. Disturbances of this balance may result in bone diseases with too little bone, osteoporosis, or too much bone, osteopetrosis. Both diseases result in bones that are prone to break. Osteoporosis is quite common, especially amongst the elderly, and can be treated quite well today. However, osteopetrosis comes with a range of additional symptoms, is often fatal, and has very limited treatment options.

Osteopetrotic diseases are hereditary, rare, and come in different forms with different levels of severity. Infantile malignant osteopetrosis (IMO) is the most severe form. IMO is very debilitating and features a range of symptoms, including stunted growth, frequent fractures, progressive blindness—caused by the cranium growing inwards and compressing the nerves to the eyes—and death, often before the age of 10. 50% of IMO cases are caused by mutations in the *TCIRG1* gene. *TCIRG1* generates a protein that is a crucial to the osteoclasts' ability to secrete the acid needed for degrading bone. IMO patients with *TCIRG1* mutations usually have no TCIRG1 protein in their osteoclasts, and as a result cannot secrete acid and degrade bone. Since osteoclasts form from blood stem cells, which reside in the bone marrow, a bone marrow blood stem cell transplant can be used to replace the defective blood stem cells with healthy ones, and normalize the skeleton over time.

It is critical to perform a transplant early to have the best possible outcome and reduce permanent damage that cannot be treated, such as blindness. To minimize the risk of a severe immune response to the new cells, the stem cells should come from a suitable close relative. However, finding a suitable donor can take time. As

an alternative, we aimed to develop a gene therapy that holds the potential to treat the patient's own stem cells, thus eliminating the need for a stem cell donor. Samples of the patient's blood stem cells are collected, treated with a modified virus—called a vector—that inserts a functional *TCIRG1* gene, the cells are transplanted back into the patient, and they will then form functional osteoclasts in the patient's body. Pre-clinical IMO gene therapy experiments in mice and in cell cultures have been promising. In **Papers I-III**, we present the most recent developments in IMO gene therapy with regard to efficacy and safety testing, as well as for making the vector suitable for human use.

In **Paper I**, we investigated how TCIRG1 protein generated from the vector is regulated during osteoclast formation in IMO cell cultures. TCIRG1 protein was present specifically in the osteoclasts, not the stem cells or other non-osteoclast cells formed from the stem cells, indicating that the therapy only affects the intended cell type. Only a very small fraction of treated IMO stem cells (2.5%) mixed with non-treated IMO cells was required to substantially increase bone degradation in osteoclasts, and only 30% healthy cells mixed with IMO cells was enough to reach normal bone degradation levels—indicating that even a low vector efficacy would still be enough to restore osteoclast function.

For **Paper II**, we used a new version of the vector, which only contained components that would be suitable for human use to further reduce the risk of side effects. We transplanted treated IMO blood stem cells into mice, collected them from the mice after 2–5 months, and generated osteoclasts in cell cultures. Treated stem cells from 9/11 mice generated completely or partially functional osteoclasts, while non-treated stem cells did not. This indicates that the new vector is effective long-term, but the efficacy could be further improved. We also assessed the vector's risk of causing cancer, which has been an issue with gene therapy in the past, but found no measurable risk.

In **Paper III**, we attempted to generate human osteoclasts in mice, which would allow us to test that the treatment is effective after transplanting human cells. However, this is normally not possible as it requires the human cell signaling protein macrophage colony-stimulating factor (M-CSF), and mouse M-CSF cannot stimulate human cells. We used gene therapy to insert the human M-CSF gene into human blood stem cells. These stem cells formed osteoclasts in cell cultures without the addition of M-CSF. Transplanted mice had human M-CSF in their blood and we detected increased numbers of human cell types formed from blood stem cells stimulated with M-CSF, but we could not detect human osteoclasts.

In summary, these results show that our gene therapy is effective and safe. Further experiments using gene therapy-treated stem cells from mice with IMO transplanted into IMO mice are needed before human testing can begin, but **Papers I-III** represent important progress for developing effective and safe IMO gene therapy.

How Osteoclasts Degrade Cartilage

Cartilage, consisting mainly of type II collagen, is another important ECM of the human skeletal structure. Cartilage allows the bones in human joints to slide smoothly against each other without causing damage. Osteoclasts can degrade cartilage, and this is known to occur when bone replaces cartilage during bone growth. Cartilage damage, bone damage, and joint pain are key features of rheumatic diseases, including rheumatoid arthritis and osteoarthritis. Osteoclasts have been proposed to play a role in this disease-related cartilage degradation, but how osteoclasts degrade cartilage in these diseases is not known—although MMPs and cathepsin K are thought to be important. Animal studies have shown that drugs that inhibit osteoclasts have a beneficial effect on cartilage integrity and pain. Current treatment options for rheumatic diseases, especially to prevent or delay cartilage degradation, are limited. Therefore, new cell culture models and improved tools for clinical characterization of the patients, such as biomarkers, would be valuable assets for developing and testing new drugs for rheumatic diseases.

In order to explore how osteoclasts degrade cartilage, we developed a cell culture model where human osteoclasts generated from blood stem cells degrade cartilage from the knee joints of cows. The osteoclasts were treated with inhibitors of MMPs or cathepsin K, and we used antibody-based tests to measure biomarkers of cartilage degradation to test if MMPs or cathepsin K enzymes were important for cartilage degradation by osteoclasts. In **Paper IV**, we showed that MMPs contributed strongly to the release of C2M from cartilage, a biomarker detecting a degradation fragment of type II collagen, but the contribution of cathepsin K to C2M release was low. This study clearly showed that osteoclasts can degrade cartilage, and that the processes involved can be measured in cell cultures using biomarkers.

In **Paper V**, we developed the biomarker $GPDPLQ_{1237}$ based on CTX-II. Arguably, CTX-II is currently the best biomarker for detecting cartilage degradation when measured in human urine or the synovial fluid in joints. $GPDPLQ_{1237}$ and CTX-II both use antibody-based tests to detect very similar degradation fragments of type II collagen, but the antibody in $GPDPLQ_{1237}$ binds to slightly larger fragments than the antibody in CTX-II. Using the previously developed model of cartilage degradation by osteoclasts, we demonstrated that both MMPs and cathepsin K contributed strongly to $GPDPLQ_{1237}$ release, with increased effect when combining the inhibitors, while only MMPs contributed to CTX-II release. Despite this, we were unable to detect $GPDPLQ_{1237}$ in human blood or urine. A possible explanation could be that either $GPDPLQ_{1237}$ fragments are not present, or that the biomarker assay needs to be more sensitive. Taken together, we can now measure how osteoclasts degrade cartilage using MMPs and cathepsin K with the new cell culture model and the biomarkers we tested in it. These tools may be useful for testing new drugs and biomarkers for cartilage degradation.

Populärvetenskaplig sammanfattning

Återställning av osteoklasters funktion med genterapi

Osteoklaster är de enda mänskliga cellerna som kan bryta ned ben. De bryter ned den kalciuminnehållande komponenten av ben genom att utsöndra saltsyra som löser upp mineralerna. För att bryta ned proteinkomponenten av ben, som mestadels består av kollagen typ I, utsöndrar osteoklasterna enzymer, såsom katepsin K och matrixmetalloproteinaser (MMPs).

Ben, tillsammans med brosk, är ett viktigt extracellulär matrix (ECM) eftersom det utgör det mänskliga skelettet som skyddar våra inre organ och ger kroppen strukturellt stöd. Osteoklaster bryter ned ben och osteoblaster bildar ben på nytt i en kontinuerlig balansgång som är nödvändig för normal tillväxt och reparation av skelettet. Störningar i denna balans kan resultera i bensjukdomar med för lite ben, osteoporos, eller för mycket ben, osteopetros. Båda sjukdomarna resulterar i en ökad risk för benbrott. Osteoporos är ganska vanligt, framförallt bland äldre, och kan behandlas relativt väl idag. Osteopetros, å andra sidan, kommer med fler symptom, är ofta dödlig, och har väldigt begränsade behandlingsmöjligheter.

Osteopetroser är ärftliga, ovanliga, kommer i olika former, och kan variera i allvarlighetsgrad. Infantil malign osteopetros (IMO) är den allvarligaste formen. IMO är mycket handikappande och ger upphov till en rad olika symptom, t.ex. kortvuxenhet, benbrott, tilltagande synnedsättning orsakad av att kraniet växer inåt och utsätter nerverna till ögonen för tryck, och död ofta före 10 års ålder. Cirka 50 % av alla IMO-fall orsakas av mutationer i genen *TCIRG1*. *TCIRG1* generar ett protein som är vitalt för osteoklasters förmåga att utsöndra den syra som behövs för att bryta ned ben. IMO patienter med mutationer i *TCIRG1* har oftast inget TCIRG1 protein i sina osteoklaster och de kan därför inte utsöndra syra och bryta ned ben. Eftersom osteoklaster bildas från blodstamceller, som finns i benmärgen, kan en transplantation av blodstamceller från benmärgen användas för att ersätta de defekta blodstamcellerna med friska stamceller och normalisera skelettet över tid.

För att uppnå nästa möjliga resultat och för att minska permanenta skador som inte kan behandlas, till exempel blindhet, är det viktigt att en transplantation utförs så tidigt som möjligt. Stamcellerna bör komma från en lämplig nära släkting för att minska risken för en allvarlig immunreaktion. Att hitta en lämplig donator kan dock

ta tid. Vi vill utveckla en genterapi med potential att behandla patientens egna stamceller för att kringgå behovet av donerade stamceller. Prover av patients egna stamceller samlas in, behandlas med ett modifierat virus kallat en vektor som sätter in en funktionell kopia av genen *TCIRG1*, transplanteras tillbaka till patienten och bildar sedan funktionella osteoklaster i patientens kropp. Prekliniska experiment med IMO genterapi i möss och i cellodlingar har visat lovande resultat. I **Artikel I-III** presenterar vi de senaste utvecklingarna inom IMO genterapi, beträffande effektivitet, säkerhet, och att göra vektorn lämplig för människligt bruk.

I **Artikel I** undersökte vi hur TCIRG1 protein genererat från vektorn regleras när osteoklaster bildas i IMO cellodlingar. TCIRG1 protein var endast närvarande i osteoklaster, inte i stamceller eller andra icke-osteoklast celler som bildades från stamcellerna, vilket indikerar att behandlingen endast påverkar den avsedda celltypen. Enbart en liten andel behandlade IMO stamceller (2.5 %) blandade med obehandlade IMO celler krävdes för en betydlig ökning av nedbrytningsprodukter av ben. 30 % friska celler blandade med IMO celler var tillräckligt för att nå normala nivåer av bennedbrytning, vilket indikerar att även en låg effektivitet från vektorn vore tillräcklig för att återställa osteoklasternas funktion.

För **Artikel II** använde vi en ny version av vektorn som endast innehöll komponenter som vore lämpliga för mänskligt bruk, för att ytterligare minska risken för bieffekter. Vi transplanterade behandlade IMO blodstamceller till möss, samlade in dem från mössen 2–5 månader senare, och genererade osteoklaster i cellodlingar. Behandlade stamceller från 9/11 möss genererade fullständigt eller delvis funktionella osteoklaster. Detta indikerar att vektorn är långsiktigt effektiv, men effektiviteten kan fortfarande förbättras. Vi testade också vektorns risk för att orsaka cancer, vilket har varit ett problem med genterapi förr, men fann ingen mätbar risk.

I **Artikel III** försökte vi genera mänskliga osteoklaster i möss. Detta skulle göra det möjligt att testa behandlingens effektivitet efter transplantation med mänskliga celler. Detta är normalt sett inte möjligt eftersom det kräver cellsignaleringsproteinet makrofagkolonistimulerande faktor (M-CSF) och M-CSF från möss kan inte stimulera mänskliga celler. Vi satte in den mänskliga genen för M-CSF i mänskliga blodstamceller med genterapi. Stamcellerna bildade då osteoklaster i cellodlingar utan tillsatt M-CSF. Transplanterade möss hade mänskligt M-CSF i blodet och celler som bildas från blodstamceller som stimulerats med M-CSF ökade i antal, men vi kunde inte hitta några mänskliga osteoklaster i mössen.

Sammanfattningsvis så visar dessa resultat att vår genterapi är effektiv och säker. Fortsatta experiment där stamceller från möss med IMO behandlas med genterapi och transplanteras till IMO möss behövs innan mänskliga test kan påbörjas, men **Artiklarna I-III** representerar viktiga framsteg för utvecklingen av effektiv och säker IMO genterapi.

Hur osteoklaster bryter ned brosk

Brosk består i huvudsak av kollagen typ II och är ett annat viktigt ECM i det mänskliga skelettet. Brosk låter benen i leder glida friktionsfritt mot varandra utan att ta skada. Osteoklaster kan bryta ned brosk och det är känt att det förekommer när brosk ersätts av ben när ben växer. Skador på brosk och/eller ben och ledvärk är typiska symptom vid reumatiska sjukdomar, till exempel ledgångsreumatism och artros. Det har föreslagits att osteoklaster kan bidra till den sjukdomsrelaterade nedbrytningen av brosk. Även om MMPs och katepsin K tros vara av vikt så är det inte känt hur osteoklaster bryter ned brosk vid de här tillstånden. Djurförsök har visat att läkemedel som hämmar osteoklaster har en välgörande effekt på broskets integritet och på smärta. Behandlingar för reumatiska sjukdomar, i synnerhet behandlingar som förhindrar eller minskar nedbrytning av brosket, är för närvarande begränsade. Därför vore nya cellodlingsmetoder samt förbättrade verktyg för klinisk karakterisering av patienterna, till exempel biomarkörer, en tillgång för att utveckla och testa nya läkemedel för reumatiska sjukdomar.

För att utforska hur osteoklaster bryter ned brosk så utvecklade vi en ny cellodlingsmetod där mänskliga osteoklaster genererade från blodstamceller bryter ned brosk från knäleder från kor. Osteoklasterna behandlades med MMP- och katepsin K-inhibitorer och med hjälpa av antikroppsbaserade tester mätte vi biomarkörer för brosknedbrytning för att testa om MMPs eller katepsin K enzymer var viktiga för att osteoklaster ska kunna bryta ned brosk. I **Artikel IV** visade vi att MMPs bidrog starkt till frisättning av C2M, en biomarkör som mäter ett nedbrytningsfragment av kollagen typ II, men att katepsin K hade ett begränsat bidrag. Den här studien visade tydligt att osteoklaster kan bryta ned brosk och att de processer som bidrar kan mätas i cellodlingar med hjälp av biomarkörer.

I **Artikel V** utvecklade vi biomarkören $GPDPLQ_{1237}$ som är baserade på CTX-II. CTX-II är troligtvis den för närvarande bästa biomarkören för brosknedbrytning när den mäts i mänsklig urin eller ledvätska. Både $GPDPLQ_{1237}$ och CTX-II använder antikroppsbaserade tester för att detektera väldigt snarlika nedbrytningsfragment av kollagen typ II, men antikroppen i $GPDPLQ_{1237}$ binder till lite större fragment än antikroppen i CTX-II. Med hjälp av metoden för brosknedbrytning av osteoklaster som vi redan utvecklat demonstrerade vi att både MMPs och katepsin K bidrog starkt till frisättning av $GPDPLQ_{1237}$, med en ökad effekt när inhibitorerna kombinerades, och att endast MMPs bidrog till frisättning av CTX-II. Trots det kunde vi inte detektera $GPDPLQ_{1237}$ i mänskliga blod- eller urinprov. En möjlig förklaring kan vara antingen att $GPDPLQ_{1237}$ fragmenten inte är närvarande eller att testet för $GPDPLQ_{1237}$ behöver vara mer känsligt. Sammanfattningsvis så kan vi nu mäta hur osteoklaster bryter ned brosk med MMPs och katepsin K med den nya cellodlingsmetoden samt biomarkörerna vi testade i den. Dessa verktyg kan vara användbara för att testa nya läkemedel och biomarkörer för brosknedbrytning.

List of Abbreviations

AE2	Anion exchanger 2
BEX	Bovine cartilage explant
Ca^{2+}	Calcium ion
CAII	Carbonic anhydrase II
CB	Cord blood
ChimP	Chimeric myeloid promoter
ClC-7	Chloride voltage-gated channel 7
CSF1R	Colony stimulating factor 1 receptor
CTX-I	C-telopeptide of type I collagen
CTX-II	C-telopeptide of type II collagen
ECM	Extracellular matrix
EFS	Elongation factor 1α short
EFS-G	EFS-GFP vector
EFS-T	EFS-TCIRG1 vector
EFS-TG	EFS-TCIRG1/GFP vector
GFP	Green fluorescent protein
hM-CSF	Human macrophage colony-stimulating factor
HSC	Hematopoietic stem cell
HSCT	Hematopoietic stem cell transplantation
HSPC	Hematopoietic stem and progenitor cell
IMO	Infantile malignant osteopetrosis
IVIM	*In vitro* immortalization
M-CSF	Macrophage colony-stimulating factor

MSC	Mesenchymal stem cell
MMP	Matrix metalloproteinase
NSG	NOD-scid IL2rγ^{null}
OA	Osteoarthritis
OSM	Oncostatin M
OSTM1	Osteopetrosis-associated transmembrane protein 1
PBMC	Peripheral blood mononuclear cell
RA	Rheumatoid arthritis
RANK	Receptor activator of nuclear factor κB
RANKL	Receptor activator of nuclear factor κB ligand
SFFV	Spleen focus-forming virus
SFFV-G	SFFV-GFP vector
SFFV-TG	SFFV-TCIRG1/GFP vector
SIN	Self-inactivating vector
TCIRG1	T-cell immune regulator 1
TNFα	Tumor necrosis factor α
TRAP	Tartrate-resistant acid phosphatase
V-ATPase	Vacuolar-type H^+-ATPase

Introduction

The Human Skeleton

The human skeleton is composed of bone and cartilage. The skeleton serves many functions, both mechanical and metabolic in nature. The mechanical functions include structural support, attachment points for muscles, tendons and ligaments, locomotion, and protection of internal organs. Metabolic functions include homeostasis of calcium ions (Ca^{2+}) as well as of other ions[1], acid–base balance[1], serving as a growth factor and cytokine depot[2], and providing the microenvironment required for hematopoiesis (blood formation) in the bone marrow[3].

Bone

Bone Structure

Bone is the main structural component of the human skeleton. Approximately 80% of human bone is cortical bone and 20% is trabecular bone, also known as cancellous bone, albeit with large variations in the ratio of the two bone types between different skeletal sites[4]. Cortical bone is dense and solid and surrounds the marrow space, whereas trabecular bone is composed of a honeycomb-like network of trabecular plates and rods interspersed in the bone marrow compartment. The bones of the human skeleton can be divided into four main categories: long bones, short bones, flat bones, and irregular bones. The long bones are of particular interest as they contain most of the bone marrow in adult humans. The structure of long bones is divided into the diaphysis, metaphyses and epiphyses (Figure 1). At the center of a long bone is the diaphysis, a hollow shaft mainly composed of dense and solid cortical bone, which houses the bone marrow. At the ends of the diaphysis, the bone widens out into the cone-shaped metaphyses, followed by the growth plates and finally the rounded epiphyses above the growth plates. The metaphysis and epiphysis are mainly composed of trabecular bone, surrounded by a thin layer of cortical bone. Where long bones meet in joints, the epiphyses are covered by a layer of articular cartilage.

Bone Composition

The bone itself consists of an extracellular matrix (ECM) interspersed with osteocytes, in units called osteons. The bone ECM is composed of a calcified (or inorganic) bone matrix—approximately 60% of the bone by weight[5]—consisting of $Ca_{10}(PO_4)_6(OH)_2$ calcium hydroxyapatite mineral[6], and a non-calcified (or organic) bone matrix consisting of approximately 90% type I collagen, 5% non-collagenous proteins, and 2% lipids by weight[7]. A number of cell types are found in or on the bone matrix, including osteocytes, osteoblasts, bone-lining cells (BLCs), reversal cells and osteoclasts, which will be covered in the following sections. Under normal conditions, osteocytes are the only cells that are permanently present within the bone matrix. In addition to the bone ECM and its resident cells, bone is vascularized and innervated which allows for both oxygen and nutrient supply as well as regulation of bone homeostasis[8].

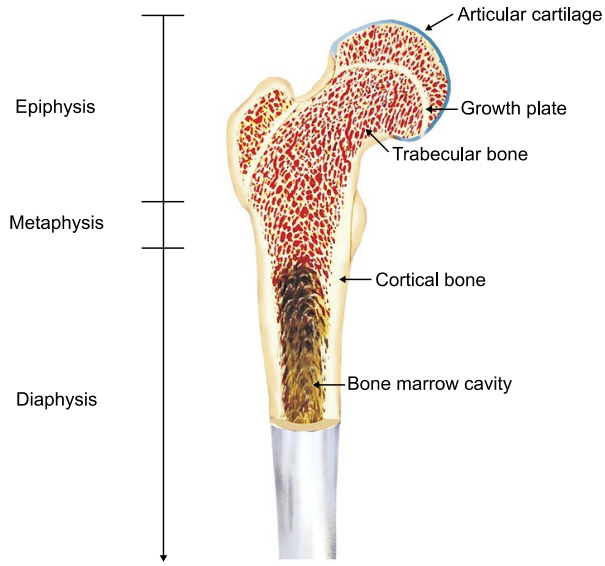

Figure 1. The Structure of a Long Bone.
The structural organization of the proximal end of a femoral long bone.
Illustration from *Asklepios Atlas of the Human Anatomy*, image provided by Science Photo Library. Adapted with permission from Encyclopædia Britannica: Encyclopædia Britannica; Britannica ImageQuest; *Structure of long bone, artwork*; 31 Aug 2017; https://quest.eb.com/search/132_1486049/1/132_1486049/cite; Accessed 18 Jun 2018.

Bone Formation

Bone is formed by osteoblasts, a type of mononuclear cell derived from pluripotent mesenchymal stem cells (MSCs) that are found in the bone marrow[9]. During development, bone formation takes the form of two different processes: intramembranous ossification and endochondral ossification. While some bones of the human skeleton, such as the flat bones of the cranium, are generated through

intramembranous ossification, endochondral ossification is responsible for most of the bone formation during both fetal development and postnatal growth. During intramembranous ossification, osteoblasts are formed from clusters of cells derived from MSCs and will then directly go on to form bone[10]. On the other hand, during endochondral ossification, the MSC clusters instead generate chondrocytes[10]. The chondrocytes proliferate and go into hypertrophy, after which the hypertrophic chondrocytes lay down a type II collagen-rich cartilage matrix to serve as a cartilage skeletal model which later becomes calcified[11]. Hypertrophic chondrocytes eventually die and the cartilage matrix surrounding them is degraded. The cartilage degradation is mediated by proteases from the hypertrophic chondrocytes—mainly matrix metalloproteinases (MMP)-9 and MMP-13 as well as, presumably, a disintegrin and metalloproteinase with thrombospondin motifs (ADAMTS)-4 and ADAMTS-5—as well as by osteoclasts[11], which will be covered in greater depth in later sections. Osteoclasts are probably the main contributor to the degradation of calcified cartilage during endochondral ossification, as deficiencies in the cysteine protease cathepsin K, predominantly expressed in osteoclasts[12], is known to result in severe metabolic bone diseases with inclusions of calcified cartilage in bones[13]. MMP-deficiencies typically only result in minor bone defects[14]. The degradation of the cartilage allows for invasion of blood vessels, osteoclasts, osteoblast precursors and bone marrow cells, and the differentiating osteoblasts form bone on the remaining cartilage scaffold[11].

The bone formation process during endochondral ossification can be divided into two main steps: synthesis and deposition of osteoid, and mineralization. Newly formed non-mineralized bone matrix consisting mainly of type I collagen and other non-collagenous proteins are synthesized and deposited in layers called osteoid, followed by mineralization of the bone matrix with hydroxyapatite crystals. The amount of mineralization is crucial for the mechanical properties of bone; human bone is about 60% mineralized[5]. Increased bone mineral density (BMD) increases the stiffness of bones at the expense of flexibility[15], possibly resulting in brittle bones, while decreased BMD renders the bone too flexible, allowing it to break during normal loading[16]. Once bone formation is completed, osteoblasts either become embedded in the bone as osteocytes, differentiate into bone lining cells (BLCs), or undergo apoptosis[9,17,18].

The osteocyte is the main cell population in bone and is a major orchestrator of activities within the skeleton; osteocytes both sense and integrate mechanical and chemical signals from their environment to regulate bone formation and bone resorption[19]. Osteocyte cell bodies reside in small cavities within the bone (lacunae) and are characterized by dendritic processes of the cell membrane (filopodia) that extend through channels in the bone (canaliculi) to form networks between osteocytes, as well as between osteocytes and the bone surface[19]. These filopodia

are not only important mechanosensors[20] that detect mechanical loading, but they are also important for osteocyte survival and signaling.

The BLCs cover all bone surfaces that are not being actively remodeled, called quiescent bone surfaces, and serve as a functional barrier between bone and bone marrow[21]. In addition to their inherent function, they are also a major source of osteoblasts in adulthood[22].

Articular Cartilage

Cartilage Structure

Articular cartilage is a smooth layer of connective tissue that covers the surfaces of bones where they meet in diarthrodial joints (also known as synovial joints)[23]. This type of cartilage serves two major functions in the human skeletal structure: 1) providing near frictionless motion and 2) counteracting the impact of the compressive forces experienced across the joint during use[23]. The superficial zone of the cartilage is in direct contact with the synovial fluid within the joint capsule which lubricates the joint, whereas the deep zone transitions into a layer of calcified cartilage that is attached to the underlying subchondral bone.

Cartilage Composition

The articular cartilage consists of both cells and an ECM. Chondrocytes derived from MSCs are sparsely distributed throughout cartilage and constitute only 2% of the total articular cartilage volume[24], although their distribution varies throughout the cartilage (Figure 2). The chondrocytes are crucial for maintaining the cartilage ECM and its lack of vascularization[25]. Of the cartilage ECM, tissue fluid represents between 65% and 80% of the total weight of articular cartilage[26]. The flow of water through the cartilage and across the articular surface helps to transport and distribute nutrients to chondrocytes, in addition to providing joint lubrication[27]. Collagens and proteoglycans account for the majority of the remaining dry weight, but lipids, phospholipids, non-collagenous proteins, and glycoproteins are also present in smaller quantities[27]. The most abundant structural macromolecule in the joint cartilage ECM is collagen, approximately 60% of the dry weight, of which type II collagen represents 90–95%[27]. Minor cartilage collagens, including types I, IV, V, VI, IX, and XI, help form and stabilize the type II collagen fibril network[27]. Type II collagen is a fibril-forming collagen and is composed of three identical α1(II) chains[28] that form a trimeric collagen triple helix[29]. In the cartilage, type II collagen is typically co-assembled with type XI collagen by covalent cross-linkage where it interacts with small leucine-rich proteoglycans that influence the fibrillar structure and function[30]. The stability and strength of type II collagen provide the cartilage with structural integrity and resistance to stress[29]. Proteoglycans, such as aggrecan,

constitute 10% to 15% of the wet weight[27]. Aggrecan is important for fluid pressurization of articular cartilage, which helps support the articular cartilage surface[31,32]. The ability of cartilage to resist compression is directly associated with high levels of aggrecan in the cartilage ECM[23]. Like all proteoglycans, aggrecan consists of a core protein with covalently attached sulfated glycosaminoglycans (GAGs)[23]. By retaining large amounts of water, primarily due to the negative charges of the GAGs, the cartilage can resist compressive forces as the aggrecans repel one another[24].

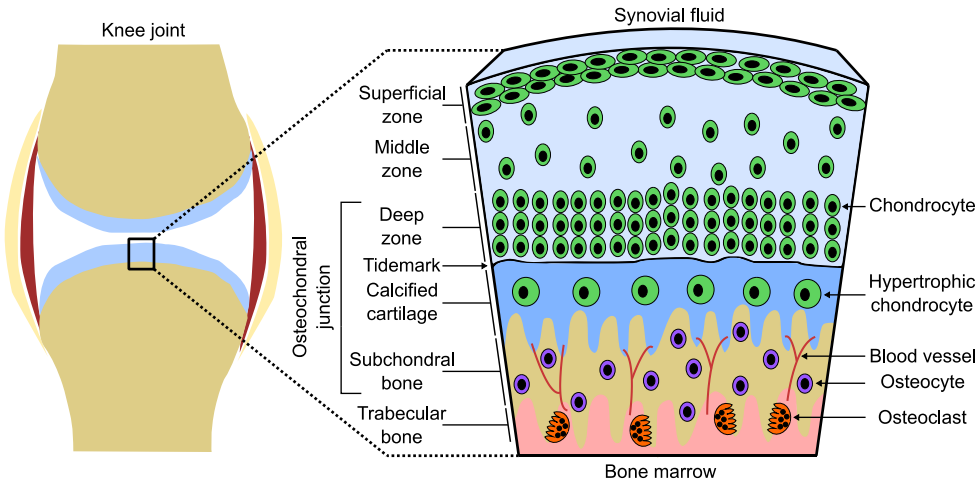

Figure 2. Schematic Representation of the Bone–Cartilage Interface in a Diarthrodial Joint.
This figure illustrates the principal organization of the bone–cartilage interface in a diarthrodial joint, using the knee joint as an example. The non-calcified articular cartilage can be divided into three zones, the superficial, the middle and the deep zone. These zones have some differences in chondrocyte organization and ECM composition. The tidemark separates the non-calcified cartilage from the calcified cartilage. The calcified cartilage has a composition that is similar to the non-calcified cartilage, but it is calcified with hydroxyapatite mineral and contains hypertrophic chondrocytes. Unlike non-calcified cartilage, which is avascular, calcified cartilage is vascularized. The non-calcified cartilage, calcified cartilage and underlying subchondral bone together form the osteochondral junction, which is crucial for transforming shear stress into compressive and tensile stress during loading and motion. The subchondral bone, which is cortical in nature, transitions into trabecular bone which is interspersed with bone marrow. The bone is inhabited by osteocytes, and osteoclasts degrade the subchondral bone during remodeling.

Bone–Cartilage Interface

Beneath the non-calcified articular cartilage, separated by the tidemark, lies a layer of calcified cartilage (Figure 2). The calcified cartilage differs from non-calcified cartilage in several aspects, particularly with regard to its mineralization, vascularization and innervation, and the hypertrophic state of the chondrocytes[33]. Non-calcified cartilage is normally aneural and avascular[34], but calcified cartilage has a blood supply via vascular channels through the subchondral bone[35]. The calcified cartilage anchors the cartilage into the subchondral bone and, together with the non-calcified cartilage and the subchondral bone, form the osteochondral junction. The osteochondral junction transforms shear stress from loading and

motion into compressive and tensile stress via undulations in the ECMs[36,37]. In addition to the osteochondral junction's role in resisting stress during loading, recent studies have suggested that there may be direct signaling and transportation of solutes between subchondral bone and the articular cartilage by diffusion through pores in their ECMs[38,39]. This cross-talk across the bone–cartilage interface is affected by the thickness and porosity of the subchondral bone as well as cartilage thickness[39], which may be increased in rheumatic disease[38,39].

Osteoclasts

Osteoclasts are tartrate-resistant acid phosphatase (TRAP)-positive multinucleated cells that are uniquely capable of resorbing the calcified and non-calcified bone matrices. Although osteoclasts play a crucial role in healthy skeletal development and maintenance, they may also contribute to metabolic bone diseases and rheumatic diseases. As such, osteoclastogenesis, bone resorption and bone remodeling are normally highly regulated processes.

Osteoclastogenesis

Osteoclasts are derived from hematopoietic stem cells (HSCs) via the monocytic lineage. HSCs differentiate into $CD14^+$ monocytes directed by cytokines and transcription factors, including PU.1[40–42]. Further differentiation is extensively regulated by cytokines, many of which are derived from osteoblast lineage cells. Osteoblast lineage cells—including osteoblasts and osteocytes—are important sources of osteoclastogenesis-regulating cytokines[43] (a basic schematic overview can be found in Figure 3), the most important of which are macrophage colony-stimulating factor (M-CSF)[44–46], receptor activator of nuclear factor κB (NFκB, [RANK]) ligand (RANKL)[46–48], and osteoprotegerin (OPG)[49–51]. M-CSF primes early osteoclast precursors by binding to the colony stimulating factor 1 receptor (CSF1R), which stimulates proliferation[4], survival[4], and the expression of RANK in early osteoclast precursors[52,53]. M-CSF also plays a role in cytoskeleton rearrangement, together with the integrin $\alpha_V\beta_3$, by stimulating a c-Src-initiated signaling complex[54,55]. The RANK receptor is then stimulated by RANKL[47,48]—which can be prevented by the soluble RANKL decoy receptor OPG[56] or the membrane-bound leucine-rich repeat-containing G-protein-coupled receptor 4 (LGR4), which binds RANKL and decreases expression and activity of nuclear factor of activated T-cells, cytoplasmic 1 (NFATc1)[57]—and results in fusion and maturation of osteoclast precursors, mediated by a number of crucial pathways including tumor necrosis factor (TNF) receptor associated factor 6 (TRAF6), NFκB, NFATc1, c-Fos, c-Src, microphthalmia-associated transcription factor (MITF),

dendritic cell-specific transmembrane protein (DC-STAMP) and osteoclast-stimulatory transmembrane protein (OC-STAMP)[47,58–64]. The committed osteoclasts attach to the ECM and undergo final changes that will enable them to resorb bone, including expressing tartrate-resistant acid phosphatase (TRAP)[65], cathepsin K[66], MMPs[67], chloride voltage-gated channel 7 (ClC-7)[68], osteopetrosis-associated transmembrane protein 1 (OSTM1)[69,70], vacuolar-type H^+-ATPase (V-ATPase)[71], V-ATPase a3 subunit (also known as T-cell immune regulator 1 [TCIRG1])[72,73], carbonic anhydrase II (CAII)[74,75], and anion exchanger 2 (AE2)[76]—all of which are important for normal resorption—as well as the calcitonin receptor (CTR), which the hormone calcitonin interacts with to inhibit bone resorption[77].

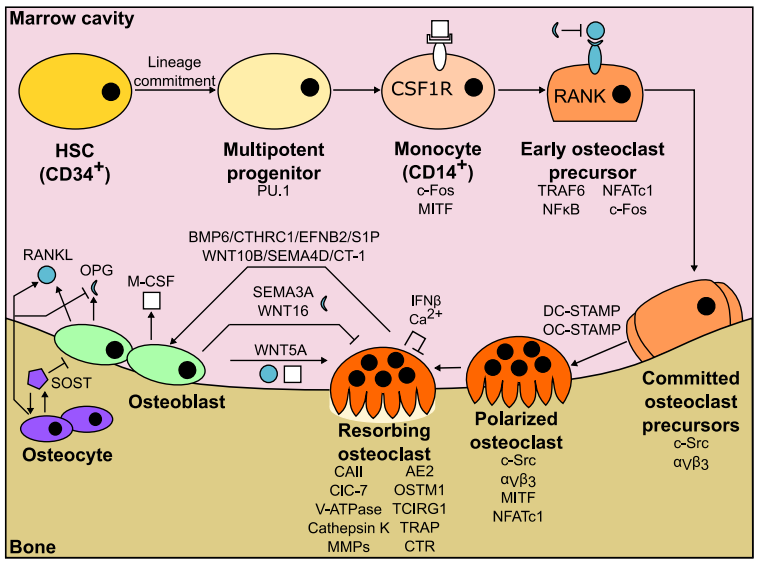

Figure 3. Schematic Overview of RANKL-Mediated Osteoclastogenesis and Coupling.
Osteoclasts are derived from HSCs that differentiate into osteoclasts via M-CSF and RANKL-mediated osteoclastogenesis. After lineage commitment of the HSCs and differentiation into monocytes, expressing the M-CSF receptor CSF1R, M-CSF primes the monocytes into becoming early osteoclast precursors that express RANK. Upon RANKL stimulation, the precursors become committed, attach to the ECM, and eventually fuse—mediated by DC-STAMP and OC-STAMP. c-Src and integrin $\alpha_V\beta_3$ mediate the required cytoskeletal rearrangement, polarization of the osteoclasts and formation of the sealing zone. The mature resorbing osteoclasts express proteases, proton pumps and other proteins required for acidification and proteolysis of the bone ECM. Throughout the whole process, M-CSF and RANKL—chiefly derived from osteoblasts and osteocytes—are required to stimulate proliferation, differentiation, survival, and resorption, which the RANKL decoy receptor OPG can inhibit. The osteoblasts, osteocytes, osteoclasts and their respective activities regulate each other throughout the process, in a phenomenon called coupling. Genes/proteins that are of particular importance have been indicated in the illustration.

The Bone Resorption Process

As the osteoclasts reach the bone surface, they attach to the bone using membrane-bound integrins. The integrin $\alpha_V\beta_3$, also known as the vitronectin receptor, facilitates the osteoclast attaching to bone by binding to the RGD (Arg-Gly-Asp) motif in bone

matrix components, such as the glycoproteins vitronectin or osteopontin that are abundant in bone[78–80]. As the osteoclasts bind to the bone matrix, this activates the osteoclast's resorptive behavior and triggers polarization signals[80]—mediated by c-Src, Syk and proline-rich tyrosine kinase 2 polarization[81–85]. Secretory lysosomes associate with microtubules and are trafficked, mediated by TCIRG1[86] interacting with Rab7, toward the bone-apposed cell membrane where they fuse with the membrane through exocytosis and form the ruffled border of the osteoclast[81]. Resorption lacunae (or Howship's lacunae) are formed as sealed compartments between the osteoclast and the bone surface that are isolated from the extracellular milieu by the sealing zone (Figure 4). The sealing zone is formed by a rearrangement of the cytoskeletal F-actin into actin rings, in response to $\alpha_V\beta_3$ binding to the bone matrix, that create a tight seal between the attached osteoclast and the bone surface[87,88].

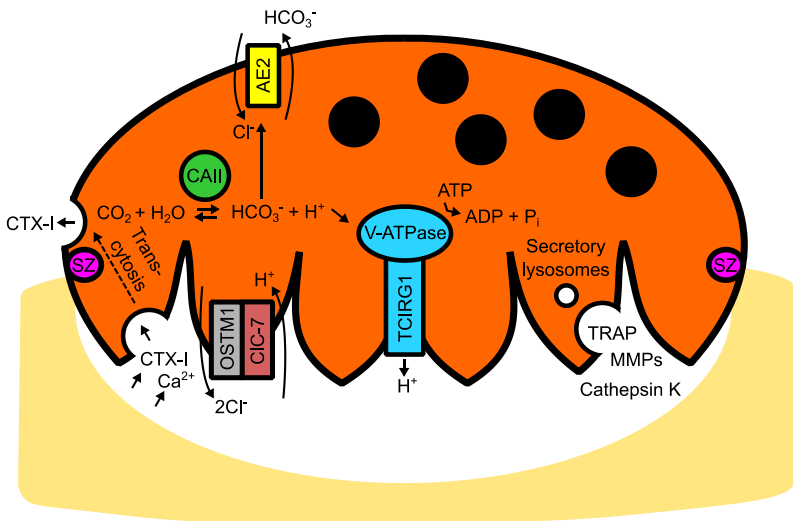

Figure 4. Schematic Representation of a Bone-Resorbing Osteoclast.
Osteoclasts attach to the bone, mediated by integrin $\alpha_V\beta_3$, and form the sealing zone. V-ATPase-containing secretory lysosomes fuse with the basolateral cell membrane to form the ruffled border. The V-ATPase dephosphorylates ATP to secrete protons—derived from the conversion of carbon dioxide and water into carbonic acid, that dissociates into bicarbonate and protons, by CAII—that acidify the resorption lacunae and dissolve the hydroxyapatite. To maintain electroneutrality, the ClC-7/OSTM1 antiporter secretes chloride ions, derived from the AE2 bicarbonate/chloride antiporter, and takes up protons. Secretory lysosomes or secretory vesicles fuse with the ruffled border to secrete TRAP, MMPs, and cathepsin K that hydrolyze the denuded collagen. Collagen and hydroxyapatite degradation products, like CTX-I, are taken up by the osteoclasts and are secreted from the functional secretory domain, located at the apical membrane (portrayed here at the lateral membrane), through transcytosis.

The mineralized bone matrix can now be dissolved through the acidification of the resorption lacunae mediated by the V-ATPase, contained in the membranes of secretory lysosomes fusing with the cell membrane[89–91] at the ruffled border, as well as the ClC-7/OSTM1 $2Cl^-/1H^+$ antiporter which maintains electroneutrality across

the cell membrane[92–95] (Figure 4). The V-ATPase dephosphorylates adenosine triphosphate (ATP), converting it into adenosine diphosphate (ADP), to pump protons into the resorption lacunae. These protons are provided through the conversion of carbon dioxide and water into carbonic acid, catalyzed by CAII[74,75,96], that then dissociates into hydrogen ions and bicarbonate. The remaining bicarbonate is removed from the osteoclast by the passive chloride-bicarbonate antiporter AE2 in the lateral and apical cell membrane[97], which also provides the chloride ions needed for electroneutrality during the acidification process. The acidification of the resorption lacunae and the resulting low pH of approximately 4.5 is sufficient to dissolve the hydroxyapatite-rich calcified bone matrix[89], thereby releasing free Ca^{2+} from the mineral. The increased Ca^{2+} levels can be sensed by the osteoclasts and exposure to high levels of extracellular Ca^{2+} levels results in less resorption and increased osteoclast apoptosis[98].

After dissolution of the inorganic matrix, the organic bone matrix is degraded by proteases secreted from the osteoclasts in secretory lysosomes or secretory vesicles (Figure 4). These proteases are mainly cysteine proteases[67]—predominantly cathepsin K[66]—and the zinc-dependent proteolytic MMPs[67]. Cathepsin K is highly dependent on an acidified resorption lacunae to function[99,100]. It is produced by osteoclasts as an inactive zymogen which is activated by low pH[101], such as that of lysosomes, endolysosomes and the resorption lacunae. Cathepsin K is highly important for bone resorption and cathepsin K deficiency is known to result in the metabolic bone disease pycnodysostosis[102], a rare autosomal recessive skeletal dysplasia that presents with increased bone density in long bones, short stature, open fontanels and cranial sutures, fractures, obtuse mandibular angle, and acroosteolysis of the distal phalanges. While MMPs have been strongly indicated to contribute to bone resorption, their specific role is less clear[103,104]. MMP deficiencies typically result in a broad range of symptoms, due to MMPs being more generally expressed and involved in the remodeling of a large number of different ECMs, depending on which specific MMP is affected[105,106]. Osteoclasts have been shown to express MMP-9,-12, -13, and -14, but no single MMP has been shown to be critical for bone resorption[107]. MMP-9,-13 and -14 have all been shown to affect bone metabolism or bone development in knockout studies in mice[105,106], but these effects do not necessarily need to be osteoclast-mediated. MMPs also play a vital role during bone development in endochondral ossification[14], where chondrocyte-derived MMPs also contribute to cartilage and type II collagen degradation. Hence, developmental bone phenotypes due to MMP deficiencies may be chondrocyte- and cartilage-related, in addition to potential osteoclast-related effects. Osteoclasts also secrete TRAP, particularly the osteoclast-specific isoform 5b[108], that produces reactive oxygen species that can degrade collagens[65]. TRAP is also present in osteoclast transcytotic vesicles, suggesting that they may also aid in degrading endocytosed

materials inside the cell[65]. The enzymatic activity of secreted TRAP 5b and TRAP can be used as an indicator of relative osteoclast numbers[108,109].

As cathepsin K and MMPs degrade the type I collagen, the protease-specific degradation fragment neo-epitope biomarkers C-telopeptide of type I collagen (CTX-I) and carboxy-terminal telopeptide of type I collagen (ICTP) are released[103,104]. CTX-I and ICTP are secreted by the osteoclasts into the extracellular space via transcytosis. Resorption by-products are taken up by the osteoclasts through endocytosis in transcytotic vesicles, where they may be degraded further, that migrate via the microtubules to the functional secretory domain (FSD) on the apical side of the osteoclast at the ECM-opposed membrane, where the contents are finally released through exocytosis[110]. After a number of resorption cycles, the osteoclasts eventually undergo apoptosis.

Bone Remodeling

Bone is a dynamic material and is constantly undergoing remodeling to maintain its strength, repair damaged bone and allow for growth of bones. The remodeling process is a highly coordinated balancing act between bone formation and bone resorption carried out by the bone remodeling unit (BRU), or basic multicellular unit (BMU), consisting of osteoclasts, osteoblasts, osteocytes, BLCs and reversal cells. The following section provides a simplified overview of some of the central concepts of the bone remodeling cycle, the BRU, and its components.

Bone Resorption Phase

The remodeling process starts with recruitment and differentiation of osteoclast precursors. Osteoclastogenesis is highly regulated on a systemic level and on a local level—through coupling between bone cells. On a systemic level, the most important regulator of osteoclastogenesis is parathyroid hormone (PTH). The synthesis and secretion of PTH is regulated by the calcium-sensing receptor (CaSR) in the parathyroid cell membrane; low levels of Ca^{2+} in blood results in low Ca^{2+} occupancy in CaSR which triggers increased PTH synthesis and secretion[111]. The effects of PTH varies and depends on the exposure. For instance, chronically elevated PTH levels such as in patients with hyperparathyroidism are known to result in bone loss, whereas intermittent PTH administration stimulates bone formation[112]. The effects of PTH on osteoclasts are mediated by the PTH receptor PTH1R, expressed in osteoblasts and osteocytes[113,114], modulating RANKL and OPG expression[115–117]. PTH also stimulates the expression of monocyte chemoattractant protein-1 (MCP-1) in osteoblasts, which increases recruitment and fusion of osteoclast precursors[118]. Through these mediators, CaSR and PTH are important regulators of Ca^{2+} homeostasis.

Another important systemic regulator of osteoclastogenesis is estrogen; estrogen has osteoprotective effects by inducing osteoclast apoptosis[119,120] or by inhibiting osteoclastogenesis[120,121], through binding to the osteoclastic estrogen receptor alpha[122,123]. Accordingly, estrogen is an important contributor to osteoporosis in postmenopausal women. Many other hormones also affect osteoclastogenesis and bone resorption, but these are outside the scope of this dissertation. Inflammatory processes may also contribute to osteoclastogenesis in ways that are relevant for this dissertation, but these will be discussed separately in the *ECM Remodeling in Rheumatic Diseases* section.

Although the above mentioned factors contribute to systemic osteoclastogenesis and osteoclast activity regulation, what exactly causes the recruitment of osteoclast precursors to a bone remodeling site is not known. However, apoptosis of osteocytes is thought to cause BLCs to form a bone remodeling compartment and signal to other osteocytes or osteoblasts to change the expression of pro- and anti-osteoclastogenic cytokines[124]. As the osteoclasts attach to the bone, the BLCs retract to give way to the osteoclasts[125]. The osteoclasts then resorb bone, as previously described (Figure 4), releasing bone degradation products and communicating with adjacent cells, e.g. osteocytes and osteoblasts, that all regulate each other through coupling (Figure 3). The bone marrow mesenchymal envelope, formed by mesenchymal cells, forms a canopy over the remodeling site and is an important source of osteoprogenitors[126]. These mesenchymal cells can differentiate into mature osteoblasts[127] which may then contribute to bone formation. The canopy also connects the remodeling sites with bone marrow capillaries[128], particularly above osteoclasts[126], which may serve as an access route for additional osteoclast and osteoblast precursors.

Reversal Phase

The precise mechanism through which the switch from bone resorption to bone formation is regulated is not known. However, many recent studies indicate that reversal cells are a crucial link between bone resorption and bone formation. The reversal cells colonize the reversal surface—the recently eroded bone—immediately after resorption, prior to osteoblasts, and are osteoblast-lineage cells that have an important role in rendering the eroded surfaces osteogenic[129]. While reversal cells tend to be placed temporally between osteoclasts and osteoblasts in the BRU concept, this is actually a too simplistic view. Reversal and resorption can in fact be a mixed state where reversal cells and osteoclasts alternate in their activity on reversal surfaces—although after bone formation has commenced, osteoclasts are no longer present[130].

The reversal cells immediately adjacent to osteoclasts have direct cell-cell contact with the osteoclasts and express the osteoblastic marker Runt-related transcription factor 2 (RUNX2) and have TRAP-positive intracellular vesicles, without

expressing any TRAP themselves[129], suggesting osteoclast-reversal cell communication. The bone matrix and the reversal surface is known to contain osteoclast products, including TRAP[131], which may stimulate osteoblastogenesis[132]. There has even been some evidence that reversal cells may progressively differentiate into bone-forming osteoblasts[129]. Bone surfaces under reversal cells have also been shown to contain the type I collagen ¾-fragment—whereas bone surfaces under osteoblasts do not—which is taken up by reversal cells; the reversal cells are MMP-13 positive and express the endocytic collagen receptor Endo180, indicating that reversal cells might secrete proteases to degrade and endocytose collagen fragments from eroded bone surfaces prior to bone formation[129] to render the reversal surface osteogenic. Furthermore, the reversal surface has a markedly increased cell density compared to the BLC density on quiescent bone surfaces, and bone formation will only be initiated on the reversal surface above a certain threshold of osteoblasts/osteoprogenitors[126,130]; bone remodeling will fail if this cell density enrichment is lacking[133].

Assuming that reversal does not fail, the bone formation phase will follow. Osteoblasts form bone as previously described on the reversal surfaces, after which the osteoblasts either undergo apoptosis or differentiate into BLCs or osteocytes.

Coupling

Another key mechanism for transitioning between bone resorption and bone formation, as well as in regulating the homeostasis between the two processes, is coupling. These coupling factors can be divided into four main categories: resorption-mediated ECM-derived signals, osteoclast-secreted factors, membrane-bound osteoclast-derived factors, and topographical changes in the bone surface mediated by the osteoclasts[134]. Additionally, coupling factors are also derived from osteoblasts and osteocytes. A plethora of coupling factors regulating osteoclastogenesis, osteoblastogenesis, bone resorption, and bone formation have been described in the scientific literature in recent years, and have been extensively reviewed elsewhere[43,135,136]. A selection of important coupling factors and their effects are listed in Table 1 and are illustrated in Figure 3, with a particular focus on paracrine signaling and coupling factors between osteoclasts, osteoblasts, and osteocytes.

One coupling factor, extracellular Ca^{2+} levels, is of particular importance for this dissertation. Similarly to their systemic regulatory role, extracellular Ca^{2+} levels are also an important regulator of resorption locally. Elevated extracellular Ca^{2+} levels induce osteoclast apoptosis[98]. Hence, osteoclasts actively resorbing the hydroxyapatite in the calcified bone matrix results in Ca^{2+} release, which in turn results in a negative feedback loop that reduces both osteoclast numbers and bone resorption.

Table 1. Overview of Coupling Factors.

Abbreviations: BMP-6, bone morphogenetic protein 6; CT-1, cardiotrophin-1; CTHRC1, collagen triple helix repeat containing 1; EFNB2, ephrin B2; EphB4, ephrin type-B receptor 4; IFNβ, interferon β; NRP1, neuropilin-1; PDGF-BB, platelet-derived growth factor BB; Ror2, receptor tyrosine kinase-like orphan receptor 2; S1P, sphingosine-1-phosphate; SEMA3A, semaphorin 3A; SEMA4D, semaphorin 4D; SOST, sclerostin.

Coupling factor	Source	Effects
Extracellular Ca^{2+}	Bone resorption	Osteoclast apoptosis[98]
SOST	Osteocytes	Decreases osteoblastogenesis[43] Decreases osteoblast activity and bone formation[137] Decreases osteocyte OPG expression[138] Increases osteocyte RANKL expression[138] Increases osteoclast CAII, cathepsin K, and TRAP expression[139]
IFNβ	Osteoclasts	Decreases osteoclastogenesis[140]
BMP-6	Osteoclasts	Increases bone formation[141,142] Decreases bone resorption[141,142] Osteoprogenitor recruitment[142,143]
CTHRC1	Osteoclasts	Increases osteoblastogenesis[144]
Secreted S1P	Osteoclasts	Increases osteoblast RANKL expression[145] Increases osteoblast survival[145] Increases osteoblast chemotaxis[145]
Intracellular S1P	Osteoclasts	Decreases osteoclastogenesis[145]
SEMA4D	Osteoclasts	Increases bone formation[146] Increases osteoblast mobility[146]
CT-1	Osteoclasts	Important for bone resorption and bone formation[147]
PDGF-BB	Osteoclasts	Increases migration and osteogenic differentiation of MSCs[148]
EFNB2 EphB4	Osteoclasts Osteoblasts	Decreases osteoclastogenesis[149] Increases bone formation[149]
Wnt10B	Osteoclasts	Increases osteoblastogenesis[150]
Wnt5A Ror2	Osteoblasts Osteoclasts	Increases osteoblast RANK expression[151,152]
Wnt16	Osteoblasts	Decreases osteoclastogenesis[153] Interfering with RANK signaling[153] Increases OPG expression in osteoblasts[153]
SEMA3A NRP1	Osteoblasts Osteoclasts	Decreases RANKL-induced osteoclastogenesis[154] Increases osteoblastogenesis[154]

Remodeling Failure

When bone remodeling fails, through failed bone resorption, failed bone formation, failed reversal, and/or uncoupling, this results in metabolic bone diseases. These can be categorized into two main groups: osteoporosis and osteopetrosis.

Osteoporosis is characterized by the World Health Organization (WHO) as a "progressive systemic skeletal disease characterized by low bone mass and microarchitectural deterioration of bone tissue, with a consequent increase in bone fragility and susceptibility to fracture"[155]. Osteoporosis is due to an imbalance between bone resorption and bone formation, where bone resorption has gained the upper hand, and is a common condition amongst the elderly. Arrested reversal surfaces, reversal surfaces where bone formation has failed to occur, has been observed in postmenopausal osteoporotic women[133]. On these surfaces, far away from ongoing resorption or bone formation, the cell density is lower than that on

active reversal surfaces and there is deficient canopy coverage[133]. Interestingly, bisphosphonate treatment—which is toxic to osteoclasts—inhibits both bone resorption as well as bone formation, and has been shown to reduce canopy coverage above resorbing osteoclasts[156]. In contrast, the antiresorptive odanacatib, a cathepsin K inhibitor, does not affect bone formation negatively or reduce canopy coverage[156].

Osteoporosis can be treated quite effectively with a range of antiresorptives and bone anabolic agents—including bisphosphonates, hormone replacement therapy (HRT), estrogen receptor modulators, recombinant PTH, and RANKL-neutralizing antibodies—but bisphosphonates are typically first line treatments due to their low cost and broad spectrum of anti-fracture efficacy[157]. Bisphosphonates are a particularly important class of antiresorptive drugs, based on chemically stable derivatives of inorganic pyrophosphate (PPi) containing a central non-hydrolyzable carbon[158]. Both bisphosphonates and PPi have very high affinity for hydroxyapatite and inhibit further calcification[159] as well as the dissolution of hydroxyapatite upon binding[160]. Due to the similarity of early bisphosphonates and PPi, it has been speculated that their metabolization into toxic non-hydrolyzable ATP analogs insides cells[161] may be an additional mode of action. Modern bisphosphonates, however, are not metabolized into ATP; rather, they contain nitrogen groups that enhance their potency by inhibiting farnesyl pyrophosphate synthase, inhibiting the mevalonate pathway, preventing prenylation of guanosine triphosphate (GTP)-binding proteins—important for cytoskeleton rearrangement, ruffled border formation, osteoclastogenesis, and survival[162]—and ultimately lead to osteoclast apoptosis[163].

Using the therapeutic approaches described above, osteoporosis can be managed relatively well today. However, osteopetrosis is a much more severe disease—albeit much rarer—with very limited treatment options and limited treatment success.

Osteopetrosis

Osteopetrosis is a heterogeneous group of rare hereditary diseases characterized by increased bone density. They are typically caused by mutations in genes related to osteoclastogenesis or osteoclast function and can range in severity from mild to lethal[164]. There are many genetic bases underlying osteopetrosis, but they can be categorized into two main groups by their inheritance pattern and severity: infantile malignant osteopetrosis (IMO)—also known as autosomal recessive osteopetrosis (ARO)—and autosomal dominant osteopetrosis (ADO), which is typically less severe. In addition to these two main groups, several syndromic forms of osteopetrosis have been reported in recent years[164]. This dissertation will focus on the most common forms of human IMO.

Infantile Malignant Osteopetrosis

IMO, is a very rare, congenital, hereditary disease, with an average incidence of around 1:300 000 births[165]. IMO can be caused by mutations in several different genes related to osteoclast function or osteoclastogenesis, as outlined in Table 2, but mutations in *TCIRG1* (51–53%) or *CLCN7* (17.5%) are the most common[164,166]—*CLCN7* mutations are also the most common cause of ADO (80%)[164]. From a clinical perspective, IMO is characterized by non-functional or absent osteoclasts, increased bone density and fractures, and typically leads to bone marrow failure, hepatosplenomegaly and eventually death, unless treated with a HSC transplant (HSCT)[167–169]—although not all forms are treatable. The increased fracture frequency is thought in part to be due to increased bone density but also due to an altered bone quality, such as an increased presence of immature woven bone and a failure to resorb calcified cartilage and replace it with bone during bone development[170]. Other IMO features present at diagnosis can include moderate to severe vision impairment, macrocephaly, hydrocephalus, fractures, short stature, need for transfusional support, developmental delay, hypocalcaemia and low serum immunoglobulin levels, depending on the genes and the mutations involved[171]. IMO patients can also suffer from a range of neurological symptoms dependent on the mutations involved, including motor delays, cognitive delays, language problems, behavioral disorders, epilepsy, and various forms of encelopathy as observed during follow-up after treatment[171], indicating that many of these symptoms are irreversible.

Table 2. Overview of Genes Involved in Human IMO.
This table is an overview of genes with known IMO-causing mutations arranged in order of frequency, as reviewed by Sobacchi et al.[166] and Palagano et al.[164]

Gene	Protein	Phenotype	Percent of IMO cases
TCIRG1	TCIRG1 (a3) & TIRC7	Osteoclast-rich/non-functional	50.0%
CLCN7	ClC-7	Osteoclast-rich/non-functional	17.5%
OSTM1	OSTM1	Osteoclast-rich/non-functional	5.0%
TNFRSF11A	RANK	Osteoclast-poor	5.0%
SNX10	SNX10	Osteoclast-rich/non-functional	4.5%
TNFRSF11	RANKL	Osteoclast-poor	2.0%
CA2	CAII	Osteoclast-rich/non-functional	$<1:10^6$
PLEKHM1	PLEKHM1	Osteoclast-rich/non-functional	2 patients reported

The loss of function of the genes described above results in IMO through several different mechanisms, but one key mechanism is the presence of non-functional osteoclasts, i.e. an osteoclast-rich phenotype, or the absence of osteoclasts, i.e. an osteoclast-poor phenotype. *TCIRG1*, *CLCN7*, *OSTM1*, *SNX10*, *CA2*, and *PLEKHM1* all encode proteins involved in the acidification of the resorption lacunae and/or in vesicular transport[164,166]. Mutations in these genes result in osteoclast-rich osteopetrosis with present but non-functional osteoclasts, whereas

TNFRSF11A and *TNFRSF11* mutations interfere with RANK/RANKL signaling and result in osteoclast-poor osteopetrosis[164,166].

TCIRG1 encodes the TCIRG1 protein, also known as the a3 isoform of the V-ATPase a subunit, as well as the T-cell immune response cDNA 7 (TIRC7) through alternative splicing[172]. TCIRG1 and TIRC7 have highly similar exon-intron organization, but have different transcription start sites[172]. TCIRG1 is essential for both normal function of the osteoclast V-ATPase as well as for secretory lysosome trafficking to the ruffled border[86] and ruffled border formation[164]. The a3 subunit of the V-ATPase is preferentially expressed in osteoclasts[173], although it has also been found in other tissues[90,174], and most other V-ATPase complexes utilize other a subunit isoforms. IMO is recapitulated in the *oc/oc* mouse strain, a naturally occurring strain with mutations in *tcirg1* resulting in the murine version of IMO[175] that presents with a highly similar phenotype. Without treatment, TCIRG1-deficient patients typically die before the age of 10[166], often due to bone marrow failure or infection[176]. However, recently described intronic *TCIRG1* mutations have been reported to cause less severe cases of IMO[177,178]. TIRC7, the alternative transcript of TCIRG1, is known to be important for T cell activation and immune response regulation; allograft rejection and inflammatory or autoimmune diseases have been shown to be associated with TIRC7 levels or TIRC7 expression[179,180]. TCIRG1-deficient IMO patients may lack TIRC7[181], but its relevance for IMO remains unclear.

CLCN7 encodes the chloride channel ClC-7 which, as previously mentioned, is an essential part of the ClC-7/OSTM1 antiporter that is crucial for maintaining electroneutrality in osteoclasts during acidification. ClC-7 may also be involved in lysosomal trafficking[182], but this requires further investigation. In addition to causing osteopetrosis[68], ClC-7 deficiency can result in a range of neurological symptoms, including hydrocephalus, neuronal lysosomal storage diseases, neurodegeneration, and other neurological symptoms[92,166,171]. Such neurological symptoms are less common in TCIRG1-deficient IMO[166,171], as several of the neurological symptoms resulting from ClC-7 deficiency are due to primary effects in neurons rather than due to the bone phenotype.

Osteopetrosis-associated transmembrane protein 1 (OSTM1) is very important for resorption, as its highly glycosylated N-terminus stabilizes ClC-7, protects it from lysosomal degradation, and contributes critically to the $2Cl^-/1H^+$ exchange[69,70]. Mutations in *OSTM1* often result in truncation, and secreted truncated OSTM1 has been shown to inhibit osteoclastogenesis *in vitro*, providing an additional potential pathogenic mechanism[183]. OSTM1 binding partners other than ClC-7 have been identified in the cytosol, suggesting a role for OSTM1 in intracellular trafficking and as an adaptor molecule for cytosolic scaffolding multi-protein complexes[184].

Patients with OSTM1-deficient IMO suffer from an extremely severe phenotype with rapidly progressing primary neurodegeneration[185,186].

Mutations in the genes encoding RANK[187,188] and RANKL[189,190]—tumor necrosis factor receptor superfamily member 11A (*TNFRSF11A)* and tumor necrosis factor receptor superfamily member 11 (*TNFRSF11)*—both directly interfere with RANK/RANKL signaling, resulting in an osteoclast-poor osteopetrosis. It is however worth noting that the RANK-deficient effects on osteoclastogenesis are mediated by cells of hematopoietic lineages, whereas RANKL-deficient effects are mediated by mesenchymal lineages—particularly the osteoblastic lineages. Although the net effect is the same, in terms of osteoclastogenesis, it makes a significant difference for therapeutic opportunities for the two genotypes.

Sorting nexin 10 (SNX10) is involved in protein sorting and membrane trafficking, mediated by protein-protein and protein-lipid interactions, and interacts with the V-ATPase to regulate its subcellular trafficking[191]. SNX10-deficient IMO results in a defective ruffled border and inability to resorb[192]. Additionally, SNX10 has also been suggested to play a role for MMP-9 trafficking and secretion[193].

Patients with CAII-deficient IMO present with osteopetrosis, renal tubular acidosis (RTA) and cerebral calcifications[194–196]. CAII-deficient IMO results in an osteoclast-rich ostepetrosis[197] with a relatively mild bone phenotype and severity for being classified as IMO[194,195], and hence the RTA and possible neurodegeneration are of greater concern than the osteopetrotic phenotype in these patients.

Pleckstrin homology domain-containing family M member 1 (PLEKHM1) is a cytosolic protein that has been implicated in endosomal trafficking through interactions with small guanosine triphosphatases (GTPases), including Rab7 and Arl8[198,199]. PLEKHM1 also participates in the fusion of autophagosomes and lysosomes[200], which is of crucial importance for protein aggregate clearance and bone resorption. *PLEKHM1* mutations may result in impaired lysosomal trafficking and secretion, ruffled border, acidification, and bone resorption[201]. Osteopetrotic mutations in *PLEKHM1* have only been reported in two patients to date[202,203].

In addition to the direct effects of having non-functional or absent osteoclasts on the bone phenotype as described above, the osteoclast-rich and osteoclast-poor phenotypes also impact the bone phenotype differently through coupling mechanisms. Although resorption levels decrease to similar levels in adult mice transplanted with HSCs from RANK-deficient mice or *oc/oc* mice, the resulting bone formation levels are not equal; adult mice with an osteoclast-rich osteopetrotic phenotype have increased bone formation parameters, such as mineral apposition rate (MAR) and bone formation rate per bone surface (BFR/BS), compared to controls while those with osteoclast-poor osteopetrosis do not[204]. This illustrates the uncoupling phenomenon that occurs when osteoclasts are present but resorption is

dysfunctional. In an osteoclast-rich osteopetrotic phenotype, osteoclasts can exert a bone anabolic role that does not occur in osteoclast-poor osteopetrosis. Hence, aberrant bone mass and bone quality in osteopetrosis is not just a matter of absent bone resorption—it may also be a result of abnormal bone formation through uncoupling.

Current Treatment

As previously stated, IMO is the most severe form of osteopetrosis and treatment as soon as possible after diagnosis is of the essence. The only treatment available today is an allogeneic HSCT. Optimal engraftment and treatment results of an HSCT are obtained when using HSCs from a human leukocyte antigen (HLA)-identical sibling. The overall survival after an HSCT is 60–65%[166,205,206] and below 50% for cases who do not have an HLA-identical sibling donor, which is approximately 70% of cases[207]. Attempts at bypassing the need for an HLA-identical donor using unrelated umbilical cord blood have so far been unsuccessful[208]. However, different strategies for transplanting HLA-haploidentical hematopoietic progenitor cells has shown some promise[207,209,210].

It should however be noted that an HSCT is not suitable for all IMO patients. For instance, patients with RANKL mutations will not be cured by an HSCT as the main sources of RANKL for osteoclastogenesis—osteoblasts and osteocytes—are of mesenchymal origin, and HSCT has been shown to not be beneficial in RANKL-deficient IMO[189]. In contrast, RANK-deficient IMO is curable by HSCT[211,212]. Furthermore, HSCT cannot prevent or treat the neurodegenerative disease that is present in a subgroup of IMO patients[213]. Patients with *OSTM1* mutations, as well as some with *CLCN7* mutations, suffer from severe neurodegenerative disease and will not survive, regardless of treatment[164]. Currently, there are no approved curative treatments available for RANKL-deficient or neurodegenerative IMO[164], although pharmacological administration of RANKL may hold potential for RANKL-deficiency[214].

Gene Therapy

Gene therapy is based on the concept of inserting genetic code into a cell with a genetic defect to restore normal functionality or, in the case of gene editing, to insert, correct or disrupt a gene. Depending on the disease and the target population of cells, numerous different approaches can be used. For the purpose of treating osteopetrosis, HSC-targeted gene therapy is ideal. HSC-targeted gene therapy with host-integrating transgenes allows for sustained transduction of self-renewing HSCs

and their daughter cells, and can therefore be used to provide long-term or permanent rescue of a phenotype derived from genetic defects in HSC-derived target cells[215]—such as osteoclasts.

Gene Therapy Targeting Hematopoietic Stem Cells

Early clinical trials of HSC-targeting gene therapy focused on the use of gammaretroviral vectors. These trials had some success in for instance X-linked severe combined immunodeficiency (X-SCID)[216,217], adenosine deaminase severe combined immunodeficiency (ADA-SCID)[218], and chronic granulomatous disease (CGD)[219]. However, gammaretroviral integration tends to be near transcription start sites[220], increasing the risk of insertional mutagenesis that may lead to increased expression of oncogenes or proto-oncogenes. Accordingly, several X-SCID patients developed leukemia due to insertional mutagenesis[221,222] as a result of their gene therapy. Lentiviral vectors, retroviral vectors that are typically based on immunodeficiency viruses, are less likely to cause mutagenesis by insertion in close proximity to proto-oncogenes, resulting in an improved safety profile[223,224]. Lentiviral vectors based on human immunodeficiency virus (HIV)-1 have been shown to be able to transduce HSCs in a stable and efficient manner[225–227]. Due to the ability of lentiviral vectors to transduce and integrate quiescent HSCs by nuclear import, unlike gammaretroviral vectors that can only integrate in dividing cells as they require the breakdown of the nuclear membrane to enter the nucleus, lentiviral vectors have become the vector system of choice for HSC-targeted gene therapy[215,228].

To make gammaretroviral vectors safer, self-inactivating (SIN) vectors were developed to abolish the endogenous enhancer and promoter activity of the vectors[229], allowing for the use of added internal promoters to drive the transgene expression instead. Subsequent clinical trials of SIN gammaretroviral vectors in X-SCID patients have maintained the treatment efficacy while having less clustering of insertion sites in lymphoid proto-oncogenes, although the long-term effects on leukemogenesis remain unknown[230]. Lentiviral SIN vectors have been developed by removing important replication and virulence genes from the viral genome[231,232], resulting in the production of replication-incompetent viral particles that are produced using multiple different plasmids. The use of multiple plasmids reduces the risk of recombination in the transfected virus production cell line (typically 293T cells), thereby reducing the risk of generating replication-competent virions[232]. As a further safety precaution, the oncogenic potential of retroviral vectors can be assessed using *in vitro* immortalization (IVIM) assays. IVIM studies have shown that SIN lentiviral vectors with physiological promoters, rather than viral promoters, have a substantially reduced risk of insertional transformation compared to gammaretroviral vectors or lentiviral vectors without these safety features[233–235].

Clinical trials of HSC-targeting lentiviral vectors have been ongoing since the mid 2000's, and a large number of lentiviral gene therapy treatments are currently in development. Several promising clinical trials of various sizes have been described in the literature, treating for instance sickle cell disease[236], metachromatic leukodystrophy[237], Wiskott-Aldrich syndrome[238,239], transfusion-dependent β-thalassemia[240], and cerebral adrenoleukodystrophy[241].

IMO Gene Therapy Development

The main advantage of gene therapy for TCIRG1-deficient IMO over allogeneic HSCT is the possibility of utilizing HSCs obtained from the IMO patients themselves to expedite treatment. IMO HSCs can potentially be treated *ex vivo* and subsequently transplanted back into the patient as an autologous graft (Figure 5), thereby minimizing any immune response to the graft and in turn circumventing the need for a suitable donor—potentially allowing for earlier treatment.

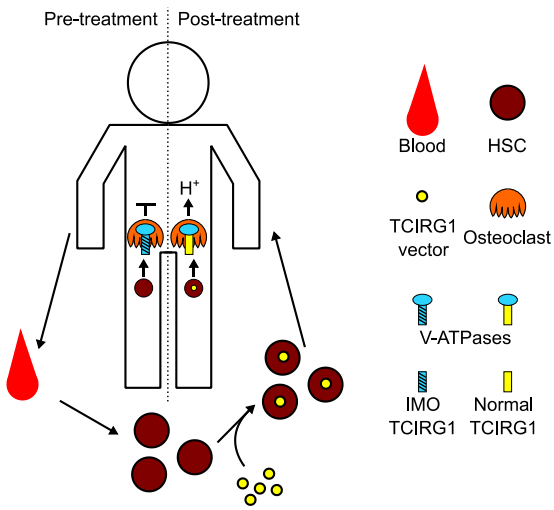

Figure 5. TCIRG1-Deficient IMO Gene Therapy Concept.
A TCIRG1-deficient IMO patient is unable to acidify resorption lacunae and resorb bone due to defects in the TCIRG1 subunit of the V-ATPase. Blood is obtained, possibly including a stem cell mobilization regimen, and HSCs are isolated. This procedure can be repeated multiple times to achieve a suitable cell population. Isolated HSCs are then treated with a TCIRG1-expressing vector *ex vivo* and the corrected HSCs are transplanted back as an autologous graft, without the need for immunosuppression due to the autologous and *ex vivo* nature of the treatment. Functional osteoclasts, capable of acidification, will then form spontaneously and normalize the bone phenotype over time.

In previous studies, the phenotype of *oc/oc* mice has been normalized by treating *oc/oc* HSCs *ex vivo* with a gammaretroviral vector expressing murine *tcirg1* complementary DNA (cDNA), followed by neonatal transplantation[242]. Due to the relatively high risk of insertional mutagenesis and aberrant gene expression of

adjacent genes after integration of the transgenes, the gammaretroviral vectors and the strong constitutively active spleen focus-forming virus (SFFV) promoter used are not optimal for clinical use. More recent studies have therefore focused on SIN lentiviral vectors.

Using a proof-of-concept SIN lentiviral vector, containing human *TCIRG1* cDNA, the SFFV promoter, and a green fluorescent protein (GFP) transgene marker, *in vitro* transduction of human $CD34^+$ cells obtained from peripheral blood—corresponding to hematopoietic stem and progenitor cells (HSPCs)—of IMO patients has been demonstrated to restore resorptive function in osteoclasts generated from these HSPCs[243]. However, as this vector system contained both the SFFV promoter and GFP, it remained unsuitable for clinical application. Interestingly, this study also observed that TCIRG1 protein was only present in mature IMO osteoclasts and not in HSPCs, despite the presence of TCIRG1 mRNA at all times[243]. This indicates that vector-derived TCIRG1 may be subjected to some form of inherent regulation within osteoclasts and osteoclast precursors, but these preliminary observations require further investigation.

These early proof-of-concept studies have assessed the potential for IMO gene therapy *in vivo* by treating *oc/oc* HSCs with gene therapy and transplanting them into *oc/oc* mice to assess phenotype rescue in mice, and *in vitro* by treating human HSCs and assess the efficacy in osteoclast cell cultures. The ideal *in vivo* model for IMO gene therapy development would be one that allowed for *ex vivo* correction of human HSCs followed by transplantation into *oc/oc* mice to assess phenotype rescue. However, human osteoclasts do not form in mice. HSC differentiation, expansion and maintenance are highly regulated by transcription factors and cytokines. In most cases, human and murine cytokine structure and function are conserved, but there are exceptions. Murine M-CSF is unable to activate human CSF1R[244]. As the M-CSF acting upon osteoclasts and osteoclast precursors is typically derived from cells of osteoblastic lineage[43], which in turn are derived from MSCs, humanized mouse models generated by a human HSCT only express murine M-CSF—thereby preventing human osteoclastogenesis in mice.

Humanized mouse models, usually generated by a human HSCT into immunodeficient mice—such as NOD-scid IL2rγ^{null} (NSG) mice—that will accept a xenograft without immune rejection, have been a valuable tool for investigating human hematopoiesis[245]. However, they have been described to only have partially functional humanized immune systems[246,247]. Previous studies have described humanized mice with a human M-CSF (hM-CSF) knock-in—that in theory should be able to support human osteoclastogenesis—resulting in more efficient differentiation and enhanced frequencies of human monocytes and macrophages in the bone marrow, spleen, peripheral blood, lungs, liver, and peritoneal cavity[248], which is highly relevant for potential human osteoclastogenesis *in vivo*. While these

findings clearly demonstrate the feasibility of overexpressing hM-CSF in humanized mice to improve reconstitution of relevant monocytic lineages, this study did not report any osteoclast-related findings. A lack of suitable mouse models for generating human osteoclasts *in vivo* still remains at present.

ECM Remodeling in Rheumatic Diseases

The role of osteoclasts in bone remodeling, in health and disease, is well established. Although osteoclasts have been strongly implied to have a role in degrading cartilage, particularly in arthritis, direct osteoclastic cartilage resorption is not universally accepted. Some researchers attribute cartilage resorption to cells termed chondroclasts. Osteoclast and chondroclasts are very similar with regard to both the expression of osteoclast markers as well as their regulation and function, and the general consensus is that they are one and the same or that chondroclasts are slightly modified osteoclasts that differ mainly in their location[249–251]. Some however do consider them different and postulate that they might have different modes of action; osteoclasts and putative chondroclasts have for instance been shown to have a difference in extracellular and intracellular distribution of TRAP[252]. Nonetheless, there is no marker to date that is capable of distinguishing between chondroclasts and osteoclasts[251], and from a practical point of view they are one and the same. However, the extent of the putative osteoclastic cartilage resorption and the processes involved are not well understood. This section will provide an overview of some of the evidence indicating a direct role of osteoclastic resorption in cartilage remodeling—and bone remodeling—in rheumatic diseases, focused on two forms of arthritis. Important non-osteoclastic mechanisms of cartilage degradation in rheumatic diseases will also be covered in this section.

Rheumatoid Arthritis

Rheumatoid arthritis (RA) is an autoimmune-mediated chronic joint disease—associated with infiltration of inflammatory cells, synovial lining hyperplasia and inflammation, and bone and cartilage destruction—that manifests as pain and loss of junction function, physical impairment and fatigue[253]. One of the hallmarks of RA is focal bone loss, and patients with RA have dramatically increased osteoclastogenesis and osteoclast activity[254] that results in bone erosion and an increased risk of osteoporosis and fractures[255]. The contribution of osteoclasts to RA bone loss is clearly demonstrated by the protective effects of bisphosphonates and the RANKL-neutralizing antibody denosumab[256], and by elevated serum RANKL:OPG ratios correlating with radiological disease progression[257]. The role of osteoclasts in RA bone loss is relatively well understood, and several mechanisms

involved in the pathological osteoclast activity have been elucidated (Figure 6). A major driving force behind the increased osteoclastogenesis and osteoclast activity in RA is inflammation; immune cells, pro-inflammatory cytokines and autoantibodies drive the inflammation in RA, which in turn drives the increased osteoclastogenesis and the increased bone erosion.

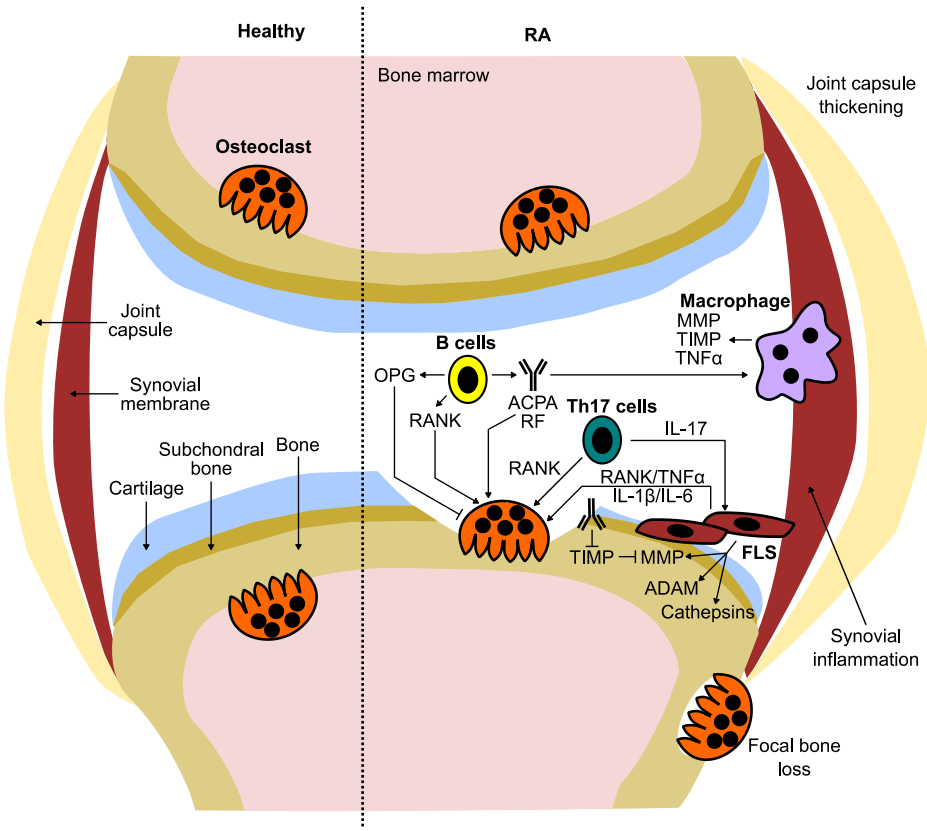

Figure 6. ECM Remodeling and Cellular Involvement in Rheumatoid Arthritis.
Overview of selected ECM pathological changes, remodeling processes, and cellular contributors to RA pathology.

During synovitis, T cells infiltrate the synovium and secrete RANKL, stimulating osteoclastogenesis[258], and the Th17 T cell subset both secretes RANKL as well as induces RANKL expression in fibroblast-like synoviocytes (FLS) via interleukin (IL)-17[259]. Activated B cells also infiltrate the synovium in RA, where they may be a source of RANKL[260]. Furthermore, activated B cells from RA patients have been demonstrated to stimulate osteoclastogenesis to a greater degree than those from healthy donors *in vitro*[261]. However, activated B cells are also a major source of OPG[262], hence their contribution to RA osteoclastogenesis is unclear. Macrophages

and monocytes also infiltrate the synovium and secrete MMPs that may contribute directly to the ECM degradation[263], but macrophages are also known to secrete tissue inhibitors of metalloproteinases (TIMPs)[264] that can neutralize the activity of MMPs. Although both MMPs and TIMPs are upregulated in RA patients, the MMP:TIMP balance becomes skewed in favor of the MMPs[265]. This may in part be due to many patients developing autoantibodies against TIMPs and thereby disturbing the MMP:TIMP balance that would normally regulate the activity of MMPs[266].

The principal function of normal FLS is to secrete synovial fluid and ECM components[267]. However, in RA the FLS transform into a cancer-like state, proliferate strongly, and escape apoptosis[267]. RA FLS become highly migratory; they invade and degrade the articular cartilage, mediated by invadosomes with upregulated matrix adhesion molecules[268] and proteases, including MMPs, a disintegrin and metalloproteinase (ADAM), and cathepsins[269]. The FLS also upregulate toll-like receptors (TLRs), sensitizing them to inflammatory signals and resulting in the release of pro-inflammatory cytokines like TNFα, IL-1β, and IL-6 upon receptor activation, further stimulating the immune response in the inflamed synovium[267]. TNFα drives osteoclastogenesis and osteoclast activity through multiple mechanisms; TNFα enhances activation of NFκB, activator protein (AP)-1, and NFATc1[270], induces RANKL expression in mesenchymal cells[271], and increases the number of circulating osteoclast precursors by upregulating CSF1R[272]. IL-6 stimulates RANKL expression in osteoblasts[273] and is correlated with radiographic joint destruction in RA[274]. IL-1β also stimulates RANKL expression and ostoeclastogenesis[273]. Antagonists against TNFα[275], IL-6[276], and IL-1β[277] have all been effective as disease-modifying antirheumatic drugs (DMARDs), particularly the TNFα inhibitors, with regard to reducing RA progression and bone erosion.

The autoantibodies rheumatoid factor (RF) and anti-citrullinated protein antibodies (ACPAs) are both associated with a more severe RA phenotype[278,279]. Immune complexes derived from RF binding the constant region of immunoglobulin G (IgG) or ACPA binding citrullinated proteins, which are common in RA, can increase TNFα expression in macrophages[280,281]. Furthermore, ACPA can bind directly to citrullinated proteins on osteoclast precursors—osteoclasts even secrete citrullinating enzymes—resulting in increased osteoclastogenesis and osteoclast activity[282]. Similarly, the Fc gamma receptor (FcγR) expressed on osteoclasts[283] can bind IgG-containing immune complexes; FcγRIV is upregulated during osteoclast maturation in mice and the cross-linking of FcγRIV by autoantibody immune complexes is critical for osteoclast development and bone erosion in inflamed joints[284].

Even if the bone erosions can be well managed by currently available treatments, RA patients appear to lack sufficient bone formation during the period of effective treatment; only few patients have bone regeneration during treatment, and typically those that do are patients that have low disease activity[285]. This lack of bone formation may be due to a lack of mature osteoblasts at sites of bone erosion[286], potentially not reaching the critical osteoblast/reversal cell density threshold required for initiating bone formation[130]. This in turn may be a result of the dysregulated osteoclast activity in RA, mediated by the inflammation and the invading immune cells, that potentially results in uncoupling of bone resorption and formation.

Osteoarthritis

Osteoarthritis Pathology

Osteoarthritis (OA) is a degenerative joint disease characterized by joint pain and a progressive deterioration of joint tissues, including cartilage erosions, alterations to the synovial tissue, and subchondral bone remodeling[287]—as well as new bone formation in the form of osteophytes[288]. OA is one of the leading causes of global disability[289] and the most common form of arthritis in adults worldwide to result in disability[290]. While the etiology of OA is poorly understood, an increased turnover of joint ECMs—including the subchondral bone and, in particular, the articular cartilage[291]—are central to the disease process. What has become very clear in recent years, is that there are many different phenotypes of OA and that many factors in the joint other than the cartilage, including subchondral bone, synovium, and inflammation, are important for OA development[292] (Figure 7). Hence, OA is unlikely to be treatable with a universal approach or single therapy, and patients are currently limited to symptomatic treatment. Although several promising drug candidates are currently in clinical trials, there are no disease-modifying OA drugs (DMOADs) available to date[293].

Little is known about the initiating events of OA, but mechanical factors[294,295], genetics[296], epigenetics[297,298] and loss of the normal chondrocyte phenotype[299] have all been implicated. Inflammation also contributes to ECM degradation in OA, although the relative contribution of inflammation compared to other factors remains a matter of debate and may differ greatly between patients. Given that many potential inflammatory mediators in OA are similar to those in RA, with the exception of autoimmunity, inflammatory mediators will not be covered in this section.

The chondrocyte is of particular interest due to its ability to maintain the cartilage structure and composition by acting as a mechanosensor that can respond to changing ECM conditions to modify both synthesis and degradation of cartilage

ECM[300]. These ECM-chondrocyte interactions are essential for regulating both embryonic bone formation and bone formation during adult bone remodeling[301]. However, pro-inflammatory cytokines are known to upregulate MMPs, ADAMTS-4, and ADAMTS-5 in chondrocytes, which leads to increased turnover of aggrecans and reduces proteoglycan synthesis[302]. This increased proteolytic activity is a key component of both OA initiation and perpetuation of cartilage degradation[303].

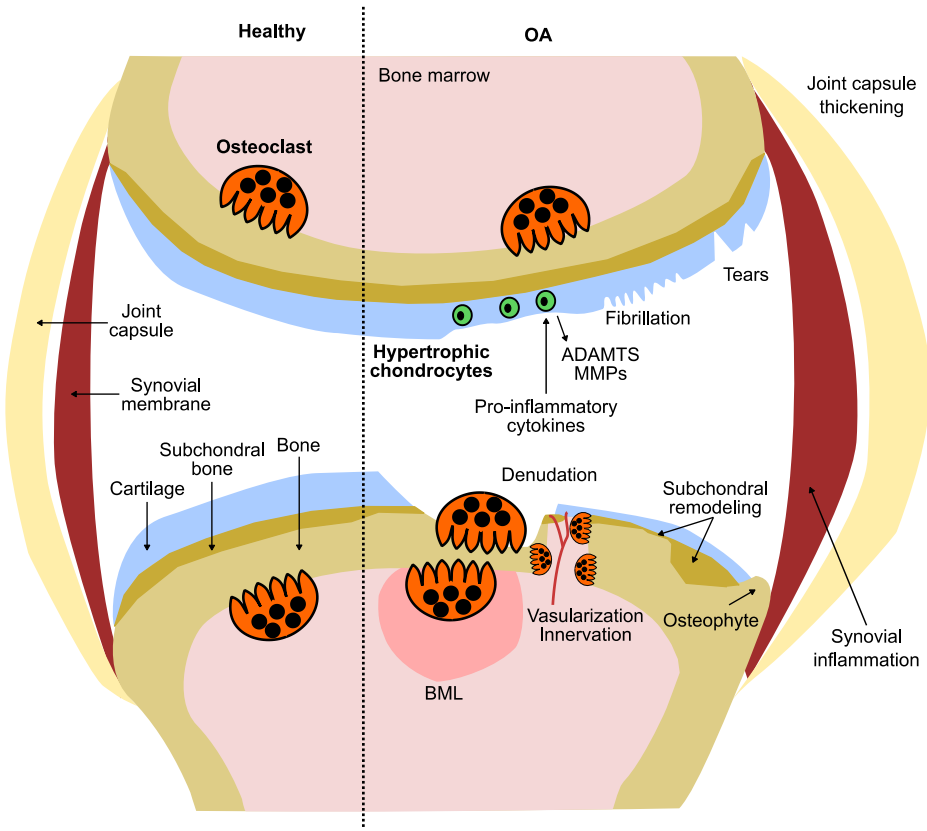

Figure 7. ECM Remodeling and Cellular Involvement in Osteoarthritis.
Overview of selected ECM pathological changes, remodeling processes, and cellular contributors to OA pathology.

An altered chondrocyte gene expression profile has also been proposed as a potential OA-initiating mechanism. For instance, the expression of transcription factor SOX-9 is high in normal articular cartilage, but is lost in OA cartilage[304]. This is accompanied by decreased aggrecan expression and certain subsets of patients also have decreased type X collagen expression as well as increased type I collagen, type II collagen, and MMP-13 expression[305]—indicating a state of increased ECM turnover, attempt at cartilage repair, and potential bone formation. Type X collagen

expression is often upregulated in OA[306], as it is in hypertrophic chondrocytes prior to bone formation[307], but there are temporal and spatial differences in its expression profile in osteoarthritis[308,309]. Furthermore, SOX-9 normally prevents osteoblastogenesis of chondrocytes by regulating RUNX2[310], further supporting the role of a chondrocyte phenotype shift toward bone remodeling rather than cartilage maintenance in OA.

Osteoclast Involvement in Osteoarthritis

Altered bone remodeling is common in OA, with subchondral bone sclerosis and changes in subchondral bone metabolism often being amongst the first detectable OA alterations[311]. Increased osteoclast activity and subchondral bone remodeling are involved in both OA development and progression[37], but their overall contributions to disease is unclear. Suppressing bone resorption using osteoclast inhibitors has resulted in beneficial secondary effects on cartilage health in several pre-clinical OA studies and increased resorption has resulted in cartilage deterioration—demonstrating that osteoclasts can contribute at least indirectly to cartilage health—although the pre-clinical chondroprotective effects of antiresorptives have been difficult to reproduce in clinical trials, despite reductions in pain outcomes[293,311,312]. For instance, the varying efficacy of bisphosphonates in OA clinical trials could potentially be attributed to different disease-stages of the patients, different OA phenotypes with different levels of bone involvement, and a lack of OA progression in control groups[293]. If the differences in efficacy are stage- and phenotype-driven, bisphosphonates therapy may only be suitable for certain patients[293]. Therefore, the use of patient stratification is essential for accurate treatment and DMOAD development.

OA cartilage degradation has been likened to the cartilage degradation that occurs as part of endochondral ossification[313], featuring chondrocyte proliferation and hypertrophy, vascularization, ECM calcification, and elevated RUNX2 expression—crucial for osteoblast differentiation and bone formation[313,314]—which suggests that osteoclasts may also have a more direct role to play. For instance, blood vessels rarely penetrate the tidemark into non-calcified cartilage in the normal patella, but this is a more common feature in OA[315]. Osteoclastic turnover of the subchondral bone and invasion of the calcified and non-calcified cartilage are likely to contribute to the increased angiogenesis and innervation of cartilage in OA[34]. The differentiation, activity and survival of osteoclasts is highly regulated in healthy individuals, whereas monocytes isolated from patients with OA exhibit increased osteoclastogenesis, elevated resorption, and reduced osteoclast apoptosis[316]. Heterozygous OPG knockout mice have been demonstrated to have increased joint destruction after surgical induction of OA, but this was proposed to be due to increased chondrocyte apoptosis[317]. Similarly, surgical induction of OA in wild type mice results in chondrocyte apoptosis and cartilage destruction that can be reduced

by the administration of exogenous OPG[317]. This effect may be mediated by TNF-related apoptosis-inducing ligand (TRAIL)[318], as OPG can bind TRAIL and inhibit TRAIL-induced apoptosis[319]. Hence, the role of the RANK/RANKL/OPG axis in OA cartilage degradation may be related to both chondrocyte health and osteoclast activity.

In recent years, there is increasing evidence indicating potential direct contribution of osteoclast activity to cartilage degradation. Resorption pits reaching from subchondral bone into articular cartilage have been described in OA[320], and GAG release has been measured from human osteoclasts cultured on cartilage[249]—although GAG release has also been demonstrated from macrophages cultured on cartilage. Additionally, osteoclasts are recruited to the subchondral bone in spontaneously occurring equine post-traumatic OA (PTOA). In PTOA, subchondral bone osteoclast numbers are correlated with articular cartilage RANKL expression as well as cartilage deterioration, and RANKL expression in calcified cartilage and subchondral bone is associated with calcified cartilage microcracks[321]. Hence, osteoclasts recruited to the subchondral bone by RANKL may potentially contribute to degradation of calcified cartilage non-calcified cartilage. Furthermore, bone marrow lesions (BMLs) have been shown to be associated with the subchondral bone areas underlying articular cartilage lesions—featuring increased MMP-13 expression, angiogenesis, cartilage formation, and increased bone turnover, suggesting an increased osteoclast-associated bone–cartilage crosstalk[322,323]. While these studies strongly imply the potential contribution of osteoclasts to cartilage degradation in OA, little is known of their actual contribution *in vivo* and the mechanisms through which osteoclasts resorb cartilage. Both MMPs[324] and cathepsin K[325] are thought to degrade cartilage, but in addition to osteoclasts there are many other potential contributors to MMP[326–328] and cathepsin K[328,329] levels in the OA joint. As such, osteoclastic cartilage resorption processes require further investigation. A translational approach incorporating tools such as *in vitro* models and biomarkers may therefore be valuable to elucidate the mechanisms involved in osteoclastic cartilage degradation *in vivo*.

Neo-Epitope Biomarkers

Biomarkers can be defined in many different ways, but biomarkers can generally be summarized as some form of objective measurement that provide an indication of the state of different processes in the body. The National Institutes of Health (NIH) Biomarkers Definitions Working Group defined a biomarker as “a characteristic that is objectively measured and evaluated as an indicator of normal biological processes, pathogenic processes, or pharmacologic responses to a therapeutic intervention”[330].

Biomarkers range from very simple to very complex in nature. An example of a simple biomarker would be to measure blood pressure, pulse, or body mass index (BMI). In comparison, more complex biomarkers may include measuring the levels of a specific protein or even just a specific modified version of a protein in blood or urine through various laboratory procedures, such as the commonly-used enzyme-linked immunosorbent assays (ELISAs). The proteolytic degradation of proteins or other post-translational modifications of proteins result in protein fragments which may expose a novel epitope that is otherwise not exposed or present, termed a neo-epitope. This dissertation will focus on neo-epitope biomarkers formed through the proteolytic degradation of ECM proteins, used as indicators of ECM turnover and as tools for investigating mechanisms involved in ECM turnover.

Cartilage Degradation Biomarkers

Personalized medicine and biomarkers have been proposed as the way forward to develop more effective and targeted therapies as well as to investigate pathophysiogical processes in diseases such as OA[293]. As previously discussed, a key feature of rheumatic diseases is the pathological degradation or remodeling of cartilage. However, the extent of the cartilage degradation and the underlying mechanisms may differ greatly between diseases, disease stages and patients. Biomarkers are a very valuable tool both clinically and pre-clinically for investigating the extent of ongoing cartilage degradation, mechanisms of degradation, and can be used to assess whether therapies are having beneficial effects on cartilage degradation. A plethora of biomarkers of cartilage degradation have been published over the years, including cartilage oligomeric matrix protein (COMP)[331], C2M[332], C2K77[333], C1,2C[334], C2C[324], C2C-HUSA[335], and the aggrecan epitopes ARGS[336,337], FFGV[336,337] and CS846[338]. Many of these biomarkers are neo-epitope biomarkers, and have been shown to have varying relevance for rheumatic diseases. However, the most relevant cartilage degradation biomarker to date arguably is the neo-epitope biomarker C-telopeptide of type II collagen (CTX-II).

CTX-II is a biomarker of type II collagen degradation, indicative of cartilage degradation. Urinary and synovial fluid CTX-II, unlike blood CTX-II, are highly relevant biomarkers for OA and are the most informative biochemical biomarkers for prediction of OA to date[339]. OA incidence and progression[340–344], severity[345–347], BMLs[348], osteophytes[349], and pain[350] have been associated with CTX-II, although pain associations have varied[350]. CTX-II has also been shown to have some relevance for RA[351]; in RA, CTX-II has been shown to predict disease progression[352–355], treatment efficacy[353], bone mineral density (BMD) reduction[356] and synovitis[356]. However, blood CTX-II has not been reported to have any clinical utility to date, although it has been demonstrated to be very useful in animal models with experimental joint destruction[357–361].

The CTX-II assay detects C-telopeptide fragments of type II collagen, the major ECM component of articular cartilage, with a neo-epitope[362] formed by the proteolytic cleavage of type II collagen ($_{1230}$EKGPDP↓LQYMR$_{1240}$)[363] during degradation of cartilage by MMPs[364–366] that results in the release of the $_{1230}$EKGPDP↓$_{1235}$ neo-epitope. This neo-epitope has been immunolocalized to areas of cartilage damage, around chondrocytes, areas of vascularization close to the subchondral bone, and the bone–cartilage interface[367]—suggesting that osteoclasts may contribute to its generation and/or release. Additional elongated versions—as well as truncated versions—of the CTX-II neo-epitope (Table 3) that are not detected by CTX-II assays have previously been described in patent literature[364–366].

Table 3. Presence and Origin of Type II Collagen C-Telopeptides in Bodily Fluids.
C-telopeptide neo-epitopes of type II collagen, as described by Eyre[366]. Abbreviations: —, absent or present in trace amounts; CC, derived from calcified cartilage; NC, derived from non-calcified cartilage.

Peptide sequence	Synovial fluid	Blood	Urine	Assays
EKGPD	—	NC	NC+CC	None
EKGPDP	NC	NC	NC+CC	CTX-II
EKGPDPL	NC	NC	NC+CC	None
EKGPDPLQ	—	CC	—	GPDPLQ$_{1237}$
EKGPDPLQYMR	NC	NC	—	None

At present, none of the elongated or truncated versions of the CTX-II neo-epitope have biomarker assays available, with the exception for the novel GPDPLQ$_{1237}$ assay that has been developed as part of **Paper V**. Furthermore, there have been no peer-reviewed scientific publications describing the other neo-epitopes. Of these elongated neo-epitopes, the $_{1230}$EKGPDPLQ↓$_{1237}$ neo-epitope is of particular interest. The EKGPDPLQ neo-epitope has been suggested to be generated by cathepsin K cleavage of calcified cartilage and, accordingly, to be osteoclast-specific[364–366]. The neo-epitope has also been described as being present only in blood, and not in synovial fluid or urine[364–366]. Proteases in the kidneys and/or liver have been suggested to remove the C-terminal -LQ of the EKGPDPLQ neo-epitope to generate the urinary forms of the C-telopeptide—EKGPDP or smaller[364–366]. This in turn is indicative that the EKGPDPLQ neo-epitope may be of interest as a potential blood-precursor to CTX-II. However, the only descriptions of this neo-epitope to date are from the patent literature[364–366]. Due to these proposed differences in the generation and/or processing as well as tissue origin compared to the EKGPDP neo-epitope, EKGPDPLQ may be a relevant blood biomarker of degenerative joint diseases. As different osteoclast substrates affect both the ECM degradation products and have been proposed to alter the osteoclast phenotype[368], assessing the degradation products of osteoclastic cartilage resorption and the processes involved in generating these products may further our understanding of pathological cartilage degradation mechanisms.

Aims of the Dissertation

The overall aim of this dissertation was to develop novel therapies, models and biomarkers for diseases with altered bone and/or cartilage turnover mediated by osteoclasts. This aim can be further sub-divided into the two following aims:

Developing Clinically Applicable IMO Gene Therapy

- To assess the efficacy, level of rescue required, and TCIRG1 protein regulation after lentiviral-mediated IMO gene therapy *in vitro* (**Paper I**).
- To develop a clinically applicable IMO gene therapy vector and assess the long-term efficacy *ex vivo* after transplantation of treated human IMO HSPCs into mice (**Paper II**).
- To develop a humanized mouse model overexpressing hM-CSF capable of sustaining human hematopoiesis and osteoclastogenesis (**Paper III**).

Investigating Osteoclastic Cartilage Resorption

- To establish a cell culture model of osteoclastic resorption of non-calcified and calcified cartilage to assess osteoclastic processes that may contribute to cartilage degradation (**Paper IV**).
- To develop a novel biomarker assay of osteoclastic cartilage resorption based on the elongated CTX-II neo-epitope EKGPDPLQ (**Paper V**).

Results

Paper I

Regulation and Function of Lentiviral Vector-Derived TCIRG1

In **Paper I**, we wanted to investigate how vector-derived TCIRG1 protein levels are regulated during the differentiation of monocytes into osteoclasts. We also investigated the ratio of healthy or vector-treated IMO stem cells to IMO stem cells required to restore osteoclast function, to get an indication of the rescue threshold for treatment of IMO.

Vector Design

The rescue vector (SFFV-TG) used in this study contains the cDNA of human *TCIRG1* in a bicistronic SIN lentiviral vector under the SFFV promoter up-stream of an internal ribosomal entry site (IRES) followed by the enhanced green fluorescent protein (GFP) gene. The bicistronic vector design allows for simultaneous expression of both TCIRG1 and GFP proteins as separate proteins. A similar vector without the TCIRG1 cDNA (SFFV-G) was used as a control for protein expression.

Vector-Derived TCIRG1 Levels are Regulated by Osteoclastogenesis

We aimed to investigate how TCIRG1 protein levels are regulated during osteoclastogenesis when using a strong constitutively active promoter. We transduced healthy $CD34^+$ cord blood (CB) or IMO HSPCs and stimulated osteoclastogenesis with M-CSF and RANKL. Our data shows that the transduction of CB HSPCs with SFFV-TG does not appear to result in ectopic expression of TCIRG1, and that the TCIRG1 expression in IMO cells transduced with SFFV-TG exhibited similar kinetics as the endogenous protein. IMO SFFV-TG TCIRG1 expression increased over time and was only present at low levels in IMO SFFV-TG and CB cells after 5 days of osteoclastogenesis, but increased after 7 and 10 days. However, GFP levels were constant regardless of the vector used, indicating that the TCIRG1 regulation was not at a transcriptional level. Hence, both endogenous and vector-derived TCIRG1 levels appear to be translationally or post-translationally regulated.

In osteoclastogenesis experiments with or without RANKL, IMO HSPCs transduced with SFFV-TG (Figure 8A) had substantial TCIRG1 expression only with RANKL stimulation after 9 and 14 days of differentiation despite constant GFP expression, indicating that even TCIRG1 derived from a viral vector is strongly regulated by osteoclastogenesis *in vitro*. Cells cultured without RANKL failed to differentiate into osteoclasts but instead differentiated toward a macrophage-like cell type. These cells only expressed limited amounts of TCIRG1 which were absent when using the SFFV-G control vector (Figure 8B), indicating that the post-translational TCIRG1 regulation is dependent on RANKL-mediated osteoclastogenesis.

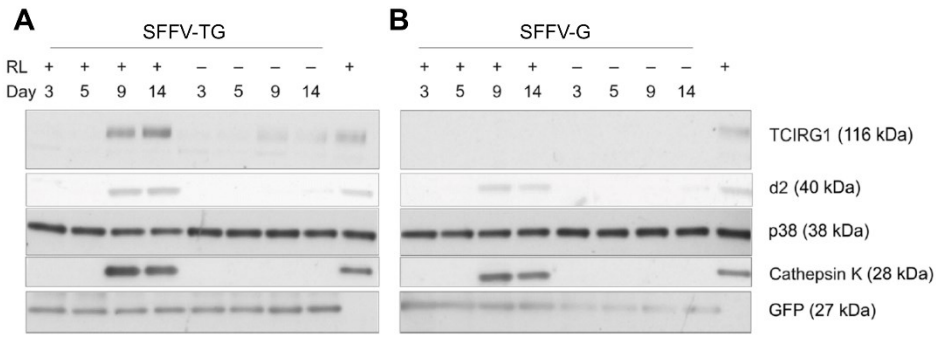

Figure 8. Osteoclastogenesis-Dependent Regulation of Vector-Derived TCIRG1.
IMO HSPCs were transduced with the SFFV-TG (**A**) or the SFFV-G (**B**) vector, and differentiated into osteoclasts in the presence of RANKL (RL +) or macrophages in the absence of RANKL (RL -). The protein expression of TCIRG1, the V-ATPase subunit d2, the osteoclast marker cathepsin K, and GFP were assessed throughout differentiation by western blot, and p38 was used as loading control. CTRL cells are positive controls, composed of mature osteoclasts generated from healthy HSPCs.
Adapted with permission from Springer Nature: Springer; Calcified Tissue International; *Regulation and Function of Lentiviral Vector-Mediated TCIRG1 Expression in Osteoclasts from Patients with Infantile Malignant Osteopetrosis: Implications for Gene Therapy*; Thudium CS, Moscatelli I, Löfvall H, Kertész Z, Montano C, Bjurström CF, Karsdal MA, Schulz A, Richter J, Henriksen K; 2016.

TCIRG1 Glycosylation is Dependent on Cell Type

We also investigated how vector-derived TCIRG1 protein may be regulated in a non-osteoclast cell type of a non-hematopoietic lineage. Cells from the fibrosarcoma cell line HT1080—of mesenchymal lineage—were transduced with SFFV-TG, followed by TCIRG1 mRNA and protein analyses. TCIRG1 mRNA and protein was present already after 3 days in HT1080 cells and the relative distribution between high-molecular weight and low-molecular weight TCIRG1 was reversed, compared to TCIRG1 in osteoclast cell lysates where the high-molecular weight form is predominant (Figure 9). As TCIRG1 has been reported to have different molecular weights in its fully glycosylated and its core-glycosylated form[369], we investigated if the molecular weights we observed were due to the glycosylation status. This was achieved by deglycosylating osteoclast cell lysates using the endoglycosidases PNGase F and Endo H. PNGase F is capable of deglycosylating fully glycosylated

and core-glycosylated TCIRG1, whereas Endo H can only deglycosylate core-glycosylated TCIRG1[369]. We found that the two different TCIRG1 molecular weights in both osteoclasts and HT1080 cells corresponded to the fully glycosylated and the core-glycosylated TCIRG1 (Figure 9). Hence, the difference in glycosylation of TCIRG1 between osteoclasts and HT1080 cells indicates that glycosylation may be relevant to potentially lineage-specific TCIRG1 regulation.

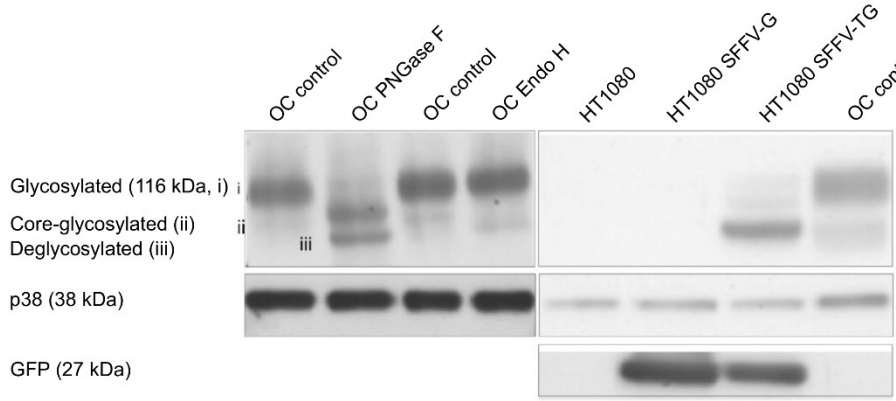

Figure 9. Differences in TCIRG1 Glycosylation Between Osteoclasts and HT1080 cells.
HT1080 cells were transduced with the SFFV-TG or SFFV-G vector, or left non-transduced, and were cultured for 3 days followed by TCIRG1 expression analysis by western blot. The HT1080 TCIRG1 bands were compared to those in osteoclast (OC) lysates that had been deglycosylated using PNGase F or Endo H. GFP expression was assessed to verify transduction, and p38 was used as loading control.
Adapted with permission from Springer Nature: Springer; Calcified Tissue International; *Regulation and Function of Lentiviral Vector-Mediated TCIRG1 Expression in Osteoclasts from Patients with Infantile Malignant Osteopetrosis: Implications for Gene Therapy*; Thudium CS, Moscatelli I, Löfvall H, Kertész Z, Montano C, Bjurström CF, Karsdal MA, Schulz A, Richter J, Henriksen K; 2016.

Phenotype Restoration Threshold

A crucial issue for gene therapy is the level of correction required to achieve phenotype restoration. We addressed this by mixing $CD34^+$ CB HSPCs or IMO HSPCs transduced with SFFV-TG with non-transduced IMO HSPCs and differentiating the mixtures into osteoclasts on bone with M-CSF and RANKL. As little as 2.5% of CB HSPCs mixed with 97.5% IMO HSPCs was sufficient to significantly increase the resorption per osteoclast, as measured by CTX-I/TRAP activity in culture media, and 30% CB HSPCs mixed with 70% IMO HSPCs resorbed at similar levels as the 100% CB HSPCs (Figure 10A). Similarly, 2.5% of transduced IMO HSPCs resulted in significantly increased resorption per osteoclast, and the resorption increased substantially with increasing levels of transduced cells (Figure 10B). These results indicate that even low levels of transduction and engraftment are sufficient to rescue the phenotype.

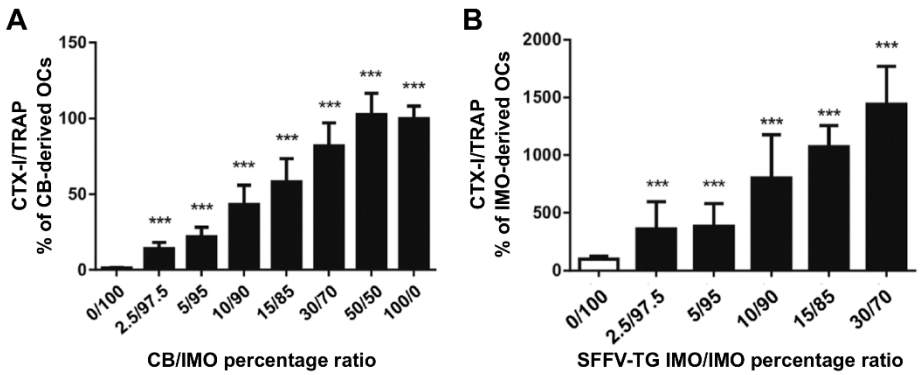

Figure 10. Correctional Effects of Mixing Normal CB or Treated IMO HSPCs with IMO HSPCs.
CB HSPCs (**A**) or IMO HSPCs transduced with SFFV-TG (**B**) were mixed with IMO HSPCs at different ratios followed by osteoclast differentiation on bone and measurements of CTX-I and TRAP activity to calculate resorption per osteoclast (CTX-I/TRAP). Data in **A** are expressed as percent of 100% CB-derived osteoclasts and data in **B** are expressed as percent of 100% IMO-derived osteoclasts, error bars represent the standard error of the mean (SEM). Statistical significance levels relative to 100% IMO are indicated by ***p < 0.001.
Adapted with permission from Springer Nature: Springer; Calcified Tissue International; *Regulation and Function of Lentiviral Vector-Mediated TCIRG1 Expression in Osteoclasts from Patients with Infantile Malignant Osteopetrosis: Implications for Gene Therapy*; Thudium CS, Moscatelli I, Löfvall H, Kertész Z, Montano C, Bjurström CF, Karsdal MA, Schulz A, Richter J, Henriksen K; 2016.

Paper II

Gene Therapy Corrects IMO in NSG-Engrafting Human HSPCs

In **Paper II**, we investigated if human IMO HSPCs treated with a clinically applicable lentiviral vector and transplanted into immunodeficient mice long-term would be capable of generating functional osteoclasts *ex vivo*—as there are no suitable osteopetrotic models that will engraft human HSPCs.

Vector Design

All vectors used in this study are SIN lentiviral vectors. For comparing the viral proof-of-concept vector promoter to different mammalian promoters *in vitro*, vectors containing the cDNA of human TCIRG1 under the SFFV promoter, the elongation factor 1a short (EFS) promoter, or the chimeric myeloid promoter (ChimP), followed by an IRES and GFP were used—named SFFV-TG, EFS-TG, and ChimP-TG, respectively. After validating the promoters, a vector expressing TCIRG1 cDNA alone under the EFS promoter (EFS-T) was used for transplantation experiments. Control vectors expressed GFP alone under the SFFV or EFS promoters (SFFV-G, EFS-G).

Mammalian Promoters Maintain the Gene Therapy Efficacy In Vitro

Osteoclasts were generated from $CD34^+$ IMO HSPCs with M-CSF and RANKL, and similar levels of Ca^{2+} and CTX-I release were detected regardless of the vector used. As EFS-TG appeared to result in increased TCIRG1 and resorption levels compared to ChimP-TG, EFS was used for developing a clinically applicable vector. EFS-T transduction of IMO HSPCs followed by *in vitro* osteoclastogenesis with M-CSF and RANKL resulted in Ca^{2+} and CTX-I release that was comparable to that of CB cells transduced with EFS-G or EFS-T. Compared to the EFS-TG, EFS-T exhibited trends toward increased resorption, increased TCIRG1 protein levels, and reduced TRAP activity—indicating increased reversal of the osteopetrotic phenotype. The mutagenic potential of EFS-T was assessed in IVIM assays that revealed that the vector had a strongly reduced risk of *in vitro* immortalization, compared to gammaretroviral or lentiviral vectors with the SFFV promoter.

EFS-T-HSPCs Maintain Osteoclastogenic Potential Post-Transplant

$CD34^+$ IMO HSCPs transduced with EFS-T or EFS-G, or CB HSPCs, were transplanted into 8–15 weeks old NSG mice. Similar bone marrow engraftment levels (on average 35%) as well as B cell, T cell and myeloid lineage reconstitution were observed in all three conditions at 9–19 weeks post-transplantation. Human $CD34^+$ bone marrow cells were isolated and used for *ex vivo* osteoclastogenesis with M-CSF and RANKL. On average, the *ex vivo* osteoclastogenesis resulted in a fully

normalized Ca^{2+} release in the IMO EFS-T condition (Figure 11A), while the CTX-I release was increased to 33% of the CTX-I levels obtained from of CB-derived osteoclasts (Figure 11B). However, the IMO EFS-T condition did not have reduced TRAP activity compared to the IMO EFS-G condition.

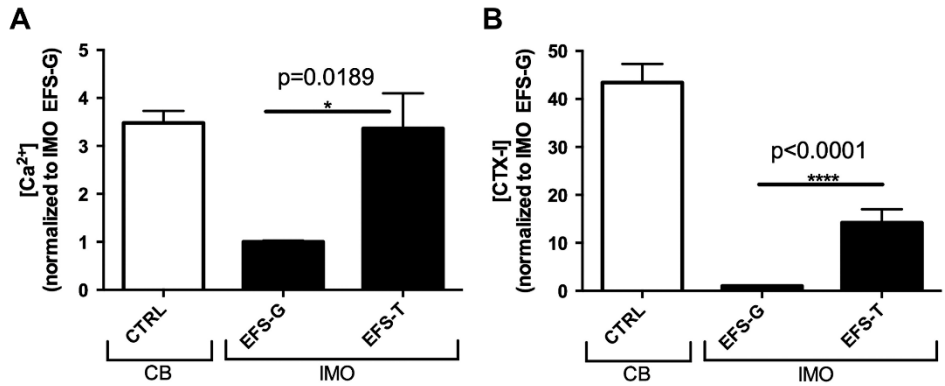

Figure 11. NSG-Transplanted Vector-Corrected IMO HSPCs Generate Functional Osteoclasts *Ex Vivo*.
Human $CD34^+$ cells were isolated from the NSG mice, expanded for 2 weeks, seeded on bone slices, and differentiated into osteoclasts. The concentrations of Ca^{2+} (**A**) and CTX-I (**B**) were measured in the media. The data are presented as fractions of the IMO EFS-G control, error bars represent the SEM. Statistical significance levels relative to the IMO EFS-G are indicated by *p < 0.05, and ****p < 0.0001.
Adapted with permission from Mary Ann Liebert, Inc.: Mary Ann Liebert, Inc.; Human Gene Therapy; *Targeting NSG Mice Engrafting Cells with a Clinically Applicable Lentiviral Vector Corrects Osteoclasts in Infantile Malignant Osteopetrosis*; Moscatelli I, Löfvall H, Thudium CS, Rothe M, Montano C, Kertész Z, Sirin M, Schulz A, Schambach A, Henriksen K, Richter J; 2018.

On an individual level, the bone-resorbing phenotype was completely restored in 1/11 mice with IMO EFS-T cells, and partially restored in 8/11 mice (Table 4). Furthermore, TCIRG1 protein was detectable in 4/8 assessed IMO EFS-T osteoclast cell lysates. The vector copy number (VCN) was in the range of 0.10–0.46 per human ($CD45^+$) cell in IMO EFS-T mice with no or partial rescue, whereas the individual with complete rescue had a VCN of 1.96 per human cell (Table 4), indicating that transduction and integration efficacy may be linked to rescue efficacy.

Table 4. *Ex Vivo* Rescue Efficacy in Transplanted NSG Mice.

Rescue efficacy was estimated by comparing the relative increase of Ca^{2+} and CTX-I, as well as decrease of TRAP activity, to negative (IMO EFS-G) and positive (CB) controls within the same transplantation experiment. Data from Moscatelli et al.[370]. Abbreviations: #1–4, transplantation experiment 1–4; n/a, not applicable; n.d., not determined; VCN_{CD45}, VCN per human $CD45^+$ cell.

Transplantation		VCN_{CD45}	TCIRG1 Band intensity	$[Ca^{2+}]$ % of IMO EFS-G	[CTX-I] % of IMO EFS-G	TRAP % of IMO EFS-G	Rescue
#1	IMO EFS-T	n.d.	n.d.	638	1619	300	Partial
	IMO EFS-T	n.d.	None	728	1850	162	Partial
	IMO EFS-T	n.d.	Weak	717	2313	89	Partial
	IMO EFS-G	n.d.	n/a	100	100	100	n/a
	IMO EFS-G	n.d.	n/a	100	100	100	n/a
#2	IMO EFS-T	0.33	n.d.	96	106	89	None
	IMO EFS-T	0.11	None	88	124	109	None
	IMO EFS-T	0.46	Weak	212	1062	66	Partial
	IMO EFS-T	0.25	Weak	205	1080	65	Partial
	IMO EFS-G	0.85	n/a	100	100	100	n/a
	IMO EFS-G	1.09	n/a	100	100	100	n/a
	CB	0.04	n/a	328	4922	33	n/a
#3	IMO EFS-T	1.96	Strong	277	2715	33	Complete
	IMO EFS-G	39.86	n/a	88	96	124	n/a
	IMO EFS-G	3.89	n/a	112	104	76	n/a
	CB	0.13	n/a	433	4422	23	n/a
	CB	0	n/a	280	2856	35	n/a
#4	IMO EFS-T	0.21	None	328	2210	82	Partial
	IMO EFS-T	0.33	None	272	2155	84	Partial
	IMO EFS-T	0.1	n.d.	142	423	78	Partial
	IMO EFS-G	2.27	n/a	100	100	100	n/a
	CB	0	n/a	359	4526	24	n/a
	CB	0	n/a	340	4992	23	n/a

Paper III

Monocyte and Osteoclast Formation of HSPCs Expressing hM-CSF

In **Paper III**, we investigated if a humanized mouse model generated by transplantation of human HSPCs expressing hM-CSF, by means of a lentiviral hM-CSF vector, would have improved reconstitution of the human monocyte population and would be capable of sustaining human osteoclastogenesis both *in vivo* and *in vitro*.

Vector Design

The SIN lentiviral vector used in this study contained the cDNA of hM-CSF under the SFFV promoter, followed by an IRES and the dTomato transgene marker. A similar vector, using a non-coding spacer sequence instead of M-CSF cDNA, was used as a control.

hM-CSF-Expressing HSPCs Generate Cells of Myeloid Lineages In Vitro

Transduction of human $CD34^+$ CB HSPCs with the hM-CSF vector resulted in an hM-CSF secretion of 15902 pg/ml, whereas the control vector only resulted in 98 pg/ml. The transduced HSPCs had increased differentiation into the $hCD14^+$ monocyte population, as well as $hCD14^+hCD33^+$ and $hCD14^+hCD11b^+$ populations. Additionally, the transduced HSPCs also stimulated non-transduced HSPCs in a paracrine manner, increasing the non-transduced $hCD14^+$ population.

hM-CSF Vector Supports Osteoclastogenesis In Vitro

Transduced HSPCs were used for osteoclastogenesis cultures on bone by stimulating the cells with different combinations of hM-CSF, human RANKL, and mouse RANKL. The hM-CSF vector was capable of sustaining osteoclastogenesis with the addition of either human or murine RANKL (Figure 12A) and resulted in Ca^{2+} release from the bone (Figure 12B). However, the addition of exogenous hM-CSF did not further increase osteoclastogenesis or resorption. The control vector could only sustain osteoclastogenesis with addition of exogenous hM-CSF.

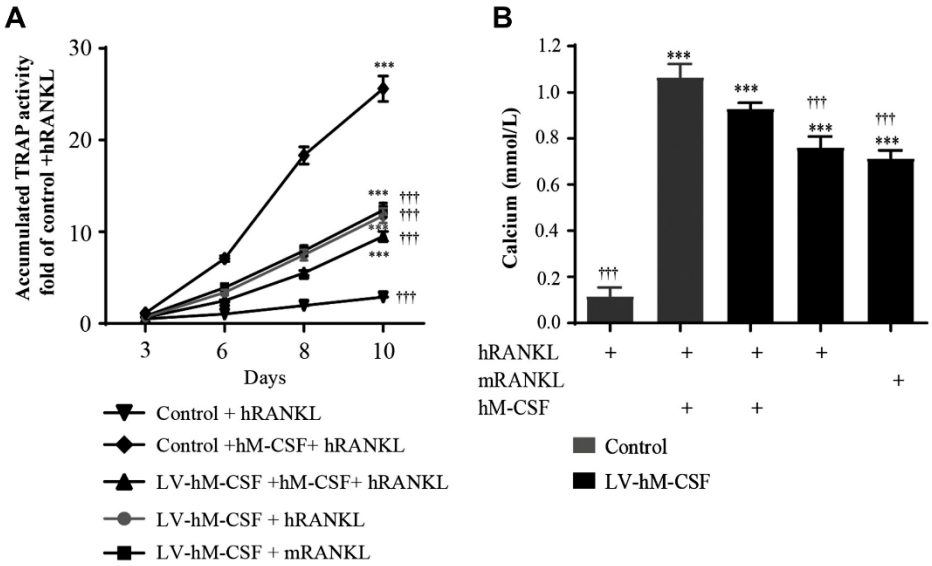

Figure 12. hM-CSF-HSPCs Generate Functional Osteoclasts *In Vitro* Without Exogenous hM-CSF.
HSPCs transduced with the hM-CSF vector (LV-hM-CSF) were seeded on bone slices and differentiated into osteoclasts using different combinations of hM-CSF, human RANKL (hRANKL), and mouse RANKL (mRANKL). Accumulated TRAP activity over time (**A**) and Ca^{2+} release (**B**) after 10 days of osteoclastogenesis were measured in cell culture supernatants. Statistical significance levels relative to control + hRANKL and control + hM-CSF + hRANKL are indicated by ***$p < 0.001$ and $^{\dagger\dagger\dagger}p < 0.001$, respectively. Error bars represent the standard deviation.
Adapted with permission from Johan Wiley and Sons: John Wiley & Sons Ltd; European Journal of Haematology; *Forced Expression of Human Macrophage Colony-Stimulating Factor in CD34⁺ Cells Promotes Monocyte Differentiation In Vitro and In Vivo but Blunts Osteoclastogenesis In Vitro*; Montano Almendras CP, Thudium CS, Löfvall H, Moscatelli I, Schambach A, Henriksen K, Richter J; 2017.

Transplanting Transduced HSPCs Results in Improved Myeloid Reconstitution

The transduced HSPCs were transplanted into newborn mice of the immunodeficient NSG strain. The transplantation of transduced HSPCs resulted in 2875 pg/ml serum hM-CSF, whereas mice transplanted with control-HSPCs only had 82 pg/ml hM-CSF—which is close to the lower detection limit of the hM-CSF ELISA (78 pg/ml). The engraftment of human ($CD45^+$) cells was similar using both the hM-CSF and control vectors. The human monocyte ($hCD14^+$) cell population was significantly increased 8 weeks post-transplant of transduced HSPCs, compared to control HSPCs, in both peripheral blood and bone marrow (Figure 13A). The $hCD14^+hCD33^+hCD45^+$ population was also increased in peripheral blood, but not in bone marrow (Figure 13B). Overall, these results demonstrate that hM-CSF expression in human HSPCs increases the reconstitution of myeloid lineages, which has important implications for potential human osteoclastogenesis *in vivo.*

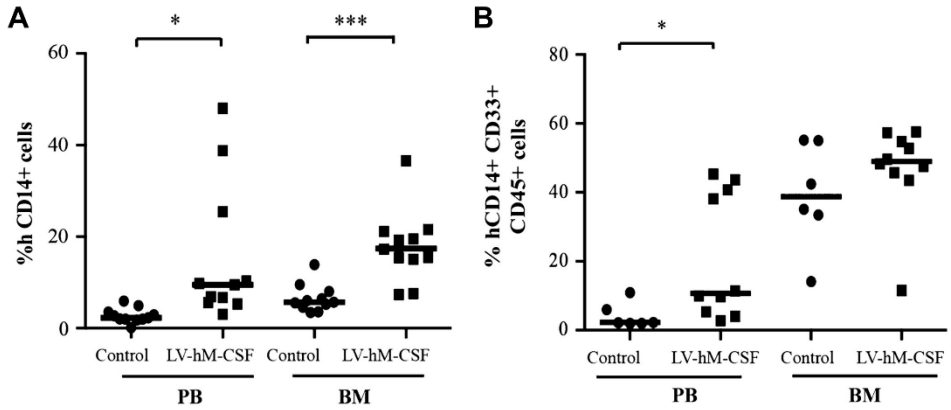

Figure 13. Vector-Derived hM-CSF Increases Monocyte Differentiation of Human HSPCs in NSG mice.
hM-CSF-HSPCs were transplanted into NSG mice and human monocyte populations were analyzed by flow cytometry after eight weeks: peripheral blood and bone marrow $hCD14^+$ (**A**), and peripheral blood and bone marrow $hCD45^+hCD14^+hCD33^+$ (**B**). Each symbol represents an individual mouse, and the lines represent the mean. Statistical significance levels relative to control are indicated by $*p < 0.05$ and $***p < 0.001$.
Adapted with permission from Johan Wiley and Sons: John Wiley & Sons Ltd; European Journal of Haematology; *Forced Expression of Human Macrophage Colony-Stimulating Factor in $CD34^+$ Cells Promotes Monocyte Differentiation In Vitro and In Vivo but Blunts Osteoclastogenesis In Vitro*; Montano Almendras CP, Thudium CS, Löfvall H, Moscatelli I, Schambach A, Henriksen K, Richter J; 2017.

Undetectable Human Osteoclastogenesis

Despite improved human monocyte reconstitution *in vivo*, we were unable to detect human osteoclasts *in vivo* using immunohistochemical approaches—such as dTomato/TRAP co-localization. Further studies are required to validate human osteoclastogenesis in this model system.

Paper IV

Osteoclastic Bone and Cartilage Resorption Processes

In **Paper IV**, we described a novel cell culture model for investigating the osteoclastic resorption processes involved in degrading the ECMs that are often affected in knee OA—non-calcified cartilage, calcified cartilage and subchondral bone—and characterize the ECM degradation using biomarkers.

Model Design

Human osteoclasts were generated by stimulating $CD14^+$ PBMCs with M-CSF and RANKL for two weeks. The mature osteoclasts were then cultured on bovine knee joints ECMs: non-calcified cartilage, osteochondral ECM (a mixture of calcified cartilage and subchondral bone), and cortical bone. The osteoclasts were treated with different antiresorptive compounds during the ECM resorption cultures: the V-ATPase inhibitor diphyllin[371], the cysteine protease inhibitor E-64[99]—principally inhibiting cathepsin K in an osteoclastic resorption setting—or the broad-spectrum MMP inhibitor GM6001[372]. Resorption was assessed by measuring bone (Ca^{2+} and CTX-I) and cartilage degradation (C2M) biomarkers in the culture media. The model design and the osteoclastic processes contributing to the release of the ECM degradation biomarkers are illustrated in Figure 14.

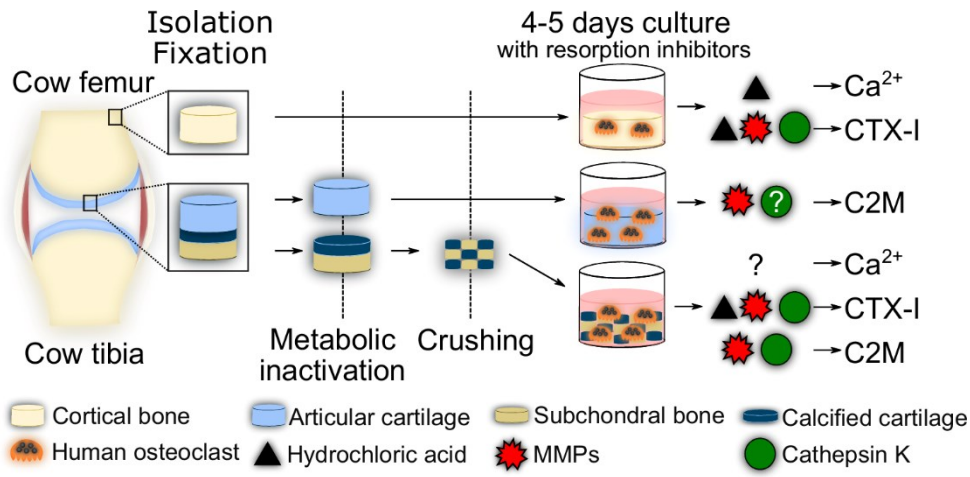

Figure 14. Overview of Osteoclastic Resorption of Knee Joint ECMs.
Cortical bone, articular cartilage and an osteochondral ECM, consisting of subchondral bone and calcified cartilage, were isolated from bovine knees, and fixed in ethanol. The articular cartilage and the osteochondral ECM were metabolically inactivated through immersion in liquid nitrogen. The osteochondral ECM was crushed to generate a plateable matrix. Human osteoclasts were cultured on the ECMs in the presence of V-ATPase, MMP and cathepsin K inhibitors, and their impact on ECM degradation was assessed using biomarkers.
Adapted from Löfvall et al.[373]

Cortical Bone Resorption

Cortical bone resorption was used as a reference to validate functional resorption. As expected, V-ATPase inhibition had strong effects on Ca^{2+} levels (58% inhibition), whereas the other inhibitors had negligible, yet statistically significant, effects (Figure 15A). Inhibition of the V-ATPase (96%), cathepsin K (77%), and MMPs (34%) all resulted in CTX-I inhibition (Figure 15B), and inhibiting both cathepsin K and MMPs had an increased effect (91%). TRAP activity in the media and culture viability was increased by V-ATPase inhibition, as expected[371], similarly to an osteoclast-rich osteopetrosis phenotype. All of these results are in line with the well-established mechanisms involved in bone resorption; acidification is crucial for hydroxyapatite dissolution and type I collagen degradation is mainly mediated by cathepsin K.

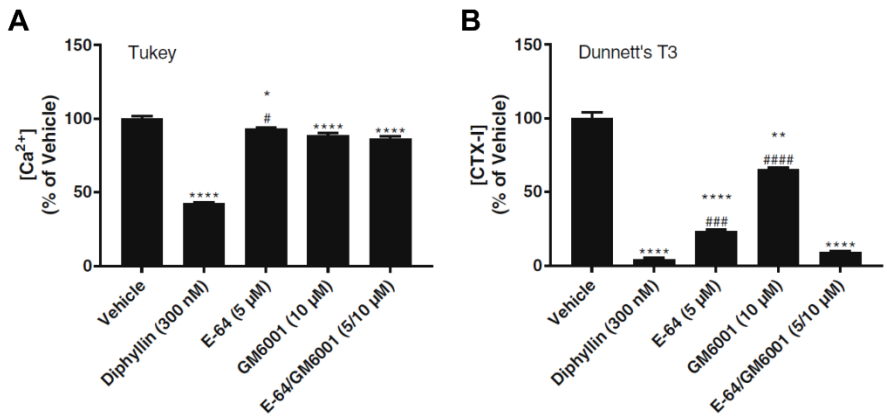

Figure 15. Ca^{2+} and CTX-I Release from Osteoclasts Cultured on Cortical Bone.
Osteoclasts were cultured on bovine femoral cortical bone in the presence or absence of resorption inhibitors. Resorption of calcified ECM and type I collagen were assessed by measuring the Ca^{2+} (**A**) and CTX-I (**B**) concentrations in the medium. Background-subtracted biomarker data are presented as percent of vehicle with error bars representing the SEM. Statistical significance is indicated by *p < 0.05, **p < 0.01, ***p < 0.001, ****p < 0.0001 for comparisons against the vehicle and $^{\#}$p < 0.05, $^{\#\#}$p < 0.01, $^{\#\#\#}$p < 0.001, $^{\#\#\#\#}$p < 0.0001 for comparisons against E-64/GM6001 (only shown for E-64 and GM6001); the post hoc test used is indicated in the corner of each graph. Adapted from Löfvall et al.[373]

Articular Cartilage Resorption

Articular cartilage resorption, as measured by the type II collagen degradation neo-epitope C2M[332] (Figure 16), was completely abrogated by MMP inhibition (100% inhibition). There was a trend toward cathepsin K inhibition reducing C2M release (69%), but this was not significant and was highly variable. V-ATPase inhibition had no significant effects on C2M and varied greatly between experiments, ranging from inhibition to stimulation. These data indicate that C2M release from non-calcified cartilage resorption is mainly mediated by MMPs, and that acidification is dispensable.

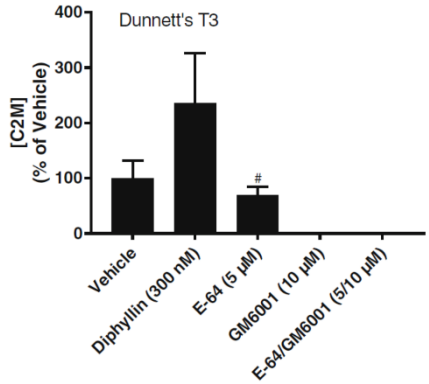

Figure 16. C2M Release from Osteoclasts Cultured on Articular Cartilage.
Osteoclasts were cultured on articular cartilage from bovine femoral condyles in the presence or absence of resorption inhibitors. Resorption of type II collagen was assessed by measuring C2M concentrations in the medium. Background-subtracted biomarker data are presented as percent of vehicle with error bars representing the SEM. Statistical significance is indicated by *p < 0.05, **p < 0.01, ***p < 0.001, ****p < 0.0001 for comparisons against the vehicle and #p < 0.05, ##p < 0.01, ###p < 0.001, ####p < 0.0001 for comparisons against E-64/GM6001 (only shown for E-64 and GM6001); the post hoc test used is indicated in the corner of the graph.
Adapted from Löfvall et al.[373]

Overall, TRAP activity and culture viability were not affected by V-ATPase inhibition, likely a result of this being a non-calcified ECM, but the results varied substantially between experiments. Some of the variation in biomarker results may be related to inter-individual differences in osteoclast and ECM quality, as different donor PBMCs and bovine knees were used for each experiment.

Osteochondral Resorption

The osteochondral ECM composition was validated by safranin O-fast green staining prior to crushing of the isolated matrix. The staining demonstrated that the articular cartilage was removed and that only bone interspersed with an aggrecan-containing matrix remained. This matrix was presumed to be calcified cartilage, but this could not be verified due to the decalcified nature of the sections used for the staining. von Kossa staining of non-decalcified matrix showed that the proximal surface was calcified, although some non-calcified matrix remained at the surface.

Osteochondral resorption resulted in release of both bone and cartilage degradation biomarkers. Although Ca^{2+} release (Figure 17A) was not reduced by any inhibitor, suggesting that the ECM was not heavily calcified, CTX-I release (Figure 17B) was inhibited by V-ATPase (50% inhibition), cathepsin K (81%), and MMP (49%) inhibitors. Inhibiting both cathepsin K and MMPs resulted in an apparent increase in CTX-I inhibition (96%). Culture viability was not affected by any antiresorptive, but V-ATPase inhibition increased TRAP activity—albeit to a lesser extent than on cortical bone. Taken together, these findings indicate that the subchondral bone component in the osteochondral ECM may be less calcified than cortical bone.

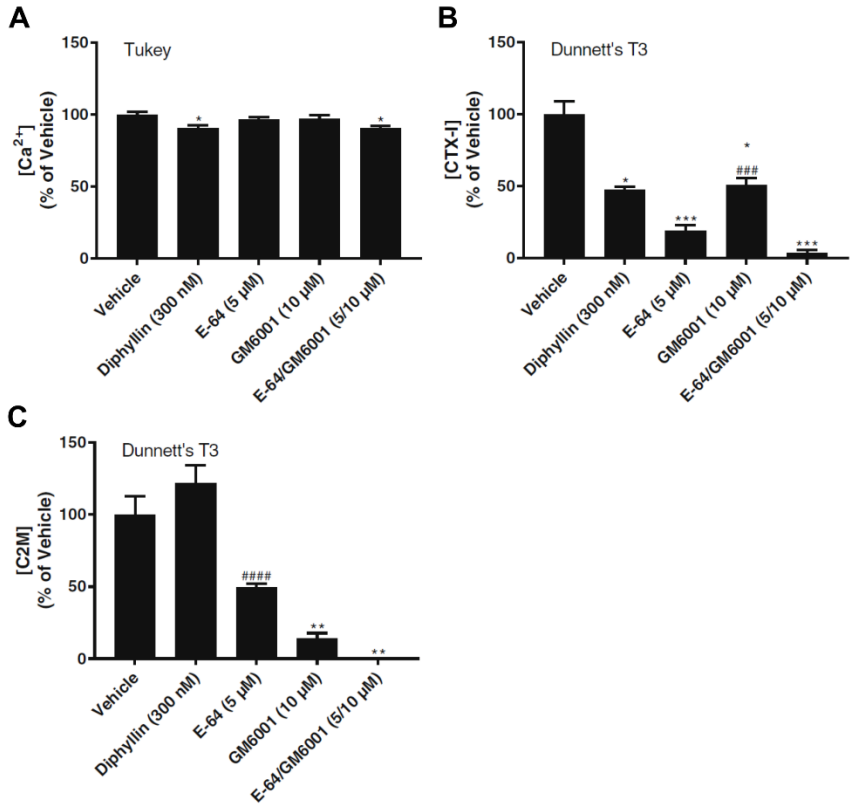

Figure 17. Ca^{2+}, CTX-I and C2M Release from Osteoclasts Cultured on Osteochondral ECM.
Osteoclasts were cultured on osteochondral ECM from bovine femoral condyles in the presence or absence of resorption inhibitors. Resorption of calcified ECM and type I collagen were assessed by measuring the Ca^{2+} (**A**) and CTX-I (**B**) concentrations in the medium. Resorption of type II collagen was assessed by measuring C2M (**C**) concentrations in the medium. Background-subtracted biomarker data are presented as percent of vehicle with error bars representing the SEM. Statistical significance is indicated by *p < 0.05, **p < 0.01, ***p < 0.001, ****p < 0.0001 for comparisons against the vehicle and #p < 0.05, ##p < 0.01, ###p < 0.001, ####p < 0.0001 for comparisons against E-64/GM6001 (only shown for E-64 and GM6001); the post hoc test used is indicated in the corner of each graph. Adapted from Löfvall et al.[373]

Osteochondral C2M release (Figure 17C) was mainly inhibited by MMP inhibitors (86%), but cathepsin K inhibition appeared to have a greater effect on osteochondral C2M release (51%) than it had on non-calcified cartilage, further supported by the apparent increase in inhibition when MMP and cathepsin K inhibitors were combined (100%). However, the effects of cathepsin K inhibition alone varied greatly between experiments. V-ATPase inhibition had negligible effects on osteochondral C2M release. These findings suggest that C2M release from calcified cartilage resorption is mainly mediated by MMPs, but cathepsin K may contribute to some extent, and that acidification is dispensable.

Paper V

GPDPLQ$_{1237}$: A Multi-Protease Cartilage Degradation Biomarker

In **Paper V**, we developed the novel competitive GPDPLQ$_{1237}$ ELISA measuring the C-terminal neo-epitope EKGPDPLQ$_{1237}$↓ of type II collagen degradation. To investigate the mechanisms involved in generating the EKGPDPLQ neo-epitope from cartilage degradation in a biologically relevant setting, we measured GPDPLQ$_{1237}$ in models of cartilage degradation in the presence of cathepsin K (E-64) and MMP (GM6001) inhibitors.

Biomarker Design

The GPDPLQ$_{1237}$ target has been previously described in patent literature[364–366]. Sequence analysis showed that the target sequence is unique to the type II collagen alpha 1 chain, and the target is fully conserved in human, cow, and rat. Antibodies were generated against the target sequence by immunizing mice with a keyhole limpet haemocyanin (KLH)-conjugated standard peptide (EKGPDPLQ). Hybridoma cells were generated through the fusion of isolated splenocytes with SP2/0 myeloma cells and limited dilution procedures were used to generate monoclonal cultures. The selectivity of the resulting monoclonal antibodies for the standard peptide—and lack of reactivity toward the CTX-II target (EKGPDP)—was verified through screening for reactivity against truncated (EKGPDP, EKGPDPL) and elongated (EKGPDPLQY, EKGPDPLQYM) standard peptides. The competitive GPDPLQ$_{1237}$ ELISA was generated using the NB427-5G11-4W3 monoclonal antibody. The technical performance of the GPDPLQ$_{1237}$ assay was validated in a series of technical tests, including tests of lower limit of detection (LLOD), upper limit of detection (ULOD), linear measurement range, inter- and intra-assay variation, and freeze/thaw stability of the analyte.

Osteoclast-Mediated GPDPLQ$_{1237}$ Release from Articular Cartilage

The release of GPDPLQ$_{1237}$ (Figure 18A) and CTX-II (Figure 18B) was measured in our osteoclastic non-calcified cartilage resorption model. GPDPLQ$_{1237}$ release was found to be mediated by both cathepsin K and MMPs. Inhibitors of cathepsin K (72.1% inhibition after subtraction of background) and MMPs (75.5%) resulted in significant inhibition of GPDPLQ$_{1237}$ release, and combination of the two inhibitors resulted in an apparent increase in GPDPLQ$_{1237}$ inhibition (91.5%), although the latter was not statistically significant compared to either inhibitor alone. CTX-II release was reduced by MMP inhibition (87.0%), but the cathepsin K inhibitor only had minimal effects (5.5%). Hence, GPDPLQ$_{1237}$ is a multi-protease biomarker of osteoclastic cartilage resorption *in vitro*, whereas CTX-II is only derived from MMP-mediated resorption.

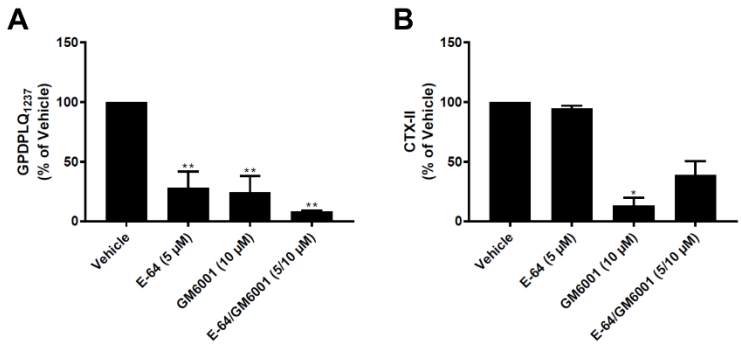

Figure 18. Osteoclast-Derived GPDPLQ$_{1237}$ and CTX-II Release from Bovine Articular Cartilage.
Osteoclasts were cultured on articular cartilage from bovine femoral condyles in the presence or absence of resorption inhibitors. Background-subtracted GPDPLQ$_{1237}$ (**A**) and CTX-II (**B**) levels in response to protease inhibitors are presented as percent of vehicle with error bars representing the SEM. Statistical significance relative to the vehicle condition is indicated by *$p < 0.05$ and **$p < 0.01$.
Adapted from **Paper V**.

Inflammation-Mediated GPDPLQ$_{1237}$ Release from Articular Cartilage

The generation of the GPDPLQ$_{1237}$ neo-epitope from bovine articular cartilage biopsies undergoing inflammation-mediated degradation was tested in samples derived from bovine cartilage explant (BEX) cultures stimulated with oncostatin M (OSM) and tumor necrosis factor α (TNFα)[374]. The neo-epitope was detected in the stimulated culture media after approximately 10 days of culture (Figure 19A), but GPDPLQ$_{1237}$ levels remained at unstimulated levels when inhibiting MMPs. Overall, GPDPLQ$_{1237}$ levels were significantly increased (Figure 19B) by OSM+TNFα stimulation (129.9 ng/ml) compared to unstimulated controls (12.0 ng/ml). The GPDPLQ$_{1237}$ increase was fully reversible by the inhibition of MMPs (10.6 ng/ml), but not by the inhibition of cysteine proteases (367.2 ng/ml). Hence, GPDPLQ$_{1237}$ is released as part of MMP-mediated degradation of inflamed cartilage *in vitro*.

GPDPLQ$_{1237}$ is Present in Rat Tibial Articular Cartilage and Growth Plates

Knees from healthy young adult female rats were used to immunolocalize the origin of the GPDPLQ$_{1237}$ neo-epitope within knee joints. Immunohistochemical analyses showed that GPDPLQ$_{1237}$ was localized to both articular cartilage and the growth plate. The articular cartilage staining was localized mainly to the ECM and pericellular spaces throughout all cartilage layers, albeit at varying intensity. The growth plates stained for GPDPLQ$_{1237}$ mainly between the columns of proliferating cells and at the proximal bone–cartilage interface. Despite its presence in relevant rat tissues, GPDPLQ$_{1237}$ was not measurable at sufficient levels in rat blood, human blood, or human urine to allow for robust technical validation of *in vivo* samples.

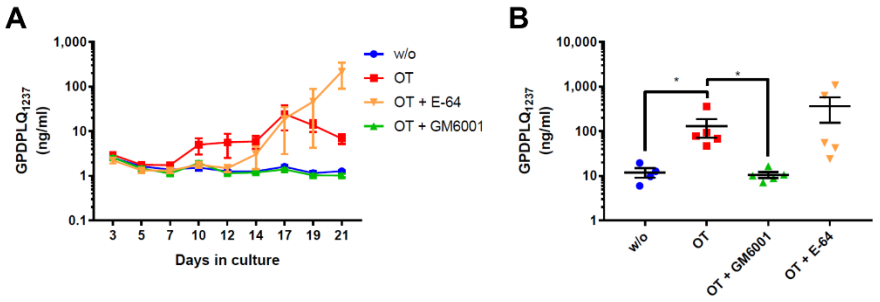

Figure 19. GPDPLQ$_{1237}$ Release into BEX Supernatants upon Stimulation and Inhibition of MMP Activity. BEX cultures were untreated (w/o), treated with OSM and TNFα (OT) without protease inhibitors, or OT with the protease inhibitors GM6001 (OT + GM6001) or E-64 (OT + E-64). Data are presented as the mean GPDPLQ$_{1237}$ levels per group at each time point throughout the experiment (**A**) and as the area under the curves (AUCs) of each individual explant (**B**). Error bars represent the SEMs. Statistical significance relative to the OT condition in the AUC data is indicated by *p < 0.05.
Adapted from **Paper V**.

Discussion

Toward Clinically Applicable Gene Therapy for IMO

The Regulation of TCIRG1

There is a medical need for new and better treatment options for IMO in addition to HSCT. In this dissertation, we have described substantial progress in the development of HSC-targeted gene therapy for TCIRG1-deficient IMO, which may facilitate and expedite treatment. A crucial issue for gene therapy application is the level of correction that is required to achieve phenotype restoration. In **Paper I**, we assessed this *in vitro* by mixing IMO HSPCs transduced with our proof-of-concept vector—using the SFFV promoter, TCIRG1 cDNA and a GFP transgene—or CB HSPCs with IMO HSPCs. Our results indicate that the level of correction needed, at least *in vitro*, is low. Similar findings have been reported in mice *in vivo*. The transplantation of lineage-depleted bone marrow cells into *oc/oc* mice without prior conditioning is sufficient for long-term survival and reversal of the phenotype, even though engraftment was only 3–5% as measured in peripheral blood[375]. These results combined with our new findings are very promising indicators of the feasibility of IMO gene therapy.

During this study, we also discovered that vector-derived TCIRG1 expression in IMO cells closely mimicked that of endogenous TCIRG1 in CB cells; without RANKL-mediated osteoclastogenesis, the TCIRG1 protein was absent. These findings indicate that the transduction protocol results in the expression of TCIRG1 specifically in osteoclasts, reducing the risk for potential off-target effects, though these effects have not been tested in other myeloid or immune cell lineages.

Different proportions of high- and low-molecular weight versions of TCIRG1 were observed between cell types in this study, and our results suggest that these different molecular weights were due to TCIRG1 being differentially glycosylated in different cell lineages. After transduction, the low-molecular weight TCIRG1 was predominant in the MSC-derived cell line HT1080, whereas the high-molecular weight TCIRG1 was predominant in HSC-derived osteoclasts. Given that TCIRG1 has different glycosylated forms and different osteopetrotic mutations can alter the ability of TCIRG1 to become glycosylated, resulting in endoplasmic reticulum retention[369], we hypothesize that glycosylations may be a contributing factor to

osteoclastogenesis-related regulation of TCIRG1. Since our study was published, new studies have shown that mutations at putative TCIRG1 N-glycosylation sites that prevent glycosylation results in increased TCIRG1 turnover by proteasomal degradation compared to the N-glycosylated forms[376]. Furthermore, non-glycosylated TCIRG1 is retained in the endoplasmic reticulum and cannot associate with the V-ATPase assembly chaperone, VMA21[376]. Hence, glycosylation is crucial for TCIRG1 stability and functional incorporation into V-ATPase complexes[376]. These findings suggest that differences in glycosylation of TCIRG1 between cell types may indeed play a role in post-translational regulation of vector-derived TCIRG1 in osteoclasts, and the absence thereof in non-osteoclast cells. The increased relative prevalence of core-glycosylated TCIRG1 in HT1080 cells compared to osteoclasts suggests that HT1080 cells do not regulate TCIRG1 through the same mechanisms as osteoclasts. However, this would need to be further studied in additional cell types, and preferably in normal rather than cancerous cell types, to get a greater understanding of whether this phenomenon is specific to osteoclastic or hematopoietic lineages. It would have been interesting to investigate this further in the transduced macrophage-like cells from the RANKL-free cultures, but this would not have been suitable due to the very limited levels of TCIRG1 detected by western blot under those conditions.

Safe and Effective IMO Gene Therapy

In **Paper II**, we used NSG mice transplanted with the corrected human IMO HSPCs to assess the rescue efficacy through *ex vivo* osteoclastogenesis of human HSPCs isolated from the mice. We evaluated a clinically relevant vector—using the EFS promoter and TCIRG1 cDNA, without a transgene marker—and found that it had maintained rescue efficacy *in vitro* and was capable of achieving partial or complete phenotype rescue *ex vivo*. As indicated by the VCN per human cell (1.96 in the complete rescue and 0.10–0.46 in the partial or no rescue), improving transduction and integration efficacy may be an important aspect for further improvement of the vector—although the VCN per human cell did not correlate with the multiplicity of infection (MOI) used for transductions. Increasing TCIRG1 expression may also prove beneficial, as several of the partial rescues had TCIRG1 levels that were not detectable by western blot, but this needs to be delicately balanced with safe levels of promoter activity. The EFS promoter used to develop the clinical vector in this paper is an intron-less form of the elongation factor 1 α (EF-1α) promoter. The EF-1α promoter is currently in use in clinical trials for X-SCID, and early data indicates that HSC-targeted gene therapy using EF-1α is effective and safe[377]. Similarly, in our experiments we demonstrated that not only was the EFS-T vector relatively effective, it also had a substantially improved safety profile in IVIM assays. Having found the clinically applicable gene therapy vector to have good efficacy and safety profiles, further development will focus on *in vivo* testing. Given currently available technology, these studies will focus on testing the rescue efficacy of hTCIRG1-

transduced *oc/oc* HSPCs in *oc/oc* mice, as this is currently the most relevant model available to test the clinical vector *in vivo*.

Generating New Models

In **Paper III**, we aimed to produce a humanized mouse model overexpressing hM-CSF in the transplanted human HSPCs to assess its potential for generating human osteoclasts *in vitro* and *in vivo*. Using lentiviral vectors to create this mouse model with HSPCs expressing hM-CSF, we obtained improvements in terms of hematopoiesis and monocyte and myeloid reconstitution, as has been previously reported in hM-CSF-expressing humanized mice[248,378]. Despite our ability to generate functional human osteoclasts from the HSPCs *in vitro* without exogenous M-CSF stimulation, we were unable to detect human osteoclasts with immunohistochemical analyses of tibial and femoral growth plates using e.g. reporter transgene and TRAP co-localization techniques. Attempts at identifying human-derived osteoclasts were further complicated by a lack of available antibodies that are suitable for the specific detection of human cells or human osteoclasts in mouse xenograft models. None of the antibodies we tested for these purposes were successful. However, hM-CSF administration also stimulates murine osteoclastogenesis *in vivo*[379], and hence both mouse osteoclasts and possibly mouse-human hybrid osteoclasts may make detection of human-derived osteoclasts difficult in our model, if spontaneous reconstitution of murine hematopoietic and osteoclastic lineages occur.

The verification of human osteoclastogenesis in our hM-CSF humanized mouse model, or a similar humanized mouse model, would make for an interesting and highly valuable model for testing whether gene therapy-treated human IMO osteoclasts differentiated *in vivo* have increased resorption, by measuring for instance serum CTX-I—assuming that endogenous osteoclast activity can be ablated. However, generating human osteoclasts in mice following gene therapy would require both a TCIRG1 transgene as well as some source of exogenous hM-CSF, which could potentially be achieved by injection[379] to avoid using additional transgenes. In order to generate a more relevant gene therapy model, *oc/oc* mice could be cross-bred with NSG mice to potentially result in immunodeficient osteopetrotic mice. Such a model could greatly facilitate the pre-clinical development of IMO gene therapy by allowing for the transplantation of corrected human HSPCs into mice to investigate if the corrected human cells are sufficient to achieve functional correction *in vivo*—but such a model system would still require exogenous hM-CSF. Given the success of the monocyte reconstitution in the hM-CSF humanized mouse, IMO HSPCs transduced with a bicistronic vector expressing both hM-CSF and human TCIRG1 could be considered an option for testing in NSG or *oc/oc*-NSG hybrid mice, and the efficacy could be tested by serum CTX-I. As we have not been able to demonstrate human osteoclasts in NSG-based

models at present, it is unclear whether such experiments are feasible due to successful treatment being dependent on generating osteoclasts that incorporate the TCIRG transgene. To date, attempts at generating *oc/oc*-NSG hybrid mice have been unsuccessful, as the off-spring seldom survives (Montano Almendras et al., unpublished data). Furthermore, in the event that NSG mice transplanted with human HSPCs have spontaneous reconstitution of murine hematopoietic and osteoclastic lineages (a highly plausible event), any effects of the transplantation may be masked by the endogenous resorption.

Other methods for developing osteopetrotic mouse strains capable of being transplanted with human HSPCs and potentially supporting human osteoclastogenesis are currently being explored. However, since these are in the very early stages, they will not be discussed in this dissertation. Another interesting possibility would be to use human bone marrow ossicles in mice. Recent studies of xenograft humanized bone marrow ossicles generated through *in situ* differentiation of human bone marrow-derived MSCs in NSG mice have reported an improved engraftment of xenotransplanted human HSCs in a humanized bone marrow niche[380]. If such a model system would be capable of sustaining a sufficient population of human osteoblasts secreting hM-CSF, this could potentially allow for human osteoclastogenesis after HSCT. However, the practical utility of such a model may be limited, given the localized nature of the model and that the model is unlikely to be devoid of normally functioning murine cells; the effects of transplanting human IMO cells with or without treatment into humanized ossicles would most likely be difficult to detect due to interfering murine cells and the lack of a systemic osteopetrotic phenotype.

Novel Approaches for IMO Treatment

In addition to the gene therapy described in this dissertation, other interesting developments that may improve the treatability of IMO have recently been described. For instance, the generation of transplantable HSCs by direct conversion of other cell types may be another option to generate a large amount of autologous HSCs[381,382] for transplantation. Similarly, *oc/oc* induced pluripotent stem cells (iPSCs) have already been developed and have shown promise in *in vitro* tests of TCIRG1-targeting gene therapy using bacterial artificial chromosomes (BACs)[383]. Human SNX10-deficient iPSCs have also been developed, but osteoclastogenesis, osteopetrotic phenotype, and functional correction have yet to be investigated in these cells[384]. Due to the rarity of IMO samples, human TCIRG1-deficient IMO iPSCs would be a valuable asset for the continued development of IMO gene therapy, and as a potential source of HSCs for gene correction and subsequent transplantation.

Remaining Questions

Regardless of the promising progress in IMO gene therapy, additional questions regarding the risk of off-target effects of IMO gene therapy remain unanswered. As previously mentioned, the *TCIRG1* gene also encodes TIRC7 through alternative splicing[172], which is a transmembrane receptor expressed on activated T cells[385]. TIRC7 is an inhibitory receptor with important roles in regulating immune responses[386]. Increased intragraft TIRC7 mRNA levels in cardiac transplants has been associated with acute rejection and TIRC7 mRNA levels are reduced in PBMCs of transplant recipients with acute cardiac rejection[387,388]. Similarly, TIRC7 plasma and mRNA levels have been observed to be elevated in patients with acute graft-versus-host disease (aGVHD), where they are associated with aGVHD severity, and decline in response to treatment[389]. TIRC7 plasma and mRNA levels have also been found to be elevated in immune thrombocytopenia patients, and to decline in response to treatment[180]. Hence, TIRC7 appears to have a role in both graft rejection and autoimmune diseases. The role of TIRC7 in osteopetrosis, if any, remains unclear, though TCIRG1-deficient IMO patients may lack TIRC7[181] depending on their TCIRG1 mutations. All TIRC7 exons, except for most of exon 1 which is a major component of its 5' untranslated region (5'UTR), including the transcription and translation start sites are included in TCIRG1 cDNA[172]. As such, following transcription of TCIRG1 cDNA, the resulting mRNA will code for the full TIRC7 amino acid sequence. Despite this, TIRC7 is unlikely to be normally expressed from the TCIRG1 cDNA, as the 5'UTR is important for translational regulation. Any ectopic TIRC7 expression from the vector should be excluded *in vitro* prior to clinical trials.

Furthermore, many IMO patients present with neurological symptoms and it is unlikely that HSC-targeted IMO gene therapy would alleviate most of these neurological symptoms, since many of these symptoms persist after HSCT[171]. It has been shown to be possible to achieve CNS-based therapeutic effects based on HSC gene therapy in e.g. early-onset metachromatic leukodystrophy[237]. However, any such therapeutic benefits in the CNS is likely to be heavily dependent on whether the HSCs and/or their progeny can enter the CNS and generate the required progeny to correct the required phenotype. In the case of the primary neurodegeneration and neuronal lysosomal storage disorders in e.g. OSTM1- and ClC-7 deficient IMO, HSC-targeted gene therapy is unlikely to be beneficial. As with HSCT for IMO, gene therapy for IMO is probably best suited for patients that do not exhibit severe neurodegenerative symptoms, as those with neurodegenerative symptoms are unlikely to benefit sufficiently enough to merit treatment.

Osteoclastic Cartilage Resorption Processes

$GPDPLQ_{1237}$ is a Multi-Protease Biomarker of Cartilage Resorption

While cartilage resorption has been described previously[249], the processes osteoclasts use when degrading cartilage have not been quantified until now; in this dissertation, we have clearly demonstrated osteoclastic resorption of cartilage and some of the processes involved *in vitro*. Using our model of osteoclastic cartilage resorption, developed in **Paper IV**, we have been able to explore some of the osteoclastic resorption processes that contribute to cartilage resorption. In **Paper V**, we used the $GPDPLQ_{1237}$ multi-protease biomarker of type II collagen degradation to demonstrate that osteoclastic resorption of type II collagen, like resorption of type I collagen, is mediated by both MMPs and cathepsin K. The weak effects of cathepsin K inhibition on the C2M and CTX-II neo-epitopes are likely due to these neo-epitopes being released mainly through MMP-mediated type II collagen degradation, rather than due to the experimental model—as cathepsin K effects on $GPDPLQ_{1237}$ were evident. Our findings clearly demonstrate that osteoclasts can resorb cartilage using MMPs and cathepsin K independently of acidification, further supporting the notion that chondroclasts are simply osteoclasts located on cartilage rather than on bone.

The Role of Acidification in Cartilage Resorption

In our studies, the main difference in resorption mechanisms between the two types of collagen-containing ECMs appears to lie in the acidification of the ECM rather than the proteases used; type I collagen in cortical bone cannot be resorbed without acidification of the resorption lacunae, in comparison to type II collagen in calcified and non-calcified cartilage which can be resorbed independently of acidification. These findings appear to be contradicted by the calcified cartilage accumulation in bones in both human and murine TCIRG1-deficient osteopetrosis[390,391]. However, this accumulation in osteopetrosis is a result of a developmental phenotype, and the effects of inhibited acidification in mature osteoclasts cultured on calcified cartilage or non-calcified cartilage *in vitro* may be different. The dispensability of acidification in our studies is likely a result of low calcification of the cartilage ECMs, at least for the non-calcified cartilage. For the calcified cartilage, it may also be due to calcified cartilage having a different mineral distribution than e.g. subchondral bone—despite having a similar mineral content[392]. Our osteochondral Ca^{2+}, cell viability and TRAP activity data indicate that the osteochondral ECM—including both calcified cartilage and subchondral bone—is less calcified than cortical bone; osteochondral Ca^{2+} release and cell viability were not affected by any antiresorptive and TRAP activity was less impacted by the V-ATPase inhibitor diphyllin than on cortical bone. Similarly, CTX-I release from osteochondral ECM

was inhibited less by diphyllin than that from cortical bone. These findings suggest that acidification was dispensable for osteochondral resorption in our model.

However, the effects of diphyllin on C2M release from both calcified and non-calcified cartilage were not consistent between experiments, ranging from inhibition to stimulation. A possible explanation is the differences in matrix content in the osteochondral ECM between matrix batches, as different batches were used for each experiment. The matrix isolation procedure may have affected the effects of diphyllin on osteochondral C2M release by altering the ratio of calcified cartilage, non-calcified cartilage and subchondral bone in the osteochondral matrix. If the osteochondral ECM contains a large proportion of non-calcified cartilage, the detected C2M may be originating from the non-calcified cartilage—which is unlikely to require acidification to be resorbed. However, the matrix isolation would not explain the inconsistent effects on C2M release from the non-calcified cartilage matrix.

Previous studies have demonstrated that osteoclasts from a Dock5 knockout mouse are unable to form sealing zones due to abnormal podosome arrangement, and as a result cannot dissolve calcified ECM[393]. Despite this, they still secrete normal levels of active cathepsin K, have unaffected lysosomal acidification and are able to resorb calcified cartilage[393]—possibly due to the differences in mineral distribution of calcified cartilage and bone[392]. However, given that both human and murine TCIRG1-deficient osteopetrosis results in the accumulation of calcified cartilage[390,391], further investigation into the role of acidification in resorbing the calcified cartilage is warranted. While the overall lack of effect of diphyllin on C2M release from either type of cartilage indicates that acidification was not required, the reason for the large variance in response to diphyllin between experiments, particularly on the non-calcified cartilage, remains unclear.

In contrast to the effects of diphyllin on C2M release from non-calcified cartilage, the effects of diphyllin on $GPDPLQ_{1237}$ release were more consistent between experiments. Unpublished data (Löfvall et al.) showed that diphyllin resulted in a reproducible inhibition (50.3%) of $GPDPLQ_{1237}$ release from resorbed non-calcified cartilage, whereas CTX-II was not inhibited. Hence, it appears that reduced acidification may negatively affect the release of type II collagen neo-epitopes that are mediated by cathepsin K, such as $GPDPLQ_{1237}$, but not those that are MMP-mediated. Given that acidification is required for cathepsin K to be activated and to be functional[394], these results indicate that the effect of V-ATPase inhibition on $GPDPLQ_{1237}$ is likely due to a suboptimal pH for cathepsin K activation and function. A previous study has indicated similar effects for type I collagen resorption from decalcified cortical bone where decalcification greatly reduced the impact of cathepsin K inhibition on CTX-I release but increased the impact of MMP inhibition[100]. Type I collagen is mainly degraded by cathepsin K[103,104], but the

relative contributions of cathepsin K and MMP are altered under decalcified conditions[100], possibly due to decreased acidification of the resorption lacunae. Furthermore, V-ATPase inhibition still reduces CTX-I release from decalcified bone, potentially through cathepsin K-mediated effects, albeit to a lesser extent than from calcified bone[100]. Additionally, cathepsin K has recently been shown to be able to activate MMP-9 in an acidic extracellular milieu[395]. However, we did not observe any effects of acidification inhibition on MMP-mediated biomarkers of cartilage resorption and this appears contradictory to the increased MMP contribution to CTX-I release from decalcified bone[100]. Given that MMPs are pH-neutral[104], a decreased acidification of the resorption lacunae might explain their increased contribution to CTX-I release on decalcified bone.

Mature murine osteoclasts seeded on calcified cartilage do not appear to form a sealing zone[393], indicating that resorption lacunae would not form and that extracellular acidification would be greatly impaired when osteoclasts are cultured on cartilage. Similarly, mature human osteoclasts seeded on decalcified bone do not form acting rings, but rather have a large number of podosomes[100]. Some osteopetrotic TCIRG1 mutations affect lysosomal acidification—which is essential for resorption of both the calcified and the non-calcified bone matrices[100]—and osteoclast-rich osteopetrosis results in an inability of osteoclasts to resorb calcified cartilage[166,170]. These studies combined with our findings indicate that acidification of the resorption lacunae is dispensable for cathepsin K-mediated cartilage resorption, at least on non-calcified cartilage, and MMP-mediated cartilage resorption in both murine and human osteoclasts, provided that lysosomal acidification remains functional. An interesting option to further explore the role of acidification and cathepsin K in generating cartilage degradation biomarkers would be to utilize osteoclasts derived from TCIRG1-deficient IMO patients carrying different mutations that affect either lysosomal acidification or lysosomal trafficking, if mutations acting in such specific ways could be found. Osteoclasts with either defective lysosomal acidification or lysosomal trafficking should both have a greatly impaired ability to generate $GPDPLQ_{1237}$ through cathepsin K-mediated proteolysis; acidic lysosomal or endolysosomal pH contributes to cathepsin K's activation and stability[396], and defective lysosomal trafficking prevents the fusion of secretory lysosomes with the ruffled border—and presumably the corresponding non-ruffled border in osteoclasts on cartilage. The role of lysosomal acidification in cathepsin K-mediated cartilage degradation could also be investigated further using lysosomotropic antiresorptives. For such experiments, the agent used to inhibit lysosomal acidifications should not affect processes that are crucial to acidifying the resorption lacunae, such as diphyllin which inhibits the V-ATPase[371]. Compounds such as chloroquine which increase the pH of lysosomes[101] and thereby inhibit bone resorption[397] could potentially be used to inhibit the pH-mediated activation of cathepsin K in lysosomes. Chloroquine may also increase the

pH in resorption lacunae to reduce cathepsin K activity in the lacunae[398], as well as increase the activity of the pH-neutral MMPs—which can be assessed using e.g. CTX-II and C2M. However, in the absence of sealing zones and lacunae acidification—as would be expected when osteoclasts are cultured on cartilage—the effects of chloroquine on cathepsin K-mediated cartilage degradation biomarkers should be due to inhibition of lysosomal acidification. However, given the lack of ruffled borders when osteoclasts are cultured on cartilage, the inhibitory effect of diphyllin on $GPDPLQ_{1237}$ is likely mediated through the same processes as those of chloroquine.

The Tissue and Protease Origins of the EKGPDPLQ Neo-Epitope

Our findings contradict the previously proposed mechanisms for generating the $GPDPLQ_{1237}$ neo-epitope as well as its proposed tissue and cellular origin. We were able to generate its release from non-calcified cartilage in both the resorption model and in the OSM+TNFα-stimulated explants, and demonstrated that both cathepsin K and MMPs can contribute to its release from cartilage resorption and that MMP contributes to its release from inflamed cartilage *in vitro*. The lack of effect of cathepsin K inhibition in the cartilage explants is likely due to this model system being predominantly MMP-mediated[333,374]. The lack of peer-reviewed scientific literature available on the neo-epitope makes it difficult to ascertain how it was originally discovered, how it was found to be present in blood, and why it was speculated to be derived specifically from cathepsin K and calcified cartilage. We performed immunohistochemistry on rat knees to investigate which knee joint compartments the neo-epitope may potentially originate from. The localization of $GPDPLQ_{1237}$ to articular cartilage suggests that $GPDPLQ_{1237}$ may be a feature of physiological articular cartilage turnover in rats, unlike CTX-II which is only present in the articular cartilage during arthritis[358]. Both $GPDPLQ_{1237}$ and CTX-II[399] are localized to the growth plate, which indicates that they are both generated during endochondral ossification. Hence, it appears that both calcified and non-calcified cartilage may generate this neo-epitope *in vivo*.

We measured the release of $GPDPLQ_{1237}$ from the osteochondral ECM in an attempt to verify its release from a calcified cartilage-containing matrix. However, the results were inconclusive (Löfvall et al., unpublished data). In some osteochondral $GPDPLQ_{1237}$ experiments, the results were very similar to those of non-calcified cartilage—with high MMP and cathepsin K contribution, along with potentially increased effect when inhibiting both proteases—but in others the protease contributions differed greatly. Hence, the osteochondral $GPDPLQ_{1237}$ data were not considered reliable, and the osteochondral ECM likely requires further optimization and refinement for use in biomarker and drug validation. The matrix isolation procedure may require better control of the relative ratio between the different

matrices included in the osteochondral ECM, and should ideally be a pure calcified cartilage matrix, to further test $GPDPLQ_{1237}$ release from calcified cartilage.

Detecting the $GPDPLQ_{1237}$ Analyte in Body Fluids

Despite $GPDPLQ_{1237}$ being a highly promising biomarker of multi-protease osteoclastic cartilage resorption *in vitro* and being present in rat cartilage, we were unable to detect it at relevant levels in animal or human body fluids. Although the neo-epitope has been proposed to be a blood-precursor to CTX-II[364–366], in most samples the $GPDPLQ_{1237}$ assay was either not able to detect the neo-epitope or the levels were too low for robust technical validation. Even blood and urine samples derived from OA and RA patients—or aggressive animal models of RA—were very low, clustered around the LLOD of the assay, and were similar to controls. These may not be the most ideal populations for testing the $GPDPLQ_{1237}$ assay; screening other patient populations with increased cartilage turnover, such as ankylosing spondylitis (AS) patients[338,400], may be another way to find human samples with strong $GPDPLQ_{1237}$ signals. Osteoclastogenesis of monocytes isolated from AS patients has been shown to be elevated *in vitro*[401], indicating that osteoclasts may play a potential role in the osteopenia observed in AS patients and potentially in cartilage degradation. To further investigate the pathological relevance of $GPDPLQ_{1237}$ *in vitro*, it would be interesting to assess if osteoclasts from AS, OA or RA patients, have altered cartilage resorption properties, similarly to previous studies of OA osteoclasts on bone[316].

According to the patents[364–366] that the $GPDPLQ_{1237}$ biomarker was based on, the neo-epitope may be degraded into the shorter neo-epitopes (including the CTX-II neo-epitope), by proteases in the kidneys and/or liver, which are later secreted in urine. How this was investigated is not clear to us, as this has not been published beyond the aforementioned patents, but the neo-epitope may only be present transiently in the blood before being further processed *in vivo*—thereby reducing the neo-epitope's blood levels to levels that are not detectable. This could be a plausible explanation as to why urine and synovial fluid CTX-II are such valuable biomarkers of human cartilage degradation whereas blood CTX-II is not; synovial fluid CTX-II is measured close to its biological source and urine CTX-II is measured after clearing, processing and filtration in the liver and kidneys (possibly resulting in the up-concentration of analytes), whereas blood CTX-II may be degraded, rapidly cleared, or be too dilute for reliable measurement. In that case, synovial fluid may be a more relevant matrix for measuring $GPDPLQ_{1237}$, but synovial fluid is not ideal for clinical use as it is not readily available and is highly invasive to sample. Furthermore, the patents also claim that the neo-epitope is only present in blood and is absent or only present at trace levels in urine and synovial fluid[364–366]. Hence there are still many questions remaining regarding the biological generation, processing and clearing of the $GPDPLQ_{1237}$ neo-epitope that may affect its utility as an *in vivo*

biomarker. The neo-epitope may also be present in other forms; the CTX-II assay uses a sandwich approach and therefore only detects multimers of neo-epitope-containing fragments. In comparison $GPDPLQ_{1237}$ is a competitive ELISA and detects both monomers and multimers. The ability of $GPDPLQ_{1237}$ to bind neo-epitopes that are dimerized between the lysine residues has been verified (Löfvall et al., unpublished data), but *in vivo* the detection of multimers may depend on the specific types of dimerization.

Technical optimization or redesigning the assay could potentially improve the sensitivity to allow for $GPDPLQ_{1237}$ detection *in vivo*. Such optimization measures could include new immunizations to produce antibodies with improved sensitivity, using other types of assay buffers, implementing sample pre-treatments before measurements, or switching the assay over to other technical platforms, e.g. sandwich ELISA, radioimmunoassay (RIA), chemiluminescence immunoassay (CLIA), electrochemiluminescence immunoassay (ECLIA), or mass spectrometry-based platforms. Except the sandwich ELISA redesign, which did not prove effective as of yet, the above listed measures have not been tested in practice to date. It remains possible that other elongated CTX-II neo-epitopes described in the patents[364–366] may have greater relevance *in vivo*, but this has yet to be tested and no assays are currently available for any of the other neo-epitopes. Further optimization of $GPDPLQ_{1237}$ and development of novel assays may shed light on the generation, processing, and release of CTX-II and CTX-II-like biomarkers that may have clinical implications for diseases, such as rheumatic diseases, with pathological cartilage turnover.

Concluding Remarks

In this dissertation, we have performed research aimed at furthering our understanding of osteoclast regulation and function—which may have important clinical implications for metabolic bone diseases and rheumatic diseases—by developing novel therapies, models, and biomarkers for osteoclast-related diseases.

The regulation of proteins that are crucial for osteoclast function are important to consider for the development of gene therapy. The risk of having ectopic transgene expression versus obtaining effective levels of gene product is a delicate balance. We have demonstrated that the risk of ectopic expression and insertional mutagenesis is low using our gene therapy vectors, and that the success rate of *ex vivo*-generated osteoclasts from transplanted HSPCs is promising for future development. Thus, we have made substantial progress toward the clinical implementation of IMO gene therapy. Further studies will focus on testing and optimizing the *in vivo* efficacy of the clinical vector construct in murine HSPCs and transplantation experiments.

Osteoclasts have long been suspected to contribute indirectly as well as directly to cartilage degradation in rheumatic diseases, but the mechanisms involved in the latter are less understood. Although we were not able to demonstrate *in vivo* relevance of $GPDPLQ_{1237}$, our studies clearly illustrate the importance of having suitable models and good biomarkers for investigating mechanisms involved in ECM turnover and biomarker generation—as e.g. protease-specific biomarkers may not be able to detect the effects of other relevant proteases on ECM turnover. Using our novel cartilage resorption model and the $GPDPLQ_{1237}$ biomarker, we demonstrated that osteoclasts degrade cartilage using both MMPs and cathepsin K in a biologically relevant setting, and that the $GPDPLQ_{1237}$ neo-epitope can be generated through MMP-mediated cartilage degradation in pro-inflammatory cartilage explants—findings that contradict the original hypothesis regarding the neo-epitope's origin and generation. Compared to our C2M and CTX-II findings from cartilage resorption, the role of cathepsin K was much more pronounced for $GPDPLQ_{1237}$—similarly to the differences in protease contribution between CTX-I and ICTP. The $GPDPLQ_{1237}$ multi-protease neo-epitope biomarker may therefore be a valuable tool to provide further pan-protease insight into cartilage degradation.

Acknowledgements

I would like to thank everyone who contributed to this dissertation and who supported me during my PhD studies.

First of all, I would like to thank **Kim Henriksen**, my supervisor at Nordic Bioscience. Without your support and guidance in osteoclast research, this work would not have been possible. I have learned so much from you and I will never forget it. Working with you has been a pure pleasure.

Secondly, I would like to thank my supervisor at Lund University, **Johan Richter**. Thank you for all your supervision and guidance, especially for the gene therapy parts of the project as well as the academic work required as part of the PhD studies. My PhD journey started with you and Ilana; first I did a summer research project in your group, followed by my Master's thesis, and now finally my PhD studies. You got me started in osteoclast biology, which was initially a sidetrack for me as I was more interested in gene therapy. I used to say to my friends that the ECM was boring, but now osteoclastic ECM remodeling is one of my specialties. It was also in your lab I met Kim Henriksen for the first time, and where I learned that Kim was looking for a PhD student, which opened so many doors for me. Thank you very much, Johan!

Deep thanks to my Nordic Bioscience co-supervisor **Christian Thudium**, who spent countless hours in the lab teaching me the methods I needed to learn, discussing data and so much more.

Another big thank you to **Ilana Moscatelli** and **Carmen Montano Almendras**, my colleagues at Lund University without whom the gene therapy aspects of this project would not have been possible. Thanks also to **Zsuzsanna Kertész** for your help during Ilana's maternity leave.

Thank you **Morten Karsdal**, CEO of Nordic Bioscience. Our discussions have taught me a lot regarding the business aspects of biomarker development, and how we make good biomarkers and create value in life science. Your insight into my work has been very valuable.

Thank you to everyone who has shared the bone office at Nordic Bioscience with me over the years, and especially the so-called "Henrik's team" who deserve special thanks: **Anna Katri**, **Hannah Newbould**, and **Aneta Dąbrowska.** Thank you for

helping me with essential parts of my research. Particular thanks to Anna, whom I have been sharing an office with for 3 years, thank you for making the work days more fun and for helping out whenever needed.

A big thank you to our technicians **Inge Kolding** and **Marianne Ladefoged**. Your technical expertise and helpful ways made the project run so much smoother than it would have done without you. Thanks also to **Susanne Djarnis** and her team for measuring calcium levels in my never-ending flow of osteoclast media.

Thank you **Anne-Christine Bay-Jensen** and **Shu Sun** for your guidance during assay development. Despite the many failures and discarded biomarker projects, I made a working biomarker in the end thanks to your guidance. Thanks to **Ditte Jonesco** for all the discussions we have had on assay development during our PhD studies.

Thank you also to all other **Nordic Bioscience colleagues** who are not specifically mentioned here. There are lots of you who made my work easier, more interesting, and more fun. I would happily fix the microscope for you any day.

Special thanks to our external collaborators **Ansgar Schulz**, **Christopher Baum**, **Axel Schambach**, **Adrian Thrasher**, **Manuel Grez**, and **Michael Rothe** who provided essential patient material, vector constructs, and performed IVIM assays.

Importantly, this project would not have been possible without the Marie Curie ITN **Euroclast**. The training and funding from Euroclast during the first three years of my PhD studies were invaluable. Thank you to all the other Euroclast PhD students—**Emma McDermott**, **Anh Tran**, **Vikte Lionikaite**, **Sara Sprangers**, **Giuliana Ascone**, **Laia Mira Pascual**, **Sandra Segeletz**, **David Massa**, **Yixuan Cao**, and **Arjen Gebraad**—for making it an unforgettable time. I hope I will get to see you all again. Thanks also to **Teun de Vries**, who was my mentor within Euroclast. Our discussions were very rewarding and they definitely helped me develop both my project and myself.

Thank you **Magnus Gustafsson**, and other members of **MentLife**, for enriching the last year of my PhD studies and giving me all the skills needed to look for jobs outside academia. We had good talks Magnus and I learned a lot from you.

Huge thanks to my **family**. To my parents, **Eva** and **Anders**, for your unconditional love and support that have enabled me to get this far. Thanks to my brother, **Erik**, for always making it fun to come home and visit. Hugs and kisses to my dear **Rachel Cheong**; thank you Rachel for making me happy, despite all the PhD student anxiety you have had to endure, and for supporting me in all my endeavors.

A special thanks to my good friends and PhD buddies **Jonatan Dereke** and **Erik Tenland**. Our time together, from biomedicine bachelor to PhD students, has been

the time of my life. I will cherish this time and I look forward to many more years of fun, hopefully with less stress from PhD studies.

Thanks to my good friend **Jacob Gustavsson**. Being friends since high school has meant a lot to me. Even though we don't get to meet as much as I wished, your friendship and support is something that I could always count on.

Finally I would like to thank the funding sources that made this research possible; thanks to **Euroclast**, **Nordic Bioscience A/S**, **The Swedish Childhood Cancer Foundation**, **The Foundations of Lund University Hospital**, **The Danish Research Foundation**, and **Rocket Pharma**.

References

1. Bushinsky, D. A. Acid-base imbalance and the skeleton. *Eur. J. Nutr.* **40,** 238–44 (2001).
2. Mohan, S. & Baylink, D. J. Bone growth factors. *Clin. Orthop. Relat. Res.* 30–48 (1991).
3. Taichman, R. S. Blood and bone: two tissues whose fates are intertwined to create the hematopoietic stem-cell niche. *Blood* **105,** 2631–9 (2005).
4. Clarke, B. Normal bone anatomy and physiology. *Clin. J. Am. Soc. Nephrol.* **3 Suppl 3,** S131-9 (2008).
5. Seeman, E. & Delmas, P. D. Bone quality—the material and structural basis of bone strength and fragility. *N. Engl. J. Med.* **354,** 2250–61 (2006).
6. Boskey, A. L. Mineralization of Bones and Teeth. *Elements* **3,** 385–391 (2007).
7. Young, M. F. Bone matrix proteins: their function, regulation, and relationship to osteoporosis. *Osteoporos. Int.* **14 Suppl 3,** S35-42 (2003).
8. Marrella, A. *et al.* Engineering vascularized and innervated bone biomaterials for improved skeletal tissue regeneration. *Mater. Today* **21,** 362–376 (2018).
9. Capulli, M., Paone, R. & Rucci, N. Osteoblast and osteocyte: games without frontiers. *Arch. Biochem. Biophys.* **561,** 3–12 (2014).
10. Kronenberg, H. M. Developmental regulation of the growth plate. *Nature* **423,** 332–6 (2003).
11. Mackie, E. J., Ahmed, Y. A., Tatarczuch, L., Chen, K.-S. & Mirams, M. Endochondral ossification: how cartilage is converted into bone in the developing skeleton. *Int. J. Biochem. Cell Biol.* **40,** 46–62 (2008).
12. Fonović, M. & Turk, B. Cysteine cathepsins and extracellular matrix degradation. *Biochim. Biophys. Acta* **1840,** 2560–70 (2014).
13. Fratzl-Zelman, N. *et al.* Decreased bone turnover and deterioration of bone structure in two cases of pycnodysostosis. *J. Clin. Endocrinol. Metab.* **89,** 1538–47 (2004).
14. Ortega, N., Behonick, D. J. & Werb, Z. Matrix remodeling during endochondral ossification. *Trends Cell Biol.* **14,** 86–93 (2004).
15. Currey, J. D. The mechanical consequences of variation in the mineral content of bone. *J. Biomech.* **2,** 1–11 (1969).
16. Ciarelli, T. E., Fyhrie, D. P. & Parfitt, A. M. Effects of vertebral bone fragility and bone formation rate on the mineralization levels of cancellous bone from white females. *Bone* **32,** 311–5 (2003).

17. Manolagas, S. C. Birth and death of bone cells: basic regulatory mechanisms and implications for the pathogenesis and treatment of osteoporosis. *Endocr. Rev.* **21,** 115–37 (2000).
18. Aubin, J. E. Regulation of osteoblast formation and function. *Rev. Endocr. Metab. Disord.* **2,** 81–94 (2001).
19. Schaffler, M. B., Cheung, W.-Y., Majeska, R. & Kennedy, O. Osteocytes: master orchestrators of bone. *Calcif. Tissue Int.* **94,** 5–24 (2014).
20. Heckman, C. A. & Plummer, H. K. Filopodia as sensors. *Cell. Signal.* **25,** 2298–311 (2013).
21. Wein, M. N. Bone Lining Cells: Normal Physiology and Role in Response to Anabolic Osteoporosis Treatments. *Curr. Mol. Biol. Reports* **3,** 79–84 (2017).
22. Matic, I. *et al.* Quiescent Bone Lining Cells Are a Major Source of Osteoblasts During Adulthood. *Stem Cells* **34,** 2930–2942 (2016).
23. Roughley, P. J. & Mort, J. S. The role of aggrecan in normal and osteoarthritic cartilage. *J. Exp. Orthop.* **1,** 8 (2014).
24. Alford, J. W. & Cole, B. J. Cartilage restoration, part 1: basic science, historical perspective, patient evaluation, and treatment options. *Am. J. Sports Med.* **33,** 295–306 (2005).
25. Bay-Jensen, A. C., Thudium, C. S. & Mobasheri, A. Development and use of biochemical markers in osteoarthritis: current update. *Curr. Opin. Rheumatol.* **30,** 121–128 (2018).
26. Mow, V. C., Ratcliffe, A. & Poole, A. R. Cartilage and diarthrodial joints as paradigms for hierarchical materials and structures. *Biomaterials* **13,** 67–97 (1992).
27. Sophia Fox, A. J., Bedi, A. & Rodeo, S. A. The basic science of articular cartilage: structure, composition, and function. *Sports Health* **1,** 461–8 (2009).
28. Gudmann, N. S. & Karsdal, M. A. Type II Collagen. in *Biochemistry of Collagens, Laminins and Elastin* **1,** 13–20 (Elsevier, 2016).
29. Gelse, K., Pöschl, E. & Aigner, T. Collagens—structure, function, and biosynthesis. *Adv. Drug Deliv. Rev.* **55,** 1531–46 (2003).
30. Kannu, P., Bateman, J. & Savarirayan, R. Clinical phenotypes associated with type II collagen mutations. *J. Paediatr. Child Health* **48,** E38-43 (2012).
31. Dabiri, Y. & Li, L. P. Influences of the depth-dependent material inhomogeneity of articular cartilage on the fluid pressurization in the human knee. *Med. Eng. Phys.* **35,** 1591–8 (2013).
32. Moore, A. C. & Burris, D. L. An analytical model to predict interstitial lubrication of cartilage in migrating contact areas. *J. Biomech.* **47,** 148–53 (2014).
33. Mahjoub, M., Berenbaum, F. & Houard, X. Why subchondral bone in osteoarthritis? The importance of the cartilage bone interface in osteoarthritis. *Osteoporos. Int.* **23 Suppl 8,** S841-6 (2012).
34. Mapp, P. I. & Walsh, D. A. Mechanisms and targets of angiogenesis and nerve growth in osteoarthritis. *Nat. Rev. Rheumatol.* **8,** 390–8 (2012).
35. Clark, J. M. The structure of vascular channels in the subchondral plate. *J. Anat.* **171,** 105–15 (1990).

36. Goldring, S. R. & Goldring, M. B. Changes in the osteochondral unit during osteoarthritis: structure, function and cartilage-bone crosstalk. *Nat. Rev. Rheumatol.* **12,** 632–644 (2016).
37. Burr, D. B. & Gallant, M. a. Bone remodelling in osteoarthritis. *Nat. Rev. Rheumatol.* **8,** 665–73 (2012).
38. Pan, J. *et al.* Elevated cross-talk between subchondral bone and cartilage in osteoarthritic joints. *Bone* **51,** 212–7 (2012).
39. Pouran, B. *et al.* Solute transport at the interface of cartilage and subchondral bone plate: Effect of micro-architecture. *J. Biomech.* **52,** 148–154 (2017).
40. Shalhoub, V. *et al.* Characterization of osteoclast precursors in human blood. *Br. J. Haematol.* **111,** 501–12 (2000).
41. Way, K. J. *et al.* The generation and properties of human macrophage populations from hemopoietic stem cells. *J. Leukoc. Biol.* **85,** 766–78 (2009).
42. Tondravi, M. M. *et al.* Osteopetrosis in mice lacking haematopoietic transcription factor PU.1. *Nature* **386,** 81–4 (1997).
43. Han, Y., You, X., Xing, W., Zhang, Z. & Zou, W. Paracrine and endocrine actions of bone-the functions of secretory proteins from osteoblasts, osteocytes, and osteoclasts. *Bone Res.* **6,** 16 (2018).
44. Fuller, K. *et al.* Macrophage colony-stimulating factor stimulates survival and chemotactic behavior in isolated osteoclasts. *J. Exp. Med.* **178,** 1733–44 (1993).
45. Tanaka, S. *et al.* Macrophage colony-stimulating factor is indispensable for both proliferation and differentiation of osteoclast progenitors. *J. Clin. Invest.* **91,** 257–63 (1993).
46. Quinn, J. M., Elliott, J., Gillespie, M. T. & Martin, T. J. A combination of osteoclast differentiation factor and macrophage-colony stimulating factor is sufficient for both human and mouse osteoclast formation in vitro. *Endocrinology* **139,** 4424–7 (1998).
47. Lacey, D. L. *et al.* Osteoprotegerin ligand is a cytokine that regulates osteoclast differentiation and activation. *Cell* **93,** 165–76 (1998).
48. Yasuda, H. *et al.* Osteoclast differentiation factor is a ligand for osteoprotegerin/osteoclastogenesis-inhibitory factor and is identical to TRANCE/RANKL. *Proc. Natl. Acad. Sci. U. S. A.* **95,** 3597–602 (1998).
49. Simonet, W. S. *et al.* Osteoprotegerin: a novel secreted protein involved in the regulation of bone density. *Cell* **89,** 309–19 (1997).
50. Tsuda, E. *et al.* Isolation of a novel cytokine from human fibroblasts that specifically inhibits osteoclastogenesis. *Biochem. Biophys. Res. Commun.* **234,** 137–42 (1997).
51. Hakeda, Y. *et al.* Osteoclastogenesis inhibitory factor (OCIF) directly inhibits bone-resorbing activity of isolated mature osteoclasts. *Biochem. Biophys. Res. Commun.* **251,** 796–801 (1998).
52. Arai, F. *et al.* Commitment and differentiation of osteoclast precursor cells by the sequential expression of c-Fms and receptor activator of nuclear factor kappaB (RANK) receptors. *J. Exp. Med.* **190,** 1741–54 (1999).
53. Yao, G.-Q., Sun, B. H., Weir, E. C. & Insogna, K. L. A role for cell-surface CSF-1 in osteoblast-mediated osteoclastogenesis. *Calcif. Tissue Int.* **70,** 339–46 (2002).

54. Faccio, R., Takeshita, S., Zallone, A., Ross, F. P. & Teitelbaum, S. L. c-Fms and the alphavbeta3 integrin collaborate during osteoclast differentiation. *J. Clin. Invest.* **111,** 749–58 (2003).
55. Zou, W., Reeve, J. L., Liu, Y., Teitelbaum, S. L. & Ross, F. P. DAP12 couples c-Fms activation to the osteoclast cytoskeleton by recruitment of Syk. *Mol. Cell* **31,** 422–31 (2008).
56. Theoleyre, S. *et al.* The molecular triad OPG/RANK/RANKL: involvement in the orchestration of pathophysiological bone remodeling. *Cytokine Growth Factor Rev.* **15,** 457–75 (2004).
57. Luo, J. *et al.* LGR4 is a receptor for RANKL and negatively regulates osteoclast differentiation and bone resorption. *Nat. Med.* **22,** 539–46 (2016).
58. Ross, F. P. RANKing the importance of measles virus in Paget's disease. *J. Clin. Invest.* **105,** 555–8 (2000).
59. Takayanagi, H. *et al.* Induction and activation of the transcription factor NFATc1 (NFAT2) integrate RANKL signaling in terminal differentiation of osteoclasts. *Dev. Cell* **3,** 889–901 (2002).
60. Wang, Z. Q. *et al.* Bone and haematopoietic defects in mice lacking c-fos. *Nature* **360,** 741–5 (1992).
61. Li, J. *et al.* RANK is the intrinsic hematopoietic cell surface receptor that controls osteoclastogenesis and regulation of bone mass and calcium metabolism. *Proc. Natl. Acad. Sci. U. S. A.* **97,** 1566–71 (2000).
62. Zhao, Q., Shao, J., Chen, W. & Li, Y.-P. Osteoclast differentiation and gene regulation. *Front. Biosci.* **12,** 2519–29 (2007).
63. Yagi, M. *et al.* DC-STAMP is essential for cell-cell fusion in osteoclasts and foreign body giant cells. *J. Exp. Med.* **202,** 345–51 (2005).
64. Yang, M. *et al.* Osteoclast stimulatory transmembrane protein (OC-STAMP), a novel protein induced by RANKL that promotes osteoclast differentiation. *J. Cell. Physiol.* **215,** 497–505 (2008).
65. Halleen, J. M. *et al.* Intracellular fragmentation of bone resorption products by reactive oxygen species generated by osteoclastic tartrate-resistant acid phosphatase. *J. Biol. Chem.* **274,** 22907–10 (1999).
66. Lecaille, F., Brömme, D. & Lalmanach, G. Biochemical properties and regulation of cathepsin K activity. *Biochimie* **90,** 208–26 (2008).
67. Everts, V. *et al.* Degradation of collagen in the bone-resorbing compartment underlying the osteoclast involves both cysteine-proteinases and matrix metalloproteinases. *J. Cell. Physiol.* **150,** 221–31 (1992).
68. Kornak, U. *et al.* Loss of the ClC-7 chloride channel leads to osteopetrosis in mice and man. *Cell* **104,** 205–15 (2001).
69. Leisle, L., Ludwig, C. F., Wagner, F. A., Jentsch, T. J. & Stauber, T. ClC-7 is a slowly voltage-gated 2Cl(-)/1H(+)-exchanger and requires Ostm1 for transport activity. *EMBO J.* **30,** 2140–52 (2011).

70. Lange, P. F., Wartosch, L., Jentsch, T. J. & Fuhrmann, J. C. ClC-7 requires Ostm1 as a beta-subunit to support bone resorption and lysosomal function. *Nature* **440,** 220–3 (2006).
71. Saroussi, S. & Nelson, N. The little we know on the structure and machinery of V-ATPase. *J. Exp. Biol.* **212,** 1604–10 (2009).
72. Frattini, A. *et al.* Defects in TCIRG1 subunit of the vacuolar proton pump are responsible for a subset of human autosomal recessive osteopetrosis. *Nat. Genet.* **25,** 343–346 (2000).
73. Kornak, U. *et al.* Mutations in the a3 subunit of the vacuolar H(+)-ATPase cause infantile malignant osteopetrosis. *Hum. Mol. Genet.* **9,** 2059–63 (2000).
74. Gay, C. V & Mueller, W. J. Carbonic anhydrase and osteoclasts: localization by labeled inhibitor autoradiography. *Science* **183,** 432–4 (1974).
75. Lehenkari, P., Hentunen, T. A., Laitala-Leinonen, T., Tuukkanen, J. & Väänänen, H. K. Carbonic anhydrase II plays a major role in osteoclast differentiation and bone resorption by effecting the steady state intracellular pH and Ca2+. *Exp. Cell Res.* **242,** 128–37 (1998).
76. Jansen, I. D. C. *et al.* Ae2(a,b)-deficient mice exhibit osteopetrosis of long bones but not of calvaria. *FASEB J.* **23,** 3470–81 (2009).
77. Pondel, M. Calcitonin and calcitonin receptors: bone and beyond. *Int. J. Exp. Pathol.* **81,** 405–22 (2000).
78. Horton, M. A., Taylor, M. L., Arnett, T. R. & Helfrich, M. H. Arg-Gly-Asp (RGD) peptides and the anti-vitronectin receptor antibody 23C6 inhibit dentine resorption and cell spreading by osteoclasts. *Exp. Cell Res.* **195,** 368–75 (1991).
79. Helfrich, M. H., Nesbitt, S. A., Dorey, E. L. & Horton, M. A. Rat osteoclasts adhere to a wide range of RGD (Arg-Gly-Asp) peptide-containing proteins, including the bone sialoproteins and fibronectin, via a beta 3 integrin. *J. Bone Miner. Res.* **7,** 335–43 (1992).
80. Chambers, T. J. & Fuller, K. How are osteoclasts induced to resorb bone? *Ann. N. Y. Acad. Sci.* **1240,** 1–6 (2011).
81. Abu-Amer, Y., Ross, F. P., Schlesinger, P., Tondravi, M. M. & Teitelbaum, S. L. Substrate recognition by osteoclast precursors induces C-src/microtubule association. *J. Cell Biol.* **137,** 247–58 (1997).
82. Teitelbaum, S. L. Osteoclasts: what do they do and how do they do it? *Am. J. Pathol.* **170,** 427–435 (2007).
83. Boyle, W. J., Simonet, W. S. & Lacey, D. L. Osteoclast differentiation and activation. *Nature* **423,** 337–42 (2003).
84. Zou, W. & Teitelbaum, S. L. Integrins, growth factors, and the osteoclast cytoskeleton. *Ann. N. Y. Acad. Sci.* **1192,** 27–31 (2010).
85. Zou, W. *et al.* Syk, c-Src, the alphavbeta3 integrin, and ITAM immunoreceptors, in concert, regulate osteoclastic bone resorption. *J. Cell Biol.* **176,** 877–88 (2007).
86. Matsumoto, N. *et al.* Essential Role of the a3 Isoform of V-ATPase in Secretory Lysosome Trafficking via Rab7 Recruitment. *Sci. Rep.* **8,** 6701 (2018).

87. Väänänen, H. K. & Horton, M. The osteoclast clear zone is a specialized cell-extracellular matrix adhesion structure. *J. Cell Sci.* **108 (Pt 8,** 2729–32 (1995).

88. Lakkakorpi, P., Tuukkanen, J., Hentunen, T., Järvelin, K. & Väänänen, K. Organization of osteoclast microfilaments during the attachment to bone surface in vitro. *J. Bone Miner. Res.* **4,** 817–25 (1989).

89. Baron, R., Neff, L., Louvard, D. & Courtoy, P. J. Cell-mediated extracellular acidification and bone resorption: evidence for a low pH in resorbing lacunae and localization of a 100-kD lysosomal membrane protein at the osteoclast ruffled border. *J. Cell Biol.* **101,** 2210–22 (1985).

90. Toyomura, T., Oka, T., Yamaguchi, C., Wada, Y. & Futai, M. Three subunit a isoforms of mouse vacuolar H(+)-ATPase. Preferential expression of the a3 isoform during osteoclast differentiation. *J. Biol. Chem.* **275,** 8760–5 (2000).

91. Blair, H. C., Teitelbaum, S. L., Ghiselli, R. & Gluck, S. Osteoclastic bone resorption by a polarized vacuolar proton pump. *Science* **245,** 855–7 (1989).

92. Kasper, D. *et al.* Loss of the chloride channel ClC-7 leads to lysosomal storage disease and neurodegeneration. *EMBO J.* **24,** 1079–91 (2005).

93. Schaller, S., Henriksen, K., Sørensen, M. G. & Karsdal, M. A. The role of chloride channels in osteoclasts: ClC-7 as a target for osteoporosis treatment. *Drug News Perspect.* **18,** 489–95 (2005).

94. Schlesinger, P. H., Blair, H. C., Teitelbaum, S. L. & Edwards, J. C. Characterization of the osteoclast ruffled border chloride channel and its role in bone resorption. *J. Biol. Chem.* **272,** 18636–43 (1997).

95. Henriksen, K. *et al.* Characterization of osteoclasts from patients harboring a G215R mutation in ClC-7 causing autosomal dominant osteopetrosis type II. *Am. J. Pathol.* **164,** 1537–45 (2004).

96. Henriksen, K. *et al.* Ion transporters involved in acidification of the resorption lacuna in osteoclasts. *Calcif. Tissue Int.* **83,** 230–42 (2008).

97. Teti, A. *et al.* Extracellular protons acidify osteoclasts, reduce cytosolic calcium, and promote expression of cell-matrix attachment structures. *J. Clin. Invest.* **84,** 773–80 (1989).

98. Lorget, F. *et al.* High extracellular calcium concentrations directly stimulate osteoclast apoptosis. *Biochem. Biophys. Res. Commun.* **268,** 899–903 (2000).

99. Bossard, M. J. *et al.* Proteolytic activity of human osteoclast cathepsin K. *J. Biol. Chem.* **271,** 12517–12524 (1996).

100. Henriksen, K. *et al.* Degradation of the organic phase of bone by osteoclasts: a secondary role for lysosomal acidification. *J. Bone Miner. Res.* **21,** 58–66 (2006).

101. Otto, H.-H. & Schirmeister, T. Cysteine Proteases and Their Inhibitors. *Chem. Rev.* **97,** 133–172 (1997).

102. Gelb, B. D., Shi, G. P., Chapman, H. A. & Desnick, R. J. Pycnodysostosis, a lysosomal disease caused by cathepsin K deficiency. *Science* **273,** 1236–8 (1996).

103. Delaissé, J.-M. *et al.* Matrix metalloproteinases (MMP) and cathepsin K contribute differently to osteoclastic activities. *Microsc. Res. Tech.* **61,** 504–13 (2003).

104. Garnero, P. *et al.* The type I collagen fragments ICTP and CTX reveal distinct enzymatic pathways of bone collagen degradation. *J. Bone Miner. Res.* **18,** 859–67 (2003).
105. Page-McCaw, A., Ewald, A. J. & Werb, Z. Matrix metalloproteinases and the regulation of tissue remodelling. *Nat. Rev. Mol. Cell Biol.* **8,** 221–33 (2007).
106. Rodríguez, D., Morrison, C. J. & Overall, C. M. Matrix metalloproteinases: what do they not do? New substrates and biological roles identified by murine models and proteomics. *Biochim. Biophys. Acta* **1803,** 39–54 (2010).
107. Hou, P. *et al.* Matrix metalloproteinase-12 (MMP-12) in osteoclasts: new lesson on the involvement of MMPs in bone resorption. *Bone* **34,** 37–47 (2004).
108. Halleen, J. M. *et al.* Tartrate-resistant acid phosphatase 5b: a novel serum marker of bone resorption. *J. Bone Miner. Res.* **15,** 1337–45 (2000).
109. Minkin, C. Bone acid phosphatase: tartrate-resistant acid phosphatase as a marker of osteoclast function. *Calcif. Tissue Int.* **34,** 285–90 (1982).
110. Nesbitt, S. A. & Horton, M. A. Trafficking of matrix collagens through bone-resorbing osteoclasts. *Science* **276,** 266–9 (1997).
111. Egbuna, O. I. & Brown, E. M. Hypercalcaemic and hypocalcaemic conditions due to calcium-sensing receptor mutations. *Best Pract. Res. Clin. Rheumatol.* **22,** 129–48 (2008).
112. Silva, B. C. & Bilezikian, J. P. Parathyroid hormone: anabolic and catabolic actions on the skeleton. *Curr. Opin. Pharmacol.* **22,** 41–50 (2015).
113. Fermor, B. & Skerry, T. M. PTH/PTHrP receptor expression on osteoblasts and osteocytes but not resorbing bone surfaces in growing rats. *J. Bone Miner. Res.* **10,** 1935–43 (1995).
114. Datta, N. S. & Abou-Samra, A. B. PTH and PTHrP signaling in osteoblasts. *Cell. Signal.* **21,** 1245–54 (2009).
115. Lee, S. K. & Lorenzo, J. A. Parathyroid hormone stimulates TRANCE and inhibits osteoprotegerin messenger ribonucleic acid expression in murine bone marrow cultures: correlation with osteoclast-like cell formation. *Endocrinology* **140,** 3552–61 (1999).
116. Kanzawa, M., Sugimoto, T., Kanatani, M. & Chihara, K. Involvement of osteoprotegerin/osteoclastogenesis inhibitory factor in the stimulation of osteoclast formation by parathyroid hormone in mouse bone cells. *Eur. J. Endocrinol.* **142,** 661–4 (2000).
117. O'Brien, C. A., Nakashima, T. & Takayanagi, H. Osteocyte control of osteoclastogenesis. *Bone* **54,** 258–63 (2013).
118. Li, X. *et al.* Parathyroid hormone stimulates osteoblastic expression of MCP-1 to recruit and increase the fusion of pre/osteoclasts. *J. Biol. Chem.* **282,** 33098–106 (2007).
119. Kameda, T. *et al.* Estrogen inhibits bone resorption by directly inducing apoptosis of the bone-resorbing osteoclasts. *J. Exp. Med.* **186,** 489–95 (1997).

120. Song, T. *et al.* Regulation of TRPV5 transcription and expression by E2/ERα signalling contributes to inhibition of osteoclastogenesis. *J. Cell. Mol. Med.* (2018). doi:10.1111/jcmm.13718
121. García Palacios, V. *et al.* Negative regulation of RANKL-induced osteoclastic differentiation in RAW264.7 Cells by estrogen and phytoestrogens. *J. Biol. Chem.* **280,** 13720–7 (2005).
122. Nakamura, T. *et al.* Estrogen prevents bone loss via estrogen receptor alpha and induction of Fas ligand in osteoclasts. *Cell* **130,** 811–23 (2007).
123. Denger, S., Reid, G. & Gannon, F. Expression of the estrogen receptor during differentiation of human osteoclasts. *Steroids* **73,** 765–74 (2008).
124. Bellido, T. Osteocyte-driven bone remodeling. *Calcif. Tissue Int.* **94,** 25–34 (2014).
125. Perez-Amodio, S., Beertsen, W. & Everts, V. (Pre-)osteoclasts induce retraction of osteoblasts before their fusion to osteoclasts. *J. Bone Miner. Res.* **19,** 1722–31 (2004).
126. Kristensen, H. B., Andersen, T. L., Marcussen, N., Rolighed, L. & Delaisse, J.-M. Osteoblast recruitment routes in human cancellous bone remodeling. *Am. J. Pathol.* **184,** 778–89 (2014).
127. Bi, L. X., Mainous, E. G., Yngve, D. A. & Buford, W. L. Cellular isolation, culture and characterization of the marrow sac cells in human tubular bone. *J. Musculoskelet. Neuronal Interact.* **8,** 43–9 (2008).
128. Kristensen, H. B., Andersen, T. L., Marcussen, N., Rolighed, L. & Delaisse, J.-M. Increased presence of capillaries next to remodeling sites in adult human cancellous bone. *J. Bone Miner. Res.* **28,** 574–85 (2013).
129. Abdelgawad, M. E. *et al.* Early reversal cells in adult human bone remodeling: osteoblastic nature, catabolic functions and interactions with osteoclasts. *Histochem. Cell Biol.* **145,** 603–15 (2016).
130. Lassen, N. E. *et al.* Coupling of Bone Resorption and Formation in Real Time: New Knowledge Gained From Human Haversian BMUs. *J. Bone Miner. Res.* **32,** 1395–1405 (2017).
131. Wergedal, J. E. & Baylink, D. J. Distribution of acid and alkaline phosphatase activity in undemineralized sections of the rat tibial diaphysis. *J. Histochem. Cytochem.* **17,** 799–806 (1969).
132. Sheu, T.-J. *et al.* A phage display technique identifies a novel regulator of cell differentiation. *J. Biol. Chem.* **278,** 438–43 (2003).
133. Andersen, T. L. *et al.* Understanding coupling between bone resorption and formation: are reversal cells the missing link? *Am. J. Pathol.* **183,** 235–46 (2013).
134. Sims, N. A. & Martin, T. J. Coupling Signals between the Osteoclast and Osteoblast: How are Messages Transmitted between These Temporary Visitors to the Bone Surface? *Front. Endocrinol. (Lausanne).* **6,** 41 (2015).
135. Henriksen, K., Karsdal, M. A. & Martin, T. J. Osteoclast-derived coupling factors in bone remodeling. *Calcif. Tissue Int.* **94,** 88–97 (2014).
136. Sims, N. A. & Martin, T. J. Coupling the activities of bone formation and resorption: a multitude of signals within the basic multicellular unit. *Bonekey Rep.* **3,** 481 (2014).

137. Winkler, D. G. *et al.* Osteocyte control of bone formation via sclerostin, a novel BMP antagonist. *EMBO J.* **22,** 6267–76 (2003).

138. Wijenayaka, A. R. *et al.* Sclerostin stimulates osteocyte support of osteoclast activity by a RANKL-dependent pathway. *PLoS One* **6,** e25900 (2011).

139. Kogawa, M. *et al.* Sclerostin regulates release of bone mineral by osteocytes by induction of carbonic anhydrase 2. *J. Bone Miner. Res.* **28,** 2436–48 (2013).

140. Takayanagi, H. *et al.* RANKL maintains bone homeostasis through c-Fos-dependent induction of interferon-beta. *Nature* **416,** 744–9 (2002).

141. Simic, P. *et al.* Systemically administered bone morphogenetic protein-6 restores bone in aged ovariectomized rats by increasing bone formation and suppressing bone resorption. *J. Biol. Chem.* **281,** 25509–21 (2006).

142. Garimella, R. *et al.* Expression and synthesis of bone morphogenetic proteins by osteoclasts: a possible path to anabolic bone remodeling. *J. Histochem. Cytochem.* **56,** 569–77 (2008).

143. Pederson, L., Ruan, M., Westendorf, J. J., Khosla, S. & Oursler, M. J. Regulation of bone formation by osteoclasts involves Wnt/BMP signaling and the chemokine sphingosine-1-phosphate. *Proc. Natl. Acad. Sci. U. S. A.* **105,** 20764–9 (2008).

144. Takeshita, S. *et al.* Osteoclast-secreted CTHRC1 in the coupling of bone resorption to formation. *J. Clin. Invest.* **123,** 3914–24 (2013).

145. Ryu, J. *et al.* Sphingosine 1-phosphate as a regulator of osteoclast differentiation and osteoclast-osteoblast coupling. *EMBO J.* **25,** 5840–51 (2006).

146. Negishi-Koga, T. *et al.* Suppression of bone formation by osteoclastic expression of semaphorin 4D. *Nat. Med.* **17,** 1473–80 (2011).

147. Walker, E. C. *et al.* Cardiotrophin-1 is an osteoclast-derived stimulus of bone formation required for normal bone remodeling. *J. Bone Miner. Res.* **23,** 2025–32 (2008).

148. Kreja, L. *et al.* Non-resorbing osteoclasts induce migration and osteogenic differentiation of mesenchymal stem cells. *J. Cell. Biochem.* **109,** 347–55 (2010).

149. Zhao, C. *et al.* Bidirectional ephrinB2-EphB4 signaling controls bone homeostasis. *Cell Metab.* **4,** 111–21 (2006).

150. Bennett, C. N. *et al.* Regulation of osteoblastogenesis and bone mass by Wnt10b. *Proc. Natl. Acad. Sci. U. S. A.* **102,** 3324–9 (2005).

151. Maeda, K. *et al.* Wnt5a-Ror2 signaling between osteoblast-lineage cells and osteoclast precursors enhances osteoclastogenesis. *Nat. Med.* **18,** 405–12 (2012).

152. Kobayashi, Y., Uehara, S., Koide, M. & Takahashi, N. The regulation of osteoclast differentiation by Wnt signals. *Bonekey Rep.* **4,** 713 (2015).

153. Movérare-Skrtic, S. *et al.* Osteoblast-derived WNT16 represses osteoclastogenesis and prevents cortical bone fragility fractures. *Nat. Med.* **20,** 1279–88 (2014).

154. Li, Z. *et al.* The Role of Semaphorin 3A in Bone Remodeling. *Front. Cell. Neurosci.* **11,** 40 (2017).

155. Kanis, J. A., Melton, L. J., Christiansen, C., Johnston, C. C. & Khaltaev, N. The diagnosis of osteoporosis. *J. Bone Miner. Res.* **9,** 1137–41 (1994).

156. Jensen, P. R. *et al.* A supra-cellular model for coupling of bone resorption to formation during remodeling: lessons from two bone resorption inhibitors affecting bone formation differently. *Biochem. Biophys. Res. Commun.* **443,** 694–9 (2014).
157. Compston, J. *et al.* UK clinical guideline for the prevention and treatment of osteoporosis. *Arch. Osteoporos.* **12,** 43 (2017).
158. Drake, M. T., Clarke, B. L. & Khosla, S. Bisphosphonates: mechanism of action and role in clinical practice. *Mayo Clin. Proc.* **83,** 1032–45 (2008).
159. Fleisch, H., Russell, R. G. & Straumann, F. Effect of pyrophosphate on hydroxyapatite and its implications in calcium homeostasis. *Nature* **212,** 901–3 (1966).
160. Russell, R. G., Mühlbauer, R. C., Bisaz, S., Williams, D. A. & Fleisch, H. The influence of pyrophosphate, condensed phosphates, phosphonates and other phosphate compounds on the dissolution of hydroxyapatite in vitro and on bone resorption induced by parathyroid hormone in tissue culture and in thyroparathyroidectomised rats. *Calcif. Tissue Res.* **6,** 183–96 (1970).
161. Frith, J. C., Mönkkönen, J., Blackburn, G. M., Russell, R. G. & Rogers, M. J. Clodronate and liposome-encapsulated clodronate are metabolized to a toxic ATP analog, adenosine 5'-(beta, gamma-dichloromethylene) triphosphate, by mammalian cells in vitro. *J. Bone Miner. Res.* **12,** 1358–67 (1997).
162. Hall, A. Rho GTPases and the actin cytoskeleton. *Science* **279,** 509–14 (1998).
163. Luckman, S. P. *et al.* Nitrogen-containing bisphosphonates inhibit the mevalonate pathway and prevent post-translational prenylation of GTP-binding proteins, including Ras. *J. Bone Miner. Res.* **13,** 581–9 (1998).
164. Palagano, E., Menale, C., Sobacchi, C. & Villa, A. Genetics of Osteopetrosis. *Curr. Osteoporos. Rep.* **16,** 13–25 (2018).
165. Fasth, A. & Porras, O. Human malignant osteopetrosis: pathophysiology, management and the role of bone marrow transplantation. *Pediatr. Transplant.* **3 Suppl 1,** 102–7 (1999).
166. Sobacchi, C., Schulz, A., Coxon, F. P., Villa, A. & Helfrich, M. H. Osteopetrosis: genetics, treatment and new insights into osteoclast function. *Nat. Rev. Endocrinol.* **9,** 522–36 (2013).
167. Balemans, W., Van Wesenbeeck, L. & Van Hul, W. A clinical and molecular overview of the human osteopetroses. *Calcif. Tissue Int.* **77,** 263–74 (2005).
168. Del Fattore, A. *et al.* Clinical, genetic, and cellular analysis of 49 osteopetrotic patients: implications for diagnosis and treatment. *J. Med. Genet.* **43,** 315–25 (2006).
169. Villa, A., Guerrini, M. M., Cassani, B., Pangrazio, A. & Sobacchi, C. Infantile malignant, autosomal recessive osteopetrosis: the rich and the poor. *Calcif. Tissue Int.* **84,** 1–12 (2009).
170. Henriksen, K. *et al.* Dissociation of bone resorption and bone formation in adult mice with a non-functional V-ATPase in osteoclasts leads to increased bone strength. *PLoS One* **6,** e27482 (2011).
171. Mazzolari, E. *et al.* A single-center experience in 20 patients with infantile malignant osteopetrosis. *Am. J. Hematol.* **84,** 473–9 (2009).

172. Heinemann, T. *et al.* Genomic organization of the gene coding for TIRC7, a novel membrane protein essential for T cell activation. *Genomics* **57,** 398–406 (1999).

173. Li, Y. P., Chen, W. & Stashenko, P. Molecular cloning and characterization of a putative novel human osteoclast-specific 116-kDa vacuolar proton pump subunit. *Biochem. Biophys. Res. Commun.* **218,** 813–21 (1996).

174. Sun-Wada, G.-H. *et al.* The a3 isoform of V-ATPase regulates insulin secretion from pancreatic beta-cells. *J. Cell Sci.* **119,** 4531–40 (2006).

175. Marks, S. C., Seifert, M. F. & Lane, P. W. Osteosclerosis, a recessive skeletal mutation on chromosome 19 in the mouse. *J. Hered.* **76,** 171–6 (1985).

176. Wilson, C. J. & Vellodi, A. Autosomal recessive osteopetrosis: diagnosis, management, and outcome. *Arch. Dis. Child.* **83,** 449–52 (2000).

177. Sobacchi, C. *et al.* As little as needed: The extraordinary case of a mild recessive osteopetrosis owing to a novel splicing hypomorphic mutation in the TCIRG1 gene. *J. Bone Miner. Res.* **29,** 1646–1650 (2014).

178. Palagano, E. *et al.* Buried in the middle but guilty: Intronic mutations in the TCIRG1 gene cause human autosomal recessive osteopetrosis. *J. Bone Miner. Res.* **30,** 1814–1821 (2015).

179. Utku, N., Heinemann, T. & Milford, E. L. T-cell immune response cDNA 7 in allograft rejection and inflammation. *Curr. Opin. Investig. Drugs* **8,** 401–10 (2007).

180. Zhu, F. *et al.* Elevated levels of T-cell immune response cDNA 7 in patients with immune thrombocytopenia. *Hematology* **19,** 477–82 (2014).

181. Taranta, A. *et al.* Genotype-phenotype relationship in human ATP6i-dependent autosomal recessive osteopetrosis. *Am. J. Pathol.* **162,** 57–68 (2003).

182. Schulz, P., Werner, J., Stauber, T., Henriksen, K. & Fendler, K. The G215R mutation in the Cl-/H+-antiporter ClC-7 found in ADO II osteopetrosis does not abolish function but causes a severe trafficking defect. *PLoS One* **5,** e12585 (2010).

183. Shin, B. *et al.* Secretion of a truncated osteopetrosis-associated transmembrane protein 1 (OSTM1) mutant inhibits osteoclastogenesis through down-regulation of the B lymphocyte-induced maturation protein 1 (BLIMP1)-nuclear factor of activated T cells c1 (NFATc1) axis. *J. Biol. Chem.* **289,** 35868–81 (2014).

184. Pandruvada, S. N. M. *et al.* Role of Ostm1 Cytosolic Complex with Kinesin 5B in Intracellular Dispersion and Trafficking. *Mol. Cell. Biol.* **36,** 507–21 (2016).

185. Chalhoub, N. *et al.* Grey-lethal mutation induces severe malignant autosomal recessive osteopetrosis in mouse and human. *Nat. Med.* **9,** 399–406 (2003).

186. Pangrazio, A. *et al.* Mutations in OSTM1 (grey lethal) define a particularly severe form of autosomal recessive osteopetrosis with neural involvement. *J. Bone Miner. Res.* **21,** 1098–105 (2006).

187. Guerrini, M. M. *et al.* Human osteoclast-poor osteopetrosis with hypogammaglobulinemia due to TNFRSF11A (RANK) mutations. *Am. J. Hum. Genet.* **83,** 64–76 (2008).

188. Pangrazio, A. *et al.* RANK-dependent autosomal recessive osteopetrosis: characterization of five new cases with novel mutations. *J. Bone Miner. Res.* **27,** 342–51 (2012).

189. Sobacchi, C. *et al.* Osteoclast-poor human osteopetrosis due to mutations in the gene encoding RANKL. *Nat. Genet.* **39,** 960–2 (2007).

190. Lo Iacono, N. *et al.* RANKL cytokine: from pioneer of the osteoimmunology era to cure for a rare disease. *Clin. Dev. Immunol.* **2013,** 412768 (2013).

191. Chen, Y. *et al.* A SNX10/V-ATPase pathway regulates ciliogenesis in vitro and in vivo. *Cell Res.* **22,** 333–45 (2012).

192. Stattin, E.-L. *et al.* SNX10 gene mutation leading to osteopetrosis with dysfunctional osteoclasts. *Sci. Rep.* **7,** 3012 (2017).

193. Zhou, C. *et al.* SNX10 Plays a Critical Role in MMP9 Secretion via JNK-p38-ERK Signaling Pathway. *J. Cell. Biochem.* **118,** 4664–4671 (2017).

194. Sly, W. S., Hewett-Emmett, D., Whyte, M. P., Yu, Y. S. & Tashian, R. E. Carbonic anhydrase II deficiency identified as the primary defect in the autosomal recessive syndrome of osteopetrosis with renal tubular acidosis and cerebral calcification. *Proc. Natl. Acad. Sci. U. S. A.* **80,** 2752–6 (1983).

195. Sly, W. S. *et al.* Carbonic anhydrase II deficiency in 12 families with the autosomal recessive syndrome of osteopetrosis with renal tubular acidosis and cerebral calcification. *N. Engl. J. Med.* **313,** 139–45 (1985).

196. Hu, P. Y. *et al.* Carbonic anhydrase II deficiency: single-base deletion in exon 7 is the predominant mutation in Caribbean Hispanic patients. *Am. J. Hum. Genet.* **54,** 602–8 (1994).

197. Margolis, D. S., Szivek, J. A., Lai, L.-W. & Lien, Y.-H. H. Phenotypic characteristics of bone in carbonic anhydrase II-deficient mice. *Calcif. Tissue Int.* **82,** 66–76 (2008).

198. Fujiwara, T. *et al.* PLEKHM1/DEF8/RAB7 complex regulates lysosome positioning and bone homeostasis. *JCI insight* **1,** e86330 (2016).

199. Marwaha, R. *et al.* The Rab7 effector PLEKHM1 binds Arl8b to promote cargo traffic to lysosomes. *J. Cell Biol.* **216,** 1051–1070 (2017).

200. McEwan, D. G. *et al.* PLEKHM1 regulates autophagosome-lysosome fusion through HOPS complex and LC3/GABARAP proteins. *Mol. Cell* **57,** 39–54 (2015).

201. Witwicka, H. *et al.* TRAFD1 (FLN29) Interacts with Plekhm1 and Regulates Osteoclast Acidification and Resorption. *PLoS One* **10,** e0127537 (2015).

202. Del Fattore, A. *et al.* A new heterozygous mutation (R714C) of the osteopetrosis gene, pleckstrin homolog domain containing family M (with run domain) member 1 (PLEKHM1), impairs vesicular acidification and increases TRACP secretion in osteoclasts. *J. Bone Miner. Res.* **23,** 380–91 (2008).

203. Bo, T. *et al.* Characterization of a Relatively Malignant Form of Osteopetrosis Caused by a Novel Mutation in the PLEKHM1 Gene. *J. Bone Miner. Res.* **31,** 1979–1987 (2016).

204. Thudium, C. S. *et al.* A comparison of osteoclast-rich and osteoclast-poor osteopetrosis in adult mice sheds light on the role of the osteoclast in coupling bone resorption and bone formation. *Calcif. Tissue Int.* **95,** 83–93 (2014).

205. Orchard, P. J. *et al.* Hematopoietic stem cell transplantation for infantile osteopetrosis. *Blood* **126,** 270–6 (2015).

206. Driessen, G. J. A. *et al.* Long-term outcome of haematopoietic stem cell transplantation in autosomal recessive osteopetrosis: an EBMT report. *Bone Marrow Transplant.* **32,** 657–63 (2003).
207. Pronk, C. J. *et al.* Transplantation of Haploidentical TcRaß-Depleted Hematopoietic Cells Allows for Optimal Timing and Sustained Correction of the Metabolic Defect in Children With Infantile Osteopetrosis. *J. Bone Miner. Res.* **32,** 82–85 (2017).
208. Chiesa, R. *et al.* Outcomes after Unrelated Umbilical Cord Blood Transplantation for Children with Osteopetrosis. *Biol. Blood Marrow Transplant.* **22,** 1997–2002 (2016).
209. Schulz, A. S. *et al.* HLA-haploidentical blood progenitor cell transplantation in osteopetrosis. *Blood* **99,** 3458–60 (2002).
210. Bahr, T. L., Lund, T., Sando, N. M., Orchard, P. J. & Miller, W. P. Haploidentical transplantation with post-transplant cyclophosphamide following reduced-intensity conditioning for osteopetrosis: outcomes in three children. *Bone Marrow Transplant.* **51,** 1546–1548 (2016).
211. Porta, F. *et al.* Partial depletion of TCR alpha/beta(+)/ CD19(+) cells in matched unrelated transplantation of three patients with osteopetrosis. *Bone Marrow Transplant.* **50,** 1583–5 (2015).
212. Natsheh, J. *et al.* Improved Outcomes of Hematopoietic Stem Cell Transplantation in Patients With Infantile Malignant Osteopetrosis Using Fludarabine-Based Conditioning. *Pediatr. Blood Cancer* **63,** 535–40 (2016).
213. Steward, C. G. Neurological aspects of osteopetrosis. *Neuropathol. Appl. Neurobiol.* **29,** 87–97 (2003).
214. Lo Iacono, N. *et al.* Osteopetrosis rescue upon RANKL administration to Rankl(-/-) mice: a new therapy for human RANKL-dependent ARO. *J. Bone Miner. Res.* **27,** 2501–10 (2012).
215. Morgan, R. A., Gray, D., Lomova, A. & Kohn, D. B. Hematopoietic Stem Cell Gene Therapy: Progress and Lessons Learned. *Cell Stem Cell* **21,** 574–590 (2017).
216. Cavazzana-Calvo, M. *et al.* Gene therapy of human severe combined immunodeficiency (SCID)-X1 disease. *Science* **288,** 669–72 (2000).
217. Gaspar, H. B. *et al.* Gene therapy of X-linked severe combined immunodeficiency by use of a pseudotyped gammaretroviral vector. *Lancet* **364,** 2181–7 (2004).
218. Aiuti, A. *et al.* Correction of ADA-SCID by stem cell gene therapy combined with nonmyeloablative conditioning. *Science* **296,** 2410–3 (2002).
219. Ott, M. G. *et al.* Correction of X-linked chronic granulomatous disease by gene therapy, augmented by insertional activation of MDS1-EVI1, PRDM16 or SETBP1. *Nat. Med.* **12,** 401–9 (2006).
220. De Rijck, J. *et al.* The BET family of proteins targets moloney murine leukemia virus integration near transcription start sites. *Cell Rep.* **5,** 886–94 (2013).
221. Hacein-Bey-Abina, S. *et al.* A serious adverse event after successful gene therapy for X-linked severe combined immunodeficiency. *N. Engl. J. Med.* **348,** 255–6 (2003).
222. Hacein-Bey-Abina, S. *et al.* LMO2-associated clonal T cell proliferation in two patients after gene therapy for SCID-X1. *Science* **302,** 415–9 (2003).

223. Cattoglio, C. *et al.* Hot spots of retroviral integration in human CD34+ hematopoietic cells. *Blood* **110,** 1770–8 (2007).
224. Neschadim, A., McCart, J. A., Keating, A. & Medin, J. A. A roadmap to safe, efficient, and stable lentivirus-mediated gene therapy with hematopoietic cell transplantation. *Biol. Blood Marrow Transplant.* **13,** 1407–16 (2007).
225. Naldini, L. *et al.* In vivo gene delivery and stable transduction of nondividing cells by a lentiviral vector. *Science* **272,** 263–7 (1996).
226. Case, S. S. *et al.* Stable transduction of quiescent CD34(+)CD38(-) human hematopoietic cells by HIV-1-based lentiviral vectors. *Proc. Natl. Acad. Sci. U. S. A.* **96,** 2988–93 (1999).
227. Miyoshi, H., Smith, K. A., Mosier, D. E., Verma, I. M. & Torbett, B. E. Transduction of human CD34+ cells that mediate long-term engraftment of NOD/SCID mice by HIV vectors. *Science* **283,** 682–6 (1999).
228. Matreyek, K. A. & Engelman, A. Viral and cellular requirements for the nuclear entry of retroviral preintegration nucleoprotein complexes. *Viruses* **5,** 2483–511 (2013).
229. Yu, S. F. *et al.* Self-inactivating retroviral vectors designed for transfer of whole genes into mammalian cells. *Proc. Natl. Acad. Sci. U. S. A.* **83,** 3194–8 (1986).
230. Hacein-Bey-Abina, S. *et al.* A modified γ-retrovirus vector for X-linked severe combined immunodeficiency. *N. Engl. J. Med.* **371,** 1407–17 (2014).
231. Zufferey, R., Nagy, D., Mandel, R. J., Naldini, L. & Trono, D. Multiply attenuated lentiviral vector achieves efficient gene delivery in vivo. *Nat. Biotechnol.* **15,** 871–5 (1997).
232. Dull, T. *et al.* A third-generation lentivirus vector with a conditional packaging system. *J. Virol.* **72,** 8463–71 (1998).
233. Modlich, U. *et al.* Cell-culture assays reveal the importance of retroviral vector design for insertional genotoxicity. *Blood* **108,** 2545–53 (2006).
234. Zychlinski, D. *et al.* Physiological promoters reduce the genotoxic risk of integrating gene vectors. *Mol. Ther.* **16,** 718–25 (2008).
235. Modlich, U. *et al.* Insertional transformation of hematopoietic cells by self-inactivating lentiviral and gammaretroviral vectors. *Mol. Ther.* **17,** 1919–28 (2009).
236. Ribeil, J.-A. *et al.* Gene Therapy in a Patient with Sickle Cell Disease. *N. Engl. J. Med.* **376,** 848–855 (2017).
237. Sessa, M. *et al.* Lentiviral haemopoietic stem-cell gene therapy in early-onset metachromatic leukodystrophy: an ad-hoc analysis of a non-randomised, open-label, phase 1/2 trial. *Lancet (London, England)* **388,** 476–87 (2016).
238. Morris, E. C. *et al.* Gene therapy for Wiskott-Aldrich syndrome in a severely affected adult. *Blood* **130,** 1327–1335 (2017).
239. Aiuti, A. *et al.* Lentiviral hematopoietic stem cell gene therapy in patients with Wiskott-Aldrich syndrome. *Science* **341,** 1233151 (2013).
240. Thompson, A. A. *et al.* Gene Therapy in Patients with Transfusion-Dependent β-Thalassemia. *N. Engl. J. Med.* **378,** 1479–1493 (2018).

241. Eichler, F. *et al.* Hematopoietic Stem-Cell Gene Therapy for Cerebral Adrenoleukodystrophy. *N. Engl. J. Med.* **377,** 1630–1638 (2017).
242. Johansson, M. K. *et al.* Hematopoietic stem cell-targeted neonatal gene therapy reverses lethally progressive osteopetrosis in oc/oc mice. *Blood* **109,** 5178–85 (2007).
243. Moscatelli, I. *et al.* Lentiviral gene transfer of TCIRG1 into peripheral blood CD34+ cells restores osteoclast function in infantile malignant osteopetrosis. *Bone* **57,** 1–9 (2013).
244. Gow, D. J. *et al.* Cloning and expression of porcine Colony Stimulating Factor-1 (CSF-1) and Colony Stimulating Factor-1 Receptor (CSF-1R) and analysis of the species specificity of stimulation by CSF-1 and Interleukin 34. *Cytokine* **60,** 793–805 (2012).
245. Shultz, L. D., Ishikawa, F. & Greiner, D. L. Humanized mice in translational biomedical research. *Nat. Rev. Immunol.* **7,** 118–30 (2007).
246. Yu, H. *et al.* A novel humanized mouse model with significant improvement of class-switched, antigen-specific antibody production. *Blood* **129,** 959–969 (2017).
247. Kooreman, N. G. *et al.* Alloimmune Responses of Humanized Mice to Human Pluripotent Stem Cell Therapeutics. *Cell Rep.* **20,** 1978–1990 (2017).
248. Rathinam, C. *et al.* Efficient differentiation and function of human macrophages in humanized CSF-1 mice. *Blood* **118,** 3119–28 (2011).
249. Knowles, H. J. *et al.* Chondroclasts are mature osteoclasts which are capable of cartilage matrix resorption. *Virchows Arch.* **461,** 205–10 (2012).
250. Włodarski, K. H., Brodzikowska, A. & Kuzaka, B. Are chondroclasts and osteoclasts identical? *Folia Biol. (Praha).* **62,** 143–7 (2014).
251. Odgren, P. R., Witwicka, H. & Reyes-Gutierrez, P. The cast of clasts: catabolism and vascular invasion during bone growth, repair, and disease by osteoclasts, chondroclasts, and septoclasts. *Connect. Tissue Res.* **57,** 161–74 (2016).
252. Nordahl, J., Andersson, G. & Reinholt, F. P. Chondroclasts and osteoclasts in bones of young rats: comparison of ultrastructural and functional features. *Calcif. Tissue Int.* **63,** 401–8 (1998).
253. Firestein, G. S. Evolving concepts of rheumatoid arthritis. *Nature* **423,** 356–61 (2003).
254. Harre, U. & Schett, G. Cellular and molecular pathways of structural damage in rheumatoid arthritis. *Semin. Immunopathol.* **39,** 355–363 (2017).
255. Spector, T. D., Hall, G. M., McCloskey, E. V & Kanis, J. A. Risk of vertebral fracture in women with rheumatoid arthritis. *BMJ* **306,** 558 (1993).
256. Hoes, J. N., Bultink, I. E. M. & Lems, W. F. Management of osteoporosis in rheumatoid arthritis patients. *Expert Opin. Pharmacother.* **16,** 559–71 (2015).
257. van Tuyl, L. H. D. *et al.* Baseline RANKL:OPG ratio and markers of bone and cartilage degradation predict annual radiological progression over 11 years in rheumatoid arthritis. *Ann. Rheum. Dis.* **69,** 1623–8 (2010).
258. Crotti, T. N., Dharmapatni, A. A. S. S. K., Alias, E. & Haynes, D. R. Osteoimmunology: Major and Costimulatory Pathway Expression Associated with Chronic Inflammatory Induced Bone Loss. *J. Immunol. Res.* **2015,** 281287 (2015).

259. Sato, K. *et al.* Th17 functions as an osteoclastogenic helper T cell subset that links T cell activation and bone destruction. *J. Exp. Med.* **203,** 2673–82 (2006).

260. Yeo, L. *et al.* Cytokine mRNA profiling identifies B cells as a major source of RANKL in rheumatoid arthritis. *Ann. Rheum. Dis.* **70,** 2022–8 (2011).

261. Meednu, N. *et al.* Production of RANKL by Memory B Cells: A Link Between B Cells and Bone Erosion in Rheumatoid Arthritis. *Arthritis Rheumatol. (Hoboken, N.J.)* **68,** 805–16 (2016).

262. Li, Y. *et al.* B cells and T cells are critical for the preservation of bone homeostasis and attainment of peak bone mass in vivo. *Blood* **109,** 3839–48 (2007).

263. Zhou, M. *et al.* Immunolocalization of MMP-2 and MMP-9 in human rheumatoid synovium. *Int. J. Clin. Exp. Pathol.* **7,** 3048–56 (2014).

264. Newby, A. C. Metalloproteinase production from macrophages - a perfect storm leading to atherosclerotic plaque rupture and myocardial infarction. *Exp. Physiol.* **101,** 1327–1337 (2016).

265. Cunnane, G., Fitzgerald, O., Beeton, C., Cawston, T. E. & Bresnihan, B. Early joint erosions and serum levels of matrix metalloproteinase 1, matrix metalloproteinase 3, and tissue inhibitor of metalloproteinases 1 in rheumatoid arthritis. *Arthritis Rheum.* **44,** 2263–74 (2001).

266. Bokarewa, M., Dahlberg, L. & Tarkowski, A. Expression and functional properties of antibodies to tissue inhibitors of metalloproteinases (TIMPs) in rheumatoid arthritis. *Arthritis Res. Ther.* **7,** R1014-22 (2005).

267. Bhattaram, P. & Chandrasekharan, U. The joint synovium: A critical determinant of articular cartilage fate in inflammatory joint diseases. *Semin. Cell Dev. Biol.* **62,** 86–93 (2017).

268. Linder, S. Invadosomes at a glance. *J. Cell Sci.* **122,** 3009–13 (2009).

269. Paterson, E. K. & Courtneidge, S. A. Invadosomes are coming: new insights into function and disease relevance. *FEBS J.* **285,** 8–27 (2018).

270. Braun, T. & Zwerina, J. Positive regulators of osteoclastogenesis and bone resorption in rheumatoid arthritis. *Arthritis Res. Ther.* **13,** 235 (2011).

271. Schett, G. & Gravallese, E. Bone erosion in rheumatoid arthritis: mechanisms, diagnosis and treatment. *Nat. Rev. Rheumatol.* **8,** 656–64 (2012).

272. Yao, Z. *et al.* Tumor necrosis factor-alpha increases circulating osteoclast precursor numbers by promoting their proliferation and differentiation in the bone marrow through up-regulation of c-Fms expression. *J. Biol. Chem.* **281,** 11846–55 (2006).

273. Mori, T. *et al.* IL-1β and TNFα-initiated IL-6-STAT3 pathway is critical in mediating inflammatory cytokines and RANKL expression in inflammatory arthritis. *Int. Immunol.* **23,** 701–12 (2011).

274. Kotake, S. *et al.* Interleukin-6 and soluble interleukin-6 receptors in the synovial fluids from rheumatoid arthritis patients are responsible for osteoclast-like cell formation. *J. Bone Miner. Res.* **11,** 88–95 (1996).

275. Radner, H. & Aletaha, D. Anti-TNF in rheumatoid arthritis: an overview. *Wien. Med. Wochenschr.* **165,** 3–9 (2015).

276. Zerbini, C. A. F. *et al.* Biologic therapies and bone loss in rheumatoid arthritis. *Osteoporos. Int.* **28,** 429–446 (2017).
277. Jiang, Y. *et al.* A multicenter, double-blind, dose-ranging, randomized, placebo-controlled study of recombinant human interleukin-1 receptor antagonist in patients with rheumatoid arthritis: radiologic progression and correlation of Genant and Larsen scores. *Arthritis Rheum.* **43,** 1001–9 (2000).
278. Bax, M., Huizinga, T. W. J. & Toes, R. E. M. The pathogenic potential of autoreactive antibodies in rheumatoid arthritis. *Semin. Immunopathol.* **36,** 313–25 (2014).
279. Toes, R. E. M. & Huizinga, T. J. W. Update on autoantibodies to modified proteins. *Curr. Opin. Rheumatol.* **27,** 262–7 (2015).
280. Mathsson, L., Lampa, J., Mullazehi, M. & Rönnelid, J. Immune complexes from rheumatoid arthritis synovial fluid induce FcgammaRIIa dependent and rheumatoid factor correlated production of tumour necrosis factor-alpha by peripheral blood mononuclear cells. *Arthritis Res. Ther.* **8,** R64 (2006).
281. Clavel, C. *et al.* Induction of macrophage secretion of tumor necrosis factor alpha through Fcgamma receptor IIa engagement by rheumatoid arthritis-specific autoantibodies to citrullinated proteins complexed with fibrinogen. *Arthritis Rheum.* **58,** 678–88 (2008).
282. Harre, U. *et al.* Induction of osteoclastogenesis and bone loss by human autoantibodies against citrullinated vimentin. *J. Clin. Invest.* **122,** 1791–802 (2012).
283. Harre, U. *et al.* Moonlighting osteoclasts as undertakers of apoptotic cells. *Autoimmunity* **45,** 612–9 (2012).
284. Seeling, M. *et al.* Inflammatory monocytes and Fcγ receptor IV on osteoclasts are critical for bone destruction during inflammatory arthritis in mice. *Proc. Natl. Acad. Sci. U. S. A.* **110,** 10729–34 (2013).
285. Walsh, N. C. & Gravallese, E. M. Bone remodeling in rheumatic disease: a question of balance. *Immunol. Rev.* **233,** 301–12 (2010).
286. Walsh, N. C. *et al.* Osteoblast function is compromised at sites of focal bone erosion in inflammatory arthritis. *J. Bone Miner. Res.* **24,** 1572–85 (2009).
287. Loeser, R. F., Goldring, S. R., Scanzello, C. R. & Goldring, M. B. Osteoarthritis: a disease of the joint as an organ. *Arthritis Rheum.* **64,** 1697–707 (2012).
288. Pap, T. & Korb-Pap, A. Cartilage damage in osteoarthritis and rheumatoid arthritis—two unequal siblings. *Nat. Rev. Rheumatol.* **11,** 606–15 (2015).
289. Cross, M. *et al.* The global burden of hip and knee osteoarthritis: estimates from the global burden of disease 2010 study. *Ann. Rheum. Dis.* **73,** 1323–30 (2014).
290. Johnson, V. L. & Hunter, D. J. The epidemiology of osteoarthritis. *Best Pract. Res. Clin. Rheumatol.* **28,** 5–15 (2014).
291. Rahmati, M., Nalesso, G., Mobasheri, A. & Mozafari, M. Aging and osteoarthritis: Central role of the extracellular matrix. *Ageing Res. Rev.* **40,** 20–30 (2017).
292. Berenbaum, F. Osteoarthritis as an inflammatory disease (osteoarthritis is not osteoarthrosis!). *Osteoarthr. Cartil.* **21,** 16–21 (2013).

293. Karsdal, M. A. *et al.* Disease-modifying treatments for osteoarthritis (DMOADs) of the knee and hip: lessons learned from failures and opportunities for the future. *Osteoarthr. Cartil.* **24,** 2013–2021 (2016).
294. Felson, D. T. Osteoarthritis as a disease of mechanics. *Osteoarthr. Cartil.* **21,** 10–5 (2013).
295. Wluka, A. E., Lombard, C. B. & Cicuttini, F. M. Tackling obesity in knee osteoarthritis. *Nat. Rev. Rheumatol.* **9,** 225–35 (2013).
296. Kerkhof, H. J. M. *et al.* Recommendations for standardization and phenotype definitions in genetic studies of osteoarthritis: the TREAT-OA consortium. *Osteoarthr. Cartil.* **19,** 254–64 (2011).
297. Rushton, M. D. *et al.* Characterization of the cartilage DNA methylome in knee and hip osteoarthritis. *Arthritis Rheumatol. (Hoboken, N.J.)* **66,** 2450–60 (2014).
298. Moazedi-Fuerst, F. C. *et al.* Epigenetic differences in human cartilage between mild and severe OA. *J. Orthop. Res.* **32,** 1636–45 (2014).
299. Sherwood, J. *et al.* A homeostatic function of CXCR2 signalling in articular cartilage. *Ann. Rheum. Dis.* **74,** 2207–15 (2015).
300. O'Conor, C. J., Leddy, H. A., Benefield, H. C., Liedtke, W. B. & Guilak, F. TRPV4-mediated mechanotransduction regulates the metabolic response of chondrocytes to dynamic loading. *Proc. Natl. Acad. Sci. U. S. A.* **111,** 1316–21 (2014).
301. DeLise, A. M., Fischer, L. & Tuan, R. S. Cellular interactions and signaling in cartilage development. *Osteoarthr. Cartil.* **8,** 309–34 (2000).
302. Sherwood, J. C., Bertrand, J., Eldridge, S. E. & Dell'Accio, F. Cellular and molecular mechanisms of cartilage damage and repair. *Drug Discov. Today* **19,** 1172–7 (2014).
303. Troeberg, L. & Nagase, H. Proteases involved in cartilage matrix degradation in osteoarthritis. *Biochim. Biophys. Acta* **1824,** 133–45 (2012).
304. Haag, J., Gebhard, P. M. & Aigner, T. SOX gene expression in human osteoarthritic cartilage. *Pathobiology* **75,** 195–9 (2008).
305. Brew, C. J., Clegg, P. D., Boot-Handford, R. P., Andrew, J. G. & Hardingham, T. Gene expression in human chondrocytes in late osteoarthritis is changed in both fibrillated and intact cartilage without evidence of generalised chondrocyte hypertrophy. *Ann. Rheum. Dis.* **69,** 234–40 (2010).
306. He, Y. *et al.* Type X collagen levels are elevated in serum from human osteoarthritis patients and associated with biomarkers of cartilage degradation and inflammation. *BMC Musculoskelet. Disord.* **15,** 309 (2014).
307. Shen, G. The role of type X collagen in facilitating and regulating endochondral ossification of articular cartilage. *Orthod. Craniofac. Res.* **8,** 11–7 (2005).
308. Aigner, T. *et al.* Type X collagen expression in osteoarthritic and rheumatoid articular cartilage. *Virchows Arch. B. Cell Pathol. Incl. Mol. Pathol.* **63,** 205–11 (1993).
309. Walker, G. D., Fischer, M., Gannon, J., Thompson, R. C. & Oegema, T. R. Expression of type-X collagen in osteoarthritis. *J. Orthop. Res.* **13,** 4–12 (1995).
310. Dy, P. *et al.* Sox9 directs hypertrophic maturation and blocks osteoblast differentiation of growth plate chondrocytes. *Dev. Cell* **22,** 597–609 (2012).

311. Karsdal, M. A. *et al.* Should subchondral bone turnover be targeted when treating osteoarthritis? *Osteoarthr. Cartil.* **16,** 638–46 (2008).
312. Karsdal, M. A. *et al.* The coupling of bone and cartilage turnover in osteoarthritis: opportunities for bone antiresorptives and anabolics as potential treatments? *Ann. Rheum. Dis.* **73,** 336–48 (2014).
313. Dreier, R. Hypertrophic differentiation of chondrocytes in osteoarthritis: the developmental aspect of degenerative joint disorders. *Arthritis Res. Ther.* **12,** 216 (2010).
314. Kawaguchi, H. Endochondral ossification signals in cartilage degradation during osteoarthritis progression in experimental mouse models. *Mol. Cells* **25,** 1–6 (2008).
315. Bonde, H. V, Talman, M. L. M. & Kofoed, H. The area of the tidemark in osteoarthritis—a three-dimensional stereological study in 21 patients. *APMIS* **113,** 349–52 (2005).
316. Durand, M. *et al.* Monocytes from patients with osteoarthritis display increased osteoclastogenesis and bone resorption: the In Vitro Osteoclast Differentiation in Arthritis study. *Arthritis Rheum.* **65,** 148–58 (2013).
317. Shimizu, S. *et al.* Prevention of cartilage destruction with intraarticular osteoclastogenesis inhibitory factor/osteoprotegerin in a murine model of osteoarthritis. *Arthritis Rheum.* **56,** 3358–65 (2007).
318. Lee, S. W. *et al.* TRAIL induces apoptosis of chondrocytes and influences the pathogenesis of experimentally induced rat osteoarthritis. *Arthritis Rheum.* **50,** 534–42 (2004).
319. Sandra, F., Hendarmin, L. & Nakamura, S. Osteoprotegerin (OPG) binds with tumor necrosis factor-related apoptosis-inducing ligand (TRAIL): suppression of TRAIL-induced apoptosis in ameloblastomas. *Oral Oncol.* **42,** 415–20 (2006).
320. Shibakawa, A. *et al.* The role of subchondral bone resorption pits in osteoarthritis: MMP production by cells derived from bone marrow. *Osteoarthr. Cartil.* **13,** 679–87 (2005).
321. Bertuglia, A. *et al.* Osteoclasts are recruited to the subchondral bone in naturally occurring post-traumatic equine carpal osteoarthritis and may contribute to cartilage degradation. *Osteoarthr. Cartil.* **24,** 555–66 (2016).
322. Kuttapitiya, A. *et al.* Microarray analysis of bone marrow lesions in osteoarthritis demonstrates upregulation of genes implicated in osteochondral turnover, neurogenesis and inflammation. *Ann. Rheum. Dis.* **76,** 1764–1773 (2017).
323. Roemer, F. W. *et al.* Change in MRI-detected subchondral bone marrow lesions is associated with cartilage loss: the MOST Study. A longitudinal multicentre study of knee osteoarthritis. *Ann. Rheum. Dis.* **68,** 1461–5 (2009).
324. Billinghurst, R. C. *et al.* Enhanced cleavage of type II collagen by collagenases in osteoarthritic articular cartilage. *J. Clin. Invest.* **99,** 1534–45 (1997).
325. Dejica, V. M. *et al.* Increased type II collagen cleavage by cathepsin K and collagenase activities with aging and osteoarthritis in human articular cartilage. *Arthritis Res. Ther.* **14,** R113 (2012).

326. Xue, M. *et al.* Endogenous MMP-9 and not MMP-2 promotes rheumatoid synovial fibroblast survival, inflammation and cartilage degradation. *Rheumatology* **53,** 2270–9 (2014).

327. Kaspiris, A. *et al.* Macrophage-specific metalloelastase (MMP-12) immunoexpression in the osteochondral unit in osteoarthritis correlates with BMI and disease severity. *Pathophysiology* **22,** 143–51 (2015).

328. Sanchez, C. *et al.* Chondrocyte secretome: a source of novel insights and exploratory biomarkers of osteoarthritis. *Osteoarthr. Cartil.* **25,** 1199–1209 (2017).

329. Konttinen, Y. T. *et al.* Acidic cysteine endoproteinase cathepsin K in the degeneration of the superficial articular hyaline cartilage in osteoarthritis. *Arthritis Rheum.* **46,** 953–60 (2002).

330. Biomarkers Definitions Working Group. Biomarkers and surrogate endpoints: preferred definitions and conceptual framework. *Clin. Pharmacol. Ther.* **69,** 89–95 (2001).

331. Saxne, T. & Heinegård, D. Cartilage oligomeric matrix protein: a novel marker of cartilage turnover detectable in synovial fluid and blood. *Br. J. Rheumatol.* **31,** 583–91 (1992).

332. Bay-Jensen, A.-C. *et al.* Enzyme-linked immunosorbent assay (ELISAs) for metalloproteinase derived type II collagen neoepitope, CIIM—increased serum CIIM in subjects with severe radiographic osteoarthritis. *Clin. Biochem.* **44,** 423–9 (2011).

333. Noé, B. *et al.* C2K77 ELISA detects cleavage of type II collagen by cathepsin K in equine articular cartilage. *Osteoarthr. Cartil.* **25,** 2119–2126 (2017).

334. Matyas, J. R., Atley, L., Ionescu, M., Eyre, D. R. & Poole, A. R. Analysis of cartilage biomarkers in the early phases of canine experimental osteoarthritis. *Arthritis Rheum.* **50,** 543–52 (2004).

335. Robin Poole, A. *et al.* Ability of a urine assay of type II collagen cleavage by collagenases to detect early onset and progression of articular cartilage degeneration: Results from a population-based cohort study. *J. Rheumatol.* **43,** 1864–1870 (2016).

336. Sumer, E. U. *et al.* MMP and non-MMP-mediated release of aggrecan and its fragments from articular cartilage: a comparative study of three different aggrecan and glycosaminoglycan assays. *Osteoarthr. Cartil.* **15,** 212–21 (2007).

337. Karsdal, M. A. *et al.* Induction of increased cAMP levels in articular chondrocytes blocks matrix metalloproteinase-mediated cartilage degradation, but not aggrecanase-mediated cartilage degradation. *Arthritis Rheum.* **56,** 1549–58 (2007).

338. Kim, T.-H. *et al.* Cartilage biomarkers in ankylosing spondylitis: relationship to clinical variables and treatment response. *Arthritis Rheum.* **52,** 885–91 (2005).

339. Valdes, A. M. *et al.* Large scale meta-analysis of urinary C-terminal telopeptide, serum cartilage oligomeric protein and matrix metalloprotease degraded type II collagen and their role in prevalence, incidence and progression of osteoarthritis. *Osteoarthr. Cartil.* **22,** 683–9 (2014).

340. Reijman, M. *et al.* A new marker for osteoarthritis: cross-sectional and longitudinal approach. *Arthritis Rheum.* **50,** 2471–8 (2004).

341. Kraus, V. B. *et al.* Predictive validity of biochemical biomarkers in knee osteoarthritis: data from the FNIH OA Biomarkers Consortium. *Ann. Rheum. Dis.* **76,** 186–195 (2017).

342. Dam, E. B., Byrjalsen, I., Karsdal, M. A., Qvist, P. & Christiansen, C. Increased urinary excretion of C-telopeptides of type II collagen (CTX-II) predicts cartilage loss over 21 months by MRI. *Osteoarthr. Cartil.* **17,** 384–9 (2009).

343. Sowers, M. F. *et al.* Longitudinal changes of serum COMP and urinary CTX-II predict X-ray defined knee osteoarthritis severity and stiffness in women. *Osteoarthr. Cartil.* **17,** 1609–14 (2009).

344. Garnero, P., Gineyts, E., Christgau, S., Finck, B. & Delmas, P. D. Association of baseline levels of urinary glucosyl-galactosyl-pyridinoline and type II collagen C-telopeptide with progression of joint destruction in patients with early rheumatoid arthritis. *Arthritis Rheum.* **46,** 21–30 (2002).

345. Garnero, P. *et al.* Cross sectional evaluation of biochemical markers of bone, cartilage, and synovial tissue metabolism in patients with knee osteoarthritis: relations with disease activity and joint damage. *Ann. Rheum. Dis.* **60,** 619–26 (2001).

346. Jordan, K. M. *et al.* Urinary CTX-II and glucosyl-galactosyl-pyridinoline are associated with the presence and severity of radiographic knee osteoarthritis in men. *Ann. Rheum. Dis.* **65,** 871–7 (2006).

347. Leung, Y. Y., Huebner, J. L., Haaland, B., Wong, S. B. S. & Kraus, V. B. Synovial fluid pro-inflammatory profile differs according to the characteristics of knee pain. *Osteoarthr. Cartil.* **25,** 1420–1427 (2017).

348. Garnero, P., Peterfy, C., Zaim, S. & Schoenharting, M. Bone marrow abnormalities on magnetic resonance imaging are associated with type II collagen degradation in knee osteoarthritis: a three-month longitudinal study. *Arthritis Rheum.* **52,** 2822–9 (2005).

349. Van Spil, W. E. *et al.* The ability of systemic biochemical markers to reflect presence, incidence, and progression of early-stage radiographic knee and hip osteoarthritis: data from CHECK. *Osteoarthr. Cartil.* **23,** 1388–97 (2015).

350. Thudium, C. S., Löfvall, H., Karsdal, M. A., Bay-Jensen, A.-C. & Bihlet, A. R. Protein biomarkers associated with pain mechanisms in osteoarthritis. *J. Proteomics* (2018). doi:10.1016/j.jprot.2018.04.030

351. Krabben, A., Huizinga, T. W. J. & Mil, A. H. M. van der H. Biomarkers for radiographic progression in rheumatoid arthritis. *Curr. Pharm. Des.* **21,** 147–69 (2015).

352. Garnero, P. *et al.* Association of baseline levels of markers of bone and cartilage degradation with long-term progression of joint damage in patients with early rheumatoid arthritis: the COBRA study. *Arthritis Rheum.* **46,** 2847–56 (2002).

353. Landewé, R. *et al.* Markers for type II collagen breakdown predict the effect of disease-modifying treatment on long-term radiographic progression in patients with rheumatoid arthritis. *Arthritis Rheum.* **50,** 1390–9 (2004).

354. Young-Min, S. *et al.* Biomarkers predict radiographic progression in early rheumatoid arthritis and perform well compared with traditional markers. *Arthritis Rheum.* **56,** 3236–47 (2007).
355. Marotte, H., Gineyts, E., Miossec, P. & Delmas, P. D. Effects of infliximab therapy on biological markers of synovium activity and cartilage breakdown in patients with rheumatoid arthritis. *Ann. Rheum. Dis.* **68,** 1197–200 (2009).
356. Freeston, J. E. *et al.* Urinary type II collagen C-terminal peptide is associated with synovitis and predicts structural bone loss in very early inflammatory arthritis. *Ann. Rheum. Dis.* **70,** 331–3 (2011).
357. Oestergaard, S. *et al.* The utility of measuring C-terminal telopeptides of collagen type II (CTX-II) in serum and synovial fluid samples for estimation of articular cartilage status in experimental models of destructive joint diseases. *Osteoarthr. Cartil.* **14,** 670–9 (2006).
358. Oestergaard, S. *et al.* Early elevation in circulating levels of C-telopeptides of type II collagen predicts structural damage in articular cartilage in the rodent model of collagen-induced arthritis. *Arthritis Rheum.* **54,** 2886–90 (2006).
359. Oestergaard, S. *et al.* Effects of ovariectomy and estrogen therapy on type II collagen degradation and structural integrity of articular cartilage in rats: implications of the time of initiation. *Arthritis Rheum.* **54,** 2441–51 (2006).
360. Nielsen, R. H., Christiansen, C., Stolina, M. & Karsdal, M. A. Oestrogen exhibits type II collagen protective effects and attenuates collagen-induced arthritis in rats. *Clin. Exp. Immunol.* **152,** 21–7 (2008).
361. Duclos, M. E. *et al.* Significance of the serum CTX-II level in an osteoarthritis animal model: a 5-month longitudinal study. *Osteoarthr. Cartil.* **18,** 1467–76 (2010).
362. Schaller, S. *et al.* In vitro, ex vivo, and in vivo methodological approaches for studying therapeutic targets of osteoporosis and degenerative joint diseases: how biomarkers can assist? *Assay Drug Dev. Technol.* **3,** 553–80 (2005).
363. Christgau, S. *et al.* Collagen type II C-telopeptide fragments as an index of cartilage degradation. *Bone* **29,** 209–15 (2001).
364. Eyre, D. R. Cartilage resorption assays. US6255056B1. (2001).
365. Eyre, D. R. Cartilage resorption assays measuring type II collagen fragments. US6348320B1. (2002).
366. Eyre, D. R. Synthetic peptides of type II collagen for cartilage resorption assays. US6566492B2. (2003).
367. Bay-Jensen, A.-C. *et al.* Biochemical markers of type II collagen breakdown and synthesis are positioned at specific sites in human osteoarthritic knee cartilage. *Osteoarthr. Cartil.* **16,** 615–23 (2008).
368. Rody, W. J. *et al.* The use of cell culture platforms to identify novel markers of bone and dentin resorption. *Orthod. Craniofac. Res.* **20 Suppl 1,** 89–94 (2017).
369. Bhargava, A. *et al.* Osteopetrosis mutation R444L causes endoplasmic reticulum retention and misprocessing of vacuolar H+-ATPase a3 subunit. *J. Biol. Chem.* **287,** 26829–39 (2012).

370. Moscatelli, I. *et al.* Targeting NSG Mice Engrafting Cells with a Clinically Applicable Lentiviral Vector Corrects Osteoclasts in Infantile Malignant Osteopetrosis. *Hum. Gene Ther.* **29,** 938–949 (2018).

371. Sørensen, M. G., Henriksen, K., Neutzsky-Wulff, A. V, Dziegiel, M. H. & Karsdal, M. A. Diphyllin, a novel and naturally potent V-ATPase inhibitor, abrogates acidification of the osteoclastic resorption lacunae and bone resorption. *J. Bone Miner. Res.* **22,** 1640–8 (2007).

372. Hao, J. L. *et al.* Effect of galardin on collagen degradation by Pseudomonas aeruginosa. *Exp. Eye Res.* **69,** 595–601 (1999).

373. Löfvall, H. *et al.* Osteoclasts degrade bone and cartilage knee joint compartments through different resorption processes. *Arthritis Res. Ther.* **20,** 67 (2018).

374. Hui, W., Rowan, A. D., Richards, C. D. & Cawston, T. E. Oncostatin M in combination with tumor necrosis factor alpha induces cartilage damage and matrix metalloproteinase expression in vitro and in vivo. *Arthritis Rheum.* **48,** 3404–18 (2003).

375. Flores, C. *et al.* Nonablative neonatal bone marrow transplantation rapidly reverses severe murine osteopetrosis despite low-level engraftment and lack of selective expansion of the osteoclastic lineage. *J. Bone Miner. Res.* **25,** 2069–77 (2010).

376. Esmail, S. *et al.* N-linked glycosylation of a subunit isoforms is critical for vertebrate vacuolar H+ -ATPase (V-ATPase) biosynthesis. *J. Cell. Biochem.* **119,** 861–875 (2018).

377. De Ravin, S. S. *et al.* Lentiviral hematopoietic stem cell gene therapy for X-linked severe combined immunodeficiency. *Sci. Transl. Med.* **8,** 335ra57 (2016).

378. Li, Y. *et al.* Induction of functional human macrophages from bone marrow promonocytes by M-CSF in humanized mice. *J. Immunol.* **191,** 3192–9 (2013).

379. Kodama, H. *et al.* Congenital osteoclast deficiency in osteopetrotic (op/op) mice is cured by injections of macrophage colony-stimulating factor. *J. Exp. Med.* **173,** 269–72 (1991).

380. Reinisch, A., Hernandez, D. C., Schallmoser, K. & Majeti, R. Generation and use of a humanized bone-marrow-ossicle niche for hematopoietic xenotransplantation into mice. *Nat. Protoc.* **12,** 2169–2188 (2017).

381. Lis, R. *et al.* Conversion of adult endothelium to immunocompetent haematopoietic stem cells. *Nature* **545,** 439–445 (2017).

382. Sugimura, R. *et al.* Haematopoietic stem and progenitor cells from human pluripotent stem cells. *Nature* **545,** 432–438 (2017).

383. Neri, T. *et al.* Targeted Gene Correction in Osteopetrotic-Induced Pluripotent Stem Cells for the Generation of Functional Osteoclasts. *Stem cell reports* **5,** 558–68 (2015).

384. Xu, M., Stattin, E.-L., Murphy, M. & Barry, F. Generation of induced pluripotent stem cells (ARO-iPSC1-11) from a patient with autosomal recessive osteopetrosis harboring the c.212+1G>T mutation in SNX10 gene. *Stem Cell Res.* **24,** 51–54 (2017).

385. Utku, N. *et al.* Prevention of acute allograft rejection by antibody targeting of TIRC7, a novel T cell membrane protein. *Immunity* **9,** 509–18 (1998).

386. Utku, N. *et al.* TIRC7 deficiency causes in vitro and in vivo augmentation of T and B cell activation and cytokine response. *J. Immunol.* **173,** 2342–52 (2004).

387. Morgun, A. *et al.* Cytokine and TIRC7 mRNA expression during acute rejection in cardiac allograft recipients. *Transplant. Proc.* **33,** 1610–1611 (2001).

388. Shulzhenko, N. *et al.* Monitoring of intragraft and peripheral blood TIRC7 expression as a diagnostic tool for acute cardiac rejection in humans. *Hum. Immunol.* **62,** 342–7 (2001).

389. Zhu, F. *et al.* Increased expression of T cell immune response cDNA 7 in patients with acute graft-versus-host disease. *Ann. Hematol.* **94,** 1025–32 (2015).

390. Segovia-Silvestre, T. *et al.* Advances in osteoclast biology resulting from the study of osteopetrotic mutations. *Hum. Genet.* **124,** 561–577 (2009).

391. Helfrich, M. H. Osteoclast diseases. *Microsc. Res. Tech.* **61,** 514–32 (2003).

392. Gupta, H. S. *et al.* Two different correlations between nanoindentation modulus and mineral content in the bone-cartilage interface. *J. Struct. Biol.* **149,** 138–48 (2005).

393. Touaitahuata, H., Cres, G., de Rossi, S., Vives, V. & Blangy, A. The mineral dissolution function of osteoclasts is dispensable for hypertrophic cartilage degradation during long bone development and growth. *Dev. Biol.* **393,** 57–70 (2014).

394. Lecaille, F. *et al.* Selective inhibition of the collagenolytic activity of human cathepsin K by altering its S2 subsite specificity. *Biochemistry* **41,** 8447–54 (2002).

395. Christensen, J. & Shastri, V. P. Matrix-metalloproteinase-9 is cleaved and activated by cathepsin K. *BMC Res. Notes* **8,** 322 (2015).

396. Vizovišek, M., Fonović, M. & Turk, B. Cysteine cathepsins in extracellular matrix remodeling: Extracellular matrix degradation and beyond. *Matrix Biol.* (2018). doi:10.1016/j.matbio.2018.01.024

397. Al-Bari, M. A. A., Shinohara, M., Nagai, Y. & Takayanagi, H. Inhibitory effect of chloroquine on bone resorption reveals the key role of lysosomes in osteoclast differentiation and function. *Inflamm. Regen.* **32,** 222–231 (2012).

398. Fuller, K. *et al.* The resorptive apparatus of osteoclasts supports lysosomotropism and increases potency of basic versus non-basic inhibitors of cathepsin K. *Bone* **46,** 1400–7 (2010).

399. Bay-Jensen, A.-C. *et al.* The response to oestrogen deprivation of the cartilage collagen degradation marker, CTX-II, is unique compared with other markers of collagen turnover. *Arthritis Res. Ther.* **11,** R9 (2009).

400. Bay-Jensen, A. C. *et al.* Circulating protein fragments of cartilage and connective tissue degradation are diagnostic and prognostic markers of rheumatoid arthritis and ankylosing spondylitis. *PLoS One* **8,** e54504 (2013).

401. Im, C. H. *et al.* Receptor activator of nuclear factor kappa B ligand-mediated osteoclastogenesis is elevated in ankylosing spondylitis. *Clin. Exp. Rheumatol.* **27,** 620–5 (2009).

Paper I

Calcif Tissue Int (2016) 99:638–648
DOI 10.1007/s00223-016-0187-6

ORIGINAL RESEARCH

Regulation and Function of Lentiviral Vector-Mediated TCIRG1 Expression in Osteoclasts from Patients with Infantile Malignant Osteopetrosis: Implications for Gene Therapy

Christian Schneider Thudium[1] · Ilana Moscatelli[2] · Henrik Löfvall[1,2] · Zsuzsanna Kertész[2] · Carmen Montano[2] · Carmen Flores Bjurström[2] · Morten Asser Karsdal[1] · Ansgar Schulz[3] · Johan Richter[2] · Kim Henriksen[1]

Received: 29 June 2016 / Accepted: 8 August 2016 / Published online: 19 August 2016

Abstract Infantile malignant osteopetrosis (IMO) is a rare, recessive disorder characterized by increased bone mass caused by dysfunctional osteoclasts. The disease is most often caused by mutations in the TCIRG1 gene encoding a subunit of the V-ATPase involved in the osteoclasts capacity to resorb bone. We previously showed that osteoclast function can be restored by lentiviral vector-mediated expression of TCIRG1, but the exact threshold for restoration of resorption as well as the cellular response to vector-mediated TCIRG1 expression is unknown. Here we show that expression of TCIRG1 protein from a bicistronic TCIRG1/GFP lentiviral vector was only observed in mature osteoclasts, and not in their precursors or macrophages, in contrast to GFP expression, which was observed under all conditions. Thus, vector-mediated TCIRG1 expression appears to be post-transcriptionally regulated, preventing overexpression and/or ectopic expression and ensuring protein expression similar to that of wild-type osteoclasts. Codon optimization of TCIRG1 led to increased expression of mRNA but lower levels of protein and functional rescue. When assessing the functional rescue threshold in vitro, addition of 30 % CB $CD34^+$ cells to IMO $CD34^+$ patient cells was sufficient to completely normalize resorptive function after osteoclast differentiation. From both an efficacy and a safety perspective, these findings will clearly be of benefit during further development of gene therapy for osteopetrosis.

Keywords Osteoclast · Osteopetrosis · Gene therapy · Lentivirus · TCIRG1

Introduction

Osteopetrosis is a heterogeneous group of rare diseases characterized by the inability of the osteoclasts to resorb bone [1, 2]. The most severe form is called infantile malignant osteopetrosis (IMO). Mutations in the *TCIRG1* gene, encoding the a3 subunit of the osteoclastic V-ATPase, account for up to 50 % of all IMO cases [3, 4] and are also the cause of osteopetrosis in the *oc/oc* model [5]. The mutations may lead to an absence of the a3 subunit in osteoclasts [6, 7]. The disease itself presents as an increase in bone mass, but despite increased density the bones are brittle and prone to fracture. The cellular phenotype is characterized by an increased amount of osteoclasts, which are unable to resorb bone [7]. The disease is fatal, and unless treated, most patients die within the first 6 years of life. As osteoclasts derive from the hematopoietic stem cells via the monocytic lineage, the preferred treatment is hematopoietic stem cell transplantation performed as early as possible after diagnosis [8, 9].

TCIRG1 (also known as a3) comprises the largest subunit of the osteoclastic V-ATPase. The main function of the V-ATPase in osteoclasts is to deliver protons to the ongoing acidification of the resorption lacunae during bone resorption [10]. Located in the membrane-embedded V_0

Electronic supplementary material The online version of this article (doi:10.1007/s00223-016-0187-6) contains supplementary material, which is available to authorized users.

✉ Johan Richter
Johan.Richter@med.lu.se

[1] Nordic Bioscience, Herlev, Denmark

[2] Department of Molecular Medicine and Gene Therapy, Lund Strategic Center for Stem Cell Biology, BMC A12, 221 84 Lund, Sweden

[3] Department of Pediatrics and Adolescent Medicine, University Medical Center, Ulm, Germany

domain of the V-ATPase, the TCIRG1 contains two hemi channels allowing access of protons for transport across the plasma membrane [11]. It provides a structural scaffold on which the other V_0 subunits assemble, and is believed to be important for targeting the V-ATPase to the plasma membrane [12, 13]. This subunit is, thus, crucial for V-ATPase functionality.

We have previously shown that the murine *oc/oc* disease model of osteopetrosis can be rescued by gene therapy using gammaretroviral vectors to target hematopoietic stem cells [14]. We have further shown that the resorptive function of human IMO osteoclasts can be restored in vitro by lentiviral-mediated gene transfer of the *TCIRG1* cDNA into $CD34^+$ cells from peripheral blood of IMO patients expanded in culture and differentiated on bone slices to mature bone-resorbing osteoclasts [6].

As a part of the continued development of lentiviral-mediated clinical gene therapy for IMO, we here wanted to study regulation of lentiviral vector-mediated expression of TCIRG1 in human osteoclasts and non-hematopoietic cells in comparison with the expression of the endogenous gene. Furthermore, we wanted to determine whether the use of a vector with a codon-optimized version of TCIRG1 would lead to an increased level of expression of the protein and also increased functional correction. Finally, we wanted to investigate in more detail what levels (percentages) of normal cells or vector-corrected cells were needed to achieve significant correction of the bone resorption capacity of human osteoclasts from IMO patients in vitro.

Materials and Methods

$CD34^+$ Cell Isolation, Culture and Expansion

Samples of peripheral blood from IMO patients (University Medical Center Ulm) or umbilical cord blood from normal deliveries (University Hospital Lund) were obtained after informed consent under protocols approved by institutional ethical boards. The IMO patient mutations are described in Suppl. Table 1, and cells were isolated, cultured and expanded as previously described [6]. Briefly, mononuclear cells from these cell sources were isolated using Ficoll density centrifugation medium and $CD34^+$ cells were subsequently separated from the mononuclear cell fraction using MACS columns (Miltenyi Biotec, Bergisch Gladbach, Germany). Cells were cultured in SFEM StemSpan medium (StemCell Technologies, Vancouver, BC), with the following human recombinant cytokines: M-CSF (50 ng/ml), GM-CSF (30 ng/ml), SCF (200 ng/ml), IL-6 (10 ng/ml) and Flt3L (50 ng/ml) all from R&D Systems (Minneapolis, MN, USA). $CD34^+$ cells were plated at a density of 5×10^4 cells in 1-ml medium using 24-well bacteriological plates and incubated for 1 week at 37 °C before collection and replating at a density of 1×10^5/well. From day 7, the medium was exchanged every 2–3 days by demi-depletion.

Vectors, Viral Production and Transduction of $CD34^+$ Cells

The rescue vector used in this study (based on the pRRL lentiviral vector backbone), named LV-TCIRG1/GFP, contains the cDNA of human *TCIRG1* inserted into a self-inactivating lentiviral vector under the spleen focus-forming virus (SFFV) promoter up-stream of an internal ribosomal entry site (IRES) which is followed by the gene for enhanced green fluorescent protein (GFP). A lentiviral vector expressing only GFP (LV-GFP) was used as control. In addition, a vector named LV-coTCIRG1/GFP containing a codon-optimized version of human *TCIRG1* synthesized by GeneArt (Life Technologies, Regensburg, Germany) was generated. In LV-coTCIRG1/GFP, the cDNA sequence was modified to eliminate splice sites, poly(A) signals and TATA boxes that may negatively influence expression. Codon usage was optimized based on transfer RNA frequencies in human so that the Codon Adaptation Index was increased from 0.86 to 0.95. Also the GC content was increased to 62 % to promote RNA stability. All vectors were produced by transient transfection of the vector plasmids in human 293T cells along with packaging plasmid (pCMV ΔR8.91) and envelope plasmid (VSV-G pMDG). $CD34^+$ cells were transduced once on day 0–3 for 6 h in 24-well plates coated with RetroNectin (Takara Bio, Otsu, Japan) at a multiplicity of infection (MOI) of 30. After transduction, cells were cultured as described above and transduction efficiency was tested at different time points by flow cytometry analysis of cells expressing GFP. Cells received a second round of transduction at MOI 30 on day 7 for 6 h to ensure that transduction efficiency was around 30–40 % at the end of the 2-week expansion period (Suppl Fig. 1, adapted from [6]).

Osteoclastogenesis

After 2 weeks, the expanded cells were reseeded into 96-well plates on bovine cortical bone slices at a density of 1×10^5/well for cell assays or they were reseeded 12-well plates at a density of 1.2×10^6/well for western blot (WB). The cells were incubated, at 37 °C and 5 % CO_2, in αMEM containing 10 % fetal bovine serum (FBS), 100 units/ml penicillin, 100 µg/ml streptomycin and 388 µg/L thymidine. They were expanded for 3 days in the presence of 50 ng/ml M-CSF. RANKL, 50 ng/ml, was added on day 3, and media were changed every 2–3 days hereafter. After 10 days, cells were fixed in 4 % formaldehyde for further

analyses. Resorption was assessed by the presence of CTX-I and Ca^{2+} in the cell supernatant, and osteoclast differentiation was assessed by TRAP activity.

Osteoclasts derived from $CD14^+$ monocytes were generated as previously described [15, 16]. In brief, $CD14^+$ monocytes were obtained from peripheral blood of healthy donors by density gradient centrifugation using Ficoll medium and were subsequently cultured at a density of 1.5×10^5 cells/cm^2, at 37 °C and 5 % CO_2, in αMEM containing 10 % FBS, 100 units/ml penicillin, 100 µg/ml streptomycin and 388 µg/L thymidine. The cells were expanded for 2–3 days in the presence of 25 ng/ml M-CSF and were subsequently differentiated into osteoclasts by adding 25 ng/ml of RANKL for an additional 10 days of culture with medium changes every 2–3 days.

HT1080 Cultures and Transduction

Human fibrosarcoma HT1080 cells were maintained in Dulbecco's modified Eagle's medium/High Glucose (Thermo scientific) supplemented with 10 % FBS and penicillin/streptomycin at 37 °C and 5 % CO_2.

HT1080 cells were transduced once on day 1 for 6 h in 24-well plates at an MOI of 10. After 72 h, transduction efficiency was tested by flow cytometry analysis of cells expressing GFP and TCIRG1 expression was tested by qRT-PCR and WB.

Deglycosylation

The mature $CD14^+$-derived osteoclasts were harvested into RIPA buffer, and the protein concentration was measured using the Bio-Rad protein measurement assay (Bio-Rad, Hercules, CA, USA). The cell lysate was deglycosylated using either PNGase F or Endo H, both from Promega (Madison, WI, USA), according to the manufacturer's instructions. In brief, 8 µg of total protein was mixed with the respective denaturing buffers and was subsequently denatured at 95 °C for 5 min followed by a deglycosylation reaction with PNGase F or Endo H in the respective enzyme buffers at 37 °C for 2 h. As non-deglycosylated controls, denatured protein solution was incubated in enzyme buffers without enzyme. Samples equivalent to 5 µg of total cell lysate protein were used for immunoblotting alongside 6 µg of total protein from the transduced HT1080 cells.

Mixing Experiments

After expansion, cord blood or rescued IMO $CD34^+$ cells (transduced twice with LV-TCIRG1/GFP at MOI 30) were mixed with non-rescued IMO $CD34^+$ cells in increasing cell to cell ratio. The cells were then seeded into 96-well plates on bovine cortical bone slices at a density of 1×10^5/well for cell assays or at a density of 1.2×10^6/well on plastic in 12-well plates for western blot. Cells were then differentiated into osteoclasts as described above, during a period of 10–12 days.

Resorption Biomarkers

The release of the c-terminal type I collagen fragments (CTX-I) from mineralized bone slices was determined in the culture supernatants using the CrossLaps for Culture kit (IDS, Boldon, UK), according to the manufacturer's instructions. The concentration of total calcium was measured in culture supernatants after resorption, by using a colorimetric assay and a Hitachi 912 Automatic Analyzer (Roche Diagnostics, Basel, Switzerland) following the assay method validated and warranted by Roche Diagnostics [17].

TRAP Activity Measurements

TRAP activity was measured as previously described [6, 18]. Briefly, 2–20 µl of conditioned media from 96-well cell cultures on either bone or plastic was added to a 96-well plate together with 80 µl freshly prepared reaction buffer (0.33 M acetic acid, 0.167 % Triton X-100, 0.33 M NaCl, 3.33 mM EDTA at pH 5.5, 1.5 mg/ml of ascorbic acid, 7.66 mg/ml of disodium tartrate, 3 mg/ml of 4-nitrophenylphosphate). The reaction was incubated at 37 °C for 1 h in the dark and then stopped by adding 100 µl of 0.3 M NaOH. Colorimetric changes were measured at 405 nm with 650 nm as reference using a Spectramax M5 ELISA reader.

Quantitative RT-PCR

RNA was isolated using the RNeasy Mini Kit (Qiagen, Hilden, Germany) and reverse transcribed with random primers and Superscript III (Invitrogen, Burlington, Canada). Quantitative PCR was performed on a LightCycler (Roche Diagnostics) using standard conditions with cDNA equivalent to 10 ng RNA and 1:20,000 dilution of SYBR Green I [14]. The following primers were used: ACTIN: Fw 5′-CCATTGGCAATGAGCGGTT -3′; Rv 5′-GCGCTCAGGAGGAGCAA-3′; TCIRG1: Fw 5′-CAGC TCTTTCTGCCCACAG-3′; Rv 5′-CTGCAGGAAGGTGA AGGTCT-3′ (NCBI Reference Sequence: NM_006019.3); coTCIRG1: Fw 5′-CAGCTGTTTCTGCCCACCG-3′; Rv 5′-CTGCAGAAAGGTGAAGGTCT-3′. Both TCIRG1 primer sets amplify at the same efficiency when tested on transduced HT1080 cells and are designed to distinguish between the TCIRG1 expressed by the two different vectors (data not shown). Differences in gene expression were calculated using the $2^{-\Delta\Delta Ct}$ method.

Immunoblotting

Immunoblotting was performed as previously described [6]. Cells were harvested into RIPA lysis buffer. Protein concentrations were measured using the Bio-Rad protein measurement assay (Bio-Rad, Hercules, CA, USA). A total of 15 μg of total protein in SDS sample buffer were loaded onto a 7.5 % SDS-PAGE gel, followed by blotting onto a nitrocellulose membrane. Membranes were then blocked in TBS, 0.1 % Tween 20 with 5 % skim milk powder for 1 h at room temperature, followed by incubation with primary antibody overnight at 4 °C in TBS, 0.1 % Tween 20, 5 % skim milk powder, with the following dilutions: mouse anti-TCIRG1 (Abnova, Taipei, Taiwan) 1:1000, mouse anti-cathepsin K (Millipore, Billerica, MA, USA) 1:1000, rabbit anti-GFP (Abcam, Cambridge, UK) 1:2000, mouse anti-ATP6V0D2 (Abnova, Taipei, Taiwan) 1:1000 and p38 MAPK (Cell Signaling Technology, Danvers, MA, USA) 1:1000. The blots were then washed 3 times for 10 min and incubated with a corresponding HRP-conjugated secondary antibody for 1 h at room temperature followed by washing 3 times for 10 min in TBS buffer. Blots were developed using the ECL kit (GE Healthcare, Waukesha, WI, USA).

Statistics

Statistical analysis was performed on log-transformed data using one-way ANOVA with Dunnett's multiple comparisons test against respective controls. * indicates $p < 0.05$; ** indicates $p < 0.01$; *** indicates $p < 0.001$; ns indicates $p > 0.05$.

Results

Lentiviral-Mediated TCIRG1 Expression in Osteoclasts Differentiated from IMO CD34$^+$ Cells Follows the Regulation Pattern of Endogenous TCIRG1 Protein

To characterize the expression of TCIRG1 as a function of lentiviral transduction, we transduced CD34$^+$ cells from normal cord blood or IMO patients with either a bicistronic lentiviral vector containing the TCIRG1 cDNA together with a marker gene (LV-TCIRG1/GFP) or a control GFP vector (LV-GFP). The CD34$^+$ cells were then expanded for 2 weeks, and as previously observed, transduction with LV-TCIRG1/GFP led to an increase in TCIRG1 mRNA in expanded CD34$^+$ cells, while no change was observed in expanded CD34$^+$ cells transduced with LV-GFP compared to untransduced controls (data not shown and [6]). Subsequent to expansion, cells were differentiated into mature osteoclasts in the presence of M-CSF and RANKL. In LV-TCIRG1/GFP-transduced cord blood cells induced to undergo osteoclastogenesis, TCIRG1 protein expression was increased with osteoclast maturation from day 5 onward (Figs. 1a, 2). TCIRG1 expression levels were similar compared to LV-GFP-transduced cord blood-derived controls. Previous studies showed no differences in TCIRG1 expression between LV-GFP-transduced and non-transduced cord blood cells (data not shown and [6]). In IMO patient cells, LV-TCIRG1/GFP transduction led to a differentiation-dependent increase in expression of TCIRG1, corresponding to the pattern seen in normal CB cells undergoing osteoclastogenesis, while TCIRG1 protein expression was absent at all time points of differentiation in LV-GFP-transduced IMO patient cells (Fig. 1b–d). In contrast to TCIRG1 protein, GFP was expressed at a constant high level in both LV-GFP and LV-TCIRG1/GFP conditions at all time points during osteoclastogenesis (Fig. 1a–d).

Lentiviral Expression of TCIRG1 Follows RANKL-Induced Osteoclastogenesis

To further characterize the effect of differentiation on lentiviral-mediated TCIRG1 expression, we transduced IMO cells with the LV-TCIRG1/GFP vector or the LV-GFP control vector and following expansion cultured the cells with M-CSF in the presence or absence of RANKL. IMO cells transduced with LV-TCIRG1/GFP and treated with RANKL exhibited a differentiation-dependent increase in TCIRG1 expression as described above, which was accompanied by the normal increase in cathepsin K expression with osteoclastogenesis (Fig. 2a, lanes 3 and 4). As expected, cells exposed only to M-CSF failed to differentiate into osteoclasts, did not express cathepsin K and instead differentiated toward a macrophage-like cell type. These macrophage-like cells expressed only very minor amounts of exogenous TCIRG1 at day 9 and 14 (Fig. 2a, lane 7 and 8). IMO cells transduced with LV-GFP failed to express TCIRG1 both when exposed to RANKL in combination with M-CSF or with M-CSF alone, while the osteoclast markers cathepsin K and the d2 subunit of the V-ATPase were expressed on day 9 and 14 in cells exposed to both M-CSF and RANKL. Expression of d2 was only affected by osteoclast differentiation, and it was not affected by the lentiviral-mediated expression of TCIRG1 (Fig. 2a). Cells transduced with either LV-TCIRG1/GFP or LV-GFP and differentiated with or without RANKL expressed GFP throughout differentiation.

In summary, the data from these two first sets of experiments indicate that expression of TCIRG1 protein during osteoclastogenesis is regulated at the post-transcriptional level in a manner similar to the endogenous protein even when expressed from a lentiviral vector with a strong generic promoter as SFFV.

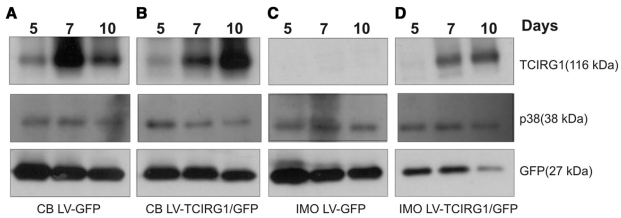

Fig. 1 Lentiviral-mediated TCIRG1 expression in osteoclasts differentiated from IMO CD34$^+$ cells follows the regulation pattern of the endogenous protein. CD34$^+$ cells from IMO patients or normal CB CD34$^+$ cells were transduced with LV-TCIRG1/GFP or LV-GFP. Transduced cells were expanded for 2 weeks and then differentiated on plastic into osteoclasts, as described in "Materials and Methods" section, followed by western blot analysis of protein expression. Samples were run on western blot using antibodies against TCIRG1, GFP and p38 as a loading control

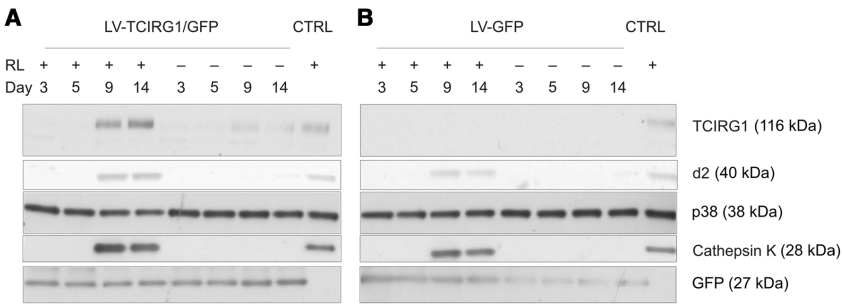

Fig. 2 Lentiviral-mediated expression of TCIRG1 is dependent on RANKL. IMO CD34$^+$ cells were transduced with LV-TCIRG1/GFP (**a**) or LV-GFP (**b**) and expanded for 2 weeks and then differentiated into osteoclasts in the presence of RANKL (+RL) or macrophages in the absence of RANKL (−RL). The protein expression of TCIRG1, the V-ATPase subunit d2, the osteoclast marker cathepsin K and GFP was assessed throughout differentiation, and p38 was used as loading control. The *last lanes* in each of the two panels represent mature osteoclasts generated from CD34$^+$ cord blood cells

Differences in TCIRG1 Glycosylation Between Cell Types Suggest a Regulatory Role in Osteoclasts

To investigate whether the regulation mechanism is cell lineage specific, we used LV-TCIRG1/GFP to express TCIRG1 in HT1080 cells, a fibrosarcoma cell line not normally expressing this protein. At day 3, after transduction TCIRG1 was highly expressed at the mRNA level (Fig. 3a) and protein level (Fig. 3b). However, the molecular weight of the protein was lower than that observed for TCIRG1 expressed in osteoclasts. Previous studies have shown that TCIRG1 exists in a fully glycosylated (mature) form and a core-glycosylated form when expressed in osteoclasts [19]. By immunoblotting, we identified two distinct bands with different molecular weights in osteoclast cell lysates (Figs. 1, 2). Importantly, the band at 116 kDa was more intense than the lower molecular weight band, indicating that this is the dominant form in osteoclasts. In contrast, in the HT1080 cells, the predominant form is corresponding to the low molecular weight form in osteoclasts (Fig. 3b). We therefore hypothesized that this modification may serve to protect the protein from degradation in the mature osteoclast. Upon transduction of the HT1080 cells using LV-TCIRG1/GFP, the cells readily expressed both TCIRG1 mRNA (Fig. 3a) and protein (Fig. 3b) after 3 days without RANKL stimulation. Using the enzymes PNGase F and Endo H, we verified that TCIRG1 existed in both a fully glycosylated and a core-glycosylated form in the osteoclasts (Fig. 3b) where PNGase F is capable of deglycosylating the fully glycosylated and the core-glycosylated form, whereas Endo H can only deglycosylate the core-glycosylated form. In contrast, TCIRG1 was only present in the core-glycosylated form of the protein in HT1080 cells transduced with the LV-TCIRG1/GFP vector as can be seen by comparing the molecular weight of TCIRG1 in the HT1080 samples to the deglycosylated osteoclast samples (Fig. 3b). Furthermore, as the HT1080 cells expressed both TCIRG1 mRNA and protein after 3 days, these cells did not seem to possess the same form of RANKL-dependent TCIRG1

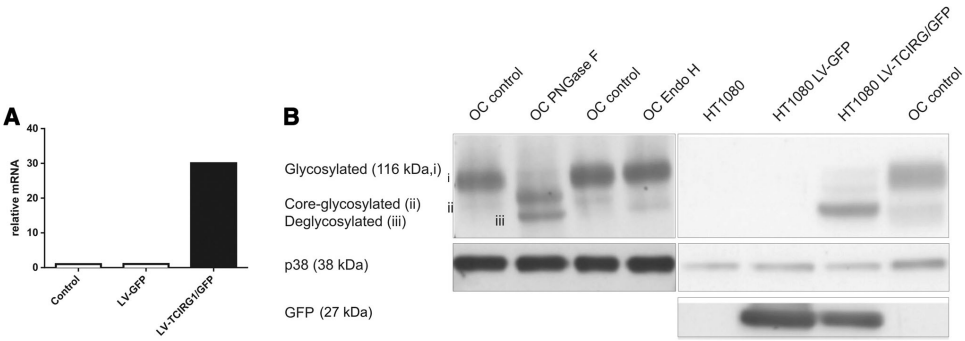

Fig. 3 TCIRG1 is differentially glycosylated in osteoclasts and HT1080 cells. HT1080 cells were transduced with the LV-TCIRG1/GFP vector, the LV-GFP vector or left non-transduced and were cultured for 3 days followed by analysis of TCIRG1 mRNA levels by qPCR (**a**). Cell lysates of osteoclasts differentiated from $CD14^+$ monocytes were deglycosylated using PNGase F or Endo H and the glycosylations of TCIRG1 in the transduced HT1080 cells, and the deglycosylated osteoclast lysates were analyzed by western blot (**b**)

regulation observed in osteoclast lineage cells (Fig. 2a). As both the cord blood control cells and the IMO $CD34^+$ cells transduced with the LV-TCIRG1 vector contain the same two forms of TCIRG1 and mainly the fully glycosylated form (Fig. 2a), it is possible that the glycosylation mechanism may be restricted to cells of the osteoclastic lineage.

A Lentiviral Vector with Codon-Optimized TCIRG1 Generates Higher Levels of RNA but Lower Levels of Protein and Bone Resorption in Osteoclasts as Compared to the Non-Optimized Vector

In an effort to increase expression of TCIRG1 and possibly the resorptive function of corrected IMO cells, we constructed a lentiviral vector with a codon-optimized version of TCIRG1 (LV-coTCIRG1/GFP) as described in "Materials and Methods" section. This vector, in all other features identical with LV-TCIRG1/GFP, was then compared to LV-TCIRG1/GFP.

IMO cells were transduced (MOI 30, 2 hits) with LV-GFP, LV-TCIRG1/GFP or LV-coTCIRG1/GFP and expanded for 2 weeks, and transduction efficiency was similar for all vectors. qRT-PCR analysis performed showed that the relative mRNA levels of *TCIRG1* in IMO cells transduced with LV-TCIRG1/GFP or LV-coTCIRG1/GFP were about 10- and 200-fold higher than in LV-GFP-transduced cells, respectively (Fig. 4a). However, in five patient samples tested, cells transduced with LV-TCIRG1/GFP exhibited higher TCIRG1 protein levels as analyzed by western blot compared to those transduced with LV-coTCIRG1/GFP (one example shown in Fig. 4b). This was somewhat unexpected and thus in stark contrast to expression of *TCIRG1* at the mRNA level, although the previously presented regulation mechanism could be involved in this.

Furthermore, when these expanded IMO cells were differentiated into osteoclasts on bovine bone slices, the resorptive function, determined by CTX-I release, was inferior in osteoclasts generated from LV-coTCIRG1/GFP cells as compared to LV-TCIRG1/GFP cells (Fig. 4c), correlating well with the lower protein expression.

Mixing Increasing Numbers of Expanded CB $CD34^+$ Cells into IMO $CD34^+$ Cells Followed by Osteoclast Generation Results in a Dose-Dependent Increase in Resorptive Function

In gene therapy, a central question is the level of correction needed at the cellular level in order to correct the disease. In the *oc/oc* mouse model of osteopetrosis, we previously found that engraftment of as little as 4 % wild-type mononuclear GFP-marked cells in non-irradiated recipients could correct the disease [20]. We also observed that 30 % of the osteoclasts in these mice were green, indicating fusion of GFP-positive cells with non-marked cells to form green osteoclasts [20]. Here we wanted to determine the percentage of normal wild-type cells needed to correct the human form of the disease in vitro. To do so we mixed different ratios of $CD34^+$ cells from healthy CB donors with $CD34^+$ cells from IMO patients with mutations in TCIRG1 and assessed their total capacity to resorb bone after osteoclast maturation. First, CB and IMO $CD34^+$ cells expanded for 2 weeks as described in "Methods" section were mixed at increasing CB to IMO $CD34^+$ cell ratio as specified in Fig. 5 and then differentiated into osteoclasts on plastic or on bone slices in the presence of M-CSF and RANKL. The protein expression of TCIRG1 in

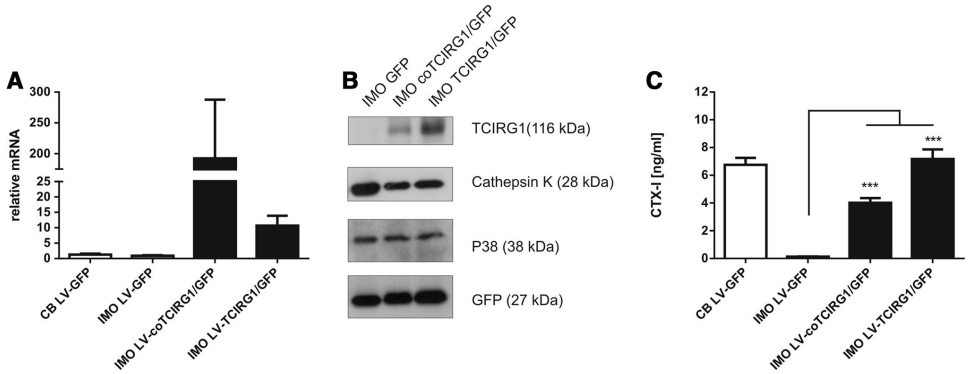

Fig. 4 A lentiviral vector with codon-optimized TCIRG1 generates higher levels of RNA but lower levels of protein and bone resorption in osteoclasts as compared to the non-optimized vector. IMO CD34$^+$ cells were transduced (MOI 30, 2 hits) with LV-GFP, LV-TCIRG1/GFP or LV-coTCIRG1/GFP, expanded for 2 weeks and compared to LV-GFP-transduced and expanded CD34$^+$ cells. mRNA was isolated after 14 days of expansion, qRT-PCR was performed, and the graph shows the average relative *TCIRG1* levels (±SEM) of three patient samples and cord blood controls, respectively (**a**). Western blot analysis was performed on lysates from mature osteoclasts after 10 days of differentiation. G = LV-GFP; co = LV-coTCIRG1/GFP; T = LV-TCIRG1/GFP (**b**). Organic bone resorption was assessed on day 10 by measuring CTX-I concentration in the supernatant (**c**). Statistical analysis was done using one-way ANOVA with a Dunnett post-test

the mixing cultures increased with the increasing percentage ratios of CB cells in a dose-dependent manner (Fig. 5a). We then determined osteoclast formation measured as TRAP (Fig. 5b), bone resorption measured by CTX-I release (Fig. 5c) and calculated the resorptive capacity per osteoclast assessed as CTX-I/TRAP ratio (Fig. 5d). For comparison purposes data were normalized to values obtained from osteoclasts differentiated from 100 % CB cells. Increasing percentage ratios of CB cells reduced the number of osteoclasts (Fig. 5b). Increased bone resorptive activity measured by CTX-I release was observed already at a CB cell to IMO cell ratio of 2.5/97.5 %, and at 10 % CB cells, resorptive capacity was restored to about half of that obtained from the pure CB-derived osteoclast population.

Mixing Increasing Ratios of LV-TCIRG1/GFP-Transduced and Expanded IMO CD34$^+$ Cells into Non-Corrected IMO CD34$^+$ Cells Followed by Osteoclast Generation Results in a Dose-Dependent Increase in Bone Resorption

To come as close as possible to a future gene therapy setting in the next experiment, we added LV-TCIRG1/GFP-transduced and expanded IMO CD34$^+$ cells to non-corrected expanded IMO CD34$^+$ cells at different ratios and differentiated these into osteoclasts on plastic or bone slices in the presence of M-CSF and RANKL. The transduction (2 hits MOI 30, efficiency 30 %) and expansion protocols are described in "Methods" section. The highest percentage ratio corrected versus non-corrected IMO cells was limited to 30/70 % as this was the transduction efficiency obtained in the corrected IMO cell population. Lacking a full rescue comparison, data were normalized to those obtained from 100 % non-corrected IMO osteoclasts. Western blot analysis showed a dose-dependent increase in expression of TCIRG1 with increasing amounts of corrected IMO cells, similar to what was observed for CB cells, but with slightly lower expression. Addition of LV-TCIRG1/GFP-transduced IMO cells to non-corrected cells led to a decrease in TRAP, which surprisingly increased slightly with rescued cell dose (Fig. 6b). At day 10, CTX-I was increased at a percentage ratio of as little as 2.5/97.5 % corrected IMO cells, while a 30/70 % ratio corrected cells resulted in a 12-fold increase in resorption compared to non-corrected IMO cells alone, as measured by CTX-I release (Fig. 6c), and a 14-fold increase in resorption per osteoclast (Fig. 6d).

In summary, these data support that at least some degree of in vitro rescue can be obtained using vector-transduced CD34$^+$ cells at doses as low as 2.5–5 % of the total cell population.

Discussion

Aiming at gene transfer correction of infantile malignant osteopetrosis, we introduced the TCIRG1 cDNA into IMO patient CD34$^+$ cells using a lentiviral vector followed by differentiation into mature osteoclasts as previously shown

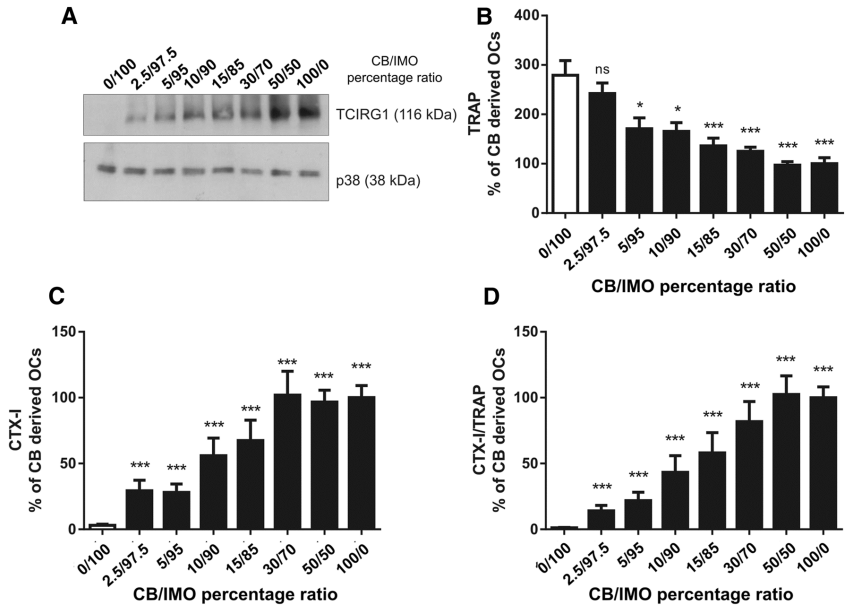

Fig. 5 Correctional effect of mixing normal CB and IMO cells. Normal CB CD34$^+$ cells and IMO CD34$^+$ were expanded, mixed at increasing CB to IMO ratio and then differentiated into mature osteoclasts on either plastic (western blot) or bovine cortical bone (for resorption assays). At day 10, cells were lysed and protein expression of TCIRG1 was analyzed by western blot and p38 was used as loading control (**a**). TRAP activity (**b**) and CTX-I (**c**) were measured at day 10, and the bone resorption per osteoclast (CTX-I/TRAP) (**d**) was calculated. *Data* in **b**–**d** are expressed as values compared to those obtained from osteoclasts generated from 100 % CB CD34$^+$ cells. Statistical analysis was done using one-way ANOVA with a Dunnett post-test comparing to 100 % IMO CD34$^+$ cells

[6]. Normally, driving transgene expression with a generic, non-tissue-specific promoter causes the transgene to be ectopically expressed at all time points and in all cell lineages derived from the transduced cells. However, despite high expression of the TCIRG1 mRNA in pre-osteoclasts, TCIRG1 protein was not detectable in LV-TCIRG1/GFP-transduced IMO pre-osteoclasts and early during osteoclastogenesis and no overexpression was observed in LV-TCIRG1/GFP-transduced CB cells. Our findings indicate that even vector-mediated TCIRG1 expression is restricted in a manner similar to what is observed during normal, RANKL-induced osteoclastogenesis and endogenous transcriptional regulation of TCIRG1 [21, 22].

In addition, we showed that when CD34$^+$ cells transduced with LV-TCIRG1/GFP were differentiated into macrophages instead of osteoclasts, by excluding RANKL, TCIRG1 protein expression was suppressed. The minor levels observed are likely explained by residual osteoclastogenesis, which is sometimes observed when cells are grown on plastic even without RANKL [15, 16]. In our experiments, the marker gene in our bicistronic vector, GFP, was expressed at high levels throughout all steps of expansion and differentiation, excluding a vector-specific regulation of protein expression.

Beranger and colleagues previously showed that TCIRG1 expression is regulated by transcription factors downstream of RANKL. The *TCIRG1* gene is repressed by the poly(ADP-ribose) polymerase-1 (PARP-1) in pre-osteoclasts [21]. Presence of RANKL causes release of the negative regulation by PARP-1 during osteoclastogenesis and leads to up-regulation of TCIRG1 through JunD proto-oncogene (JunD) and Fos-related antigen (Fra-2) [22]. However, our data strongly suggest that the expression of TCIRG1 is also regulated through post-transcriptional mechanisms linked to osteoclastogenesis. This mechanism is without consideration for whether the transcript is expressed from the lentiviral vector used here, a feature that is clearly beneficial when considering gene therapy of IMO.

Although the exact mechanism behind the post-transcriptional regulation is unclear, our data may indicate that glycosylation of the protein is involved. When ectopically

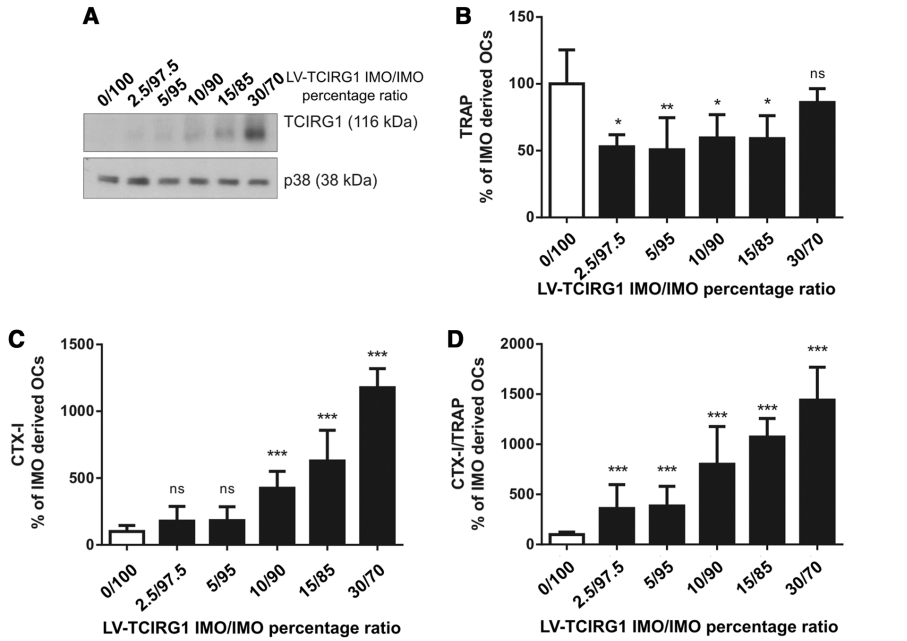

Fig. 6 Correctional effect of mixing LV-TCIRG1/GFP-corrected and non-corrected IMO cells. IMO $CD34^+$ cells and LV-TCIRG1/GFP-corrected $CD34^+$ IMO cells were expanded, mixed at increasing LV-TCIRG1/GFP-corrected IMO to non-corrected IMO cell ratio and then differentiated into mature osteoclasts on either plastic (western blot) or bovine cortical bone (for resorption assays). At day 10, cells were lysed and protein expression of TCIRG1 was analyzed by western blot and p38 was used as loading control (**a**). TRAP activity (**b**) and CTX-I (**c**) were measured at day 10, and the bone resorption per osteoclast (CTX-I/TRAP) was calculated (**d**). *Data* in **b**–**d** are expressed as values compared to those obtained from osteoclasts generated from 100 % non-corrected IMO $CD34^+$ cells. Statistical analysis was done using one-way ANOVA with a Dunnett post-test comparing to 100 % non-corrected IMO $CD34^+$ cells

expressing TCIRG1 in the HT1080 cells, both mRNA and protein were present within 72 h; however, the molecular weight was lower compared to the 116-kDa form seen in osteoclasts. Interestingly, deglycosylation in osteoclasts led to the presence of the 100-kDa form, showing that osteoclasts do glycosylate TCIRG1 as expected [19], most likely to protect it against degradation in the lysosomes. Importantly, this glycosylation is not seen when ectopically expressing TCIRG1 in HT1080 cells. However, further data are needed to fully clarify whether this is the mechanism behind the tightly controlled TCIRG1 expression in osteoclasts.

Another hypothesis may be that the TCIRG1 levels are dependent on the proper assembly of the V-ATPase complex. Studies have shown that correct assembly of the V-ATPase V_0 complex is necessary for protein stability [23]. Thus, it is possible that overexpression of TCIRG1 in the absence of other V_0 subunits results in TCIRG1 degradation, and only as the expression of the other subunits increases with osteoclastogenesis, TCIRG1 is stabilized and detectable by western blot. Indeed, the d2 subunit was shown to increase with osteoclastogenesis (Fig. 2a). However, the finding that TCIRG1 is readily expressed and detectable on WB in LV-TCIRG1/GFP-transduced HT1080 cells suggests that TCIRG1 is not dependent on the expression of the remaining subunits, at least in the HT1080 cell line. Alternatively, RNA-binding proteins could regulate translation of the TCIRG1 mRNA; however, at present this is unknown [24]. The dissection of these mechanisms is clearly of future interest, but beyond the scope of the current work.

Codon optimization has become a commonly employed technique in the field of viral gene transfer to increase expression of the protein of interest and thereby also the degree of functional correction [25, 26]. In an attempt to increase expression of TCIRG1 and the resorptive function of corrected IMO cells, we codon-optimized our transgene according to state-of-the-art methodology. However, even

though mRNA expression increased 20-fold, TCIRG1 protein expression and functional correction were consistently lower in all five patient samples tested when compared to our standard vector, while level of expression of GFP appeared to be the same from the two vectors as judged by western blot. Recently, published findings may explain the discrepancy in TCIRG1-mRNA and protein expression observed [27]. As reviewed by Mauro and Chappell, codon optimization appears to be more complex than initially considered [27]. For example, codon usage may influence ribosomal elongation rhythm, which may affect protein folding, and possibly also protein stability. Mauro and Chappell further suggested that constructs for human therapeutic applications primarily should be restricted to unmodified natural gene sequences if possible [27]. In line with this suggestion, the vector with the unmodified TCIRG1 cDNA, LV-TCIRG1/GFP, was used for further experiments.

For future development of gene therapy of osteopetrosis, an important question is to which level osteoclast function needs be restored in order to achieve correction of the disease phenotype in vivo. In our study, we found that normal $CD34^+$ cells amounting to as low as 5 % were able to incur a significant rescue of IMO patient cells. The findings were similar when using corrected IMO $CD34^+$ cells to incur rescue of IMO patient cells, a setting resembling a gene therapy treatment where the patient's own $CD34^+$ cells are isolated from peripheral blood, corrected ex vivo and infused back into the patient. The magnitude of the increase was higher in both scenarios than explained by the 5 % corrected cells, suggesting that corrected and non-corrected pre-osteoclasts may fuse and give rise to a larger number of functional osteoclasts. This is in line with previous findings showing that osteoclast progenitors transduced with a lentiviral vector containing a GFP marker gene may give rise to high numbers of GFP-expressing mature osteoclasts both in vitro and in vivo [6, 20]. In this context, it is worth to remember that patients with mutations in *TCIRG1* in only one allele do not exhibit any symptoms of osteopetrosis. Furthermore, recent findings in a case of mild autosomal recessive osteopetrosis caused by a mutation in intron 15 of *TCIRG1*, suggest that only minor gene doses are necessary for functional correction [28, 29].

One limitation in the current study when it comes to going forward toward a clinical gene therapy for IMO is the use of the SFFV-promoter. In a clinical setting, this promoter needs to be replaced with a mammalian promoter such as the elongation factor 1 short (EFS) for safety reasons [30, 31]; however, as exemplified here, regulation of TCIRG1 protein expression is to some extent promoter independent, and hence, it is likely that similar data will be obtained with a clinically applicable promoter.

In summary, we here show that lentiviral-mediated expression of *TCIRG1* is regulated in the same manner as the endogenous gene product despite being expressed by a lentiviral vector with a generic promoter. In addition, we established that the natural *TCIRG1* gene sequence leads to higher level of protein expression and functional rescue in osteoclasts than a codon-optimized cDNA of the gene, even though mRNA levels from the latter were considerably higher. Furthermore, only a low fraction of human pre-osteoclasts with a functional TCIRG1 is needed to significantly increase resorptive function in vitro [20]. From both an efficacy and a safety perspective, our findings are encouraging for the further development of gene therapy for osteopetrosis.

Acknowledgments We thank Christopher Baum and Axel Schambach (Hannover Medical School, Germany) for providing us with the lentiviral vector backbone. KH is supported by the Danish Research Foundation (Den Danske Forskningsfond). JR is supported by grants from the Swedish Childhood Cancer Foundation, a Clinical Research Award, from Lund University Hospital, the Foundations of Lund University Hospital. AS is partially supported by grants of the EU (ERARE initiative, project OSTEOPETR). HL is supported by Marie Curie Initial Training Networks (Euroclast, FP7-People-2013-ITN: # 607446). The Lund Stem Cell Center is supported by a Center of Excellence grant in life sciences from the Swedish Foundation for Strategic Research. The funders had no role in study design, data collection and analysis, decision to publish or preparation of the manuscript.

Compliance with Ethical Standards

Conflict of interest Morten Asser Karsdal owns stock in Nordic Bioscience. Christian Schneider Thudium, Ilana Moscatelli, Henrik Löfvall, Zsuzsanna Kertész, Carmen Montano, Carmen Flores Bjurström, Ansgar Schulz, Johan Richter and Kim Henriksen declare no competing financial interests.

Human and Animal Rights All procedures involving human subjects were approved by the local Human Investigation Ethics Committee.

Informed Consent Written informed consent was obtained from all subjects.

References

1. Segovia-Silvestre T, Neutzsky-Wulff AV, Sorensen MG, Christiansen C, Bollerslev J, Karsdal MA, Henriksen K (2009) Advances in osteoclast biology resulting from the study of osteopetrotic mutations. Hum Genet 124:561–577
2. Tolar J, Teitelbaum SL, Orchard PJ (2004) Osteopetrosis. N Engl J Med 351:2839–2849
3. Frattini A, Orchard PJ, Sobacchi C, Giliani S, Abinun M, Mattsson JP, Keeling DJ, Andersson AK, Wallbrandt P, Zecca L, Notarangelo LD, Vezzoni P, Villa A (2000) Defects in TCIRG1 subunit of the vacuolar proton pump are responsible for a subset of human autosomal recessive osteopetrosis. Nat Genet 25:343–346

4. Sobacchi C, Schulz A, Coxon FP, Villa A, Helfrich MH (2013) Osteopetrosis: genetics, treatment and new insights into osteoclast function. Nat Rev Endocrinol 9:522–536
5. Scimeca JC, Franchi A, Trojani C, Parrinello H, Grosgeorge J, Robert C, Jaillon O, Poirier C, Gaudray P, Carle GF (2000) The gene encoding the mouse homologue of the human osteoclast-specific 116-kDa V-ATPase subunit bears a deletion in osteosclerotic (oc/oc) mutants. Bone 26:207–213
6. Moscatelli I, Thudium CS, Flores C, Schulz A, Askmyr M, Gudmann NS, Andersen NM, Porras O, Karsdal MA, Villa A, Fasth A, Henriksen K, Richter J (2013) Lentiviral gene transfer of TCIRG1 into peripheral blood CD34(+) cells restores osteoclast function in infantile malignant osteopetrosis. Bone 57:1–9
7. Taranta A, Migliaccio S, Recchia I, Caniglia M, Luciani M, De Rossi G, Dionisi-Vici C, Pinto RM, Francalanci P, Boldrini R, Lanino E, Dini G, Morreale G, Ralston SH, Villa A, Vezzoni P, Del Principe D, Cassiani F, Palumbo G, Teti A (2003) Genotype-phenotype relationship in human ATP6i-dependent autosomal recessive osteopetrosis. Am J Pathol 162:57–68
8. Orchard PJ, Fasth AL, Le Rademacher J, He W, Boelens JJ, Horwitz EM, Al-Seraihy A, Ayas M, Bonfim CM, Boulad F, Lund T, Buchbinder DK, Kapoor N, O'Brien TA, Perez MAD, Veys PA, Eapen M (2015) Hematopoietic stem cell transplantation for infantile osteopetrosis. Blood 126:270–276
9. Schulz AS, Classen CF, Mihatsch WA, Sigl-Kraetzig M, Wiesneth M, Debatin K-M, Friedrich W, Müller SM (2002) HLA-haploidentical blood progenitor cell transplantation in osteopetrosis. Blood 99:3458–3460
10. Thudium CS, Jensen VK, Karsdal MA, Henriksen K (2012) Disruption of the V-ATPase functionality as a way to uncouple bone formation and resorption—a novel target for treatment of osteoporosis. Curr Protein Pept Sci [Internet] 13:141–151. http://www.ncbi.nlm.nih.gov/pubmed/22044152
11. Forgac M (2007) Vacuolar ATPases: rotary proton pumps in physiology and pathophysiology. Nat Rev Mol Cell Biol 8(11):917–929
12. Toei M, Saum R, Forgac M (2010) Regulation and isoform function of the V-ATPases. Biochemistry 49(23):4715–4723
13. Toyomura T, Murata Y, Yamamoto A, Oka T, Sun-Wada GH, Wada Y, Futai M (2003) From lysosomes to the plasma membrane. Localization of vacuolar type H+-ATPase with the a3 isoform during osteoclast differentiation. J Biol Chem 278:22023–22030
14. Johansson MK, De Vries TJ, Schoenmaker T, Ehinger M, Brun ACM, Fasth A, Karlsson S, Everts V, Richter J (2007) Hematopoietic stem cell-targeted neonatal gene therapy reverses lethally progressive osteopetrosis in oc/oc mice. Blood 109(12):5178–5185
15. Sørensen MG, Henriksen K, Schaller S, Henriksen DB, Nielsen FC, Dziegiel MH, Karsdal MA (2007) Characterization of osteoclasts derived from CD14+ monocytes isolated from peripheral blood. J Bone Miner Metab 25(1):36–45
16. Henriksen K, Karsdal MA, Taylor A, Tosh D, Coxon FP (2012) Generation of human osteoclasts from peripheral blood. Methods Mol Biol 816:159–175
17. Sørensen MG, Henriksen K, Neutzsky-Wulff AV, Dziegiel MH, Karsdal MA (2007) Diphyllin, a novel and naturally potent V-ATPase inhibitor, abrogates acidification of the osteoclastic resorption lacunae and bone resorption. J Bone Miner Res 22:1640–1648
18. Karsdal MA, Hjorth P, Henriksen K, Kirkegaard T, Nielsen KL, Lou H, Delaissé JM, Foged NT (2003) Transforming growth factor-β controls human osteoclastogenesis through the p38 MAPK and regulation of RANK expression. J Biol Chem 278:44975–44987
19. Bhargava A, Voronov I, Wang Y, Glogauer M, Kartner N, Manolson MF (2012) Osteopetrosis mutation R444L causes endoplasmic reticulum retention and misprocessing of vacuolar H+-ATPase a3 subunit. J Biol Chem 287:26829–26839
20. Flores C, De Vries TJ, Moscatelli I, Askmyr M, Schoenmaker T, Langenbach GEJ, Ehinger M, Everts V, Richter J (2010) Non-ablative neonatal bone marrow transplantation rapidly reverses severe murine osteopetrosis despite low-level engraftment and lack of selective expansion of the osteoclastic lineage. J Bone Miner Res 25(9):2069–2077
21. Beranger GE, Momier D, Rochet N, Quincey D, Guigonis J-M, Samson M, Carle GF, Scimeca J-C (2006) RANKL treatment releases the negative regulation of the poly(ADP-ribose) polymerase-1 on Tcirg1 gene expression during osteoclastogenesis. J Bone Miner Res 21:1757–1769
22. Beranger GE, Momier D, Guigonis J-M, Samson M, Carle GF, Scimeca J-C (2007) Differential binding of poly(ADP-Ribose) polymerase-1 and JunD/Fra2 accounts for RANKL-induced Tcirg1 gene expression during osteoclastogenesis. J Bone Miner Res 22:975–983
23. Kane PM, Tarsio M, Liu J (1999) Early steps in assembly of the yeast vacuolar H+-ATPase. J Biol Chem [Internet] [cited 2016 May 10], 274:17275–17283. http://www.ncbi.nlm.nih.gov/pubmed/10358087
24. Glisovic T, Bachorik JL, Yong J, Dreyfuss G (2008) RNA-binding proteins and post-transcriptional gene regulation. FEBS Lett 582(14):1977–1986
25. Athanasopoulos T, Foster H, Foster K, Dickson G (2011) Codon optimization of the microdystrophin gene for Duchene muscular dystrophy gene therapy. Methods Mol Biol 709:21–37
26. Suwanmanee T, Hu G, Gui T, Bartholomae CC, Kutschera I, von Kalle C, Schmidt M, Monahan PE, Kafri T (2014) Integration-deficient lentiviral vectors expressing codon-optimized R338L human FIX restore normal hemostasis in Hemophilia B mice. Mol Ther 22:567–574
27. Mauro VP, Chappell SA (2014) A critical analysis of codon optimization in human therapeutics. Trends Mol Med 20:604–613
28. Sobacchi C, Pangrazio A, Lopez AG-M, Gomez DP-V, Caldana ME, Susani L, Vezzoni P, Villa A (2014) As little as needed: the extraordinary case of a mild recessive osteopetrosis owing to a novel splicing hypomorphic mutation in the TCIRG1 gene. J Bone Miner Res 29:1646–1650
29. Palagano E, Blair HC, Pangrazio A, Tourkova I, Strina D, Angius A, Cuccuru G, Oppo M, Uva P, Van Hul W, Boudin E, Superti-Furga A, Faletra F, Nocerino A, Ferrari MC, Grappiolo G, Monari M, Montanelli A, Vezzoni P, Villa A, Sobacchi C (2015) Buried in the middle but guilty: intronic mutations in the TCIRG1 gene cause human autosomal recessive osteopetrosis. J Bone Miner Res 30:1814–1821
30. Modlich U, Navarro S, Zychlinski D, Maetzig T, Knoess S, Brugman MH, Schambach A, Charrier S, Galy A, Thrasher AJ, Bueren J, Baum C (2009) Insertional transformation of hematopoietic cells by self-inactivating lentiviral and gammaretroviral vectors. Mol Ther 17:1919–1928
31. Carbonaro DA, Zhang L, Jin X, Montiel-Equihua C, Geiger S, Carmo M, Cooper A, Fairbanks L, Kaufman ML, Sebire NJ, Hollis RP, Blundell MP, Senadheera S, Fu P-Y, Sahaghian A, Chan RY, Wang X, Cornetta K, Thrasher AJ, Kohn DB, Gaspar HB (2014) Preclinical demonstration of lentiviral vector-mediated correction of immunological and metabolic abnormalities in models of adenosine deaminase deficiency. Mol Ther 22:607–622

Paper II

RESEARCH ARTICLE

Targeting NSG Mice Engrafting Cells with a Clinically Applicable Lentiviral Vector Corrects Osteoclasts in Infantile Malignant Osteopetrosis

Ilana Moscatelli,[1] Henrik Löfvall,[1,2] Christian Schneider Thudium,[2] Michael Rothe,[3] Carmen Montano,[1] Zsuzsanna Kertész,[1] Mehtap Sirin,[4] Ansgar Schulz,[4] Axel Schambach,[3] Kim Henriksen,[2] and Johan Richter[1]

[1]Department of Molecular Medicine and Gene Therapy, Lund Strategic Center for Stem Cell Biology, Lund University, Lund, Sweden; [2]Nordic Bioscience, Herlev, Denmark; [3]Institute of Experimental Hematology, Hannover Medical School, Hannover, Germany; [4]Department of Pediatrics and Adolescent Medicine, University Medical Center, Ulm, Germany.

Infantile malignant osteopetrosis (IMO) is a rare, lethal, autosomal recessive disorder characterized by nonfunctional osteoclasts. More than 50% of the patients have mutations in the *TCIRG1* gene, encoding for a subunit of the osteoclast proton pump. The aim of this study was to develop a clinically applicable lentiviral vector expressing TCIRG1 to correct osteoclast function in IMO. Two mammalian promoters were compared: elongation factor 1α short (EFS) promoter and chimeric myeloid promoter (ChimP). EFS promoter was chosen for continued experiments, as it performed better. IMO osteoclasts corrected *in vitro* by a TCIRG1-expressing lentiviral vector driven by EFS (EFS-T) restored Ca^{2+} release to 92% and the levels of the bone degradation product CTX-I to 95% in the media compared to control osteoclasts. IMO $CD34^+$ cells from five patients transduced with EFS-T were transplanted into NSG mice. Bone marrow was harvested 9–19 weeks after transplantation, and human $CD34^+$ cells were selected, expanded, and seeded on bone slices. Vector-corrected IMO osteoclasts had completely restored Ca^{2+} release. CTX-I levels in the media were 33% compared to normal osteoclasts. Thus, in summary, evidence is provided that transduction of IMO CD34+ cells with the clinically applicable EFS-T vector leads to full rescue of osteoclasts *in vitro* and partial rescue of osteoclasts generated from NSG mice engrafting hematopoietic cells. This supports the continued clinical development of gene therapy for IMO.

Keywords: IMO, gene therapy, MSC, lentiviral vector

INTRODUCTION

Infantile malignant osteopetrosis (IMO) is the most severe subtype of osteopetrosis. This heterogeneous group of rare diseases is characterized by the inability of osteoclasts to resorb bone.[1,2] While the disease itself presents as an increase in bone mass, the bones are brittle and prone to fracture, despite their increased density. The cellular phenotype is characterized by an increased amount of osteoclasts that are unable to resorb bone.[3] The *TCIRG1* gene encoding the a3 subunit of the osteoclastic V-ATPase is commonly mutated in IMO patients, leading to an absence of the a3 subunit in their osteoclasts.[3,4] *TCIRG1* mutations account for up to 50% of all IMO cases.[5,6] A mutation in *TCIRG1* is also the cause of osteopetrosis in the *oc/oc* mouse model of the disease.[7] Unless treated, IMO has a fatal outcome, and most patients die within their first 6 years of life. The preferred treatment for IMO is to perform hematopoietic stem cell transplantation (HSCT) as early as possible after diagnosis, as osteoclasts are derived from hematopoietic stem cells via the monocytic lineage.[8,9] However, development of stem cell–based gene therapy for this disease might circumvent some of the complications associated with HSCT.[10]

Previous studies have rescued the murine *oc/oc* disease model of osteopetrosis with gene therapy, utilizing a gammaretroviral vector to target hematopoietic stem cells.[11] It has also been demonstrated

*Correspondence: Prof. Johan Richter, Department of Molecular Medicine and Gene Therapy, BMC A12, 221 84 Lund, Sweden. E-mail: Johan.Richter@med.lu.se

DOI: 10.1089/hum.2017.053

that the resorptive function of human IMO osteoclasts was restored *in vitro* by lentiviral-mediated gene transfer of *TCIRG1* cDNA into $CD34^+$ cells obtained from the peripheral blood of IMO patients followed by expansion of the cells in culture and differentiation on bone slices to mature bone-resorbing osteoclasts.[4] However, in that study, *TCIRG1* was driven by the spleen focus forming virus (SFFV) promoter that raises safety concerns in terms of insertional deregulation of proto-oncogenes.[12] Instead of employing strong viral promoter/enhancer sequences, having led to severe adverse events in past gene therapy trials,[13,14] the use of weaker cellular promoters can increase treatment safety.

The current work thus modified the lentiviral vector for possible use in a clinical setting. The SFFV promoter was replaced with one of two different mammalian promoters, and these were then tested for correction of IMO osteoclast function *in vitro*. The correction at the level of putative stem cells was also assessed by transplantation of gene corrected $CD34^+$ cells from IMO patients to NSG mice.

MATERIALS AND METHODS

$CD34^+$ cell isolation, culture, and expansion

Samples of peripheral blood from IMO patients (University Medical Center Ulm; Supplementary Table S1; Supplementary Data are available online at www.liebertpub.com/hum) or umbilical cord blood (CB) from normal deliveries (Lund, Malmö, and Helsingborg Hospitals) were obtained after informed consent under protocols approved by institutional ethical boards. Mononuclear cells from these sources were isolated using density gradient centrifugation with Ficoll, and $CD34^+$ cells were subsequently separated from the mononuclear cell fraction using MACS columns (Miltenyi Biotec, Bergisch Gladbach, Germany). For expansion, cells were cultured in StemSpan™ Serum-Free Expansion Medium (SFEM; StemCell Technologies, Vancouver, Canada), with the following human recombinant cytokines: macrophage colony-stimulating factor (M-CSF; 50 ng/mL), granulocyte macrophage colony-stimulating factor (GM-CSF; 30 ng/mL), stem cell factor (SCF; 200 ng/mL), interleukin-6 (IL-6; 10 ng/mL), and Flt3L (50 ng/mL), all from R&D Systems (Minneapolis, MN). $CD34^+$ cells were plated at a density of 5×10^4 cells in 1 mL of medium using 24-well bacteriological plates and incubated for a week at 37°C before collection and re-plating at a density of 1×10^5/well. From day 7, the medium was exchanged every 2–3 days by demi-depletion. For transplantation, $CD34^+$ cells were cultured for 30 h in StemSpan™ SFEM with the following human recombinant cytokines (100 ng/mL): SCF, Flt3L, and thrombopoietin (TPO), all from R&D Systems.

Vectors, viral production, and transduction of $CD34^+$ cells

All the vectors used in this study are self-inactivating (SIN) lentiviral vectors with a pRRL backbone (Supplementary Fig. S1). For comparing promoter experiments, three rescue vectors were used (SFFV-TG, EFS-TG, ChimP-TG), which contain the cDNA of human *TCIRG1* under the spleen focus-forming virus (SFFV) promoter, the elongation factor 1α short (EFS) promoter, or the chimeric myeloid promoter (ChimP),[15] respectively, upstream of an internal ribosomal entry site (IRES), which is followed by the gene for enhanced green fluorescent protein (GFP) used as a marker gene. For subsequent *in vitro* studies and for transplantations, a vector expressing *TCIRG1* alone under the EFS promoter (EFS-T) was used, without any marker gene. Control vectors expressed GFP under the SFFV or EFS promoters (SFFV-G, EFS-G). Lentiviral vectors were produced by transient transfection of the vector plasmids into 293T cells, along with packaging plasmid (pCMV ΔR8.91), and envelope plasmid (VSV-G pMDG). Transductions were carried out in 24-well plates coated with RetroNectin (Takara Bio, Otsu, Japan). For the *in vitro* experiments, $CD34^+$ cells were transduced with a first hit at a multiplicity of infection (MOI) of 30 for 6 h on day 3 and a second hit at a MOI of 30 for 6 h on day 7 followed by a week of culture with a myeloid cytokine cocktail and subsequent differentiation to osteoclasts, as described above. For the *in vivo* experiments, a shorter transduction protocol was developed to allow efficient transduction while maintaining the stem/progenitor nature of the $CD34^+$ population. Mononuclear cells were thawed, and $CD34^+$ cells were isolated and transduced with the first hit (MOI of 30 or 100) overnight followed by transduction on the following day with a second hit (MOI of 30 or 100) for 6 h, after which the cells were transplanted in the NSG mice. The total culture time of the cells prior to transplantation was <30 h.

Osteoclastogenesis

After 2 weeks, the expanded cells were reseeded into 96-well plates on plastic or on bovine cortical bone slices at a density of 1×10^5/well for cell assays and 1.0×10^6/well on plastic in a 12-well plate for Western blot. The cells were incubated at 37°C and 5% CO_2 in alpha minimum essential medium containing 10% heat-inactivated fetal bovine serum (FBS), 100 units/mL of penicillin, 100 μg/mL of

streptomycin, and 388 μg/L of thymidine. They were expanded for 3 days in the presence of 50 ng/mL of M-CSF and were differentiated for an additional 10 days in the presence of 50 ng/mL of M-CSF and 50 ng/mL of receptive activator of nuclear factor kappa-B ligand (RANKL), both from R&D Systems, with medium changes every 2–3 days. After 13 days, the cells were either fixed in 4% formaldehyde for further analyses or lysed for Western blot analysis. Resorption was assessed by CTX-I and Ca^{2+} release into the media and the formation of resorption pits. Osteoclastogenesis was assessed by tartrate-resistant acid phosphatase (TRAP) activity in the media.

Western blot

Cells were harvested into radioimmunoprecipitation assay (RIPA) buffer. Protein concentrations were measured using a Protein Assay Kit II (Bio-Rad, Hercules, CA). Total protein (15 μg) in SDS sample buffer was separated by gel electrophoresis in an SDS-PAGE 4–12% gradient gel followed by blotting onto a nitrocellulose membrane. Membranes were then blocked in Tris-buffered saline (TBS) with Tween 20 (TBST) with 5% skim milk powder for 1 h at room temperature followed by incubation with a primary antibody overnight at 4°C in TBST with 5% skim milk powder using the following antibody dilutions: mouse monoclonal anti-TCIRG1 (catalog # H00010312-M01A; Abnova, Taipei, Taiwan) 1:1000 and rabbit polyclonal anti-p38 MAPK (catalog # 9212; Cell Signaling Technology, Danvers, MA) 1:1000. The blots were then washed for 3 × 10 min and incubated with the corresponding horseradish peroxidase–conjugated secondary antibody for 1 h at room temperature followed by 3 × 10 min washes in TBS. Blots were developed using ECL Western Blotting Reagents (GE Healthcare, Waukesha, WI). To estimate the relative TCIRG1 protein expression levels between vectors, a semi-quantitative analysis of the developed Western blot films was carried out using Fiji.[16] The films were digitized as PDF files using an office scanner, and converted into 8-bit black-and-white tiff images in Fiji. The bands of interest were marked using the rectangle tool, and the band intensity peaks were plotted using the gel analysis tool. Background signals in the plots were removed by separating the peaks from the background intensity using the straight-line tool, and the area of each isolated peak was subsequently measured. The TCIRG1 peak areas were divided by the corresponding p38 peak areas, and the TCIRG1/p38 peak area ratios were normalized to that of the CB EFS-T condition, due to one experiment lacking a CB EFS-G condition, of the respective experiment ($n = 3$).

TRAP activity measurements

Between 1 and 20 μL of media from 96-well cell cultures on either bone or plastic was added to a 96-well plate and diluted with water to a volume of 20 μL. The diluted samples were incubated with 80 μL of freshly prepared reaction buffer (0.25 M acetic acid, 0.125% Triton X-100, 0.25 M NaCl, 2.5 mM EDTA, 1.1 mg/mL of ascorbic acid, 5.75 mg/mL of disodium tartrate, 2.25 mg/mL of 4-nitrophenylphosphate, pH 5.5) at 37°C for 1 h in the dark, and the reaction was then stopped by adding 100 μL of 0.3 M NaOH. Absorbance was measured at 405 nm, with 650 nm as a reference using a SpectraMax M5 (Molecular Devices, Sunnyvale, CA) plate reader.

Resorption biomarkers

The release of the c-terminal type I collagen fragments (CTX-I) from resorbed bone slices was determined using the CrossLaps for Culture kit (IDS, Boldon Colliery, United Kingdom), which was used according to the manufacturer's instructions.

The release of Ca^{2+} was analyzed by measuring the concentration of total calcium in media after resorption using a colorimetric calcium (CPC) assay and an ADVIA 1800 Clinical Chemistry System (both from Siemens Healthineers, Erlangen, Germany).

Resorption pit formation

Resorption pits on the fixed bone slices were visualized by washing them with water, removing the remaining cells by lysing them with RIPA buffer, and scrubbing with a cotton swab followed by staining with hematoxylin for 7 min. Excess dye was removed by scrubbing the bones with a cotton swab. Digital micrographs were obtained using a 10 × objective and an Olympus DP71 digital camera mounted on an Olympus IX-70 microscope using the Cell-A software (Olympus, Center Valley, PA).

NSG mice and transplantations

Breeding pairs of immunodeficient NOD-scid IL2rγ^{null} (NSG) mice were obtained from Charles River Laboratories (Sulzfeld, Germany). The mice were maintained in the conventional animal facility at the Biomedical Centre, Lund University. All experiments were performed according to protocols approved by the local animal ethics committee. NSG mice (8–15 weeks old) were sub-lethally irradiated with 300 cGy and transplanted 6 h later with 1×10^5 untransduced CB $CD34^+$ cells or IMO

$CD34^+$ cells transduced with either EFS-T or EFS-G by tail-vein injection. The mice were administered ciprofloxacin via their drinking water for 2 weeks to avoid post-transplantation infections. Peripheral blood was harvested at different time points, and bone-marrow cells were harvested by crushing the femora with a mortar after termination of the mice.

Vector copy number

Vector copy number (VCN) analysis was performed on whole bone-marrow genomic DNA from samples harvested from mice 9–19 weeks after transplantation. The mean VCN per cell was determined by quantitative reverse transcription polymerase chain reaction. Samples were measured in triplicates using 100 ng of genomic DNA. Primers for the WPRE element of the vector were used to determine the amount of viral sequences, which was further normalized to a genomic reference sequence of the *Ptbp2* gene.[17] A serial dilution of a plasmid standard containing both sequences was measured in parallel to perform an absolute quantification. A cell line clone with predetermined VCN was used as an inter-plate calibrator.

In vitro immortalization assay

Three independent *in vitro* immortalization (IVIM) assays using the EFS-T vector were performed at Hannover Medical School according to previously published protocols.[18–20] For determining the incidence of positive and negative assays, potentially immortalized clones were discriminated from rare cases of background proliferation by the first quartile (Q1) expectation level of the positive control. A mutagenic vector such as RV-SF, at VCN levels above three copies, is expected to show positive assays with re-plating frequencies (RF) $>3.17\times10^4$ in 75% of the cases (experience from metadata available at Hannover Medical School). All plates with a RF between the limit of detection (LOD; 1.05×10^4) and the Q1 level cannot be distinguished from spontaneous cell proliferation.

Flow cytometric analysis of cells from transplanted NSG mice

Peripheral blood and bone marrow of transplanted NSG mice was analyzed for human reconstitution by determining the percentage of cells positive for huCD45-APC (BD Biosciences, San Jose, CA) and for transduction efficiency by determining the percentage of GFP^+ cells in the control group. For lineage analysis, the cells were stained with antibodies directed against CD33-PeCy7, CD15-PeCy7, CD19-BV605, and CD3-PE (all from BD Biosciences).

Statistics

The resorptive function of osteoclasts generated from NSG-engrafting vector-corrected IMO hematopoietic cells was analyzed statistically by comparing the EFS-T condition with the EFS-G condition using a two-sided Mann–Whitney test, where * indicates $p<0.05$, ** indicates $p<0.01$, *** indicates $p<0.001$, and **** indicates $p<0.0001$. Results are shown as the means ± standard error of the mean (SEM). For the IVIM assay, the significance of the differences between RF was calculated with Fisher's exact test, where * indicates $p<0.05$.

RESULTS

Restored resorptive function of osteoclasts from IMO patients after lentiviral-mediated TCIRG1 gene transfer driven by mammalian promoters

It was previously shown that $CD34^+$ IMO cells transduced with SFFV-TG can be differentiated into functional osteoclasts *in vitro*.[4] In this study, the efficacy of two different mammalian promoters—EFS and ChimP—were evaluated by comparing them to SFFV-TG (Supplementary Fig. S1). All three TCIRG1-expressing vectors transduced approximately 35% of IMO $CD34^+$ cells after two hits with a MOI of 30 (Fig. 1A). Transduced IMO and CB $CD34^+$ cells were differentiated into osteoclasts on plastic, and TCIRG1 protein expression was analyzed by Western blot. TCIRG1 protein was expressed in the mature rescued osteoclasts at day 13 of osteoclast culture, but TCIRG1 protein was not detected in untransduced IMO cells or cells transduced with SFFV-G (Fig. 1B). The TCIRG1 levels were highest in cells exposed to the SFFV-TG vector followed by the EFS-TG vector and lowest in cells exposed to the ChimP-TG vector. Osteoclast differentiation on bone slices was verified by assessing TRAP activity in the media, and the ability to resorb bone was evaluated by measuring the release of Ca^{2+} and CTX-I. The Ca^{2+} and CTX-I levels increased in $CD34^+$-derived IMO osteoclasts transduced with the rescue vectors compared to those transduced with the SFFV-G vector and the untransduced IMO osteoclasts, indicating an increase in resorptive activity and at least partial restoration of function (Fig. 1C and D). Once again, the levels were highest for cells transduced with SFFV-TG (Ca^{2+}: 80 ± 11%; CTX-I: 81 ± 6%, relative to CB-derived osteoclasts), followed by EFS-TG (Ca^{2+}: 72 ± 7%; CTX-I: 54 ± 16%), and finally

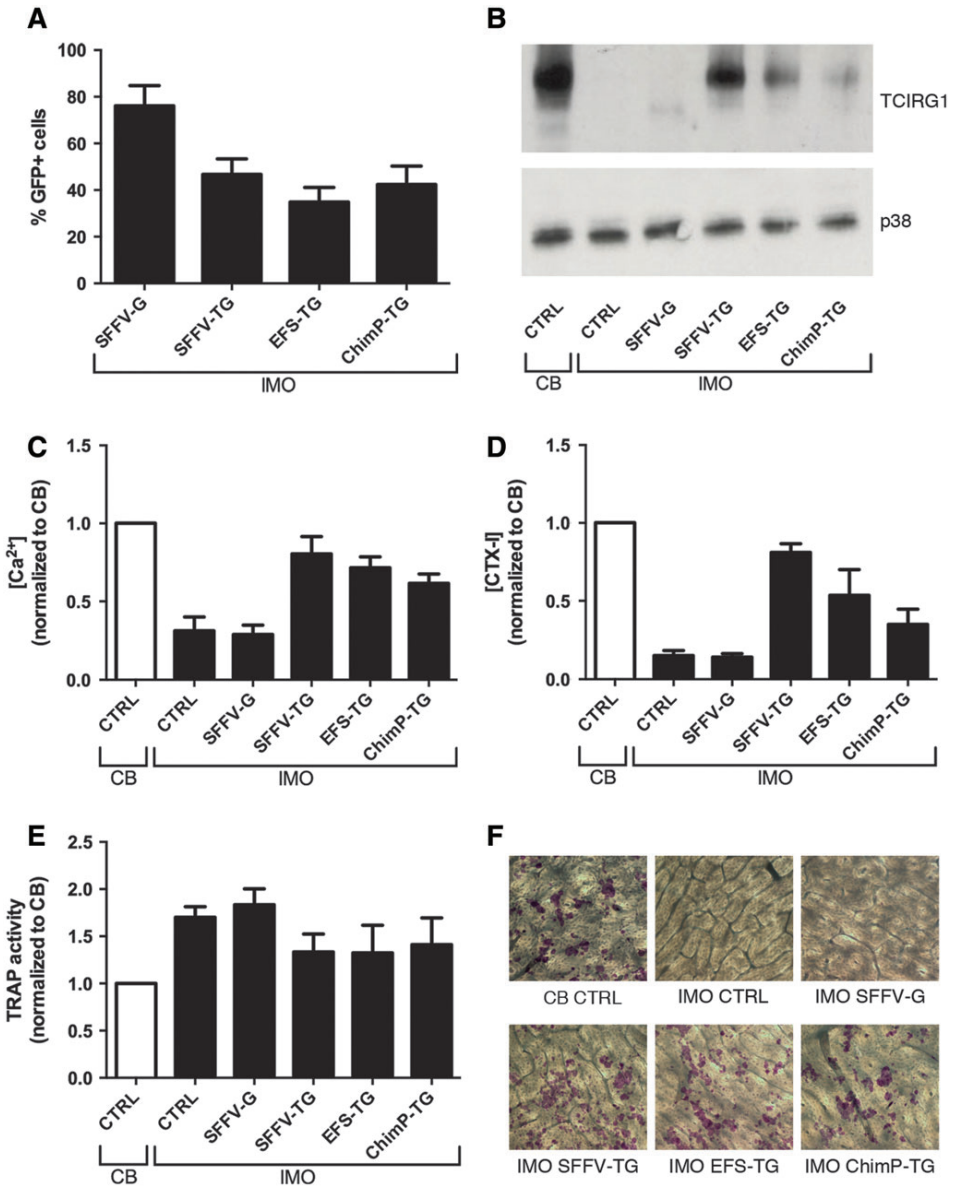

Figure 1. Lentiviral transduction of *TCIRG1* driven by mammalian promoters can restore resorption in osteoclasts differentiated from infantile malignant osteopetrosis (IMO) $CD34^+$ cells *in vitro*. $CD34^+$ cells were transduced and expanded for 2 weeks, seeded on bone slices, and differentiated into osteoclasts for 13 days in the presence of macrophage colony-stimulating factor (M-CSF) and receptive activator of nuclear factor kappa-B ligand (RANKL). **(A)** Transduction efficiency was evaluated as % of green fluorescent protein (GFP^+) cells determined by flow cytometry. **(B)** Western blot analysis was performed on lysates from mature osteoclasts after 13 days of differentiation. **(C)** Resorption of the inorganic bone matrix was evaluated by measuring Ca^{2+} release into the media. **(D)** Resorption of the organic bone matrix was assessed on day 13 by measuring the CTX-I concentration in the media. **(E)** Tartrate-resistant acid phosphatase (TRAP) activity in the media was measured for osteoclast quantification. **(F)** At day 13 of osteoclast differentiation, bone slices were stained for resorption pits, as described in Materials and Methods. Formation of resorption pits was visualized on a microscope with a 10× objective, and images are representative of three different bone slices per condition. The data are shown as means ± standard error of the mean (SEM).

ChimP-TG (Ca^{2+}: 62±6%; CTX-I: 35±9%). Ca^{2+} and CTX-I levels remained unchanged in IMO SFFV-G osteoclasts compared to untransduced IMO osteoclasts. Media from the *TCIRG1*-transduced IMO osteoclasts had a slightly lowered TRAP activity compared to both SFFV-G and IMO controls (Fig. 1E). To evaluate further the effect of lentiviral gene transfer of *TCIRG1* cDNA into IMO osteoclasts, bone slices were stained with hematoxylin to visualize resorption pits. After 13 days of differentiation, the mature IMO osteoclasts generated from cells transduced with the rescue vectors had formed a high number of clearly visible pits, whereas resorption pits were almost absent on bones with untransduced IMO cells and IMO cells transduced with SFFV-G (Fig. 1F). Although there was no statistically significant difference between the biomarker values for EFS-TG and ChimP-TG, there was a consistent trend present in four parameters (Ca^{2+}, CTX-I, TRAP, and WB expression levels) in all experiments, indicating that EFS-TG was the vector that generated the highest expression levels and the best functional outcome *in vitro* of the tested mammalian vectors.

Clinically relevant EFS-T vector can restore resorption in osteoclasts differentiated from IMO CD34$^+$ cells *in vitro*

Having chosen the EFS promoter for continued experiments, the IRES and GFP were removed from the EFS-TG vector to obtain the clinically relevant EFS-T vector, which was then tested *in vitro* for efficacy and safety (Supplementary Fig. S1). Transduced IMO and CB CD34$^+$ cells were differentiated into osteoclasts on plastic for analysis of TCIRG1 expression and on bone slices for resorption analysis. The expression of TCIRG1, evaluated by Western blot, was higher in the cells transduced with EFS-T than in those transduced with EFS-TG (Fig. 2A). Both the Ca^{2+} (Fig. 2B) and the CTX-I (Fig. 2C) levels in the media were higher when using EFS-T (Ca^{2+}: 92±5%; CTX-I: 95±6%) than when using EFS-TG (Ca^{2+}: 76±14%; CTX-I: 67±28%), and they were nearly comparable to those from CB-derived osteoclasts. TRAP activity was lower in the media from cells transduced with EFS-T than from those transduced with EFS-G, indicating a trend to normalization to the levels observed in the media of CB-derived osteoclasts (Fig. 2D). The osteoclasts derived from IMO cells transduced with EFS-T were capable of forming high numbers of resorption pits on bone slices (Fig. 2E), thus confirming the functional rescue of IMO cells *in vitro* with the EFS-T vector.

EFS-T exhibits a low mutagenic potential compared to RV-SF and LV-SF

A safety concern regarding the clinical use of integrating viral vectors is the risk of insertional mutagenesis. The IVIM assay has demonstrated the capability to detect transformation of virally transduced cells under myeloid differentiation conditions.[18] In three independent IVIM assays, the EFS-T vector was compared to a gammaretroviral vector (RV-SF) and to a lentiviral vector, with the strong viral promoter SFFV (LV-SF) as positive controls. Cells were also subject to mock transduction in similar culture conditions, without viral vector, to monitor background activity. No replating clones were seen for the mock control or the EFS-T vector, whereas RV-SF-transduced samples induced clones in 5/8 cases, and the LV-SF-transduced samples induced clones in 2/5 cases (Fig. 3). The RV-SF vector had a mean RF of 8.34×10^{-3}, the LV-SF vector had a mean RF of 1.24×10^{-3}, and the EFS-T vector only had one positive well in 2/10 cases, corresponding to a mean RF of 2.63×10^{-5}.

Long-term engraftment of transduced CB and IMO CD34$^+$ cells in NSG mice

NSG mice (8–15 weeks old) were transplanted with untransduced CB CD34$^+$ cells or IMO CD34$^+$ cells transduced with either EFS-T or EFS-G (Table 1). The mice were sacrificed 9–19 weeks post transplantation, and bone marrow was analyzed for human reconstitution, the control animals transplanted with IMO cells transduced with EFS-G also for the level of GFP marking. In all groups of transplanted mice, human CD45$^+$ cells were on average around 35% (Fig. 4A), showing that peripheral blood IMO CD34$^+$ cells have the capacity to engraft in NSG mice similarly to CB CD34$^+$ cells. In addition, GFP-marked cells were found in all mice transplanted with IMO cells transduced with EFS-G (1.1–12.6% of huCD45$^+$ cells). No differences in lineage distribution of bone-marrow cells harvested from mice transplanted with human CB CD34$^+$ cells or with IMO CD34$^+$ cells transduced with EFS-G or EFS-T were observed, indicating that EFS-T does not skew the differentiation potential of transduced CD34$^+$ cells in the NSG model (Fig. 4B).

Restored resorptive function of osteoclasts generated from NSG-engrafting vector-corrected IMO hematopoietic cells

Bone-marrow cells were harvested from NSG mice 9–19 weeks after transplantation with CB cells ($n=5$) or IMO cells transduced with EFS-G ($n=7$) or EFS-T ($n=11$). Human CD34$^+$ cells were

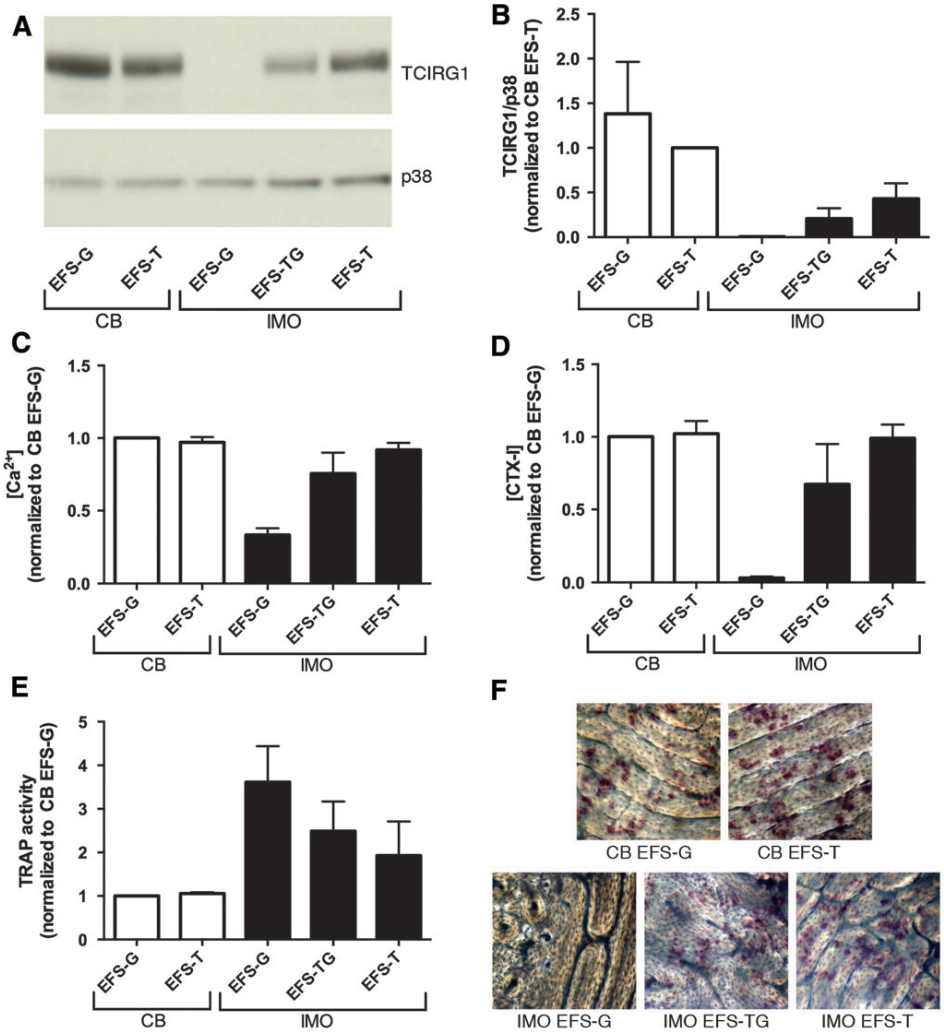

Figure 2. The clinically relevant EFS-T vector can restore resorption in osteoclasts differentiated from IMO $CD34^+$ cells *in vitro*. $CD34^+$ cells were transduced and expanded for 2 weeks, seeded on bone slices, and differentiated into osteoclasts for 13 days in the presence of M-CSF and RANKL. **(A)** Western blot analysis was performed on lysates from mature osteoclasts after 13 days of differentiation. **(B)** The relative protein expression of TCIRG1 from the Western blots ($n=3$) was analyzed by calculating the peak area ratios, as described in Materials and Methods. The concentration of Ca^{2+} **(C)** and CTX-I **(D)** as well as TRAP activity **(E)** was measured in the media at day 13. **(F)** At day 13 of osteoclast differentiation, bone slices were stained for resorption pits, as described in Materials and Methods. Formation of resorption pits was visualized on a microscope with a 10× objective, and images are representative of three different bone slices per condition. The data are shown as means ± SEM.

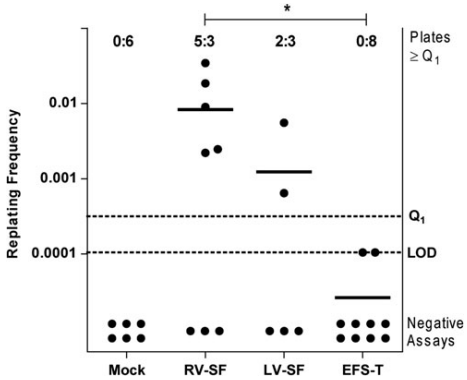

Figure 3. EFS-T exhibits a low mutagenic potential compared to RV-SF and LV-SF. Re-plating frequency (RF) of mock, RV-SF, LV-SF, and EFS-T transduced samples. *Black bar* indicates the mean RF. The *filled circles* for negative assays below the limit of detection (LOD) were manually inserted into the graph. The difference in incidence of positive (above the Q1 level) to negative assays for RV-FS to EFS-T was significant ($p=0.0256$).

isolated (range of $CD34^+$ cells per mouse 1.5–9.6%), expanded for 2 weeks, seeded on plastic or bone slices, and differentiated into osteoclasts for 13 days in the presence of M-CSF and RANKL. Western blot analysis was performed on lysates from mature osteoclasts differentiation and showed the presence of the a3 subunit after rescue in 4/8 of the mice transplanted with IMO EFS-T cells. Lysates from two different mice in this group are shown (Fig. 5A), one in which TCIRG1 could be detected and one in which it was not detected, suggesting that there was variability of rescue of NSG-engrafting cells between mice. Vector-corrected IMO osteoclasts exhibited completely restored Ca^{2+}-release ($97\pm21\%$ compared to CB-derived osteoclasts), with a 3.4-fold increase (Fig. 5B; $p=0.019$) relative to the non-corrected IMO osteoclasts. CTX-I levels in the media were partially restored ($33\pm6\%$ compared to CB-derived osteoclasts) and 14-fold ($p<0.0001$) higher than those of the non-corrected IMO osteoclasts, which failed to resorb bone (Fig. 5C). There was no difference in TRAP activity of the osteoclasts derived from mice transplanted with IMO cells transduced with EFS-G or EFS-T (Fig. 5D). VCN was assessed in eight mice transplanted with EFS-T-transduced $CD34^+$ cells and ranged from 0.10 to 0.46 VCN per human $CD45^+$ cell for all mice, except one where VCN was 1.96 (Table 1). The VCN did not correlate directly with the MOI of the transduction. In transplantation experiment 4, the use of a MOI of 100 instead of a MOI of 30 did not result in a higher VCN or higher rescue (Table 1). Overall, these data show that the EFS-T vector can at least partially restore the resorptive

Table 1. *Data from individual NSG mice transplanted with IMO or CB $CD34^+$ cells*

Transplant experiment/donor	*Vector*	*MOI*	*huCD45$^+$ cells in BM (%)*	*VCN in whole BM*	*VCN per huCD45$^+$ cell*	*TCIRG1 band in WB*	*[Ca^{2+}] x-fold of IMO EFS-G*	*[CTX-I] x-fold of IMO EFS-G*	*TRAP activity x-fold of IMO EFS-G*	*Rescue*
1/P6	EFS-T	30×2	n.d.	n.d.	n.d.	n.d.	6.38	16.19	3.00	Partial
1/P6	EFS-G	30×2	n.d.	n.d.	n.d.	—	1.00	1.00	1.00	—
1/P6	EFS-T	30×2	n.d.	n.d.	n.d.	None	7.28	18.50	1.62	Partial
1/P6	EFS-T	30×2	n.d.	n.d.	n.d.	Weak	7.17	23.13	0.89	Partial
1/P6	EFS-G	30×2	n.d.	n.d.	n.d.	—	1.00	1.00	1.00	—
2/CB	UT	—	49.00	0.02	0.04	—	3.28	49.22	0.33	—
2/P3	EFS-G	30×2	59.00	0.50	0.85	—	1.00	1.00	1.00	—
2/P4	EFS-T	30×2	36.00	0.12	0.33	n.d.	0.96	1.06	0.89	None
2/P7	EFS-T	30×2	56.00	0.06	0.11	None	0.88	1.24	1.09	None
2/P7	EFS-G	30×2	45.00	0.49	1.09	—	1.00	1.00	1.00	—
2/P3	EFS-T	30×2	59.00	0.27	0.46	Weak	2.12	10.62	0.66	Partial
2/P3	EFS-T	30×2	53.00	0.13	0.25	Weak	2.05	10.80	0.65	Partial
3/CB	UT	—	16.00	0.02	0.13	—	4.33	44.22	0.23	—
3/P1	EFS-T	30×2	28.00	0.55	1.96	Strong	2.77	27.15	0.33	Complete
3/P7	EFS-G	30×2	7.00	2.79	39.86	—	0.88	0.96	1.24	—
3/P7	EFS-G	30×2	9.00	0.35	3.89	—	1.12	1.04	0.76	—
3/CB	UT	—	40.00	0.00	0.00	—	2.80	28.56	0.35	—
4/P6	EFS-T	100×2	14.30	0.03	0.21	None	3.28	22.10	0.82	Partial
4/P6	EFS-T	100×2	24.30	0.08	0.33	None	2.72	21.55	0.84	Partial
4/P6	EFS-T	100×2	21.10	0.02	0.10	n.d.	1.42	4.23	0.78	Partial
4/P6	EFS-G	100×2	25.50	0.58	2.27	—	1.00	1.00	1.00	—
4/CB	UT	—	59.20	0.00	0.00	—	3.59	45.26	0.24	—
4/CB	UT	—	45.30	0.00	0.00	—	3.40	49.92	0.23	—

Rescue was evaluated as restoration of osteoclast resorption compared to positive and negative controls.

IMO, infantile malignant osteopetrosis; MOI, multiplicity of infection; VCN, vector copy number; P1–P7, IMO patients; CB, cord blood; UT, untransduced; n.d., not determined.

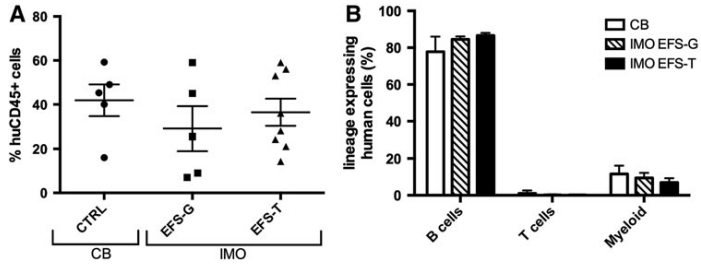

Figure 4. Long-term engraftment and lineage analysis of cord blood (CB) cells and transduced IMO CD34+ cells transplanted into NSG mice. Bone-marrow cells were harvested from NSG mice 9–19 weeks after transplantation with CB cells ($n=5$) or IMO cells transduced with the EFS-G ($n=5$) or EFS-T vector ($n=8$) and were assessed for human engraftment in total bone marrow **(A)** by analyzing the expression of CD45 and lineage distribution in the human cell compartment **(B)** by analyzing the expression of CD3, CD19, and CD33/15 markers by flow cytometry. The data are shown as means ± SEM.

function of osteoclasts differentiated *ex vivo* from NSG-engrafting vector-corrected CD34$^+$ cells from IMO patients.

DISCUSSION

The aim of the present study was to use lentiviral-mediated gene transfer of *TCIRG1* with a clinically applicable vector to rescue the phenotype of human IMO osteoclasts *in vitro* and after generation of osteoclasts from NSG-engrafting hematopoietic cells.

In a previous proof-of-principle work, sufficiently high levels of transgene expression were obtained in IMO osteoclasts *in vitro* by using the viral SFFV promoter.[4,21] In the current work, the EFS promoter

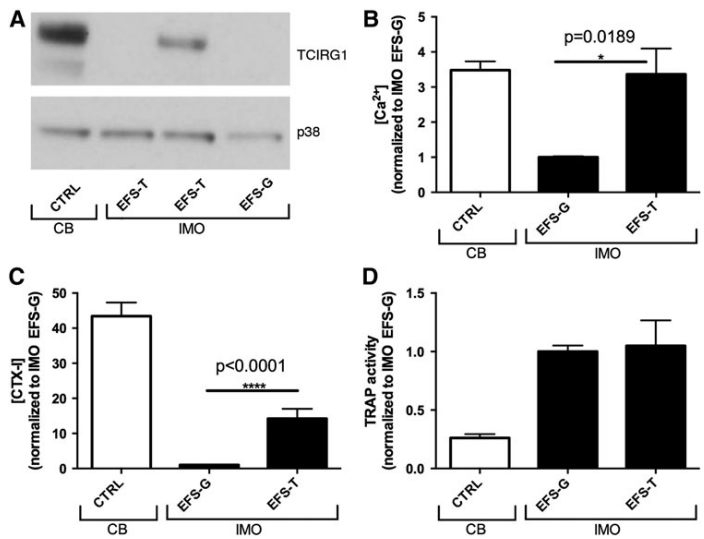

Figure 5. Vector-corrected IMO osteoclasts generated from NSG-engrafting hematopoietic cells show rescued resorption capacity. Bone-marrow cells were harvested from NSG mice 9–19 weeks after transplantation with CB cells ($n=5$) or IMO cells transduced with the EFS-G ($n=7$) or EFS-T vector ($n=11$). Human CD34$^+$ cells were expanded for 2 weeks, seeded on bone slices, and differentiated into osteoclasts for 13 days in the presence of M-CSF and RANKL. **(A)** Western blot analysis was performed on lysates from mature osteoclasts after 13 days of differentiation. Lysates from two different mice transplanted with IMO cells transduced with the EFS-T vector are shown, one in which TCIRG1 could be detected and one in which it could not. The concentration of Ca^{2+} **(B)** and CTX-I **(C)** as well as TRAP activity **(D)** was measured in the media at day 13. The data are shown as means ± SEM.

that is being used in the X-SCID[22–24] and ADA SCID[25] clinical trials and the chimeric myeloid promoter (ChimP),[15] planned to be used in the Chronic Granulomatous Disease (CGD) trial and with the advantage of being lineage specific, were tested.[26] Due to the limited patient material available, the aim was to choose the non-viral promoter that could induce the highest resorption rescue in IMO osteoclasts. Therefore, the EFS promoter and the ChimP were compared to the SFFV promoter. The EFS-TG vector mediated a higher level of protein expression and higher rescue of resorptive function of the IMO osteoclasts *in vitro* than the ChimP-TG vector, as evaluated by measuring release of calcium and the resorption marker CTX-I into the media. From a safety point of view, it has previously been shown that lentiviral-mediated expression of *TCIRG1* is regulated in the same manner as the endogenous gene product, despite being expressed by a lentiviral vector with a generic promoter.[21] Thus, the myeloid specificity of the ChimP is not strictly necessary.

Based on the results from the comparison of the three promoters *in vitro*, the clinically applicable EFS-T vector was developed, with a mammalian promoter and without GFP, for continued experiments. EFS-T-corrected IMO osteoclasts *in vitro* restored release of calcium and CTX-I into the media corresponding to $92 \pm 5\%$ and $95 \pm 6\%$ of those obtained with CB-derived osteoclasts. The overall higher rescue level observed with the EFS-T vector compared to the EFS-TG vector is most likely due to the removal of the IRES-GFP sequence allowing for a higher expression of TCIRG1.

For the *in vivo* experiments, $CD34^+$ cells from peripheral blood of five patients with different *TCIRG1* mutations were obtained without the need for mobilization due to the high percentage of circulating $CD34^+$ cells characteristic of IMO patients.[27] The cells were transduced with EFS-T or with EFS-G and transplanted into sub-lethally irradiated NSG mice; CB $CD34^+$ cells were transplanted as positive controls. It was not possible to analyze the correction of osteoclasts *in vivo*, as these cells do not develop in this xenotransplant model, probably due to the species specificity of M-CSF.[28] Therefore, the bone marrow of the mice was harvested 9–19 weeks after transplantation for analysis and osteoclast differentiation *ex vivo*. IMO $CD34^+$ cells from peripheral blood engrafted in NSG mice to the same degree as CB $CD34^+$ cells, in line with the observation that they can be used as a backup in clinical transplantations should a graft failure occur.[27] Isolated human $CD34^+$ cells were differentiated to mature osteoclasts, and resorption was assessed. The positive and negative control osteoclasts performed as expected: osteoclasts derived from mice transplanted with CB cells were capable of resorbing bone effectively *ex vivo*, while osteoclasts derived from mice transplanted with IMO EFS-G cells exhibited strongly impaired resorption.[3,29] The main objective was to assess the functional restoration of the osteoclasts derived from the mice transplanted with IMO EFS-T cells. On average, based on calcium release, resorption was completely restored compared to that of osteoclasts derived from animals transplanted with CB cells, and based on CTX-I levels, it was restored to $33 \pm 6\%$, as well as being significantly higher compared to IMO EFS-G osteoclasts. The rescue levels in individual mice were variable and can be divided into three categories: in osteoclasts derived from $CD34^+$ cells isolated from two mice, no rescue was observed; in cells derived from eight mice, partial rescue was detected; and in cells derived from one mouse, a complete rescue was observed, as assessed by an increase in calcium and CTX-I levels, a decrease in TRAP activity, and comparison to the results of osteoclasts derived from mice transplanted with CB cells. This variability is also seen in the VCN analysis that ranged from 0.10 to 0.46 per cell positive for human $CD45^+$ cells in the mice with no rescue or partial rescue, whereas it was 1.96 in the mouse whose cells conferred complete rescue. This indicates that the variability in resorption is probably due to differences in transduction efficiency of the more primitive cells. This does not seem to be directly correlated to the MOI, as an increase in VCN was not seen when using a MOI of 100 instead of a MOI of 30 for the *in vivo* experiments, but could instead be strongly influenced by the use of different patient samples and vector batches. A future aim is to optimize and standardize the vector production and transduction protocol in order to obtain a more consistent VCN ranging between 1 and 2, in the NSG-engrafting putative stem cells, which should allow a higher level of rescue to be observed in cells harvested from mice. It is possible to aim safely for a higher VCN, as the results from the IVIM assay that was performed conclude that the EFS-T vector has a strongly reduced mutagenic potential when compared to the gammaretroviral positive control vector or a SIN-lentiviral vector with a strong viral promoter/enhancer element, even at mean VCN levels above three copies per cell.

For future development and application of a clinical gene therapy protocol for treatment of IMO, a crucial question is what level of correction

of osteoclast function is needed *in vivo* to reverse the disease phenotype. It was previously shown that transplantation of gene therapy–corrected cells in *oc/oc* mice completely reversed the disease, even though the *in vitro* bone resorption capacity of these cells was only 10% of wild-type cells.[30] Furthermore, it was possible to show that transplantation of wild-type cells in *oc/oc* mice in a nonmyeloablative setting, resulting in an engraftment level of only 4–5%, was sufficient to correct the disease.[31] In terms of the human disease form, the addition of 30% umbilical CB $CD34^+$ cells to IMO $CD34^+$ cells *in vitro*, followed by osteoclast differentiation, was sufficient to restore resorptive function of these cells completely.[21] Furthermore, in the same study, levels as low as 5% CB $CD34^+$ cells or gene-corrected IMO $CD34^+$ cells mixed into non-manipulated IMO $CD34^+$ cells resulted in significant resorption, possibly due to fusion of preosteoclasts harboring normal/gene corrected TCIRG1 with TCIRG1 deficient counterparts to form osteoclasts.[4,21,31] Thus, gene correction of only a fraction of cells and partial rescue of osteoclast function may be sufficient for clinical benefit when treating patients with IMO.

In summary, this study provides evidence for almost complete rescue of IMO osteoclasts *in vitro* by a clinically applicable lentiviral vector expressing *TCIRG1* under the mammalian promoter EFS and lacking a marker gene. Furthermore, it shows partial rescue of IMO osteoclasts generated from vector-corrected, NSG mice-engrafting hematopoietic cells. These findings support further development of hematopoietic stem cell targeted gene therapy, not only of IMO, but also of other diseases affecting osteoclasts.

ACKNOWLEDGMENTS

We thank Adrian Thrasher and Manuel Grez for the ChimP construct, and Christopher Baum and Axel Schambach (Hannover Medical School, Germany) for providing us with the lentiviral vectors. K.H. is supported by the Danish Research Foundation (Den Danske Forskningsfond). J.R. is supported by grants from The Swedish Childhood Cancer Foundation and a Clinical Research Award from Lund University Hospital, The Foundations of Lund University Hospital. A.S. is partially supported by grants from the EU (ERARE initiative, project OSTEOPETR). A.S. and M.R. were supported by the EU (FP7-Health-2010-CELL-PID: #261387). H.L. is supported by Marie Curie Initial Training Networks (Euroclast, FP7-People-2013-ITN: # 607446). The Lund Stem Cell Center is supported by a Center of Excellence grant in life sciences from the Swedish Foundation for Strategic Research. The funders had no role in study design, data collection and analysis, decision to publish, or preparation of the manuscript.

AUTHOR DISCLOSURE

J.R. has subsequent to acquisition of data presented here entered into a consultancy agreement with Rocket Pharmaceutical (New York, NY) for the development of clinical gene therapy of IMO. No competing financial interests exist for the remaining authors.

REFERENCES

1. Segovia-Silvestre T, Neutzsky-Wulff AV, Sorensen MG, et al. Advances in osteoclast biology resulting from the study of osteopetrotic mutations. Hum Genet 2009;124:561–577.
2. Tolar J, Teitelbaum SL, Orchard PJ. Osteopetrosis. N Engl J Med 2004;351:2839–2849.
3. Taranta A, Migliaccio S, Recchia I, et al. Genotype–phenotype relationship in human ATP6i-dependent autosomal recessive osteopetrosis. Am J Pathol 2003;162:57–68.
4. Moscatelli I, Thudium CS, Flores C, et al. Lentiviral gene transfer of TCIRG1 into peripheral blood CD34(+) cells restores osteoclast function in infantile malignant osteopetrosis. Bone 2013;57:1–9.
5. Frattini A, Orchard PJ, Sobacchi C, et al. Defects in TCIRG1 subunit of the vacuolar proton pump are responsible for a subset of human autosomal recessive osteopetrosis. Nat Genet 2000;25:343–346.
6. Sobacchi C, Schulz A, Coxon FP, et al. Osteopetrosis: genetics, treatment and new insights into osteoclast function. Nat Rev Endocrinol 2013;9:522–536.
7. Scimeca JC, Franchi A, Trojani C, et al. The gene encoding the mouse homologue of the human osteoclast-specific 116-kDa V-ATPase subunit bears a deletion in osteosclerotic (oc/oc) mutants. Bone 2000;26:207–213.
8. Orchard P, Boelens JJ, Raymond G. Multi-institutional assessments of transplantation for metabolic disorders. Biol Blood Marrow Transplant 2013;19:S58–63.
9. Schulz AS, Classen CF, Mihatsch WA, et al. HLA-haploidentical blood progenitor cell transplantation in osteopetrosis. Blood 2002;99:3458–3460.
10. Askmyr M, Flores C, Fasth A, et al. Prospects for gene therapy of osteopetrosis. Curr Gene Ther 2009;9:150–159.
11. Thudium CS, Jensen VK, Karsdal MA, et al. Disruption of the V-ATPase functionality as a way to uncouple bone formation and resorption—a novel target for treatment of osteoporosis. Curr Protein Pept Sci 2012;13:141–151.
12. Stein S, Ott MG, Schultze-Strasser S, et al. Genomic instability and myelodysplasia with monosomy 7 consequent to EVI1 activation after gene therapy for chronic granulomatous disease. Nat Med 2010;16:198–204.
13. Braun CJ, Boztug K, Paruzynski A, et al. Gene therapy for Wiskott–Aldrich syndrome—long-term efficacy and genotoxicity. Sci Transl Med 2014;6:227ra233.
14. Hacein-Bey-Abina S, von Kalle C, Schmidt M, et al. A serious adverse event after successful gene therapy for X-linked severe combined immunodeficiency. N Engl J Med 2003;348:255–256.

15. Grez M, Reichenbach J, Schwable J, et al. Gene therapy of chronic granulomatous disease: the engraftment dilemma. Mol Ther 2011;19:28–35.

16. Schindelin J, Arganda-Carreras I, Frise E, et al. Fiji: an open-source platform for biological-image analysis. Nat Methods 2012;9:676–682.

17. Rittelmeyer I, Rothe M, Brugman MH, et al. Hepatic lentiviral gene transfer is associated with clonal selection, but not with tumor formation in serially transplanted rodents. Hepatology 2013;58: 397–408.

18. Modlich U, Bohne J, Schmidt M, et al. Cell-culture assays reveal the importance of retroviral vector design for insertional genotoxicity. Blood 2006; 108:2545–2553.

19. Zychlinski D, Schambach A, Modlich U, et al. Physiological promoters reduce the genotoxic risk of integrating gene vectors. Mol Ther 2008;16: 718–725.

20. Modlich U, Navarro S, Zychlinski D, et al. Insertional transformation of hematopoietic cells by self-inactivating lentiviral and gammaretroviral vectors. Mol Ther 2009;17:1919–1928.

21. Thudium CS, Moscatelli I, Lofvall H, et al. Regulation and function of lentiviral vector-mediated TCIRG1 expression in osteoclasts from patients with infantile malignant osteopetrosis: implications for gene therapy. Calcif Tissue Int 2016;99: 638–648.

22. De Ravin SS, Wu X, Moir S, et al. Lentiviral hematopoietic stem cell gene therapy for X-linked severe combined immunodeficiency. Sci Transl Med 2016;8:335ra357.

23. Zhou S, Ma Z, Lu T, et al. Mouse transplant models for evaluating the oncogenic risk of a self-inactivating XSCID lentiviral vector. PLoS One 2013; 8:e62333.

24. Zhou S, Mody D, DeRavin SS, et al. A self-inactivating lentiviral vector for SCID-X1 gene therapy that does not activate LMO2 expression in human T cells. Blood 2010;116:900–908.

25. Carbonaro DA, Zhang L, Jin X, et al. Preclinical demonstration of lentiviral vector-mediated correction of immunological and metabolic abnormalities in models of adenosine deaminase deficiency. Mol Ther 2014;22:607–622.

26. Santilli G, Almarza E, Brendel C, et al. Biochemical correction of X-CGD by a novel chimeric promoter regulating high levels of transgene expression in myeloid cells. Mol Ther 2011;19: 122–132.

27. Steward CG, Blair A, Moppett J, et al. High peripheral blood progenitor cell counts enable autologous backup before stem cell transplantation for malignant infantile osteopetrosis. Biol Blood Marrow Transplant 2005;11:115–121.

28. Rathinam C, Poueymirou WT, Rojas J, et al. Efficient differentiation and function of human macrophages in humanized CSF-1 mice. Blood 2011; 118:3119–3128.

29. Del Fattore A, Peruzzi B, Rucci N, et al. Clinical, genetic, and cellular analysis of 49 osteopetrotic patients: implications for diagnosis and treatment. J Med Genet 2006;43:315–325.

30. Johansson MK, de Vries TJ, Schoenmaker T, et al. Hematopoietic stem cell-targeted neonatal gene therapy reverses lethally progressive osteopetrosis in oc/oc mice. Blood 2007;109:5178–5185.

31. Flores C, de Vries TJ, Moscatelli I, et al. Nonablative neonatal bone marrow transplantation rapidly reverses severe murine osteopetrosis despite low-level engraftment and lack of selective expansion of the osteoclastic lineage. J Bone Miner Res 2010;25:2069–2077.

Received for publication April 5, 2017;
accepted after revision July 19, 2017.

Published online: July 19, 2017.

Paper III

Accepted: 25 January 2017
DOI: 10.1111/ejh.12867

ORIGINAL ARTICLE

WILEY European Journal of Haematology

Forced expression of human macrophage colony-stimulating factor in CD34$^+$ cells promotes monocyte differentiation in vitro and in vivo but blunts osteoclastogenesis in vitro

Carmen P. Montano Almendras[1] | Christian S. Thudium[2] | Henrik Löfvall[1,2] | Ilana Moscatelli[1] | Axel Schambach[3] | Kim Henriksen[2] | Johan Richter[1]

[1]Department of Molecular Medicine and Gene Therapy, BMC A12, Lund University, Lund, Sweden

[2]Nordic Bioscience, Herlev, Denmark

[3]Institute of Experimental Hematology, Hannover Medical School, Hannover, Germany

Correspondence
Johan Richter, Department of Molecular Medicine and Gene Therapy, BMC A12, Lund, Sweden.
Email: johan.richter@med.lu.se

Abstract

Objectives: Here, we tested the hypothesis that human M-CSF (hM-CSF) overexpressed in cord blood (CB) CD34$^+$ cells would induce differentiation and survival of monocytes and osteoclasts in vitro and in vivo.

Methods: Human M-CSF was overexpressed in cord blood CD34$^+$ cells using a lentiviral vector.

Results: We show that LV-hM-CSF-transduced CB CD34$^+$ cells expand 3.6- and 8.5-fold more with one or two exposures to the hM-CSF-expressing vector, respectively, when compared to control cells. Likewise, LV-hM-CSF-transduced CB CD34$^+$ cells show significantly higher levels of monocytes. In addition, these cells produced high levels of hM-CSF. Furthermore, they are able to differentiate into functional bone-resorbing osteoclasts in vitro. However, osteoclast differentiation and bone resorption were blunted compared to control CD34$^+$ cells receiving exogenous hM-CSF. NSG mice engrafted with LV-hM-CSF-transduced CB CD34$^+$ cells have physiological levels of hM-CSF production that result in an increase in the percentage of human monocytes in peripheral blood and bone marrow as well as in the spleen, lung and liver.

Conclusion: In summary, ectopic production of human M-CSF in CD34$^+$ cells promotes cellular expansion and monocyte differentiation in vitro and in vivo and allows for the formation of functional osteoclasts, albeit at reduced levels, without an exogenous source of M-CSF, in vitro.

KEYWORDS
cord blood CD34$^+$ cells, human M-CSF, lentiviral transduction, monocytes, osteoclast, transplantation

1 | INTRODUCTION

Efficient gene transfer into human hematopoietic stem cells (HSCs) provides a powerful tool for the study of gene function and as well as in the therapeutic field the possibility to treat a variety of hematopoietic and genetic disorders.[1,2] Hematopoietic stem cell transplantation can be used to durably deliver genetically modified cells to the bone marrow and subsequently induce the release of mature cells with the corrected gene into the circulation.[3,4] Here, we used this approach to overexpress human macrophage colony-stimulating factor (M-CSF) in cord blood (CB) CD34$^+$ cells, and we analyzed them in vitro and in vivo.

Macrophage colony-stimulating factor (M-CSF), also known as colony-stimulating factor-1 (CSF-1), is a pleiotropic growth factor that mediates survival, proliferation and differentiation of mononuclear/macrophage cells.[5] M-CSF is also essential for the survival and proliferation of osteoclast progenitors.[6,7] The role of M-CSF in the differentiation of mouse macrophages has been previously studied; the CSF1^{op}/CSF1^{op} mouse fails to express functional M-CSF, as a result

of a point mutation in the CSF-1 gene, which leads to osteopetrosis. Furthermore, administration of soluble M-CSF to CSF1^{op}/CSF1^{op} mice rescues the phenotype.[8,9] Similarly, Csf1^{-}/Csf1r^{-} mice also exhibit an osteopetrotic phenotype like CSF1^{op}/CSF1^{op} mice with various developmental defects in hematopoiesis, including a severe reduction of macrophages and reproductive defects.[10]

Humanized mouse models have been developed to evaluate the long-term repopulation potential of human HSCs, and these have become an indispensable tool for human HSC research.[11] Engraftment of human CD34^{+} hematopoietic stem cells in immunodeficient NSG mice leads to robust reconstitution of human T, B and NK cells, although the reconstitution of the myeloid lineage is generally poor[12] and osteoclasts development has not been reported. Cytokines play a role in HSC differentiation, expansion and maintenance; in most cases, the cytokine's general structure and function are maintained between human and mouse. However, there are some exceptions like M-CSF where murine M-CSF fails to activate the human receptor.[13]

In the present study, we utilized lentiviral-mediated gene transfer to overexpress hM-CSF in human CB CD34^{+} HSCs for the purpose of examining its effect on proliferation, monocyte differentiation and survival in vitro and in vivo after transplantation of these cells into NSG mice. We also wanted to test the hypothesis that expression of human M-CSF by the CD34^{+} cells could mediate osteoclast differentiation.

2 | MATERIALS AND METHODS

2.1 | CD34^{+} cell isolation and expansion

Umbilical cord blood cells from full-term deliveries were obtained after informed consent under a protocol approved by the institutional ethical board. Mononuclear cell and CD34^{+} cell isolation was performed as previously described.[14,15] For in vitro experiments, cells were cultured in SFEM StemSpan medium (StemCell Technologies, Vancouver, BC, Canada) with the following human recombinant cytokines: 10 ng/mL IL-6, 200 ng/mL SCF and 50 ng/mL FLT- 3L, whereas for the in vivo experiments, cells were cultured with 100 ng/mL each of SCF, TPO and FLT-3L prior to transplantation.

2.2 | Viral vectors and production

The SIN lentiviral vector used in this study was generated from the pRRL.cPPT.SFFV. idTOMATO.WPRE vector in Axel Schambach's Laboratory, Hannover, Germany. The cDNA of the soluble form of human M-CSF was inserted downstream of the SFFV promoter. A similar vector, in which the human M-CSF cDNA was replaced with a non-coding spacer sequence, was used as a control. Lentiviral vector production was performed as previously described.[14]

2.3 | Cell transduction and in vitro monocytes differentiation

Cord blood CD34^{+} cells were transduced with LV-hM-CSF or the control vector at MOI 30 and then cultured in SFEM medium containing IL6, SCF and FLT-3L. After 6 days, an aliquot of the cells was collected for flow cytometric analysis, and the remaining cells were exposed to a second hit of vector at MOI 30. The cells were then collected after 12 days for flow cytometric analysis.

2.4 | Proliferation assay

LV-hM-CSF-transduced CB CD34^{+} cells were plated at a density of 3×10^{4} cells in 24-well plates in 1-mL medium supplemented with the cytokines mentioned above. Medium was exchanged every 2-3 days by demi-depletion, and cells were cultured for 12 days and counted every 3 days. Viability was evaluated by trypan blue exclusion.

2.5 | ELISA for human M-CSF

For cytokine quantification, cell culture supernatants and serum from mice were collected and analyzed using a commercially available human M-CSF Immunoassay ELISA kit (Quantikine R&D system, Minneapolis, MN, USA). Samples were processed according to the manufacturer's instructions; the lower limit of detection of this kit is 78 pg/mL, and according to the manufacturer's description, mouse M-CSF cross-reacts approximately 0.18% with human M-CSF in this assay.

2.6 | In vitro osteoclast differentiation

CD34^{+} cells expanded for 12 days were seeded on plastic or bovine bone slices in ALPHA MEM medium (Sigma-Aldrich, St. Louis, MO, USA) supplemented with different cytokine combinations (human RANKL, murine RANKL and/or human M-CSF, 25 ng/mL of each cytokine). Cells were incubated for 10 days and refreshed with new medium every 3 days. Subsequently, cells were fixed and stained with tartrate-resistant acid phosphatase (TRAP; Sigma-Aldrich) and counter-stained using phalloidin or DAPI. Digital micrographs were obtained using an Olympus C5050 Zoom digital camera mounted on an Olympus BX-60 microscope with a 20× objective using the Cell-A software (Olympus, Center Valley, PA, USA).

2.7 | Measurement of TRAP activity and calcium release

During the osteoclast differentiation process, cell culture supernatants were collected every 3 days. TRAP activity was assayed as previously described.[14] Supernatants were diluted in TRAP solution buffer (1.5 mg/mL of L-ascorbic acid, 7.66 mg/mL of disodium tartrate and 3 mg/mL of 4-nitrophenylphosphate) and reaction buffer (1 mol/L acetate, 0.5% Triton X-100, 1 mol/L NaCl, 10 mmol/L EDTA pH=5.5) and allowed to react for 1 hour at 37°C. The reaction was stopped using NaOH, and absorbance was read at 405 nm. The concentration of total calcium was measured in culture supernatants after resorption, by using a colorimetric calcium (CPC) assay and an ADVIA 1800 Clinical Chemistry System (both from Siemens Healthineers, Erlangen, Germany).

2.8 | Western blot

Tissue samples were lysed in RIPA buffer and separated by SDS-polyacrylamide gel (4%-12% gradient gel) electrophoresis, followed by electrophoretic transfer of proteins from the gel to a nitrocellulose membrane (Bio-Rad, Hercules, CA, USA). Membranes were subsequently blocked by 1-hour incubation with 5% skim milk powder (in TBS with 0.1% Tween 20), followed by overnight incubation at 4°C with either of the primary antibodies at the following dilutions: 1:1000 mouse anti-TCIRG1 (Abnova, Taipei, Taiwan), 1:1000 mouse anti-cathepsin K (Millipore, Billerica, MA, USA) or 1:1000 rabbit anti-p38 MAPK (Cell Signaling Technology, Danvers, MA, USA). The membranes were then washed three times, and the bands were visualized by using corresponding horseradish HRP-conjugated secondary antibodies and ECL Western Blotting Reagents (GE Healthcare, Waukesha, WI, USA).

2.9 | Human CD34$^+$ cell transduction and transplantation

Frozen CB CD34$^+$ cells were thawed and prestimulated with human SCF, TPO and FLT3-L for 7 hours followed by plating in 24-well plates coated with RetroNectin (Takara Bio, Otsu, Japan). The viral particles were added to the plated cells at MOI 10, and the second transduction was performed 12 hours later. Following transduction, the cells were washed three times and transplanted via temporal vein injection into sublethally (100 cGy) irradiated newborn NSG mice.

2.10 | Mice

NOD-SCID IL2RɣʼnullNSG) mice were obtained from Charles River Laboratories, Sulzfeld, Germany. The mice were maintained in the conventional animal facility at the Biomedical Center, Lund University. All the experiments were performed according to protocols approved by the local animal ethics committee.

2.11 | Human cell analysis

Single-cell suspensions were prepared from peripheral blood, bone marrow, spleen, lung and liver as previously described.[15,16] Flow cytometry analysis was performed using FACS Aria III (BD Biosciences, San Jose, CA, USA); 10 000 events per sample were collected and analyzed using FlowJo version 9.4.10 software (TreeStarInc, Ashland, OR, USA). Cells were stained using the following antibodies specific for human CD45-APC, CD14 brilliant violet 605, CD33 PECy7 and CD11b APC (all BD Biosciences).

2.12 | Statistics

Data are presented as the mean±SEM. Differences between groups were analyzed using Student's *t* test, one-way ANOVA or two-way ANOVA with multiple comparisons using Dunnett's test. *P* values <.05 were considered to be significant. Statistical analyses were performed using GraphPad Prism 6.0c software (GraphPad Software, Inc., La Jolla, CA, USA).

3 | RESULTS

3.1 | Lentiviral-mediated expression of human M-CSF in CB CD34$^+$ cells significantly increases cell proliferation and differentiation into monocytes in vitro

Human M-CSF was expressed in human CB CD34$^+$ cells using a lentiviral gene transfer system. Cells transduced with LV-hM-CSF were analyzed for expression of the transgene by determination of dTomato fluorescence. CB CD34$^+$ cells showed high transduction efficiencies as determined by flow cytometry, reaching 45% dTomato-positive cells using the control vector and 35% in LV-hM-CSF-transduced cells. To assess the proliferation capacity, cells were cultured in SFEM media with human SCF, FLT3-L and IL-6 as described in materials and methods. Proliferation was evaluated after one or two exposures to the viral vectors. One exposure demonstrated that the LV-hM-CSF-transduced CB CD34$^+$ cells had a 227-fold increase in proliferation compared with 63-fold for cells transduced with the dTomato control vector. Thus, LV-hM-CSF-transduced CB CD34$^+$ cells exhibited a 3.6-fold higher proliferative activity than the dTomato control-transduced cells (Figure 1A). Two exposures to the viral vectors resulted in even higher proliferation of LV-hM-CSF-transduced CB CD34$^+$ cells, with a 332-fold increase compared to 39-fold increase for cells transduced with the dTomato control vector after 12 days of expansion. Therefore LV-hM-CSF-transduced CB CD34$^+$ cells have an 8.5-fold increased proliferation compared to the control-transduced cells (Figure 1B).

We next quantified the amount of human M-CSF protein secreted into the cell supernatant using an ELISA specific for human M-CSF. LV-hM-CSF-transduced CB CD34$^+$ cells produced significantly higher levels after 12 days, on average 15 902 pg/mL SD±6945.6, while cells transduced with the control vector secreted 98 pg/mL (Figure 1C).

The differentiation ability of transduced cells into myeloid lineages was assessed using flow cytometry to detect the dTomato$^+$, CD14$^+$, CD33$^+$ and CD11b$^+$ populations. LV-hM-CSF-transduced CB CD34$^+$ cells showed high levels of monocytes differentiation both at 7 and 12 days, although at 7 days there was no significant difference when comparing to the control, whereas at 12 days LV-hM-CSF-transduced CB CD34$^+$ cells showed a significant increase in monocytic differentiation, as measured by CD14$^+$ expression (Figure 1D).

Likewise, FACS analysis revealed an increase in CD14$^+$CD33$^+$ and CD14$^+$CD11b$^+$ populations in LV-hM-CSF-transduced CB CD34$^+$ cells being only significant at 12 days comparing to the control cells (Figure 1E and F).

In addition, CD33, CD11b and CD14 expressions revealed different myeloid differentiation stages in both conditions; the 7-day analysis showed a high percentage of immature myeloid CD33$^+$ or CD11b$^+$ cells and that this population decreased after 12 days of culture. In addition, the FACS plots revealed immature myeloid cells that transition to mature monocytes (CD14+) over time (Figs S1 and S2). We also observed that LV-hM-CSF-transduced CB CD34$^+$ cells showed increased monocyte maturation compared to the control cells.

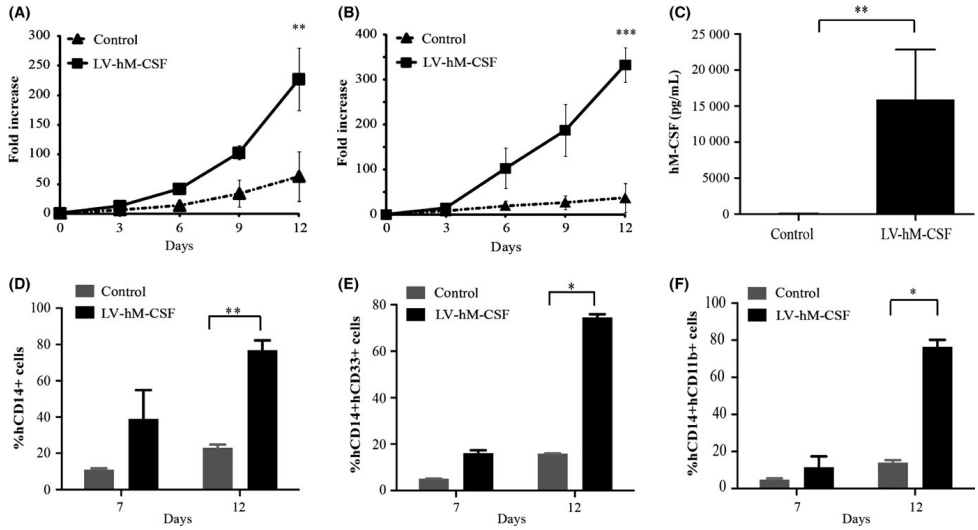

FIGURE 1 LV-hM-CSF-transduction of CB CD34$^+$ cells induces cell proliferation and differentiation in vitro as well as hM-CSF production. CB CD34$^+$ cells were transduced with LV-hM-CSF at MOI 30 as indicated in materials and methods. (A) Proliferation is displayed as fold increase after one exposure to viral vector, (B) or two exposures to the viral vector, both graphs show mean±SD of three independent experiments. (C) Human M-CSF in supernatants was determined by ELISA as described in Materials and Methods section. CB CD34$^+$ cells transduced with LV-hM-CSF or control vector were expanded for 12 days and analyzed by flow cytometry for expression of CD14, CD33 and CD11b and are presented as (D) percentage of CD14$^+$, (E) percentage of CD14$^+$/CD33$^+$ and (F) percentage of CD14$^+$/CD11b$^+$ cells. Data show mean values±SD of three independent experiments; values of *P* as determined by Student's *t* test are indicated by asterisks (**P* values <.05, ***P*<.01, ****P*<.001)

In addition, the co-expression of CD33 and C11b was analyzed at both 7 and 12 days. We show that CD33 and CD 11b are co-expressed in the same cell population, and the percentage of co-expressing cells seems to be the same at 7- or 12-day analysis (Figs S3A and S4A). Analysis of CD33 (Figs S3B and S4B) and CD11b vs side scatter (Figs S3C and S4C) revealed that the respective positive cells had the same side scatter characteristics.

Additionally, FACS analysis revealed that there was a paracrine effect of human M-CSF released into the media from LV-hM-CSF-transduced CB CD34$^+$ cells on the non-transduced (dTomato-negative) cells population as these also exhibited an increase in CD14$^+$ cells, (Figure 2B, upper left square of LV-hM-CSF). Although the control-transduced cells also had a similar fraction of dTomato$^+$ CD14$^+$ cells, the paracrine effect was not observed in these cells.

3.2 | LV-hM-CSF-transduced CB CD34$^+$ cells generate osteoclast in vitro

To determine the effect of h-M-CSF expression on *osteoclastogenesis* and osteoclasts function, transduced CD34$^+$ cells expanded for 12 days were transferred onto plastic dishes and/or bovine bone slices and were exposed to different cytokine combinations (hRANKL and hM-CSF, mRANKL alone or hRANKL alone). After 10 days of osteoclasts differentiation, the cells were fixed in 4% formaldehyde for 20 minutes and stained either with TRAP, or phalloidin and DAPI. Microscopic examination revealed that LV-hM-CSF-transduced cells were able to differentiate into multinucleated osteoclasts in the presence of murine or human RANKL alone as confirmed by phalloidin and DAPI staining (Figure 3A). In contrast, cells transduced with the control vector did not undergo osteoclastogenesis unless both hM-CSF and hRANKL were added to the medium (Figure 3A).

We then examined the expression of the marker of functional osteoclasts, TCIRG1 by Western blot. Osteoclasts differentiated from LV-hM-CSF-transduced CB CD34$^+$ cells in the presence of human or mouse RANKL expressed TCIRG1 protein at comparable levels, while control-transduced cells expressed TCIRG1 protein only in the presence of both hM-CSF and RANKL but not if hM-CSF was omitted from the medium during differentiation (Figure 3B). Similarly, another marker of osteoclasts, namely cathepsin K,[17,18] was also present in osteoclasts differentiated from LV-hM-CSF-transduced CB CD34$^+$ cells, but not in those cultured without any form of M-CSF (exogenous or expressed from the cells).

3.3 | Osteoclasts generated from LV-hM-CSF-transduced CD34$^+$ cells in vitro are functional

Next, we analyzed the function of the differentiated osteoclasts. The osteoclasts marker tartrate-resistant acid phosphatase (TRAP)[19]

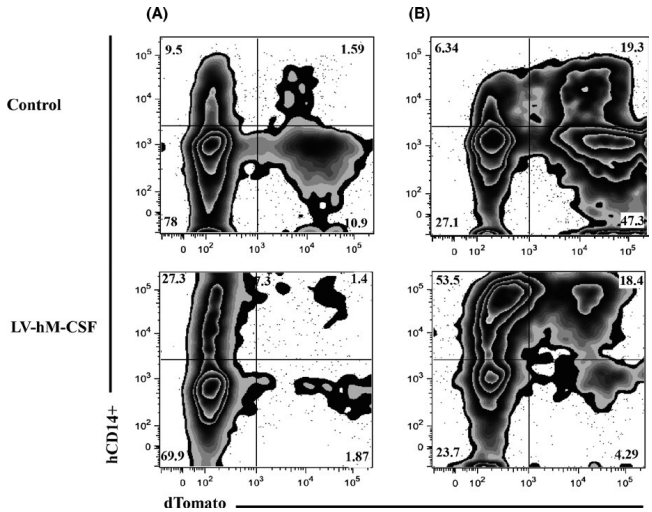

FIGURE 2 Human M-CSF produced by LV-hM-CSF-transduced CD34$^+$ cells has a paracrine effect. CB CD34$^+$ cells were transduced with LV-hM-CSF or control vector and cultured to generate monocytes in vitro as indicated in Material and Methods. Cells were stained with CD14 antibody. Data show one representative flow cytometry analysis of four; numbers indicate percentage of positive cells of total human (CD45$^+$) live population (A) analysis at 7 days (B) analysis at 12 days

was used to assess the relative numbers of osteoclasts. LV-hM-CSF-transduced CB CD34$^+$ cells show significantly higher TRAP activity both in the presence of human or mouse RANKL compared to control cells, also without added hM-CSF (Figure 4A). However, all the conditions with LV-hM-CSF and RANKL (human or murine, with or without exogenous M-CSF) displayed lower TRAP activity than control cells exposed to exogenous hM-CSF and RANKL. To analyze whether the differentiated osteoclasts resorbed bone, Ca^{2+} release into the medium was measured. Osteoclasts generated from LV-hM-CSF-transduced CB CD34$^+$ cells released high levels of Ca^{2+} from bone compared to cells transduced with the control vector, but slightly lower compared to controls cells with M-CSF and RANKL in the media (Figure 4B). Despite the lower resorption, these data confirm that LV-M-CSF-transduced cells possess resorptive capability under in vitro conditions. However, we were unable to find human-derived osteoclasts in vivo following transplantation experiments (data not shown).

3.4 | CB CD34$^+$ cells transduced with LV-hM-CSF engraft in NSG mice and produce human M-CSF in vivo

Newborn mice were sublethally irradiated (100 cGy) and transplanted with 1×10^5 of LV-hM-CSF-transduced CB CD34$^+$ cells or cells transduced with the control vector. Mice were bled 4 weeks after transplantation to confirm engraftment of human cells. Eight weeks after transplantation, mice were sacrificed and peripheral blood (PB), bone marrow (BM), spleen, liver and lungs were harvested. Analysis of PB and BM after 4 and 8 weeks showed no significant difference in the number of human CD45$^+$ cells between the groups (Figure 5A and B).

Next, we quantified the levels of human M-CSF in the serum of transplanted mice. As expected, LV-hM-CSF-transduced CB CD34$^+$ cells that transplanted mice showed high levels of human M-CSF on average 2875 pg/mL when compared to the control mice, which produced on average 82 pg/mL (Figure 5C). These results suggest that our delivery system and promoter of choice were successful in maintaining long-term gene expression of human M-CSF also in vivo.

3.5 | Differentiation of human monocytes in NSG mice transplanted with LV-hM-CSF-transduced CB CD34$^+$ cells

To analyze whether human M-CSF production supports the generation of human monocytes from CD34$^+$ cells in vivo, mice were analyzed at 4 and 8 weeks after transplantation. The 4-week analysis in PB showed a significant increase in hCD14$^+$ cells in mice transplanted with LV-hM-CSF-transduced CB CD34$^+$ cells as compared to controls (Figure 6A). The 8-week analysis showed a significant increase in the proportion of hCD14$^+$ cells in both PB and BM in mice transplanted with LV-hM-CSF-transduced CB CD34$^+$ cells (Figure 6B). The increase in the myeloid cell population was, however, lower and less significant after 8 weeks. An increase in human CD14$^+$ cells was also observed in spleen, liver and lung after 8 weeks, although levels were only significantly higher in spleen and liver (Fig. S5). Myeloid cell lineage analysis of PB after 4 weeks revealed a significant increase in CD45$^+$CD14$^+$CD33$^+$ cells, and the CD45$^+$CD14$^+$CD33$^+$ population was also increased after 8 weeks in PB but not in BM (Figure 6C and D). Analysis of myeloid cell lineages of spleen, liver and lung also showed an increase in the CD45$^+$CD14$^+$CD33$^+$ population, but these were only statistically significant in spleen and lung (Fig. S6).

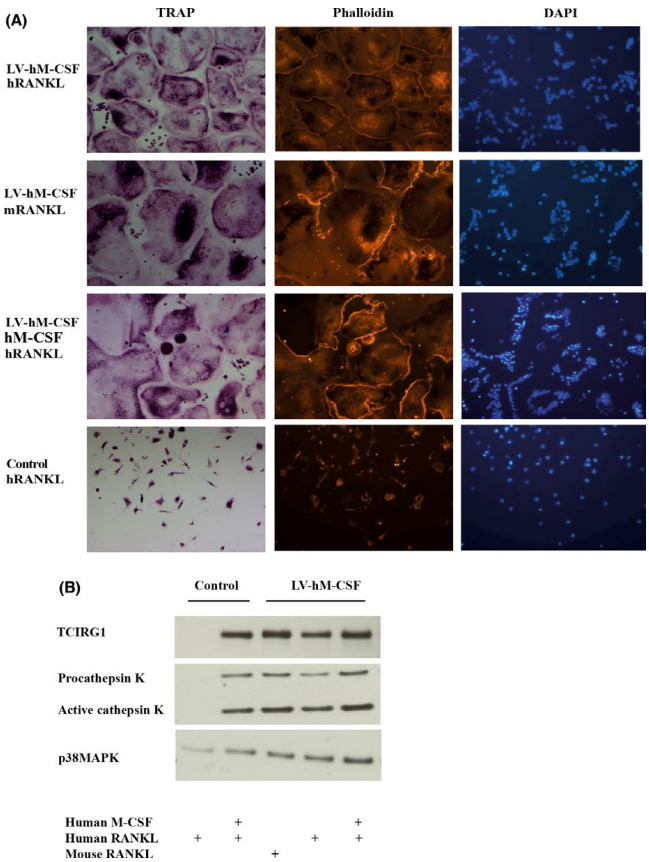

FIGURE 3 In vitro osteoclast development from LV-hM-CSF-transduced CB CD34$^+$ cells. LV-hM-CSF-transduced CB CD34$^+$ cells were expanded for 12 days and for then differentiated into osteoclasts over 10 days followed by fixation in formaldehyde and immunochemical staining with (A) TRAP (left panels), phalloidin (middle panels) and DAPI (right panels) to visualize the osteoclasts. (B) Western blot analysis was performed on lysates from mature osteoclasts after 10 days of differentiation using antibodies against TCIRG1, cathepsin K and p38MAPK

4 | DISCUSSION

Macrophage colony-stimulating factor was initially described as a hematopoietic growth factor required for survival, proliferation and differentiation of various hematopoietic lineages.[20] It is known that M-CSF acts on common myeloid progenitors (CMPs) and favors the differentiation of CMPs into the monocyte/macrophage lineages.[21,22] M-CSF signals through the M-CSF-R (Fms, CD115) where binding of M-CSF results in tyrosine phosphorylation of the receptor and subsequent activation of several downstream proteins.[23-25]

Using a lentiviral gene transfer system, we successfully overexpressed hM-CSF in CB CD34$^+$ cells. Furthermore, we showed that hM-CSF expression in CB CD34$^+$ cells significantly increased proliferation, monocyte differentiation and their ability to produce hM-CSF in vitro. We observed very low levels of hM-CSF (close to lower limit of detection of the ELISA kit used) in the control-transduced cells that might be due to cytokine production from the maturing cells that were assayed quite late (day 12) in the proliferation and differentiation cultures.

The immunophenotype stages of monocytic development are defined by a gradual increase in the expression of CD33 and CD11b antigens and subsequent acquisition of the CD14 marker by the transition to promonocytes and mature monocytes.[26] To this end, we analyzed CD33 and CD11b myeloid markers. LV-hM-CSF-transduced CB CD34$^+$ cells showed significant increase in the fraction of CD33$^+$/CD14$^+$ or CD11b$^+$/CD14$^+$ cells compared to the controls, indicating that the M-CSF released into the medium could enhance myelopoiesis and monocyte differentiation.

It has been shown that M-CSF supports survival and proliferation of myeloid progenitors[16,27] and is essential for generation of osteoclasts precursors that express RANK, the receptor for RANKL, and thus are competent to differentiate into osteoclasts in response to RANKL exposure.[28] In accordance with these findings, we show that only LV-hM-CSF-transduced CB CD34$^+$ cells were able to differentiate

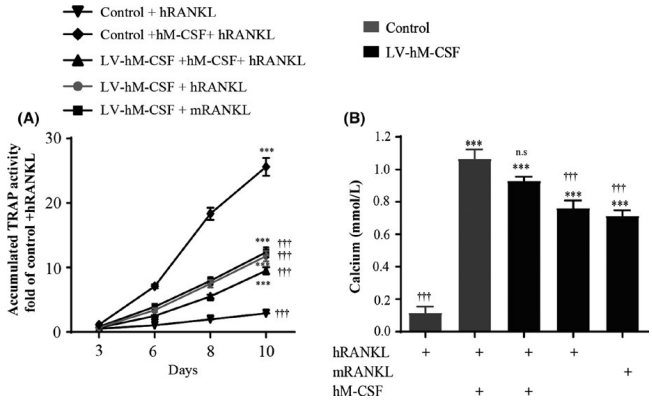

FIGURE 4 LV-hM-CSF-transduced CB CD34$^+$ cells develop into functional osteoclasts in vitro as determined by TRAP activity and calcium release. (A) Accumulated TRAP activity over time and (B) Ca^{2+} release at day 10 of osteoclastogenesis were measured in cell culture supernatants obtained during the osteoclast differentiation process on bovine bone slices. Data from one representative experiment of three performed are shown; 10 replicates from each data point. *** denotes significant difference compared to control+hRANKL and †††denote significant difference compared to control+hMCSF+hRANKL

into osteoclasts when they were stimulated with RANKL in the absence of M-CSF supplements. In addition, the TRAP activity analysis showed that LV-hM-CSF-transduced CB CD34$^+$ cells were able to generate a high number of functional bone-resorbing osteoclasts on bovine bone slices compared to the control-transduced cells.

For in vivo studies of human hematopoiesis, significant progress has been achieved in the development of mice that sustain engraftment and differentiation of human hematopoietic cells; however, several limitations remain. While human cells can be detected in engrafted NSG mice for up to 12 months, all the hematopoietic subsets begin to decline around 6 months after transplantation.[29,30] This effect is probably, at least in due to the inability of cytokines to react with receptors on the human cells, leading to survival signal deprivation in transplanted human cells. In this regard, different strategies have been developed. One of these approaches has been to inject recombinant proteins such as IL-15,[31] B cell activating factor[32] or IL-7[33] to transiently increase hematopoietic cell lineages in humanized mice. Another method is hydrodynamic injection of a plasmid-expressing human cytokines, an approach that has been used to improve reconstitution of human dendritic cells by delivery of GM-CSF and IL-4.[34] Transgenic mice have also been used to increase stable expression of human cytokines; forced expression of SCF, GM-CSF and IL-3 in NOD-SCID mice produced robust human hematopoietic reconstitution in blood, spleen, bone marrow and liver and significantly increased myeloid cell number.[35,36] Another strategy has been to engineer a knock-in mouse in which genes encoding mouse cytokines have been replaced by human counterparts. Three mice have been reported, including one that expresses human thrombopoietin,[37] another expressing both human IL-3 and GM-CSF[38] and one strain that expresses human M-CSF.[39]

In this study, we took another approach expressing a human cytokine in NSG mouse recipients by stable lentiviral-mediated transduction of human M-CSF into CB CD34$^+$ cells and subsequent transplantation to stimulate differentiation and survival of the monocytes lineage in the transplanted mice. After transplantation of LV-hM-CSF-transduced CD34$^+$ cells into NSG newborn mice, we did not observe any significant effect of hM-CSF on overall human engraftment levels in PB or BM. LV-hM-CSF- transplanted mice showed high levels of hM-CSF production in the circulation, and the amount detected is in the range of physiological levels of M-CSF in humans.[40,41] Moreover, LV-hM-CSF-transplanted mice exhibited increased differentiation potential into monocyte/myeloid lineages in PB and BM compared to controls; a finding is in line with human monocytes development in humanized CSF-1 mice previously described.[39] Likewise, we could detect human CD14$^+$ monocytes in different tissues, including spleen, lung and liver, suggesting that the obtained level of hM-CSF is sufficient to induce differentiation to and/or or migration of human monocytes into these tissues.

Appropriate conditions to generate osteoclasts in vitro from human hematopoietic stem/progenitor cells have been described by several groups.[14,42,43] However, we were not able to demonstrate human osteoclasts in NSG mice transplanted with LV-hM-CSF-transduced CB CD34$^+$ cells, even though these cells readily formed an abundance of osteoclasts in vitro in the presence of either human or murine RANKL. There may be several reasons for this negative finding, either biological or technical. It is possible that the murine bone environment does not support generation of human osteoclasts even if human M-CSF is present at relevant concentrations. Alternatively, expression of M-CSF early (priming), or at a high level, might actually blunt osteoclastogenesis as described in the murine setting.[44] This is also consistent with our in vitro findings of diminished TRAP formation and lower bone resorption from LV-hM-CSF-transduced cells during osteoclastogenesis as compared to control cells exposed to hM-CSF and RANKL. De Vries and co-workers investigated this in more detail in the murine setting and suggest that downregulation of the transcription factor NFATc1 might play a central role in this phenomenon.[44,45] Other possible explanations for not observing human osteoclasts in vivo are that factors suppressing generation of human osteoclasts may be present in the murine bone marrow or the environment selectively favoring generation of the endogenous murine osteoclasts over those generated from xenotransplanted cells. It is also possible that technical issues played a role. We tried to detect human osteoclasts by immunohistochemistry

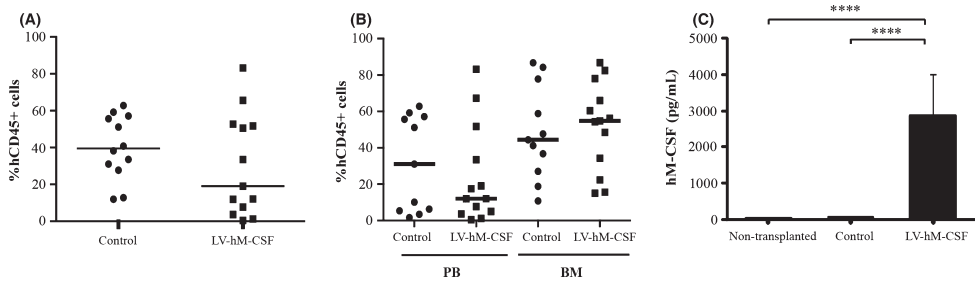

FIGURE 5 Engraftment of human cells and human M-CSF production in NSG mice transplanted with LV-hM-CSF-transduced CB CD34$^+$ cells. Newborn NSG mice were transplanted with CB CD34$^+$ cells transduced with LV-hM-CSF or with the control vector. Mice were analyzed by flow cytometry to detect the percentage of human cell engraftment. (A) Four-week peripheral blood (PB) analysis and (B) 8-week PB and bone marrow (BM) analysis, each symbol represents an individual mouse (n=11-12) and horizontal bars indicate the mean values (C) levels of human M-CSF in non-transplanted mice (n=5) and mice transplanted with CB CD34$^+$ cells transduced with LV-hM-CSF (n=8) or with the control vector (n=8), data show mean values±SD. (**** = $P \leq 0.0001$)

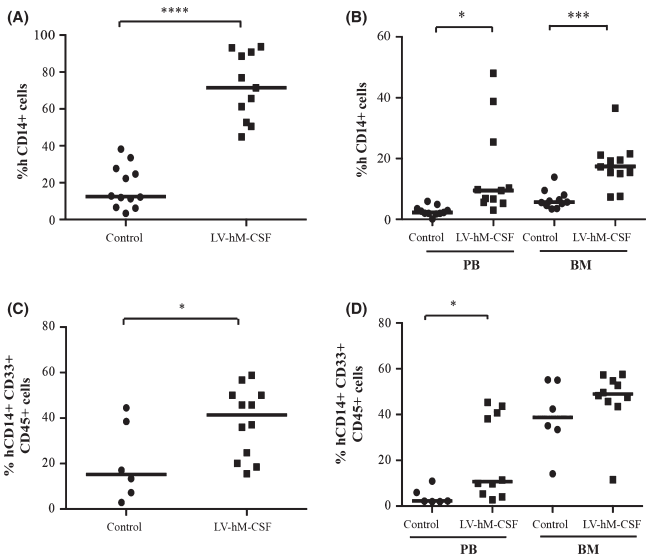

FIGURE 6 Human monocytes differentiation in NSG mice transplanted with LV-hM-CSF-transduced CB CD34$^+$ cells. NSG mice transplanted with LV-hM-CSF-transduced CB CD34$^+$ cells mice were analyzed by flow cytometry for the percentage of human CD14$^+$ cells: (A) Four-week peripheral blood analysis and (B) 8-week peripheral blood and bone marrow analysis. Cells were stained with CD45, CD14 and CD33 antibodies and analyzed by flow cytometry: (C) 4-week peripheral blood and (D) 8-week peripheral blood and bone marrow analysis. Each symbol represents an individual mouse (n=11-12), and the lines represent the mean of all analyzed mice in the respective group. Values of *P* as determined by Student's *t* test are indicated by asterisks (*P values <.05, ***P<.001 , ****$P \leq 0.0001$)

using an antibody against dTomato. While dTomato$^+$ cells were observable in the BM, we were unable to find TRAP$^+$ osteoclasts that colocalized with the dTomato stain (data not shown). As we see a paracrine effect of the hM-CSF expression on the dTomato$^-$ cell population in LV-hM-CSF-transplanted cells, it is possible that human osteoclasts that may have formed in the mice were not dTomato$^+$ making these immunohistochemical analyses flawed. The fusion of non-transduced with transduced cells has been described in vitro.[14] Furthermore, there is also the possibility that the human cells fuse with the murine cells, hence diluting the dTomato signal even further. The scarcity of specific antibodies for human osteoclasts makes it difficult to verify whether human-derived osteoclasts were present or not. This issue thus warrants further studies.

In summary, using a lentiviral-mediated gene transfer approach into human CD34$^+$ cells we first demonstrated that overexpression of human M-CSF in CD34$^+$ cells promoted proliferation, differentiation and survival of the monocyte lineages and also induced differentiation of functional osteoclasts in vitro. Moreover, transplantation of LV-hM-CSF-transduced CD34$^+$ cells into immunodeficient mice resulted in production of physiological levels of human M-CSF in vivo and increased monocyte reconstitution in tissues such as bone marrow, spleen, liver and lung.

ACKNOWLEDGEMENTS

We would like to thank Fanny Strand at the animal facility for experimental animal care. We also want to thank Beata Lindqvist at the vector unit for viral vector production. This project was supported by grants to Johan Richter from the Swedish Childhood Cancer Foundation and Lund University.

DISCLOSURE

All the authors declare no competing financial interests.

AUTHORSHIP

C.P.M.A. designed and performed experiments, interpreted data and wrote draft of the manuscript. C.S.T. and H.L. performed experiments and interpreted data. I.M. contributed to the experimental design. A.S. provided vector constructs. K.H. interpreted data and contributed to the experimental design. J.R. was the principal investigator and designed experiments, interpreted data and finalized the writing of the manuscript.

REFERENCES

1. Case SS, Price MA, Jordan CT, et al. Stable transduction of quiescent CD34(+)CD38(-) human hematopoietic cells by HIV-1-based lentiviral vectors. *Proc Natl Acad Sci USA*. 1999;96:2988-2993.
2. Ma Y, Ramezani A, Lewis R, Hawley RG, Thomson JA. High-level sustained transgene expression in human embryonic stem cells using lentiviral vectors. *Stem Cells*. 2003;21:111-117.
3. Thomas D, Mostoslavsky G. Efficient transduction of hematopoietic stem cells and its potential for gene correction of hematopoietic diseases. *Methods Mol Biol*. 2014;1114:441-450.
4. Sng J, Lufkin T. Emerging stem cell therapies: treatment, safety, and biology. *Stem Cells Int*. 2012;2012:521343.
5. Pixley FJ, Stanley ER. CSF-1 regulation of the wandering macrophage: complexity in action. *Trends Cell Biol*. 2004;14:628-638.
6. Glantschnig H, Fisher JE, Wesolowski G, Rodan GA, Reszka AA. M-CSF, TNFalpha and RANK ligand promote osteoclast survival by signaling through mTOR/S6 kinase. *Cell Death Differ*. 2003;10:1165-1177.
7. Ryan GR, Dai XM, Dominguez MG, et al. Rescue of the colony-stimulating factor 1 (CSF-1)-nullizygous mouse (Csf1(op)/Csf1(op)) phenotype with a CSF-1 transgene and identification of sites of local CSF-1 synthesis. *Blood*. 2001;98:74-84.
8. Kodama H, Nose M, Niida S, Yamasaki A. Essential role of macrophage colony-stimulating factor in the osteoclast differentiation supported by stromal cells. *J Exp Med*. 1991;173:1291-1294.
9. Wiktor-Jedrzejczak W, Bartocci A, Ferrante AW Jr, et al. Total absence of colony-stimulating factor 1 in the macrophage-deficient osteopetrotic (op/op) mouse. *Proc Natl Acad Sci USA*. 1990;87:4828-4832.
10. Dai XM, Ryan GR, Hapel AJ, et al. Targeted disruption of the mouse colony-stimulating factor 1 receptor gene results in osteopetrosis, mononuclear phagocyte deficiency, increased primitive progenitor cell frequencies, and reproductive defects. *Blood*. 2002;99:111-120.
11. Shultz LD, Brehm MA, Garcia-Martinez JV, Greiner DL. Humanized mice for immune system investigation: progress, promise and challenges. *Nat Rev Immunol*. 2012;12:786-798.
12. Shultz LD, Ishikawa F, Greiner DL. Humanized mice in translational biomedical research. *Nat Rev Immunol*. 2007;7:118-130.
13. Gow DJ, Garceau V, Kapetanovic R, et al. Cloning and expression of porcine Colony Stimulating Factor-1 (CSF-1) and Colony Stimulating Factor-1 Receptor (CSF-1R) and analysis of the species specificity of stimulation by CSF-1 and Interleukin 34. *Cytokine*. 2012;60:793-805.
14. Moscatelli I, Thudium CS, Flores C, et al. Lentiviral gene transfer of TCIRG1 into peripheral blood CD34(+) cells restores osteoclast function in infantile malignant osteopetrosis. *Bone*. 2013;57:1-9.
15. Flores C, Moscatelli I, Thudium CS, et al. Osteoclasts are not crucial for hematopoietic stem cell maintenance in adult mice. *Haematologica*. 2013;98:1848-1855.
16. Rambaldi A, Young DC, Griffin JD. Expression of the M-CSF (CSF-1) gene by human monocytes. *Blood*. 1987;69:1409-1413.
17. Saftig P, Hunziker E, Wehmeyer O, et al. Impaired osteoclastic bone resorption leads to osteopetrosis in cathepsin-K-deficient mice. *Proc Natl Acad Sci USA*. 1998;95:13453-13458.
18. Inaoka T, Bilbe G, Ishibashi O, Tezuka K, Kumegawa M, Kokubo T. Molecular cloning of human cDNA for cathepsin K: novel cysteine proteinase predominantly expressed in bone. *Biochem Biophys Res Commun*. 1995;206:89-96.
19. Tauchert S, di Liberto A, Cordes T, Thill M, Salehin D, Friedrich M. Tartrate-resistant acid phosphatase (TRAP) as a serum marker for bone resorption in breast cancer patients with bone metastases. *Clin Exp Obstet Gynecol*. 2009;36:219-225.
20. Stanley ER. The macrophage colony-stimulating factor, CSF-1. *Methods Enzymol*. 1985;116:564-587.
21. Stanley ER, Berg KL, Einstein DB, et al. Biology and action of colony–stimulating factor-1. *Mol Reprod Dev*. 1997;46:4-10.
22. Socolovsky M, Constantinescu SN, Bergelson S, Sirotkin A, Lodish HF. Cytokines in hematopoiesis: specificity and redundancy in receptor function. *Adv Protein Chem*. 1998;52:141-198.
23. Downing JR, Roussel MF, Sherr CJ. Ligand and protein kinase C downmodulate the colony-stimulating factor 1 receptor by independent mechanisms. *Mol Cell Biol*. 1989;9:2890-2896.
24. Sherr CJ. Colony-stimulating factor-1 receptor. *Blood*. 1990;75:1-12.
25. Sherr CJ. Regulation of mononuclear phagocyte proliferation by colony-stimulating factor-1. *Int J Cell Cloning*. 1990;8(suppl 1):46-60. discussion -2.
26. Garnache-Ottou F, Chaperot L, Biichle S, et al. Expression of the myeloid-associated marker CD33 is not an exclusive factor for leukemic plasmacytoid dendritic cells. *Blood*. 2005;105:1256-1264.
27. Shadle PJ, Allen JI, Geier MD, Koths K. Detection of endogenous macrophage colony-stimulating factor (M-CSF) in human blood. *Exp Hematol*. 1989;17:154-159.
28. Feng X. RANKing intracellular signaling in osteoclasts. *IUBMB Life*. 2005;57:389-395.
29. Watanabe S, Terashima K, Ohta S, et al. Hematopoietic stem cell-engrafted NOD/SCID/IL2Rgamma null mice develop human lymphoid systems and induce long-lasting HIV-1 infection with specific humoral immune responses. *Blood*. 2007;109:212-218.
30. Andre MC, Erbacher A, Gille C, et al. Long-term human CD34+ stem cell-engrafted nonobese diabetic/SCID/IL-2R gamma(null) mice show impaired CD8+ T cell maintenance and a functional arrest of immature NK cells. *J Immunol*. 2010;185:2710-2720.
31. Huntington ND, Alves NL, Legrand N, et al. IL-15 transpresentation promotes both human T-cell reconstitution and T-cell-dependent antibody responses in vivo. *Proc Natl Acad Sci USA*. 2011;108:6217-6222.
32. Schmidt MR, Appel MC, Giassi LJ, Greiner DL, Shultz LD, Woodland RT. Human BLyS facilitates engraftment of human PBL derived B cells in immunodeficient mice. *PLoS ONE*. 2008;3:e3192.
33. van Lent AU, Dontje W, Nagasawa M, et al. IL-7 enhances thymic human T cell development in "human immune system" Rag2-/-IL-2Rgammac-/- mice without affecting peripheral T cell homeostasis. *J Immunol*. 2009;183:7645-7655.
34. Chen Q, Khoury M, Chen J. Expression of human cytokines dramatically improves reconstitution of specific human-blood lineage cells in humanized mice. *Proc Natl Acad Sci USA*. 2009;106:21783-21788.
35. Nicolini FE, Cashman JD, Hogge DE, Humphries RK, Eaves CJ. NOD/SCID mice engineered to express human IL-3, GM-CSF

and Steel factor constitutively mobilize engrafted human progenitors and compromise human stem cell regeneration. *Leukemia*. 2004;18:341-347.
36. Billerbeck E, Barry WT, Mu K, Dorner M, Rice CM, Ploss A. Development of human CD4+FoxP3+ regulatory T cells in human stem cell factor-, granulocyte-macrophage colony-stimulating factor-, and interleukin-3-expressing NOD-SCID IL2Rgamma(null) humanized mice. *Blood*. 2011;117:3076-3086.
37. Rongvaux A, Willinger T, Takizawa H, et al. Human thrombopoietin knockin mice efficiently support human hematopoiesis in vivo. *Proc Natl Acad Sci USA*. 2011;108:2378-2383.
38. Willinger T, Rongvaux A, Takizawa H, et al. Human IL-3/GM-CSF knock-in mice support human alveolar macrophage development and human immune responses in the lung. *Proc Natl Acad Sci USA*. 2011;108:2390-2395.
39. Rathinam C, Poueymirou WT, Rojas J, et al. Efficient differentiation and function of human macrophages in humanized CSF-1 mice. *Blood*. 2011;118:3119-3128.
40. Gilbert HS, Praloran V, Stanley ER. Increased circulating CSF-1 (M-CSF) in myeloproliferative disease: association with myeloid metaplasia and peripheral bone marrow extension. *Blood*. 1989;74:1231-1234.
41. Janowska-Wieczorek A, Belch AR, Jacobs A, et al. Increased circulating colony-stimulating factor-1 in patients with preleukemia, leukemia, and lymphoid malignancies. *Blood*. 1991;77:1796-1803.
42. Pierelli L, Scambia G, d'Onofrio G, et al. Generation of multinuclear tartrate-resistant acid phosphatase positive osteoclasts in liquid culture of purified human peripheral blood CD34+ progenitors. *Br J Haematol*. 1997;96:64-69.
43. Way KJ, Dinh H, Keene MR, et al. The generation and properties of human macrophage populations from hemopoietic stem cells. *J Leukoc Biol*. 2009;85:766-778.
44. De Vries TJ, Schoenmaker T, Aerts D, et al. M-CSF priming of osteoclast precursors can cause osteoclastogenesis-insensitivity, which can be prevented and overcome on bone. *J Cell Physiol*. 2015;230:210-225.
45. Kim JH, Kim N. Regulation of NFATc1 in osteoclast differentiation. *J Bone Metab*. 2014;21:233-241.

SUPPORTING INFORMATION

Additional Supporting Information may be found online in the supporting information tab for this article.

How to cite this article: Montano Almendras CP, Thudium CS, Löfvall H, et al. Forced expression of human macrophage colony-stimulating factor in $CD34^+$ cells promotes monocyte differentiation in vitro and in vivo but blunts osteoclastogenesis in vitro. *Eur J Haematol*. 2017;00:1-10. https://doi.org/10.1111/ejh.12867

Paper IV

Löfvall et al. Arthritis Research & Therapy (2018) 20:67
https://doi.org/10.1186/s13075-018-1564-5

Arthritis Research & Therapy

RESEARCH ARTICLE Open Access

Osteoclasts degrade bone and cartilage knee joint compartments through different resorption processes

Henrik Löfvall[1,2], Hannah Newbould[1], Morten A. Karsdal[1], Morten H. Dziegiel[3], Johan Richter[2], Kim Henriksen[1] and Christian S. Thudium[1*]

Abstract

Background: Osteoclasts have been strongly implicated in osteoarthritic cartilage degradation, at least indirectly via bone resorption, and have been shown to degrade cartilage in vitro. The osteoclast resorption processes required to degrade subchondral bone and cartilage—the remodeling of which is important in the osteoarthritic disease process—have not been previously described, although cathepsin K has been indicated to participate. In this study we profile osteoclast-mediated degradation of bovine knee joint compartments in a novel in vitro model using biomarkers of extracellular matrix (ECM) degradation to assess the potential of osteoclast-derived resorption processes to degrade different knee joint compartments.

Methods: Mature human osteoclasts were cultured on ECMs isolated from bovine knees—articular cartilage, cortical bone, and osteochondral junction ECM (a subchondral bone-calcified cartilage mixture)—in the presence of inhibitors: the cystein protease inhibitor E-64, the matrix metalloproteinase (MMP) inhibitor GM6001, or the vacuolar-type H^+-ATPase (V-ATPase) inhibitor diphyllin. Biomarkers of bone (calcium and C-terminal type I collagen (CTX-I)) and cartilage (C2M) degradation were measured in the culture supernatants. Cultures without osteoclasts were used as background samples. Background-subtracted biomarker levels were normalized to the vehicle condition and were analyzed using analysis of variance with Tukey or Dunnett's T3 post hoc test, as applicable.

Results: Osteochondral CTX-I release was inhibited by E-64 (19% of vehicle, $p = 0.0008$), GM6001 (51% of vehicle, $p = 0.013$), and E-64/GM6001 combined (4% of vehicle, $p = 0.0007$)—similarly to bone CTX-I release. Diphyllin also inhibited osteochondral CTX-I release (48% of vehicle, $p = 0.014$), albeit less than on bone (4% of vehicle, $p < 0.0001$). Osteochondral C2M release was only inhibited by E-64 (49% of vehicle, $p = 0.07$) and GM6001 (14% of vehicle, $p = 0.006$), with complete abrogation when combined (0% of vehicle, $p = 0.004$). Cartilage C2M release was non-significantly inhibited by E-64 (69% of vehicle, $p = 0.98$) and was completely abrogated by GM6001 (0% of vehicle, $p = 0.16$).

Conclusions: Our study supports that osteoclasts can resorb non-calcified and calcified cartilage independently of acidification. We demonstrated both MMP-mediated and cysteine protease-mediated resorption of calcified cartilage. Osteoclast functionality was highly dependent on the resorbed substrate, as different ECMs required different osteoclast processes for degradation. Our novel culture system has potential to facilitate drug and biomarker development aimed at rheumatic diseases, e.g. osteoarthritis, where pathological osteoclast processes in specific joint compartments may contribute to the disease process.

Keywords: Osteoarthritis, Osteoclast, Extracellular matrix, Cartilage, Bone, Cell culture, Biomarker

* Correspondence: cst@nordicbio.com
[1]Nordic Bioscience, Herlev Hovedgade 205-207, 2730 Herlev, Denmark
Full list of author information is available at the end of the article

Background

Osteoclasts are bone-resorbing multinucleated cells derived from hematopoietic stem cells via the monocytic lineage upon stimulation with the cytokines macrophage colony-stimulating factor (M-CSF) and receptor activator of nuclear factor kappa-B ligand (RANKL) [1]. Bone is resorbed by osteoclasts through secretion of hydrochloric acid dissolving the inorganic matrix [2] and proteases, mainly the cysteine protease cathepsin K [3–5] and matrix metalloproteinases (MMPs) [6–8], degrading the organic matrix. In addition to their well-established role in normal bone turnover, osteoclasts play important roles in diseases with progressive joint destruction, in particular in bone erosion in diarthrodial joints in rheumatoid arthritis (RA) [9–13]. Their role in cartilage and subchondral bone alterations in osteoarthritis (OA) is poorly understood [14].

The osteochondral junction is a key compartment of the joint. Consisting of non-calcified articular cartilage, calcified cartilage and subchondral bone, the osteochondral junction transforms shear stress from loading and motion into compressive and tensile stress via undulations in the extracellular matrices (ECMs) [14, 15]. Subchondral bone sclerosis and changes in subchondral bone metabolism, possibly mediated by osteoclast-osteoblast coupling [16–18], are often amongst the first detectable OA alterations [19]. In conjunction, increased osteoclast activity and subchondral bone remodeling are involved in OA development and progression [15]. Suppressing bone resorption has resulted in beneficial secondary effects on cartilage health in several pre-clinical OA studies and increased resorption has resulted in cartilage deterioration [20], demonstrating how osteoclasts can contribute indirectly to cartilage health. The differentiation, activity and survival of osteoclasts is tightly regulated in healthy individuals [21] whereas monocytes isolated from patients with OA exhibit increased osteoclastogenesis, elevated resorption, and reduced osteoclast apoptosis [22].

The idea of osteoclasts being directly involved in OA cartilage degradation is gaining increased attention. Human osteoclasts can degrade cartilage [23] and equine osteoclasts are recruited to the subchondral bone in spontaneous post-traumatic OA [24]. Furthermore, bone marrow lesions have been shown to be associated with the subchondral bone areas underlying articular cartilage lesions, suggesting osteoclast-associated cartilage-bone crosstalk [25, 26]. Resorption pits reaching from subchondral bone into articular cartilage have been described in OA [27], but which osteoclast-derived resorption processes that are involved in cartilage degradation have not been investigated. Different osteoclast substrates affect the possible ECM degradation products and the phenotype of the resorbing osteoclasts [28]. This suggests that the ECM can be a determinant of osteoclast functionality, and hence there is a need for increased understanding of osteoclast effects on other ECMs of relevance to joint pathology. MMPs [6, 8, 29, 30] and cathepsin K [3, 6, 8, 31] have long been thought to degrade both bone and cartilage, but in addition to osteoclasts there are many other potential contributors to MMP [32–34] and cathepsin K [34, 35] levels in the OA joint. Therefore, the contribution of proteases specifically derived from osteoclasts to degrading these ECMs requires further investigation.

To this date direct osteoclast-derived effects and the osteoclast processes involved in degrading the articular cartilage and the osteochondral junction compartments have not been determined. To shed light on if and how osteoclasts play a role in the degradation of the different joint components, in this study we investigated matrix-dependent and enzyme-dependent degradation processes by human osteoclasts on bovine joint tissues. To this end we exploited a novel cell culture model of osteoclast-derived bovine knee joint degradation, using osteochondral ECM (a subchondral bone-calcified cartilage mixture), articular cartilage, and cortical bone as osteoclast substrates. By measuring biomarkers of ECM turnover, we investigated the effects of osteoclast-derived resorption processes in degrading the ECMs of knee joint compartments in vitro.

Methods

Isolation of bovine knee joint ECMs

Three intact bovine knees, derived from two cows, were obtained from a local butcher. Articular cartilage was isolated from the femoral condyles, using a biopsy punch and a scalpel, and was immersed in liquid nitrogen to render the cartilage metabolically inactive and prevent endogenous protease activity. The cartilage slices were then stored in 70% ethanol at 4 °C until use.

The femoral condyles were then cut sagittally into slices using a Proxxon FET circular saw with a diamond-coated blade (Proxxon, Föhren, Germany). The slices were fixated in 70% ethanol for 10 min. The remaining articular cartilage was removed with a scalpel to leave mainly subchondral bone and calcified cartilage, the cartilage between the subchondral bone and the tidemark [36], in our osteochondral ECM. Using a chisel and mallet, strips of osteochondral matrix were isolated from the proximal surface of the denuded slices down to 1 mm beneath the surface. The resulting matrix strips were immersed in liquid nitrogen and crushed into small pieces using a tissue pulverizer, thereby homogenizing the ECM and allowing for even coverage of cell culture wells, to generate the osteochondral ECM used for culture. The osteochondral ECM was then stored in 70% ethanol at 4 °C until use.

Bovine femurs were fixated in 70% ethanol for several weeks after which cortical bone biopsies were drilled from the diaphyses. The resulting bone cylinders were cut into 70-μm-thick slices using a Minitom with a diamond cut-off wheel (Struers, Ballerup, Denmark). The bone slices were then stored in 70% ethanol at 4 °C until use.

Histology

Femoral condyle slices, from before and after cartilage removal, were fixated in 4% formaldehyde and decalcified in 15% EDTA. The decalcified slices were infiltrated with paraffin using a Tissue-Tek VIP 5 Jr. (Sakura Finetek, Alphen aan den Rijn, The Netherlands), embedded in paraffin, and cut into 5–6-μm-thick sagittal sections using a HM 360 microtome (Microm International GmbH, Walldorf, Germany). The sections were stained with safranin O-fast green. Digital micrographs were obtained with an Olympus DP71 digital camera mounted on a BX-60 microscope with a 4X objective using the Olympus cellSens software (Olympus, Center Valley, PA, USA).

von Kossa staining

Osteochondral matrix strips were stained with von Kossa staining to verify the presence of calcified ECM. Cortical bone slices were used as positive controls of calcification and decalcified osteochondral strips and cortical bone slices were used as negative controls. The tissues were washed in type I ultrapure water and then stained by incubating for 5 min in 1% silver nitrate under a lamp, 2 min in 1% pyrogallol, and 5 min in 1% sodium thiosulfate, with washes between each step. Images were obtained using a digital camera.

Resorption assays

The resorption experiments were based on three independent resorption assays, including a small pilot (n = 3 per condition) and two larger trials (n = 6 per condition for each). Each trial used ECMs from one unique bovine knee and osteoclasts from one unique set of blood donors. Data from the different trials are shown individually—the pilot in Additional files 1, 2 and 3: Figures S1–S3 and the two larger trials in Additional files 4, 5 and 6: Figures S4–S6 and Figs. 2, 3 and 4, respectively—due to minor modifications in experimental setup, such as culture time, ECM and osteoclast origin, replicate numbers, and the number of conditions.

Prior to plating the ECMs, the osteochondral ECM was washed three times by centrifugation and medium replacement, whereas the slices of cortical bone and articular cartilage were washed with medium replacement only. Culture wells on 96-well culture plates were filled with 50 μl of medium followed by the addition of ECMs; osteochondral ECM was added with a spatula, until the bottoms of the wells were covered, and cortical bone or articular cartilage slices were added using forceps. Mature human osteoclasts derived from $CD14^+$ monocytes were generated as previously described [37, 38] from the peripheral blood of anonymized blood donors obtained from a blood bank. The mature osteoclasts were lifted using a trypsin/EDTA mixture and a cell scraper, counted and seeded by adding 50 μl/well of cell suspension resulting in final culture densities of 1.0×10^5 cells/well on articular cartilage and on osteochondral ECM and 5.0×10^4 cells/well on the cortical bone. Two matrix-containing wells without osteoclasts were cultured in parallel on each plate to serve as background samples for biomarker analyses, these samples were analyzed in the same manner as all other samples. The plates were incubated for 1 h at 37 °C and 5% CO_2 after which 150 μl of medium supplemented with various resorption inhibitors was added. The following inhibitors and final concentrations were selected based on previous research [39]: 300 nM diphyllin (V-ATPase inhibitor), 5 μM E-64 (cysteine protease inhibitor), 10 μM GM6001 (broad-spectrum MMP inhibitor), 5 μM E-64 and 10 μM GM6001 combined (E-64/GM6001), or dimethyl sulfoxide (DMSO) vehicle (1:2000 in medium), all of the above from Sigma-Aldrich (St. Louis, MO, USA). After 24 h the medium was changed by demi-depletion, replacing 150 μl of used medium with 150 μl of fresh medium supplemented with inhibitors, followed by another 3–4 days of culture. At the end of the culture 200 μl of medium was collected from each well and stored at − 20 °C until analysis. A graphical overview of the experimental model design can be found in Fig. 5.

Cell culture viability analysis

After collecting the cell culture supernatants, 200 μl of medium supplemented with inhibitors and 12.5% alamarBlue (Thermo Fisher Scientific, Waltham, MA, USA) was added to the wells, resulting in a final alamarBlue concentration of 10%, and the cells were incubated at 37 °C and 5% CO_2 for approximately 3 h. The relative viability of the different culture conditions was then assessed by measuring the alamarBlue fluorescence with excitation at 540 nm and emission at 590 nm using a SpectraMax M5 plate reader (Molecular Devices, Sunnyvale, CA, USA). Medim from wells containing only matrix and medium were used as background samples (data not shown).

TRAP activity analysis

Tartrate-resistant acid phosphatase (TRAP) activity was assessed as a measurement of relative osteoclast numbers in the cell cultures. 2.5 μl of media from each cell culture well was added to a 96-well plate and mixed with 17.5 μl of type I ultrapure water. The samples were incubated with 80 μl of freshly made reaction buffer (0.25 M

acetic acid, 0.125% Triton X-100, 0.25 M NaCl, 2.5 mM EDTA, 1.1 mg/ml of ascorbic acid, 5.75 mg/ml of disodium tartrate, 2.25 mg/ml of 4-nitrophenylphosphate, pH 5.5). The reaction mixture was incubated at 37 °C for 1 h in the dark and was stopped by adding 100 μl of 0.3 M NaOH. Absorbance was measured at 405 nm with 650 nm as a reference using a SpectraMax M5 plate reader (Molecular Devices, Sunnyvale, CA). Media from wells containing only matrix and medium were used as background samples (Additional file 7: Figure S7).

Biomarker measurements

Calcium release was analyzed by measuring the concentration of total calcium (Ca^{2+}) in medium after resorption using a colorimetric calcium assay, based on the *o*-cresolphthalein complexone (CPC) method, on an ADVIA 1800 Clinical Chemistry System (both from Siemens Healthineers, Erlangen, Germany). C-terminal type I collagen fragments (CTX-I) released from resorbed bone were measured using the CrossLaps for Culture ELISA (IDS, The Boldons, UK), which was used according to the manufacturer's instructions. C2M, a metabolite of MMP-mediated collagen type II degradation, was measured as previously described [40]. Biomarker levels below the detection limits of the respective assays were assigned the detection limit as their value. Medium from wells containing only matrix and medium were used as background samples in all biomarker measurements (Additional file 7: Figure S7).

Statistical analysis

For statistical analysis, the measured background samples from matrix without osteoclasts were subtracted from all osteoclast-containing samples. The background-subtracted data were normalized to the mean of the vehicle condition on the respective ECM and are presented as percentages of the vehicle. All graphs except Additional file 7: Figure S7 contain background-subtracted and vehicle-normalized data. The raw data on osteoclast-derived biomarkers levels compared to background samples (Additional file 7: Figure S7) were not statistically analyzed. All statistical comparisons were made within the same cell culture trial using all the conditions' technical replicates. These comparisons were performed using IBM SPSS Statistics v24.0.0.0 64-bit edition for Windows (IBM, Armonk, NY, USA). The data were analyzed with one-way analysis of variance (ANOVA), with the assumption that the data were normally distributed, followed by either Tukey or Dunnett's T3 (DT3) post hoc test depending on whether or not equal variances could be assumed based on Levene's test. The post hoc test used for each test is specified in every graph that was statistically analyzed and when p values are given in the "Results" section (presented as p_{Tukey} or p_{DT3}). Statistical significance was considered to be $p < 0.05$. Significance levels are reported with symbols in the figures (*comparisons to vehicle and $^{\#}$comparisons to E-64/GM6001, the latter only being shown for E-64 and GM6001 to assess synergistic effects), where $^{*}p < 0.05$, $^{**}p < 0.01$, $^{***}p < 0.001$, $^{****}p < 0.0001$ and $^{\#}p < 0.05$, $^{\#\#}p < 0.01$, $^{\#\#\#}p < 0.001$, $^{\#\#\#\#}p < 0.0001$. Graphs were plotted in GraphPad Prism v7.01 for Windows (GraphPad Software, La Jolla, CA, USA) and represent group means and their respective standard error of the mean (SEM); significance levels were inserted manually.

Results

Osteochondral ECM characterization and model optimization

The osteochondral ECM was characterized by assessing the presence of calcified cartilage interspersed with subchondral bone, by safranin O-fast green staining of femoral condyle slices, and the overall calcification of the osteochondral matrix, by von Kossa staining of non-crushed strips of osteochondral matrix. Prior to removing the remaining articular cartilage from the partially denuded femoral condyles, the subchondral bone was still covered by some articular cartilage (Fig. 1a, stained red). No detectable articular cartilage remained above the subchondral bone plate after denuding, but calcified cartilage was still present interspersed with the subchondral bone (Fig. 1b, stained red). The amount of bone and cartilage in the slices varied throughout the matrix but we do not know to what extent. The von Kossa staining verifies the calcification of the osteochondral matrix (Fig. 1c, center), as can be seen by comparing this matrix strip with a decalcified matrix strip (Fig. 1d, center), cortical bone slices (Fig. 1c–d, left), and decalcified cortical bone (Fig. 1c–d, right) slices. The calcified osteochondral matrix was intermittently covered by a thin layer of cartilage that did not stain black (Fig. 1c, center), which was likely non-calcified articular cartilage.

To verify that osteoclast-derived biomarker release could be generated from all ECMs, background samples containing only medium and ECM was measured and compared to medium from the osteoclast-containing vehicle condition. The data clearly show that the addition of osteoclasts resulted in increased biomarker levels, with the exception of articular cartilage Ca^{2+}, CTX-I, and cortical bone C2M, compared to background levels (Additional file 7: Figure S7).

To test if the crushing procedure would affect osteoclast-derived biomarker results, both cortical bone and articular cartilage were metabolically inactivated, crushed in the same manner as osteochondral ECM, and used in resorption assays. The overall effects of the different resorption inhibitors on osteoclast-derived biomarker release from crushed ECMs did not differ from

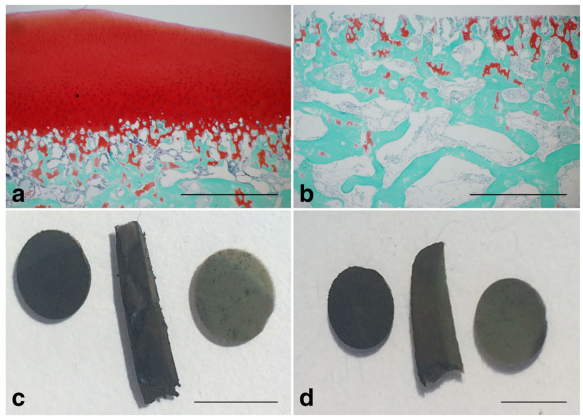

Fig. 1 Characterization of osteochondral extracellular matrix (ECM). Femoral condyles used to isolate the subchondral matrix were stained with safranin O-fast green to verify the removal of the articular cartilage and the presence of calcified cartilage interspersed with the subchondral bone (**a**–**b**). The digital micrographs represent the status of the cartilage before (**a**) and after articular cartilage removal (**b**). Isolated osteochondral ECM strips were stained for the presence of mineralized ECM using von Kossa staining (**c**–**d**). The osteochondral strip in **c** (center) was un-treated whereas the osteochondral strip in **d** (center) was decalcified prior to staining. Both strips are displayed next to cortical bone slices (**c**–**d**, left) and decalcified cortical bone slices (**c**–**d**, right), serving as references of calcified matrix. Scale bars represent 1 mm (**a**–**b**) and 6 mm (**c**–**d**)

sliced ECMs (data not shown) and only slices of cortical bone and articular cartilage were used in the optimized model.

Osteoclast effects on the cortical bone compartment

The resorption of cortical bone and the biomarkers released have been extensively described before [39]. In this study, the resorption of cortical bone in the presence of resorption inhibitors—the cysteine protease inhibitor E-64, the MMP inhibitor GM6001, and the V-ATPase inhibitor diphyllin—serve mainly as validation of functional resorption on the cortical bone slices and as a reference for the subchondral bone resorption in osteochondral ECM. For the purposes of comparing protease contribution to the different biomarker levels, the background levels were subtracted from all biomarker measurements in osteoclast-containing wells followed by normalization to the vehicle condition. Throughout this study, the cortical bone resorption parameters performed as expected (Fig. 2, Additional files 1 and 2: Figures S1 and S2). Ca^{2+} release was reduced by diphyllin (42% of vehicle, p_{Tukey} <0.0001) whereas protease inhibitors only had modest, albeit statistically significant, effects (Fig. 2a). Release of the bone resorption biomarker CTX-I was significantly reduced by all inhibitors (Fig. 2b), especially by diphyllin (4% of vehicle, p_{DT3} <0.0001) which emphasizes that the cortical bone is heavily calcified. Diphyllin increased the viability (Fig. 2c) and TRAP activity (Fig. 2d) of the cultures, as expected based on previous research [41]. C2M—a metabolite of MMP-mediated collagen type II degradation—release was not detectable above background levels (Additional file 7: Figure S7) indicating that collagen type II was not present in the matrix and was not being resorbed, nor was there any detectable cross-reactivity with resorbed collagen type I.

Osteoclast effects on the articular cartilage compartment

Cartilage degradation by osteoclasts was assessed by the release of C2M. There was a trend towards GM6001 completely abrogating the C2M release (0% of vehicle, p_{DT3} = 0.16) and E-64 reducing it to a lesser extent (69% of vehicle, p_{DT3} = 0.98), although neither was statistically significant (Fig. 3a). The effects of E-64 varied between trials (Additional files 3 and 4: Figures S3A and S4A). The diphyllin condition showed a trend towards increased C2M release (236% of vehicle, p_{DT3} = 0.79), although some data points were outside the general pattern and possibly skewed the results (Fig. 3a). This effect also varied between trials (Additional files 3 and 4: Figures S3A and S4A). There were no statistically significant effects of any inhibitor on culture viability (Fig. 3b) or osteoclast numbers (Fig. 3c). CTX-I release was not detectable above background levels (Additional file 7: Figure S7) indicating that collagen type I was not present in the matrix and was not being resorbed, nor was there any detectable cross-reactivity with resorbed collagen type II. Similarly, Ca^{2+} release was not detectable above background levels (Additional file 7: Figure S7) indicating

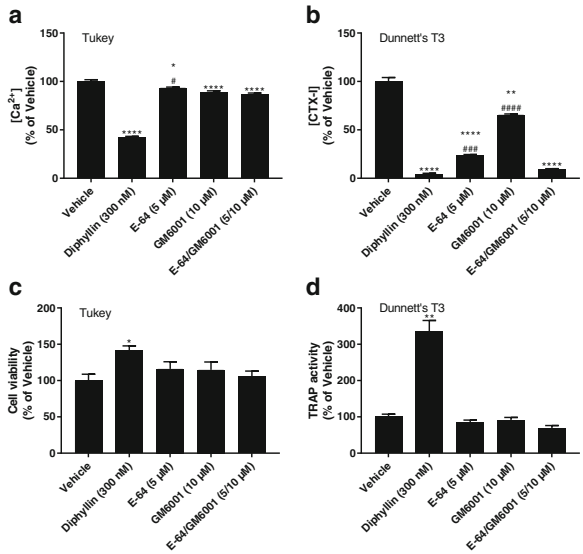

Fig. 2 Resorption biomarkers released from osteoclasts cultured on cortical bone. Osteoclasts were cultured on bovine femoral cortical bone in the presence or absence of resorption inhibitors. Resorption of calcified extracellular matrix and collagen type I was assessed by measuring the Ca^{2+} (**a**) and C-terminal type I collagen (CTX-I) (**b**) concentrations, respectively, in the medium. Cell viability was assessed using alamarBlue (**c**) and tartrate-resistant acid phosphatase (TRAP) activity in the medium was measured for relative osteoclast quantification (**d**). Data are presented as percent of vehicle with error bars representing the SEM. Statistical significance is indicated by $^{*}p < 0.05$, $^{**}p < 0.01$, $^{***}p < 0.001$, $^{****}p < 0.0001$ for comparisons against the vehicle and $^{\#}p < 0.05$, $^{\#\#}p < 0.01$, $^{\#\#\#}p < 0.001$, $^{\#\#\#\#}p < 0.0001$ for comparisons against E-64/GM6001 (only shown for E-64 and GM6001); the post hoc test used is indicated in the top left corner of each graph

that the cartilage was not calcified. ^{342}FFGV-G2, a metabolite of MMP-mediated aggrecan degradation [42], and ^{374}ARGS-G2, a metabolite of aggrecanase-mediated aggrecan degradation [42], were also measured but neither neo-epitope could be detected (data not shown).

Osteoclast effects on the osteochondral junction compartment

In the osteochondral ECM we obtained resorption of both bone and cartilage components. Interestingly, the release of CTX-I (Fig. 4b) was significantly inhibited in the presence of diphyllin (50% of vehicle, p_{DT3} = 0.014), E-64 (19% of vehicle, p_{DT3} = 0.0008), GM6001 (51% of vehicle, p_{DT3} = 0.013), and E-64/GM6001 (4% of vehicle, p_{DT3} = 0.0007) whereas Ca^{2+} release was not reduced by any inhibitor (Fig. 4a), despite using well-validated dosages of the inhibitors [39]. Although there was a trend towards E-64/GM6001 reducing CTX-I more than E-64 alone (Fig. 4b) it was not statistically significant (p_{DT3} = 0.07); E-64/GM6001 was, however, more potent than GM6001 alone (p_{DT3} = 0.007). C2M release (Fig. 4c) was reduced by GM6001 (14% of vehicle, p_{DT3} = 0.006) and to a lesser extent by E-64, which was not statistically significant (49% of vehicle, p_{DT3} = 0.07), with total abrogation of C2M release when combined (0% of vehicle, p_{DT3} = 0.004). E-64/GM6001 was significantly different from E-64 alone (p_{DT3} <0.0001) but not from GM6001 (p_{DT3} = 0.07). The effects of E-64 alone on C2M in other trials were either smaller (78% of vehicle, Additional file 5: Figure S5C) or not present (128% of vehicle, Additional file 6: Figure S6C); neither was significant (p_{DT3} = 0.98 and p_{Tukey} = 0.37, respectively). Diphyllin had a trend towards a small increase in C2M levels (Fig. 4c) but this was non-significant (122% of vehicle, p_{DT3} = 0.90) and was not present in other trials (Additional files 5 and 6: Figures S5C and S6C). There were no detectable effects on cell viability by any inhibitor (Fig. 4d). The TRAP activity (Fig. 4e) increased in the diphyllin condition on osteochondral ECM (154% of vehicle, p_{DT3} = 0.013). While E-64 and GM6001 did not affect TRAP activity significantly (76% of vehicle, p_{DT3} = 0.18 and 91% of vehicle, p_{DT3} = 0.94), E-64/GM6001 reduced it to 65% of vehicle (p_{DT3} = 0.04). Similar, but non-significant, trends were seen on cortical bone (Fig. 2d)

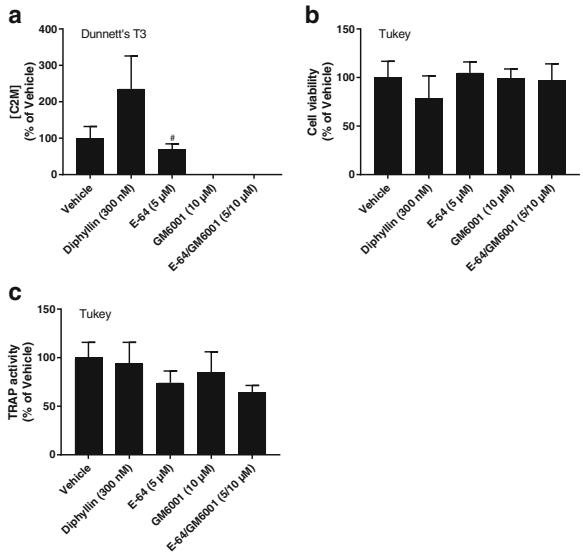

Fig. 3 Resorption biomarkers released from osteoclasts cultured on articular cartilage. Osteoclasts were cultured on articular cartilage from bovine femoral condyles in the presence or absence of resorption inhibitors. Resorption of collagen type II was assessed by measuring C2M concentrations in the medium (**a**). Cell viability was assessed using alamarBlue (**b**) and tartrate-resistant acid phosphatase (TRAP) activity in the medium was measured for relative osteoclast quantification (**c**). Data are presented as percent of vehicle with error bars representing the SEM. Statistical significance is indicated by $^{*}p < 0.05$, $^{**}p < 0.01$, $^{***}p < 0.001$, $^{****}p < 0.0001$ for comparisons against the vehicle and $^{\#}p < 0.05$, $^{\#\#}p < 0.01$, $^{\#\#\#}p < 0.001$, $^{\#\#\#\#}p < 0.0001$ for comparisons against E-64/GM6001 (only shown for E-64 and GM6001), the post hoc test used is indicated in the top left corner of each graph

and articular cartilage (Fig. 3c). ^{342}FFGV-G2 and ^{374}ARGS-G2 were also measured but neither neo-epitope was detected (data not shown).

Discussion

Inhibition of osteoclast function using bisphosphonates has underscored a potential role of targeting osteoclasts as a treatment for OA [43]. However, how osteoclasts directly affect different joint compartments in OA, except through resorption of bone, is not clear. So far clinical OA trials, in general and those inhibiting bone resorption, have failed due to lack of structural efficacy [43]. Novel approaches are needed to determine the contribution of osteoclast-derived enzymes and acidification in degrading ECMs other than bone to improve osteoclast-related structural efficacy in OA treatments. In the light of this, we conducted a study focused on osteoclast resorption mechanisms, ECM interactions and the development of a novel tool for early drug and biomarker validation.

To our knowledge no studies have previously quantified the processes degrading articular cartilage and osteochondral junction joint compartments in a setting where osteoclasts are the known and only source of degradation. In this study, we demonstrated how osteoclasts are involved in degrading these joint compartments and characterized these processes using a combination of resorption inhibitors and tissue-specific biomarkers. In brief, our study supports osteoclast-derived cathepsin K-mediated and MMP-mediated resorption of calcified cartilage and articular cartilage independently of acidification, as measured by the C2M neo-epitope. A graphical overview of the experimental model design and the osteoclast-derived resorption processes that contributed to the ECM degradation biomarkers measured in our study can be found in Fig. 5. Using this novel cell model, we were able to investigate the role of osteoclast-derived enzymes and acidification in directly degrading articular cartilage and osteochondral junction compartments.

Osteoclasts generated inhibitable Ca^{2+} release from cortical bone but not from the osteochondral ECM—the V-ATPase inhibitor diphyllin had no effect on osteochondral Ca^{2+} release—which suggests that the osteochondral Ca^{2+} was not derived from resorption. Due to this discrepancy, reference biomarker data from cortical bone are necessary for this cell culture model to verify normal resorption and validate each experiment. As Ca^{2+} was present at equal levels in all osteochondral osteoclast

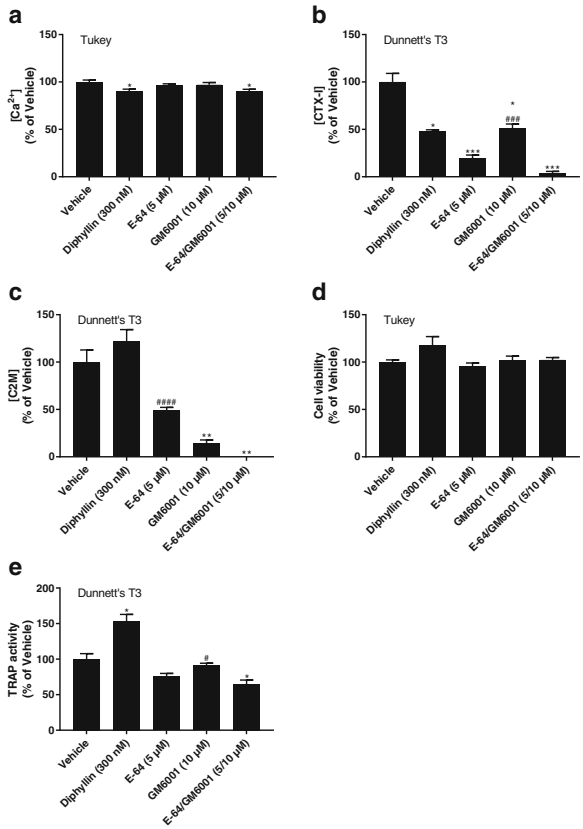

Fig. 4 Resorption biomarkers released from osteoclasts cultured on osteochondral extracellular matrix (ECM). Osteoclasts were cultured on osteochondral ECM from bovine femoral condyles in the presence or absence of resorption inhibitors. Resorption of calcified ECM and collagen type I was assessed by measuring the Ca^{2+} (**a**) and C-terminal type I collagen (CTX-I) (**b**) concentrations, respectively, in the medium. Resorption of collagen type II was assessed by measuring C2M (**c**) concentrations in the medium. Cell viability was assessed using alamarBlue (**d**) and tartrate-resistant acid phosphatase (TRAP) activity in the medium was measured for relative osteoclast quantification (**e**). Data are presented as percent of vehicle with error bars representing the SEM. Statistical significance is indicated by $^{*}p < 0.05$, $^{**}p < 0.01$, $^{***}p < 0.001$, $^{****}p < 0.0001$ for comparisons against the vehicle and $^{\#}p < 0.05$, $^{\#\#}p < 0.01$, $^{\#\#\#}p < 0.001$, $^{\#\#\#\#}p < 0.0001$ for comparisons against E-64/GM6001 (only shown for E-64 and GM6001); the post hoc test used is indicated in the top left corner of each graph

conditions, i.e. Ca^{2+} levels were increased by an equal amount in all osteoclast conditions compared to background levels, we speculate that the Ca^{2+} was derived from cellular metabolism and that the osteochondral ECM is not highly calcified like cortical bone, which appears to be supported by the von Kossa staining.

Inhibiting Ca^{2+} release by targeting the V-ATPase typically raises the viability and the TRAP activity of osteoclast cultures [41, 44], likely due to Ca^{2+} release from resorption inducing osteoclast apoptosis [45]. Accordingly, TRAP activity was raised by diphyllin to a lesser extent in the osteochondral cultures than it was in the bone cultures, and similarly viability was only marginally and non-significantly raised by diphyllin in the osteochondral cultures, further supporting that the calcification of the osteochondral ECM was relatively low.

The osteochondral CTX-I levels also support the hypothesis of low calcification as CTX-I was only moderately affected by diphyllin when compared to the effects of diphyllin on cortical bone. The apparent discrepancy between the CTX-I and calcium analyses on osteochondral ECM could however be a matter of different

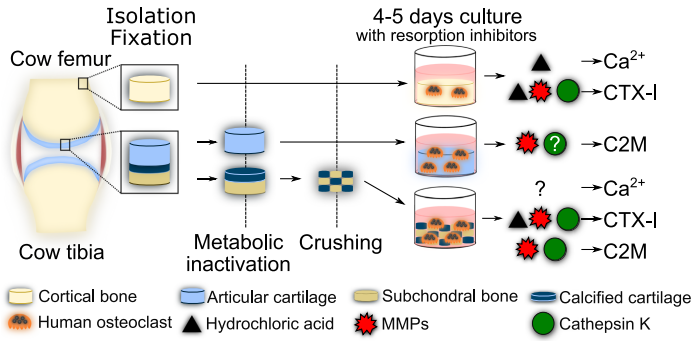

Fig. 5 Overview of the experimental model design and results. Cortical bone, articular cartilage and an osteochondral matrix, consisting of subchondral bone and calcified cartilage, were isolated from bovine femoral diaphyses and femoral condyles, and fixated in 70% ethanol. The articular cartilage and the osteochondral matrix were metabolically inactivated by immersion in liquid nitrogen. The osteochondral matrix was crushed to generate a homogeneous osteochondral extracellular matrix (ECM) for culture. Human osteoclasts derived from $CD14^+$ monocytes were cultured on the different matrices in the presence of vacuolar-type H^+-ATPase, matrix metalloproteinase (MMP) and cathepsin K inhibitors. The contributions of hydrochloric acid, MMPs and cathepsin K in degrading the ECMs were assessed by measuring biomarkers of ECM degradation in the culture supernatants. CTX-I, C-terminal type I collagen

sensitivity between the two analyses. Osteoclasts generated CTX-I from osteochondral ECM primarily through cathepsin K-mediated processes as indicated by the inhibitor panel, but secondarily also through MMP-mediated processes, in a manner similar to osteoclasts on cortical bone. Interestingly, the MMP inhibition appeared to have a stronger effect on osteochondral CTX-I release than on cortical bone CTX-I release. Similarly, osteoclasts cultured on decalcified bone display a stronger reduction in CTX-I release when MMPs are inhibited than they do on non-decalcified cortical bone, whereas the effects of cathepsin K inhibition are blunted on decalcified cortical bone, supporting that MMPs are the predominant proteases on a non-calcified matrix [8].

Osteoclast-mediated cartilage degradation has previously been demonstrated by measuring the release of glycosaminoglycans (GAGs) from osteoclasts cultured on articular cartilage [23]. In our study we instead demonstrated osteoclast-derived cartilage degradation using the C2M biomarker. C2M has previously been shown to be able to distinguish between healthy subjects and patients or between subsets of patients with arthritic diseases—such as OA [40, 46], RA [47–49] and ankylosing spondylitis [50, 51]—when measured in patient serum. Additionally, C2M has been characterized in ex vivo models of inflammatory cartilage degradation where it was shown that MMP inhibition reduces the C2M release [40]. These studies make C2M a highly relevant biomarker for both clinical studies of OA and for investigations of cartilage degradation mechanisms. Using our in vitro model we have explored additional biological mechanisms through which the C2M biomarker can be generated. Our study highlights how our model can be used for biomarker discovery and validation and for drug efficacy testing in diseases where osteoclasts may contribute to the disease process. However, it is possible that the mechanisms generating C2M in vivo and their overall contribution to C2M levels and disease may differ from the in vitro conditions.

The cartilage was degraded by osteoclast-derived MMPs in our study, as the C2M neo-epitope is mainly generated through MMP-cleavage of collagen type II and GM6001 potently inhibited the C2M release. From the osteochondral ECM we detected C2M release, which could be inhibited by E-64 and GM6001. In two of the three trials there was a trend towards cathepsin K-mediated processes contributing to C2M release from osteochondral ECM. The effect of E-64 was more apparent when it was used in combination with GM6001. This could indicate that cathepsin K contributes to release or access to the neo-epitope rather than to the generation of the neo-epitope. Cathepsin K-mediated bone resorption could also affect osteochondral C2M by enabling access to cartilage encapsulated in bone; this in turn could lead to variation in the efficacy of E-64 based on the bone-to-cartilage ratio in the matrix. Cathepsin K appeared to contribute to C2M release also on articular cartilage in two of three trials, although E-64 did not have a statistically significant effect on cartilage C2M release in any trial. The small effects of E-64 on cartilage degradation could be due to the low levels of calcification. E-64 has been shown to reduce CTX-I release from decalcified bone less than from normally calcified bone [8]. ECMs with low calcification presumably result in less acidification, thereby reducing the activity of

cathepsin K as it is most effective at an acidic pH [52]. Another factor is the biomarker itself as C2M is primarily generated by MMPs. In previous studies using a model of inflammatory cartilage degradation, E-64 had no effect on C2M release [40] even though cathepsin K is expressed in this model [29]. In our study diphyllin had no inhibitory effect on cartilage C2M or osteochondral C2M, supporting the hypothesis that both non-calcified and calcified cartilage can be resorbed independently of acidification. This is in line with the findings of Touaitahuata et al. that *Dock5*$^{-/-}$ murine osteoclasts degrade hypertrophic cartilage without acidifying the ECM due to dysfunctional sealing zones [53].

We were unable to detect the aggrecan degradation biomarkers ^{342}FFGV-G2 and ^{374}ARGS-G2 from any matrix. Although we demonstrated MMP-mediated collagen type II degradation, the MMPs present might not generate ^{342}FFGV-G2 or detectable amounts thereof, possibly due to the osteoclast source and substrate affecting which MMPs are secreted [54]. It is also possible that our matrices do not contain enough aggrecan to generate detectable levels of ^{342}FFGV-G2 or ^{374}ARGS-G2. In a model of inflammatory cartilage degradation the ^{374}ARGS-G2 neo-epitope is mainly generated by a disintegrin and metalloproteinase with thrombospondin motifs (ADAMTS)-4 [55], although ADAMTS-5 is also known to degrade aggrecan [56], but it is not known if osteoclasts express ADAMTS-4 or 5, hence, osteoclasts might not be able to generate ^{374}ARGS-G2.

While a large body of evidence supports both MMPs [6, 8, 29, 30] and cathepsin K [3, 6, 8, 31] contributing to bone and cartilage degradation, their contribution in degrading calcified cartilage or in degrading cartilage in a setting where they are known to be derived from osteoclasts has to our knowledge not been demonstrated previously. To date osteoclast inhibitors have yielded mixed results in osteoarthritis clinical trials despite promise in vivo. Hence, there is a need for elucidating the contribution of different osteoclast-derived proteases to ECM degradation. In addition to demonstrating how cysteine proteases and MMPs derived from human osteoclasts may degrade knee joint ECMs, in this study we also describe how these processes can be investigated using biomarkers directly associated with the enzymatic processing of the ECM. The in vitro model itself and the novel use of biomarkers like C2M in assessing cartilage resorption is also an important finding, in addition to demonstrating calcified cartilage resorption by MMPs and cathepsins in an acidification-independent manner. Our novel model holds potential for further studies in the early development of novel drugs and biomarkers focused on knee joint ECM remodeling.

Previous studies have suggested that the ECM is an important regulator of the osteoclast phenotype [28]. For the purposes of our study it is unclear if the relative importance of the osteoclast processes required for generating a particular biomarker was related to ECM-dependent phenotype shifts or different osteoclast subtypes. Our data do however demonstrate that osteoclast functionality is highly dependent on what matrix they are resorbing, as previously suggested [8, 28, 39, 57], since the different matrices required different osteoclast proteases and amounts of acidification for degradation. A previous study showed that monocytes from patients with OA display increased osteoclastogenesis accompanied by increased bone resorption and reduced apoptosis in vitro [22]. These findings suggest a phenotype shift in OA osteoclasts, thus it may be of interest to investigate if these osteoclasts also display increased cartilage or calcified cartilage resorption with an altered biomarker profile in future studies using our model.

Our cell culture model comes with some limitations. The amount of matrix obtained from a single knee and the large number of osteoclasts required to perform the cultures with a suitable number of technical replicates limits the number of conditions that can be used, resulting in relatively low statistical power that is sensitive to variation within conditions. Increased robustness could be achieved by investigating only the matrix and compound of interest in addition to reference matrices (cortical bone and/or articular cartilage) and reference inhibitors (diphyllin, E-64, and GM6001); this was, however, not suitable for the profiling approach of our study. Some experimental outputs varied between experiments, as can be seen by comparing the data in this article (Figs. 2, 3 and 4) with the supplementary data (Additional files 1, 2, 3, 4, 5 and 6: Figures S1–S6). This could potentially be explained by differences in osteoclast quality between donors and variations in matrix content between the knee joints, further necessitating strict use of reference matrices and inhibitors to validate each experiment. Finally, due to the in vitro design of our study, the findings cannot be directly extrapolated to the OA disease process.

In our study we decided to use a molecular in vitro approach to investigate the role of osteoclasts in degrading the knee joint ECMs rather than an in vivo approach. Considering that the contribution of osteoclasts or the different ECMs to the biomarker release cannot be precisely determined in vivo, an in vitro study provides a clearer picture of the osteoclast-derived mechanisms involved in resorbing the different ECMs. Additionally, the inter-species phenotype differences observed between human and murine osteoclasts with deficits in e.g. cathepsins (or with inhibited cathepsins) [58–60] indicate that the use of non-human osteoclasts are unlikely to be an accurate representation of the human situation. The use of bisphosphonates in clinical OA trials have yielded mixed results, despite great promise in vivo, and therefore investigations of how human osteoclasts may contribute to the degradation of knee joint ECMs is of

importance—something which, to our knowledge, has not been previously investigated in articular cartilage and osteochondral junction joint compartments.

Conclusions

In conclusion, in this study we have developed a novel cell culture model to demonstrate the osteoclasts' capability of degrading the osteochondral junction and articular cartilage joint compartments in a manner that can be assessed using tissue-specific and protease-specific biomarkers. Our study supports that osteoclasts can resorb cartilage and calcified cartilage independently of acidification. We demonstrated both MMP-mediated and cysteine protease-mediated resorption of calcified cartilage. The osteoclast functionality was highly dependent on the resorbed substrate, as different ECMs required different osteoclast processes for degradation. Our novel culture system has potential to facilitate drug and biomarker development for rheumatic diseases, e.g. osteoarthritis, with pathological osteoclast processes in specific joint compartments.

Additional files

Additional file 1: Figure S1. Resorption biomarkers released from osteoclasts cultured on cortical bone in an additional trial. Osteoclasts were cultured on bovine femoral cortical bone in the presence or absence of resorption inhibitors. Resorption of calcified ECM and collagen type I was assessed by measuring the Ca^{2+} (A) and CTX-I (B) concentrations, respectively, in the medium. Cell viability was assessed using alamarBlue (C) and TRAP activity in the medium was measured for relative osteoclast quantification (D). Data are presented as percent of vehicle with error bars representing the SEM. Statistical significance is indicated by $^{*}p < 0.05$, $^{**}p < 0.01$, $^{***}p < 0.001$, $^{****}p < 0.0001$ for comparisons against the vehicle and $^{\#}p < 0.05$, $^{\#\#}p < 0.01$, $^{\#\#\#}p < 0.001$, $^{\#\#\#\#}p < 0.0001$ for comparisons against E-64/GM6001 (only shown for E-64 and GM6001); the post hoc test used is indicated in the top left corner of each graph. (PDF 32 kb)

Additional file 2: Figure S2. Resorption biomarkers released from osteoclasts cultured on cortical bone in pilot trial. Osteoclasts were cultured on bovine femoral cortical bone in the presence or absence of resorption inhibitors. Resorption of calcified ECM and collagen type I was assessed by measuring the Ca^{2+} (A) and CTX-I (B) concentrations, respectively, in the medium. TRAP activity in the medium was measured for relative osteoclast quantification (C). Data are presented as percent of vehicle with error bars representing the SEM. Statistical significance is indicated by $^{*}p < 0.05$, $^{**}p < 0.01$, $^{***}p < 0.001$, $^{****}p < 0.0001$ for comparisons against the vehicle; the post hoc test used is indicated in the top left corner of each graph. (PDF 28 kb)

Additional file 3: Figure S3. Resorption biomarkers released from osteoclasts cultured on articular cartilage in an additional trial. Osteoclasts were cultured on articular cartilage from bovine femoral condyles in the presence or absence of resorption inhibitors. Resorption of collagen type II was assessed by measuring C2M (A) concentrations in the medium. Cell viability was assessed using alamarBlue (B) and TRAP activity in the medium was measured for relative osteoclast quantification (C). Data are presented as percent of vehicle with error bars representing the SEM. Statistical significance is indicated by $^{*}p < 0.05$, $^{**}p < 0.01$, $^{***}p < 0.001$, $^{****}p < 0.0001$ for comparisons against the vehicle and $^{\#}p < 0.05$, $^{\#\#}p < 0.01$, $^{\#\#\#}p < 0.001$, $^{\#\#\#\#}p < 0.0001$ for comparisons against E-64/GM6001 (only shown for E-64 and GM6001); the post hoc test used is indicated in the top left corner of each graph. (PDF 30 kb)

Additional file 4: Figure S4. Resorption biomarkers released from osteoclasts cultured on articular cartilage in the pilot trial. Osteoclasts were cultured on articular cartilage from bovine femoral condyles in the presence or absence of resorption inhibitors. Resorption of collagen type II was assessed by measuring C2M (A) concentrations in the medium. TRAP activity in the medium was measured for relative osteoclast quantification (B). Data are presented as percent of vehicle with error bars representing the SEM. Statistical significance is indicated by $^{*}p < 0.05$, $^{**}p < 0.01$, $^{***}p < 0.001$, $^{****}p < 0.0001$ for comparisons against the vehicle; the post hoc test used is indicated in the top left corner of each graph. (PDF 27 kb)

Additional file 5: Figure S5. Resorption biomarkers released from osteoclasts cultured on osteochondral ECM in an additional trial. Osteoclasts were cultured on osteochondral ECM from bovine femoral condyles in the presence or absence of resorption inhibitors. Resorption of calcified ECM and collagen type I was assessed by measuring the Ca^{2+} (A) and CTX-I (B) concentrations, respectively, in the medium. Resorption of collagen type II was assessed by measuring C2M (C) concentrations in the medium. Cell viability was assessed using alamarBlue (D) and TRAP activity in the medium was measured for relative osteoclast quantification (E). Data are presented as percent of vehicle with error bars representing the SEM. Statistical significance is indicated by $^{*}p < 0.05$, $^{**}p < 0.01$, $^{***}p < 0.001$, $^{****}p < 0.0001$ for comparisons against the vehicle and $^{\#}p < 0.05$, $^{\#\#}p < 0.01$, $^{\#\#\#}p < 0.001$, $^{\#\#\#\#}p < 0.0001$ for comparisons against E-64/GM6001 (only shown for E-64 and GM6001); the post hoc test used is indicated in the top left corner of each graph. (PDF 33 kb)

Additional file 6: Figure S6. Resorption biomarkers released from osteoclasts cultured on osteochondral ECM in the pilot trial. Osteoclasts were cultured on osteochondral ECM from bovine femoral condyles in the presence or absence of resorption inhibitors. Resorption of calcified ECM and collagen type I was assessed by measuring the Ca^{2+} (A) and CTX-I (B) concentrations, respectively, in the medium. TRAP activity data could not be generated in these samples. Resorption of collagen type II was assessed by measuring C2M (C) concentrations in the medium. Data are presented as percent of vehicle with error bars representing the SEM. Statistical significance is indicated by $^{*}p < 0.05$, $^{**}p < 0.01$, $^{***}p < 0.001$, $^{****}p < 0.0001$ for comparisons against the vehicle; the post hoc test used is indicated in the top left corner of each graph. (PDF 27 kb)

Additional file 7: Figure S7. Osteoclast-derived biomarker levels compared to background levels. Biomarkers were measured in medium from wells containing only matrix (Background, white) or matrix and osteoclasts (Osteoclasts, black), cultured on bovine femoral cortical bone (Bone), articular cartilage (Cartilage) or osteochondral ECM (Osteoch.). Resorption of calcified ECM and collagen type I was assessed by measuring the Ca^{2+} (A) and CTX-I (B) concentrations, respectively, in the medium. Resorption of collagen type II was assessed by measuring C2M (C) concentrations in the medium. TRAP activity in the medium was measured for relative osteoclast quantification (D). Data from one representative resorption assay are presented as the mean of the measured parameters in background wells or osteoclast-containing wells. Error bars represent the SEM. (PDF 32 kb)

Abbreviations

ADAMTS: A disintegrin and metalloproteinase with thrombospondin motifs; ANOVA: Analysis of variance; Ca^{2+}: Calcium; CPC: *o*-Cresolphthalein complexone; CTX-I: C-terminal type I collagen fragments; DMSO: Dimethyl sulfoxide; DT3: Dunnett's T3 post hoc test; ECM: Extracellular matrix; EDTA: Ethylenediaminetetraacetic acid; ELISA: Enzyme-linked immunosorbent assay; GAG: Glycosaminoglycan; M-CSF: Macrophage colony-stimulating factor; MMP: Matrix metalloproteinase; NaCl: Sodium chloride; NaOH: Sodium hydroxide; OA: Osteoarthritis; RA: Rheumatoid arthritis; RANKL: Receptor activator of nuclear factor kappa-B ligand; SEM: Standard error of the mean; TRAP: Tartrate-resistant acid phosphatase; V-ATPase: Vacuolar-type H^{+}-ATPase

Acknowledgements

Not applicable.

Funding

HL is supported by Marie Curie Initial Training Networks (Euroclast, FP7-People-2013-ITN: #607446). JR is supported by grants from The Swedish Childhood Cancer Foundation and a Clinical Research Award from Lund University Hospital, The Foundations of Lund University Hospital. KH is supported by The Danish Research Foundation (Den Danske Forskningsfond). The funders had no role in study design, data collection and analysis, decision to publish, or preparation of the manuscript.

Availability of data and materials
The datasets used and/or analyzed during the current study are available from the corresponding author on reasonable request.

Authors' contributions
HL, KH, and CST conceived of and designed the study. HL and HN acquired the data. All authors contributed to data analysis and interpretation. HL wrote the manuscript. All authors critically reviewed the manuscript for intellectual content. All authors read and approved the final manuscript.

Ethics approval and consent to participate
The use of anonymized donor material in this study was covered by the general ethical approval for research use of donor material in compliance with the Transfusion Medicine Standards (TMS) of the Danish Society of Clinical Immunology (DSKI). Written consent to participate as an anonymized healthy control was obtained from each of the participating donors as part of standard practice at the blood bank at Rigshospitalet, Copenhagen University Hospital, Copenhagen, Denmark. Donors participated in compliance with the Helsinki Declaration.

Consent for publication
Not applicable.

Competing interests
MAK, KH, and CST are employees of Nordic Bioscience A/S. MAK and KH hold stocks in Nordic Bioscience A/S. The remaining authors declare that they have no competing interests.

Publisher's Note

Author details
[1]Nordic Bioscience, Herlev Hovedgade 205-207, 2730 Herlev, Denmark. [2]Division of Molecular Medicine and Gene Therapy, Lund Strategic Center for Stem Cell Biology, Lund, Sweden. [3]Department of Clinical Immunology, Rigshospitalet, Copenhagen University Hospital, Copenhagen, Denmark.

Received: 2 November 2017 Accepted: 12 March 2018
Published online: 10 April 2018

References
1. Teitelbaum SL. Osteoclasts: what do they do and how do they do it? Am J Pathol. 2007;170:427–35. https://doi.org/10.2353/ajpath.2007.060834.
2. Roodman GD. Cell biology of the osteoclast. Exp Hematol. 1999;27:1229–41. https://doi.org/10.1016/S0301-472X(99)00061-2.
3. Gelb BD, Shi GP, Chapman HA, Desnick RJ. Pycnodysostosis, a lysosomal disease caused by cathepsin K deficiency. Science. 1996;273:1236–8. https://doi.org/10.1126/science.273.5279.1236.
4. Gowen M, Lazner F, Dodds R, Kapadia R, Feild J, Tavaria M, et al. Cathepsin K knockout mice develop osteopetrosis due to a deficit in matrix degradation but not demineralization. J Bone Miner Res. 1999;14:1654–63. https://doi.org/10.1359/jbmr.1999.14.10.1654.
5. Saftig P, Hunziker E, Wehmeyer O, Jones S, Boyde A, Rommerskirch W, et al. Impaired osteoclastic bone resorption leads to osteopetrosis in cathepsin-K-deficient mice. Proc Natl Acad Sci USA. 1998;95:13453–8. https://doi.org/10.1073/pnas.95.23.13453.
6. Delaissé J-M, Andersen TL, Engsig MT, Henriksen K, Troen T, Blavier L. Matrix metalloproteinases (MMP) and cathepsin K contribute differently to osteoclastic activities. Microsc Res Tech. 2003;61:504–13. https://doi.org/10.1002/jemt.10374.
7. Everts V, Delaissé JM, Korper W, Niehof A, Vaes G, Beertsen W. Degradation of collagen in the bone-resorbing compartment underlying the osteoclast involves both cysteine-proteinases and matrix metalloproteinases. J Cell Physiol. 1992;150:221–31. https://doi.org/10.1002/jcp.1041500202.
8. Henriksen K, Sørensen MG, Nielsen RH, Gram J, Schaller S, Dziegiel MH, et al. Degradation of the organic phase of bone by osteoclasts: a secondary role for lysosomal acidification. J Bone Miner Res. 2006;21:58–66. https://doi.org/10.1359/JBMR.050905.
9. Blaney Davidson EN, Vitters EL, van der Kraan PM, van den Berg WB. Expression of transforming growth factor-β (TGFβ) and the TGFβ signalling molecule SMAD-2P in spontaneous and instability-induced osteoarthritis: role in cartilage degradation, chondrogenesis and osteophyte formation. Ann Rheum Dis. 2006;65:1414–21. https://doi.org/10.1136/ard.2005.045971.
10. Diarra D, Stolina M, Polzer K, Zwerina J, Ominsky MS, Dwyer D, et al. Dickkopf-1 is a master regulator of joint remodeling. Nat Med. 2007;13:156–63. https://doi.org/10.1038/nm1538.
11. Schett G, Hayer S, Zwerina J, Redlich K, Smolen JS. Mechanisms of Disease: the link between RANKL and arthritic bone disease. Nat Clin Pract Rheumatol. 2005;1:47–54. https://doi.org/10.1038/ncprheum0036.
12. Schett G, Stolina M, Bolon B, Middleton S, Adlam M, Brown H, et al. Analysis of the kinetics of osteoclastogenesis in arthritic rats. Arthritis Rheum. 2005;52:3192–201. https://doi.org/10.1002/art.21343.
13. Stolina M, Adamu S, Ominsky M, Dwyer D, Asuncion F, Geng Z, et al. RANKL is a marker and mediator of local and systemic bone loss in two rat models of inflammatory arthritis. J Bone Miner Res. 2005;20:1756–65. https://doi.org/10.1359/JBMR.050601.
14. Goldring SR, Goldring MB. Changes in the osteochondral unit during osteoarthritis: structure, function and cartilage-bone crosstalk. Nat Rev Rheumatol. 2016;12:632–44. https://doi.org/10.1038/nrrheum.2016.148.
15. Burr DB, Gallant M a. Bone remodelling in osteoarthritis. Nat Rev Rheumatol. 2012;8:665–73. https://doi.org/10.1038/nrrheum.2012.130.
16. Karsdal MA, Neutzsky-Wulff AV, Dziegiel MH, Christiansen C, Henriksen K. Osteoclasts secrete non-bone derived signals that induce bone formation. Biochem Biophys Res Commun. 2008;366:483–8. https://doi.org/10.1016/j.bbrc.2007.11.168.
17. Henriksen K, Karsdal MA, Martin TJ. Osteoclast-derived coupling factors in bone remodeling. Calcif Tissue Int. 2014;94:88–97. https://doi.org/10.1007/s00223-013-9741-7.
18. Henriksen K, Andreassen KV, Thudium CS, Gudmann KNS, Moscatelli I, Crüger-Hansen CE, et al. A specific subtype of osteoclasts secretes factors inducing nodule formation by osteoblasts. Bone. 2012;51:353–61. https://doi.org/10.1016/j.bone.2012.06.007.
19. Lories RJ, Luyten FP. The bone-cartilage unit in osteoarthritis. Nat Rev Rheumatol. 2011;7:43–9. https://doi.org/10.1038/nrrheum.2010.197.
20. Karsdal MA, Leeming DJ, Dam EB, Henriksen K, Alexandersen P, Pastoureau P, et al. Should subchondral bone turnover be targeted when treating osteoarthritis? Osteoarthr Cartil. 2008;16:638–46. https://doi.org/10.1016/j.joca.2008.01.014.
21. Väänänen HK, Zhao H, Mulari M, Halleen JM. The cell biology of osteoclast function. J Cell Sci. 2000;113:377–81. http://jcs.biologists.org/content/113/3/377.
22. Durand M, Komarova SV, Bhargava A, Trebec-Reynolds DP, Li K, Fiorino C, et al. Monocytes from patients with osteoarthritis display increased osteoclastogenesis and bone resorption: the In Vitro Osteoclast Differentiation in Arthritis study. Arthritis Rheum. 2013;65:148–58. https://doi.org/10.1002/art.37722.
23. Knowles HJ, Moskovsky L, Thompson MS, Grunhen J, Cheng X, Kashima TG, et al. Chondroclasts are mature osteoclasts which are capable of cartilage matrix resorption. Virchows Arch. 2012;461:205–10. https://doi.org/10.1007/s00428-012-1274-3.
24. Bertuglia A, Lacourt M, Girard C, Beauchamp G, Richard H, Laverty S. Osteoclasts are recruited to the subchondral bone in naturally occurring post-traumatic equine carpal osteoarthritis and may contribute to cartilage degradation. Osteoarthr Cartil. 2016;24:555–66. https://doi.org/10.1016/j.joca.2015.10.008.
25. Kuttapitiya A, Assi L, Laing K, Hing C, Mitchell P, Whitley G, et al. Microarray analysis of bone marrow lesions in osteoarthritis demonstrates upregulation of genes implicated in osteochondral turnover, neurogenesis and inflammation. Ann Rheum Dis. 2017; https://doi.org/10.1136/annrheumdis-2017-211396..
26. Roemer FW, Guermazi A, Javaid MK, Lynch JA, Niu J, Zhang Y, et al. Change in MRI-detected subchondral bone marrow lesions is associated with cartilage loss: the MOST Study. A longitudinal multicentre study of knee osteoarthritis. Ann Rheum Dis. 2009;68:1461–5. https://doi.org/10.1136/ard.2008.096834.
27. Shibakawa A, Yudoh K, Masuko-Hongo K, Kato T, Nishioka K, Nakamura H. The role of subchondral bone resorption pits in osteoarthritis: MMP production by cells derived from bone marrow. Osteoarthr Cartil. 2005;13:679–87. https://doi.org/10.1016/j.joca.2005.04.010.
28. Rody WJ, Krokhin O, Spicer V, Chamberlain CA, Chamberlain M, McHugh KP, et al. The use of cell culture platforms to identify novel markers of bone and dentin resorption. Orthod Craniofac Res. 2017;20(Suppl 1):89–94. https://doi.org/10.1111/ocr.12162.
29. Sondergaard BC, Henriksen K, Wulf H, Oestergaard S, Schurigt U, Bräuer R, et al. Relative contribution of matrix metalloprotease and cysteine protease

activities to cytokine-stimulated articular cartilage degradation. Osteoarthr Cartil. 2006;14:738–48. https://doi.org/10.1016/j.joca.2006.01.016.
30. Billinghurst RC, Dahlberg L, Ionescu M, Reiner A, Bourne R, Rorabeck C, et al. Enhanced cleavage of type II collagen by collagenases in osteoarthritic articular cartilage. J Clin Invest. 1997;99:1534–45..
31. Dejica VM, Mort JS, Laverty S, Antoniou J, Zukor DJ, Tanzer M, et al. Increased type II collagen cleavage by cathepsin K and collagenase activities with aging and osteoarthritis in human articular cartilage. Arthritis Res Ther. 2012;14:R113. https://doi.org/10.1186/ar3839.
32. Xue M, McKelvey K, Shen K, Minhas N, March L, Park S-Y, et al. Endogenous MMP-9 and not MMP-2 promotes rheumatoid synovial fibroblast survival, inflammation and cartilage degradation. Rheumatology. 2014;53:2270–9. https://doi.org/10.1093/rheumatology/keu254.
33. Kaspiris A, Khaldi L, Chronopoulos E, Vasiliadis E, Grivas TB, Kouvaras I, et al. Macrophage-specific metalloelastase (MMP-12) immunoexpression in the osteochondral unit in osteoarthritis correlates with BMI and disease severity. Pathophysiology. 2015;22:143–51. https://doi.org/10.1016/j.pathophys.2015.06.001.
34. Sanchez C, Bay-Jensen A-C, Pap T, Dvir-Ginzberg M, Quasnichka H, Barrett-Jolley R, et al. Chondrocyte secretome: a source of novel insights and exploratory biomarkers of osteoarthritis. Osteoarthr Cartil. 2017;25:1199–209. https://doi.org/10.1016/j.joca.2017.02.797.
35. Konttinen YT, Mandelin J, Li T-F, Salo J, Lassus J, Liljeström M, et al. Acidic cysteine endoproteinase cathepsin K in the degeneration of the superficial articular hyaline cartilage in osteoarthritis. Arthritis Rheum. 2002;46:953–60. https://doi.org/10.1002/art.10185.
36. Simkin PA. Consider the tidemark. J Rheumatol. 2012;39:890–2. https://doi.org/10.3899/jrheum.110942.
37. Sørensen MG, Henriksen K, Schaller S, Henriksen DB, Nielsen FC, Dziegiel MH, et al. Characterization of osteoclasts derived from CD14+ monocytes isolated from peripheral blood. J Bone Miner Metab. 2007;25:36–45. https://doi.org/10.1007/s00774-006-0725-9.
38. Henriksen K, Karsdal MA, Taylor A, Tosh D, Coxon FP. Generation of human osteoclasts from peripheral blood. Methods Mol Biol. 2012;816:159–75. https://doi.org/10.1007/978-1-61779-415-5_11.
39. Neutzsky-Wulff AV, Sørensen MG, Kocijancic D, Leeming DJ, Dziegiel MH, Karsdal MA, et al. Alterations in osteoclast function and phenotype induced by different inhibitors of bone resorption - implications for osteoclast quality. BMC Musculoskelet Disord. 2010;11:109. https://doi.org/10.1186/1471-2474-11-109.
40. Bay-Jensen A-C, Liu Q, Byrjalsen I, Li Y, Wang J, Pedersen C, et al. Enzyme-linked immunosorbent assay (ELISAs) for metalloproteinase derived type II collagen neoepitope, CIIM—increased serum CIIM in subjects with severe radiographic osteoarthritis. Clin Biochem. 2011;44:423–9. https://doi.org/10.1016/j.clinbiochem.2011.01.001.
41. Sørensen MG, Henriksen K, Neutzsky-Wulff AV, Dziegiel MH, Karsdal MA. Diphyllin, a novel and naturally potent V-ATPase inhibitor, abrogates acidification of the osteoclastic resorption lacunae and bone resorption. J Bone Miner Res. 2007;22:1640–8. https://doi.org/10.1359/jbmr.070613.
42. Karsdal MA, Sumer EU, Wulf H, Madsen SH, Christiansen C, Fosang AJ, et al. Induction of increased cAMP levels in articular chondrocytes blocks matrix metalloproteinase-mediated cartilage degradation, but not aggrecanase-mediated cartilage degradation. Arthritis Rheum. 2007;56:1549–58. https://doi.org/10.1002/art.22599.
43. Karsdal MA, Bay-Jensen AC, Lories RJ, Abramson S, Spector T, Pastoureau P, et al. The coupling of bone and cartilage turnover in osteoarthritis: opportunities for bone antiresorptives and anabolics as potential treatments? Ann Rheum Dis. 2014;73:336–48. https://doi.org/10.1136/annrheumdis-2013-204111.
44. Karsdal MA, Henriksen K, Sørensen MG, Gram J, Schaller S, Dziegiel MH, et al. Acidification of the osteoclastic resorption compartment provides insight into the coupling of bone formation to bone resorption. Am J Pathol. 2005;166:467–76. https://doi.org/10.1016/S0002-9440(10)62269-9.
45. Lorget F, Kamel S, Mentaverri R, Wattel A, Naassila M, Maamer M, et al. High extracellular calcium concentrations directly stimulate osteoclast apoptosis. Biochem Biophys Res Commun. 2000;268:899–903. https://doi.org/10.1006/bbrc.2000.2229.
46. Siebuhr AS, Petersen KK, Arendt-Nielsen L, Egsgaard LL, Eskehave T, Christiansen C, et al. Identification and characterisation of osteoarthritis patients with inflammation derived tissue turnover. Osteoarthr Cartil. 2014;22:44–50. https://doi.org/10.1016/j.joca.2013.10.020.
47. Maijer KI, Gudmann NS, Karsdal MA, Gerlag DM, Tak PP, Bay-Jensen AC. Neo-epitopes—fragments of cartilage and connective tissue degradation in early rheumatoid arthritis and unclassified arthritis. PLoS One. 2016;11:e0149329. https://doi.org/10.1371/journal.pone.0149329.
48. Bay-Jensen AC, Platt A, Byrjalsen I, Vergnoud P, Christiansen C, Karsdal MA. Effect of tocilizumab combined with methotrexate on circulating biomarkers of synovium, cartilage, and bone in the LITHE study. Semin Arthritis Rheum. 2014;43:470–8. https://doi.org/10.1016/j.semarthrit.2013.07.008.
49. Bay-Jensen AC, Platt A, Siebuhr AS, Christiansen C, Byrjalsen I, Karsdal MA. Early changes in blood-based joint tissue destruction biomarkers are predictive of response to tocilizumab in the LITHE study. Arthritis Res Ther. 2016;18:13. https://doi.org/10.1186/s13075-015-0913-x.
50. Bay-Jensen AC, Leeming DJ, Kleyer A, Veidal SS, Schett G, Karsdal MA. Ankylosing spondylitis is characterized by an increased turnover of several different metalloproteinase-derived collagen species: A cross-sectional study. Rheumatol Int. 2012;32:3565–72..
51. Bay-Jensen AC, Wichuk S, Byrjalsen I, Leeming DJ, Morency N, Christiansen C, et al. Circulating protein fragments of cartilage and connective tissue degradation are diagnostic and prognostic markers of rheumatoid arthritis and ankylosing spondylitis. PLoS One. 2013;8:e54504. https://doi.org/10.1371/journal.pone.0054504.
52. Lecaille F, Choe Y, Brandt W, Li Z, Craik CS, Brömme D. Selective inhibition of the collagenolytic activity of human cathepsin K by altering its S2 subsite specificity. Biochemistry. 2002;41:8447–54. https://doi.org/10.1021/bi025638x.
53. Touaitahuata H, Cres G, de Rossi S, Vives V, Blangy A. The mineral dissolution function of osteoclasts is dispensable for hypertrophic cartilage degradation during long bone development and growth. Dev Biol. 2014;393:57–70. https://doi.org/10.1016/j.ydbio.2014.06.020.
54. Andersen TL, del Carmen OM, Kirkegaard T, Lenhard T, Foged NT, Delaissé J-M. A scrutiny of matrix metalloproteinases in osteoclasts: evidence for heterogeneity and for the presence of MMPs synthesized by other cells. Bone. 2004;35:1107–19. https://doi.org/10.1016/j.bone.2004.06.019.
55. He Y, Zheng Q, Jiang M, Sun S, Christiansen TG, Kassem M, et al. The effect of protease inhibitors on the induction of osteoarthritis-related biomarkers in bovine full-depth cartilage explants. PLoS One. 2015;10:e0122700. https://doi.org/10.1371/journal.pone.0122700.
56. Verma P, Dalal K. ADAMTS-4 and ADAMTS-5: key enzymes in osteoarthritis. J Cell Biochem. 2011;112:3507–14. https://doi.org/10.1002/jcb.23298.
57. Henriksen K, Bollerslev J, Everts V, Karsdal MA. Osteoclast activity and subtypes as a function of physiology and pathology—implications for future treatments of osteoporosis. Endocr Rev. 2011;32:31–63. https://doi.org/10.1210/er.2010-0006.
58. Brömme D, Panwar P, Turan S. Cathepsin K osteoporosis trials, pycnodysostosis and mouse deficiency models: Commonalities and differences. Expert Opin Drug Discov. 2016;11:457–72. https://doi.org/10.1517/17460441.2016.1160884.
59. James IE, Marquis RW, Blake SM, Hwang SM, Gress CJ, Ru Y, et al. Potent and selective cathepsin L inhibitors do not inhibit human osteoclast resorption in vitro. J Biol Chem. 2001;276:11507–11. https://doi.org/10.1074/jbc.M010684200.
60. Kakegawa H, Nikawa T, Tagami K, Kamioka H, Sumitani K, Kawata T, et al. Participation of cathepsin L on bone resorption. FEBS Lett. 1993;321:247–50. https://doi.org/10.1016/0014-5793(93)80118-E.

Paper V

GPDPLQ$_{1237}$—A Type II Collagen Neo-Epitope Biomarker of Osteoclast- and Inflammation-Derived Multi-Protease Cartilage Degradation In Vitro

Henrik Löfvall[1,2], Anna Katri[1,3], Aneta Dąbrowska[1], Morten A. Karsdal[1], Yunyun Luo[1], Yi He[1], Tina Manon-Jensen[1], Morten H. Dziegiel[4], Anne-Christine Bay-Jensen[1], Christian S. Thudium[1], Kim Henriksen[1*]

1. Nordic Bioscience, Herlev, Denmark.
2. Division of Molecular Medicine and Gene Therapy, Lund Strategic Center for Stem Cell Biology, Lund, Sweden.
3. Department of Drug Design and Pharmacology, Copenhagen University, Copenhagen, Denmark.
4. Department of Clinical Immunology, Rigshospitalet, Copenhagen University Hospital, Copenhagen, Denmark.

* Corresponding author

Henrik Löfvall received his Master's degree in biomedicine from Lund University in 2014. From 2014 to 2018, Henrik worked as a PhD student with the Division of Molecular Medicine and Gene Therapy, Lund University and Nordic Bioscience A/S. Henrik's research is focused on diseases with osteoclast-related degradation of bone and cartilage extracellular matrices. In this dissertation, Henrik has explored how osteoclasts resorb these matrices and has developed new methods for assessing these processes. Of clinical relevance, Henrik has also worked on a new treatment for osteopetrosis, a devastating metabolic bone disease.

Printed by Media-Tryck, Lund 2018 NORDIC SWAN ECOLABEL 3041 0903

Nordic Bioscience A/S

Department of Laboratory Medicine
Division of Molecular Medicine
and Gene Therapy

Lund University, Faculty of Medicine
Doctoral Dissertation Series 2018:108
ISBN 978-91-7619-676-2
ISSN 1652-8220

LUND UNIVERSITY

FACULTY OF MEDICINE